Refining locomotory style in the fossil record through use of 3D Geometric Morphometrics and muscle attachment sites in the fossil species *Australopithecus afarensis*

By:

Jonquil A. Mogg

A thesis submitted in partial fulfilment of the requirements for the degree of Doctor of Philosophy

The University of Sheffield
Faculty of Arts and Humanities
Department of Archaeology

November 2018

Acknowledgements

Thank you to everyone who has helped me through this journey, in particular Timothy Lister, without whom this would not have been possible. I love you dearly.

Special thanks to my best friends, and greatest support network, Kyle Billington and Isabelle Heyerdahl-King who helped me in every way possible and kept me sane when I felt like I was definitely losing it, and sometimes lost it with me.

My Aunty Dorothy, who always believed in me and is an endless source of support- thank you.

Special thanks to Pia Nystrom who taught me anatomy and then let me teach it.

Thanks to Kevin Kuykendall and Andrew Chamberlain for encouraging me on this project, and thanks to The University of Sheffield, The Powell-Cotton Museum, The Natural History Museum in London, The Museum of Central Africa, and in particular Emmanuel Gillissen.

Thanks also to Cinzia Fornai for all her support with EVAN, and Bill Sellers for his help with GaitSym.

Finally, in memory of my mother, Janet, and Oliver. I hope I fulfil all of your ambitions for me. You will be missed terribly.

ABSTRACT

Determining muscular anatomy for fossil species can be problematic. Whilst bony material does fossilise, the soft tissue elements are rarely, if ever, preserved to any useful degree and so determination of musculature is often speculative. This has meant that the exact movements of fossil species can be difficult to determine. A prime example of this problem can be seen can be seen in the controversy surrounding the locomotion of *Australopithecus afarensis*. It has been debated as to whether this fossil species walked in a way similar to modern humans (a striding biped), in a bent-hip-bent-knee style, or in some other novel way. Until relatively recently, it has not been possible to determine the way in which a hypothetical muscular system may have behaved. However, with recent advances in computing, computer modelling of locomotory behaviour has been made possible.

This study used Geometric Morphometric study of the sacrum, Os Coxa, femur and tibia to determine how similar the shape of these bones were between the fossil specimen A.L. 288-1 (*Australopithecus afarensis*) and extant apes, including *Pan paniscus, Pan troglodytes, Gorilla sp., Pongo pygmaeus* and *Homo sapiens*.

Where there was similarity in the shape of the bones, it was hypothesized that there was similarity in the attached musculature, as the species in question are closely related. This was then used to determine a theoretical musculature for the lower limb of *Australopithecus afarensis*. The properties of individual muscles for *Australopithecus afarensis* were extrapolated from the properties of the muscles of the species with the most closely shaped area of bone in the extant species, resulting in a muscular pattern most similar to modern humans at the hip, and then increasing in 'ape-like' properties distally to the knee and ankle.

This theorised musculature was then input into the forward dynamic modelling program, GaitSym, to establish whether such a muscular configuration would result in a locomotory pattern that conformed to an existing theory or to one that had not yet been proposed. The model proposed unfortunately travelled backwards, likely due to the constraints of the modelling program, however he method of this motion indicated a bipedal 'shuffle' as proposed by Hunt (1994).

Contents

Table of Figures

List of Tables

1. Introduction & Background

Since its beginning, palaeoanthropology has been dependent on comparison with extant species and the measurements available on fossil species to determine the phylogenetic relationships between ancestral and extant species. Linear measurements and ratios have been the backbone of the discipline, allowing us to make inferences for the behaviour and adaptations of fossil taxa, and ultimately, our own heritage. As the discipline of palaeoanthropology moves forward, however, it becomes increasingly important that the techniques we employ to extract the maximum information from a relatively sparse fossil record are enhanced. It is for this reason that palaeoanthropology is now becoming a digital subject where new techniques, such as 3D Geometric Morphometrics and simulation techniques, are being used to analyse our oldest ancestors. Although these techniques are used to tackle a variety of questions regarding fossil hominoids, of particular interest to this study, are those that tackle questions relating to locomotion.

Australopithecines especially have been a focus of much of this research, and in particular, the largely complete skeleton of A.L. 288-1, an individual of the species *Australopithecus afarensis*- commonly known as Lucy. Australopithecines in general are important, as they show clear bipedal traits but are near the origins of true terrestrial bipedalism in time. Further study into the locomotory styles of australopithecines serves to widen the picture of what was happening when our ancestors were becoming ground dwelling bipeds. Berge (1998) and Ward (2002) point out that various biomechanical studies of australopithecine bipedalism have suggested marked differences in the way in which australopithecines walked in comparison with modern humans. Their anatomy suggests that they perhaps moved with a waddling gait, involving large rotational movements of the pelvis and shoulders (Zihlman and Hunter, 1972; Berge, 1991, 1994; Rak, 1991). Others (Stern and Susman 1983, Susman et al. 1984, Hunt, 1994; Churchill et al., 2013; Da Silva e al. 2013) have demonstrated that the australopithecines are clearly adapted for exploitation of arboreal environments, particularly demonstrated in the morphology of the upper limb (McHenry & Berger, 1998; Green & Alemsegoed, 2012.)

Several studies have used computer simulation to assess the effectiveness of alternative gaits in *Australopithecus afarensis* (Kramer 1999; Sellers et al. 2003, 2004, 2005; Wang & Crompton 2004; Wang et al.2004 Nagano et al.2005; Crompton et al.

2010, 2012) and have demonstrated that Lucy could have been an energetically efficient biped.

A key problem regarding the determination of locomotory styles in fossil species is the paucity of information regarding musculature, as soft tissue information is rarely preserved in the fossil record. Although, through comparison to closely related extant species, we can sometimes infer some muscle attachment sites on the available osteology, a complete picture of the 'whole' can only be hypothesized. Equally, we can only hypothesize the effects such musculature would have had on the locomotory patterns that fossil species would be capable of.

To date, studies of fossil locomotion have largely focused on either comparisons of the bony morphology of the fossil species and extant species, or alternatively, on using modelling and simulations based on either modern human or ape parameters to test hypotheses of their locomotory style. This study proposes a combined approach to the problem, using both Geometric Morphometrics to compare the bony elements, and forward dynamic modelling based on the results of the Geometric Morphometric analysis to propose a locomotory style.

In order to do this, a fundamental assumption must be made. This is that similarity in osteological shape equates to similarity in musculature (and conversely, that a difference in osteological shape equates to a difference in musculature). As the species under consideration are very closely related, and as their musculature does not vary hugely in the actual muscles within the lower limb, this is not an insurmountable problem (Ruff et al., 2006). A number of studies have demonstrated that closely related species display similarity in musculature and corresponding osteology. Scott, (1957) conducted a comprehensive review (at the time) of the impacts of muscle on bone, both through ontogeny, and in relation to sex and speciation. Ashton and Oxnard (1964) suggested that these similarities could be used to assess locomotor behaviours in fossil primates, through study of the fore- and hind-limbs of extant primates and the resultant impacts of their preferred locomotory pattern on the vertebral column. Oxnard (1967; 1968) then extended this work to focus on the primate and then mammalian shoulder girdle, looking particularly at the impacts of musculature on osteology in locomotion. Corruccini and Ciochon, (1976) undertook multivariate morphometric analyses of the primate shoulder girdle, and demonstrated that there

was great similarity in myology and osteology within the extant apes, especially when allometry was accounted for. Further study on the *Papio* and *Maccaca* shoulder girdle by Kimes et al. (1981) emphasized that morphological study should by necessity be conducted on closely related groups as this would remove the possibility that structural differences observed were due to genetic or selective factors. This has become a fundamental principle in comparative anatomy and palaeoanthropological study.

1.1 Comparative Anatomy of *Australopithecus afarensis*

It has been suggested that elements of the morphology of the upper limb in *A. afarensis* indicate adaptations for locomotion in trees, including an ape-like humerus, ulna and radial neck indicative of climbing (Feldesman, 1982; Senut, 1978; 1980). A degree of arboreality is indicated in the bones of the wrist (Marzke, 1983; McHenry; 1983; Rose 1984) and by curvature of the phalanges (Paciciulli, 1995; Richmond, 1997; 1999). Additionally, the upper limbs of *A. afarensis* were relatively much longer than those of humans, as in arboreal apes (Kimbel et al., 1994).

Lovejoy (1988), however suggests that the upper limbs and fingers are relatively shorter than those of the arboreal apes, and White et al. (1993) have inferred that the upper limb, whilst remaining powerful, was not long enough to imply adaptation to regular arboreal locomotion. Gebo (1996) suggests that the features related to arboreal locomotion within the hand may simply be indicative of the retention of primitive traits in *A. afarensis,* and Ohlman (1986) has noted that the attachment for the deltoid on the clavicle is anteriorly facing, as in humans.

The pelvis is an extremely informative and useful indicator to locomotor function. This structure reflects some of the more drastic differences between bipedal humans and the extant apes as it has such a significant role in weight bearing and also forms the connection between the trunk and the lower limb. It serves as an attachment site for many muscle groups and can therefore reveal much about the form of locomotion employed by an animal. Extant non-human apes are not specialised bipeds, although all practice bipedalism on occasion, and so have pelves that have different features to those seen in our species, and other hominid and hominoid species which are adapted to the habitual extension of the lower limb necessary for traditional striding bipedal locomotion. The morphology of the pelvis is also highly dependent on maternal-foetal size and the degree of encephalization at birth (eg. Leutenegger, 1974; Wittman & Wall, 2007; Wells *et al.* 2012; Wells, 2015 etc.), although such considerations are beyond the scope of this study, which will primarily focus on the features relating to locomotory adaptation.

The pelvis of the modern bipedal human is characterised by its adaptation toward an upright striding gait. This is demonstrated by the relatively short and broad ilia, which give the pelvis a basin-like shape (Aiello and Dean, 2002). By contrast, non-human ape pelves are generally elongated in comparison to the bipedal human pelvis and do not display the same bowl-like shape (Aiello and Dean, 2002). The shape of the human pelvis allows for the support of the greater load that the trunk and internal organs place upon the lower limb – a feature not required in non-bipeds. It is broadly parallel to both the lower limb and the vertebral column thus making the sacroiliac joint extremely important in the transmission of weight onto the load bearing limbs (McHenry, 1974). As a consequence of this, the acetabular and sacroiliac joints are located nearer to each other (Leutenegger, 1974). The non-human ape pelvis contrasts with this as, although remaining parallel to the vertebral column, it is more transversely oriented to the femoral shaft (Lovejoy 1988, 2005), with the acetabular and sacroiliac joints further apart. The ilium in obligate bipeds is characterised by being wider than it is high, and is mediolaterally oriented (Waterman, 1929; Ward, 1993), for the attachment of the posterolaterally oriented gluteal muscles which are significant in the habitual extension of the lower limb. The ilium also displays a large Anterior Inferior Iliac Spine (AIIS) which is the attachment point for the rectus femoris muscle and iliofemoral ligament, which are important for stability at the hip and flexion at the knee (Palastanga *et al.* 2008).

The ilium of the non-human apes is elongated and narrow in comparison to humans, with poorly developed or absent anterior superior iliac spine. The orientation of the sacrum in bipeds also leads to the presence of a greater sciatic foramen and a posterior extension of the iliac blade, which is not seen in the extant apes (Aiello and Dean, 2002). The non-human apes however, display a relatively long iliac crest which reflects the importance of *m. latissimus dorsi* in climbing, an adaptation to the more arboreal lifestyles led by these taxa (Sonntag 1923, 1924;Waterman 1929). Its increased relative length demonstrates a greater area for the attachment of this muscle in these species. Of the extant apes, *Pongo* is the most uniquely specialised in terms of its pelvic structure as it is the only ape that routinely has the anterior superior iliac spine (Sigmon, 1974), and is adapted to a highly arboreal climbing existence.

Lovejoy (1979; 1980) suggests that the pelvis of *A. afarensis* is fully adapted to bipedality with the ilia positioned in such a way as to provide lateral attachment for

the lesser gluteal muscles. He further suggests that the attachment points the gluteus maximus and quadriceps are human-like and suggests that the groove for *m. iliopsoas* is present on the pelvis as in modern humans. However, Tuttle (1981) proposes that the ilia are actually somewhat laterally oriented in comparison to modern humans, indicating a notable degree of arborealism and Schmid (1983) infers that the pelvis of *A. afarensis* indicates suspensory rather than habitual bipedal locomotion. Some researchers (Stern and Susman, 1981; 1983; 1991; 1993; Jungers and Stern, 1983; Susman et al.. 1984; Stern and Larson, 1993; Jungers, 1991; Susman and Demes, 1994) have also suggested that some traits such as the iliopsoas groove and Anterior Superior Iliac Spine are not diagnostic of human-like bipedalism, but rather a bent hip, bent knee gait as seen in bipedally walking apes. Berge (Berge and Ponge, 1983; Berge, 1984; Berge and Kazmierczak, 1986), citing the lateral orientation of the iliac blade, the form of the iliac pillar and that of the Anterior Superior Iliac Spine, has proposed that the bipedal adaptations in *A. afarensis* were different to those seen in modern humans and that the bipedal locomotion adopted in the species would have been different in its form. She has suggested a 'waddling gait' would be the outcome of the anatomical differences (Berge, 1991; 1993; 1994).

The ischium of the extant non-human apes is also especially adapted for an arboreal lifestyle. The ischial tuberosity is everted and lower on the body of the ischium, which gives increased leverage for the muscles involved in the extension of the hip, and allows for power when climbing (Sigmon, 1974; Aiello and Dean, 2002). There is also no ischial spine (Aiello and Dean, 2002). By contrast there are prominent ischial spines in the bipedal pelvis due to the stresses placed on the ischia by the horizontally oriented pelvic floor and the weight of the abdomino-pelvic organs (Lovejoy, 1988; 2005), which it provides anchor for. The ischial spine is also important as an attachment for the sacrospinous ligament, which prevents sacral rotation and provides a narrower and more rigid pelvic floor (Abitbol, 1988). In addition to this, the ischial tuberosity is closer to the rim of the acetabulum (Aiello and Dean, 2002), which is due to the stresses placed on the ischial tuberosity and sacrum by the weight of the vertical trunk (Lovejoy, 2005).

The pubis in humans shows a well-developed pubic crest, which is the attachment for the *m. rectus abdominus*, and a well-developed pubic tubercle, which is the attachment for the inguinal ligament, both of which are vital in supporting the abdomen in bipedal

postures (Aiello and Dean, 2002). The pubis of the non-bipedal pelvis is less specifically adapted with no recognisable pubic crest or tubercle due to the smaller and less important *m. rectus abdominus* and iliofemoral ligament (Aiello and Dean, 2002). The body of the pubis is deeper and there is a narrower sub-pubic angle, and there is also no groove for the iliopsoas muscles, due to the different orientation of the thigh and pelvis (Aiello and Dean, 2002).

The acetabulum in bipeds is deep and faces inferiorly, laterally and anteriorly in order to transfer the weight of the trunk through to the lower limbs effectively and to keep the joint stable (Lovejoy, 2005).The acetabulum in non-human apes is shallow and faces laterally, allowing a wide range of motion at the hip, which is essential in climbing and an arboreal lifestyle (Lovejoy, 2005). In these behaviours, body weight is shared between the front and the hind limb which, in turn, means that the acetabular joint bears a lesser proportion of the body weight during locomotion.

In terms of musculature, the extant non-human apes are best separated from humans in the muscles of the hamstring and gluteal regions. The non-human apes have muscles in these regions that are adapted for power in climbing, whereas hominids have muscles that are largely adapted to produce speed, stability and a wide range of extension, as well as balance (Sigmon, 1974) which are necessary for habitual bipedal locomotion. The ischial tuberosity is longer and wider in apes, allowing a larger attachment for their more developed hamstrings and therefore increasing the power of the extension of the thigh, important in climbing. *M. gluteus maximus* has two parts (*m. gluteus maximus proprius* and *m. ischiofemoralis*) in non-human apes and a more extensive origin (including the distal sacrum, coccyx and ischial tuberosity) and attachment (inserting along the entire length of the femur) in apes (Aiello and Dean, 2002). *M. gluteus medius* also has a larger origin in apes, whereas *m. gluteus minimus* has a smaller origin, and is often separated, with the anterolateral portion being called *m. scansorius* (Sigmon, 1969).

Abitbol (1995), on examination of the lumbar spine and sacrum *A. afarensis* reasoned that completely upright bipedal locomotion would not have been possible, and that bipedal locomotion would have only been possible if the pelvis was tilted backwards or the trunk tilted forwards. It has also been suggested that the extremely wide hips of *A. afarensis* would not functionally allow a human like style of bipedalism (Hunt,

1994), but may have provided a stable posture for bipedal food harvesting. He inferred that any bipedal locomotion would be ‘shuffling’ in nature.

The femur of modern human bipeds is relatively much longer and grows to be much stronger than that of apes (Ruff, 2003), indicating its primary role in locomotion. This is because, as it is the primary weight bearing limb, it needs to be able to support this greater responsibility, and also provide larger muscle attachment sites for those muscles which provide the power to accomplish this form of gait and also the balance that walking on two legs requires. The bipedal femoral head is larger with a relatively longer femoral neck contrasting with the smaller femoral head and shorter femoral neck of apes (Lovejoy, 1988). This has to do with the stability required by bipeds for walking, with a larger head providing a greater contact area between the femur and pelvis, as well as a larger greater trochanter allowing greater area for muscle attachment and a greater bicondylar angle. The smaller femoral head and shorter femoral neck in the extant apes allow for the large range of motion required by the quadrupeds for climbing. In bipedal humans, but not the extant non-human apes, the intertrochanteric line on the anterior aspect of the proximal femur demarcates the attachment for the iliofemoral ligament (Aiello and Dean, 2002). The bipedal femoral shaft exhibits a high carrying angle and has elliptical femoral condyles for articulation with the tibia, contrasting with the relatively straight femoral shaft of apes and their more rounded femoral condyles (Harcourt-Smith, 2007). Due to the high carrying angle of the bipedal femur, the lateral tibial condyle is elliptical in shape, and there is a more valgus bicondylar angle at the knee when compared to apes (Lovejoy, 2007).

The modern bipedal foot is characterised by an adducted hallux which is in contrast with the abducted hallux of apes. Coupled with this is the presence of a longitudinal arch, which acts as a shock absorber and permits the medial transfer of weight during the midstance phase of walking, and the unique structure of the calcaneocuboid joint, which stabilises the midtarsal region of the foot and prevents the midtarsal break during walking (Aiello and Dean, 2002). Important for modern human bipedal locomotion are the relative proportions of the parts of the foot, with shorter digits and an adducted hallux, and the form of the ankle joint. The movement of the leg over the foot as well as the structure of the first tarsometatarsal joint and it’s prohibition of opposability in the great toe allows the modern human foot to preserve its structural integrity by dissipating kinetic energy during foot strike in walking and running and

transform into a rigid lever allowing forwards propulsion during toe-off (Lovejoy et al., 2009). It has been suggested (Lewis, 1981) that the major differences between ape feet and modern bipedal feet arise from the foot being realigned around the subtalar axis in bipeds with digits two through four moving medially towards the great toe. This would maintain the stability of the close-packed great toe, and the skeletal morphology of the modern bipedal foot is consistent with this.

Johanson and Edey (1981), argue that the pelvis, knee and toes show that *A. afarensis* was absolutely capable of a modern human-like form of bipedalism. Jungers (1984; 1991) has inferred that the relatively short lower limb and relatively long foot would have meant that bipedal locomotion in *A. afarensis* would have been energetically costly and distinctive from that of modern humans, as Jungers and Stern (1983) argue that human-like extension of the hip and thigh would not have been possible. Rak (1991) and Kramer (1999), however showed that the relatively short legs in *A. afarensis* did not represent an energetic compromise. Tardieu has extensively studied the knee in *Australopithecus afarensis* (Tardieu, 1979a; 1979b; Tardieu, 1983; 1986a, 1986b; Tardieu and Preuschoft, 1996) and concludes that it represents an early stage in hominid bipedalism, with adaptations to arboreal activity and an enhanced range of rotation of the leg, without the locking mechanism of the knee found in modern humans. Tuttle (1981) noted that there is a broad peroneal groove in the fibula of *A. afarensis* indicating arboreality. A human-like ankle and foot has also been suggested (Latimer, 1983; Latimer et al., 1987; Latimer and Lovejoy 1989; 1990a; 1990b; Ward et al. 1999), but this is contrary to Christie (1977) who suggested the medial rotation at the ankle would be much greater than in modern humans and also contrary Deloison (1991) who suggested the foot was adapted to gripping. Additionally, *A. afarensis* has been shown to have a more mobile and flatter transverse tarsal joint that of modern humans (Gomberg, 1985).

1.2 Positional Behaviours and Locomotion in Apes, Humans and *A. afarensis*

Non-human ape positional behaviours are characterised by an orthograde (upright) trunk (Hunt, 1992; Thorpe & Crompton 2006, 2007; Crompton et al., 2008; Hunt, 2016). Each species are capable of a variety of locomotor and positional behaviours however each species is can be characterised by a dominance of a particular suite.

Chimpanzees are the best studied of all non-human apes, and exhibit a variety of positional and locomotor behaviours. They combine arboreal feeding activity and terrestrial travel (Hunt, 2016), with 85% of their feeding behaviour occurring in trees and 99% of their travel occurring terrestrially. When Chimpanzees travel terrestrially, they knucklewalk 85% of the time (Doran, 1996). Arboreally, they engage in some suspensory behaviours, although rarely (Gebo, 1996), and primarily unimanual (single handed) hanging when feeding at the terminal end of branches. Chimpanzees rarely briachiate (Hunt, 1992) and are more likely to clamber or knucklewalk and palmwalk if travelling in trees (Hunt, 2016).

Bonobos are much less well studied (Hunt, 2016), but limited observations have suggested that they may be more arboreal and suspensory than chimpanzees (Doran, 1993; Doran & Hunt, 1994), although this may be a factor of limited exposure to humans.

Arboreally, gorillas largely engage in sitting and squatting behaviours, as well as some suspensory activity (Remis, 1995). When travelling travelling terrestrially, like chimpanzees, they use knucklewalking 85% of the time (Doran, 1996).

Orangutans are more arboreal than the African apes, and when travelling terrestrially will quadrupedally ‘fist walk’ unlike the knucklewalking *Pan* and *Gorilla* (Tuttle, 1969). They engage in more suspensory behaviours (Gebo, 1996) and most often practice bipedal quadrumanous climbing (Crompton et al. 2008; 2010).

Humans practice bipedalism as their primary locomotory form. The modern human gait cycle has two distinct phases: the stance phase, when the foot is in contact with the ground, and the swing phase, when it is not (Harcourt-Smith, 2007) (Figure 1-1).

Within these phases are defined periods of action (Uustal and Baerga, 2004):

1. Heel strike/initial contact

This is when the foot strikes the ground, heel first. There is flexion of the thigh at the hip and extension of the leg at the knee. The foot is dorsiflexed.

2. Foot Flat/ loading response phase

The foot then plantar flexes and force is transmitted through to the substrate along its lateral border. The thigh at the hip becomes less flexed and moves into extension, the leg begins to flex at the knee.

3. Midstance

The body is directly over the weight-bearing foot. The thigh continues to extend at the hip. The knee begins to extend. The foot became slightly dorsiflexed at the ankle and the whole body was supported by the limb.

4. Heel Off

The dominant heel leaves the floor and the foot begins to move from dorsiflexion to plantarflexion. The leg is extended at the knee, and the thigh is hyperextended.

5. Toe Off

The thigh at the hip becomes less extended. The knee is flexed and the plantarflexion of the foot at the ankle increases. This action finishes with a final push-off of the big toe.

6. Acceleration/Early Swing

The thigh and hip continue to flex and the foot moves into dorsiflexion.

7. Mid Swing

The thigh at the hip and the leg at the knee continue to flex shortening the limb to clear the substrate. The leg is now off the ground and in the swing phase, with the knee and hip both bent so as to keep the leg off the ground as it swings forward.

8. Late Swing

The thigh continues to flex and the leg begins to extend. The foot is dorsiflexed, ready for Heel Strike.

Figure 1-1: Typical Gait Cycle in Modern Human Bipedal Walking

(Taken from Uustal and Baerga, 2004)

It seems that there is little question that *A. afarensis* progressed bipedally when on the ground (contra Sarmiento, 1987; 1996). However, the nature of this bipedalism, and the degree to which it was practiced is highly debated, with broadly two camps- those who believe this locomotion to be as in modern humans (Feldesman, 1982; Lattimer, 1991; Lovejoy, 1980; Senut, 1978; 1980; Ohlman, 1986; Lattimer and Lovejoy, 1990a; 1990b; Lovejoy,1979; 1988; Gebo, 1996; Ward et al., 1999; White, 1994; White et al., 1993;Wolpoff, 1983a,1983b etc.) and those who believe that *A. afarensis's* locomotory pattern included a large arboreal component (Jungers, 1982; 1991; 1994; Jungers and Stern, 1983; Susman et al., 1984; Stern and Susman, 1981; 1983;1991; 1993; Stern and Larson, 1993; Susman and Demes, 1994; Rose, 1984; 1991; Paciciulli, 1995;Richmond, 1997; 1999 etc.), with each side quoting anatomical correlates to support these theories (summarised above).

1.3 Locomotory studies and simulation

Computer simulations and locomotory models where locomotion is actually simulated fall broadly into two types- inverse kinetic modelling and forward dynamic modelling, although other techniques, such as Finite Element Analysis have been used to determine factors important to locomotion. In inverse dynamics modelling, the motion of the model is input, or classified as 'known', and from this variables related to the motion are predicted for a specific form. Conversely, in forward dynamics, the variables are input, and a motion is predicted.

Often these models use the criteria of energy efficiency to determine the likelihood of a predicted gait- if a mode of locomotion takes a great deal of energy to produce, then it is unlikely to be used frequently, as locomotion is energetically expensive (Casey, 1992). Animals obtain their energy from the food that they ingest and metabolise and as such have a 'budget' of available energy based on this and the level of activity they partake in and other biological constraints (such as reproduction and general body maintenance) (Warren and Crompton, 1998). Exceeding this budget would result in a cost to the animal in question, and is therefore not conducive to long term survival.

Nicolas et al. (2007 and 2009) have created a model based purely on skeletal form and motion control laws, within specific parameters. Their program is designed to estimate the most energetically inexpensive and physically appropriate method for locomotion in a fossil species, although has not yet been applied to a fossil specimen, but has been tested on modern humans and bonobos with encouraging results, and has the potential to be expanded to fossil specimens in the future.

Additionally, Blemker and Delp (2005) have used 3D modelling techniques to create accurate representations of musculature. They have created models which represent the complex nature of muscle fibres and activation. This finite element analysis allows for better representations of musculature to be applied in locomotor studies, especially where simulation of movement is subsequently undertaken.

Much work has been done testing how energetically efficient various forms of locomotion for fossil species might be, taking into account the metabolic costs involved in walking bipedally in various forms. Kramer (1999) used simulation to model the locomotor energetics of *Australopithecus afarensis,* concluding that despite the relatively short length of Lucy's legs, she would not have practiced an energetically inefficient locomotor style when walking bipedally.

Similarly, Nagano et al., (2005) generated a three-dimensional reconstruction and forward-dynamic simulation of upright bipedal locomotion for *Australopithecus afarensis* and their results predicted energy expenditure was appropriate for upright bipedal walking in an individual of Lucy's body size. Conversely, Wang et al. (2004) built an inverse-dynamics musculoskeletal model of the lower limb for early hominids and modern humans, capable of estimating the patterns of muscle force during bipedal walking and tested the energetics required for *Australopithecus afarensis* and *Homo*

erectus to locomote bipedally. Their results showed that *A. afarensis* was marginally less energetically efficient when walking in the striding gait of *Homo*, and this would have been the driver for the anatomical changes in later *Homo* species. This model is however based upon the assumption of muscle attachments based on those typical of modern humans, which may mean that this model is inaccurate, as fossil species may have had an alternate muscular arrangement.

Sellers et al. (2003, 2004, 2005) have used evolutionary robotics to test locomotion in fossil species, and additionally (2010) have tested specific muscle variables, such as presence of the Achilles tendon to see how these alter gait and energy expenditure in possible locomotor strategies. The use of energy expenditure as a test parameter is valid and useful, as any species locomotory style should not be energetically too expensive, as this would imply an inefficient strategy, and one that would unlikely be used within a natural context.

Modelling current species bipedal ability has also been undertaken. This allows for better understanding of current species abilities to locomote in various forms and will also allow for this information to be extrapolated into fossil forms. D'Aout et al. (2004) have modelled bonobo gait both bipedally and quadrupedally and shown the differences between gait characteristics of bipedal locomotion and other gaits. They modelled ground reaction forces and angles at the hip, knee and ankle. They established that the ability to walk bipedally does not require specialist anatomy (though in the case of human bipedalism, where it has become the dominant form of locomotion there have been changes). Instead, apes in general, and bonobos in particular, show anatomical features that favour manoeuvrability and versatility, which allows them to relatively easily employ this mode of locomotion.

Raichlen et al. (2009) used ground reaction forces in chimpanzees to model the mechanics of hind limb weight support as demonstrated in primates (compared to most quadrupedal mammals which support the majority of their weight on their forelimbs). Their work has shown that chimpanzees support more weight on their hind limbs because they walk with a relatively protracted hindlimb, averaged over a step, and this reduces forces on the forelimb. This is likely to have allowed for the evolution of more mobile, less stable forelimb joints in primates, which in turn would have allowed for

our early ancestors to have initially undertaken an arboreal existence, and later may have been a prerequisite for bipedal locomotion.

In addition to suggestions as to how we may have become physically capable of bipedal locomotion, computer simulations have been used to model theoretical reasons as to why habitual and then obligate bipedality might have occurred in our lineage. Watson et al. (2008) have used comparisons of loaded and unloaded humans, Common chimpanzees (*Pan troglodytes*), Bonobos (*Pan paniscus*), Western lowland gorillas (*Gorilla gorilla gorilla*) and Bornean and Sumatran Orangutans (*Pongo pygmaeus* and *Pongo abelii*) to test if carrying a load (of, for example, food) may have been important in the development of habitual bipedalism.

These various techniques allow us to explore what was possible for fossil species, and even the parameters within which extant species function and are formed. They are a natural extension of comparative anatomy, and when used in conjunction with comparative anatomy can allow us to develop greater understanding of the capabilities of fossil species. They are however limited by the same constraints that apply to comparative anatomy, in that they are extrapolations from extant material, based on assumptions regarding fossil species. In addition, these techniques often require computers with extremely large processing power, and sometimes rely on simplified models. Furthermore, owing to the highly complex technical nature of computer analyses, I fear that some of these techniques are not subjected to the high level scrutiny of more traditional and well-known techniques within palaeoanthropology, and the results are open to misinterpretation.

1.4 Geometric Morphometrics

Palaeoanthropology as a field has always used the latest methods of analysis available. As Mafart et al. (2004:264) point out "Radiographic techniques have been used in palaeoanthropology and comparative anatomy since the discovery of x-rays, and each leap of medical imaging technology has been accompanied by new applications in both fields." It is therefore no surprise that this technology has been embraced so by the field. Of course, there are tremendous benefits to these methods in the study of fossils. The use of the variety of methods available to create 3D virtual objects aids the science of palaeoanthropology hugely. Fossil specimens are often extremely fragile, and repeated measurement can damage them, or at least, put them at greater

risk of being damaged. The creation of a virtual object on which measurements can be taken allows the opportunity to study a fossil to become much more widely available. Also, as fossil specimens are housed in museums across the world, these virtual objects can be shared relatively easily, encouraging a wide variety of people to study them, which can only be for the good of open science as it allows for wider access across the scientific community.

Slice (2005:5) defines Geometric Morphometrics as "the suite of methods for the acquisition, processing, and analysis of shape variables that retain *all* of the geometric information contained within the data". It encompasses the acquisition, processing, analysis, and display methods for the study of shape. Thus morphometrics is essentially the study of shape and its covariation with other variables (Bookstein, 1991, Dryden and Mardia 1998, Adams et al. 2004). It has formed a part of palaeoanthropology since its inception. Linear measurements and ratios have been the basis of comparative analysis between extant and fossil species, but these can only provide shape information within the specific boundaries of the measurements taken, failing to provide all of the geometric information, and perhaps neglecting unanticipated geometric relationships within the structure or specimens in question (Slice, 2005). With the advent of modern Geometric Morphometrics in the late 1980's and early 1990's, a change occurred in the way morphological structures were quantified and how the data were analysed, with technology allowing the study of shape to be elevated from traditional morphometrics and simple linear measurements to the complete analysis of shapes.

A further benefit is the option to undertake virtual reconstruction of fossil specimens. Previously, reconstruction would have to be undertaken, either on the fossil itself risking damage or alternatively through casts which may not be as accurate. Through virtual reconstruction, researchers are able to correct for distortion that may have occurred in the fossilisation process and experiment with a variety of alternate reconstructions relatively easily, allowing for more diverse interpretations.

The use of the techniques involved in Geometric Morphometrics on these virtual objects, allows for the manipulation of the object in virtual space but also allows for comparison of landmarks in relation to each other, giving perspective on the entire shape. As Zelditch et al. (2012) point out, individual measurements in Geometric

Morphometrics are not counted as traits or variables, but rather the complete difference in shape, with all landmark configurations becomes the variable. Coupled with this is the idea that none of the geometric information is lost in through the course of study and can be referred to, and returned to at either a later stage in the research or by others (Slice, 2005, 2007).

1.41 Structured light scanning

The first step within an analysis of Geometric Morphometrics is the initial creation of a virtual object. In order to do this, there are a variety of methods available, including CT scanning, microscribe data collection, laser scanning and structured light scanning to name but a few. This study utilises structured 3D light scanning, which is a non-contact, active optical scanner (Rocchini et al., 2001). This means that in order for a virtual object to be created, there need not be any contact between the scanner and the object (so there is less risk of damage), and that the scanner itself uses an emitter to project an illuminated pattern onto the object being scanned, and a sensor to detect the distorted pattern. Minor differences in the surface of the object being scanned are reflected in the linear pattern projected and in turn incorporated into the model. This method of creating a 3D object is extremely accurate, in this case to within approximately 30 μm (Weber and Bookstein, 2011) and also is non-invasive to the object being measured. There are, however, disadvantages to this technique as a structured light scanner will not scan reflective or transparent surfaces, although this is rarely a problem with fossil specimens.

Structured light scanning allows for only a surface model of an object to be created, in comparison to CT scanning which allows for the complete internal structure to be mapped also. The use of CT scanning is also non-invasive and allows for the collection of a great deal of data from a specimen. However, it is also expensive and requires that the objects be brought to the scanner as it is not a portable device.

Laser scanners are another non-invasive optical technology, and unlike CT scanners can be portable. However, like CT scanners, they can also be expensive, and depending on the model of scanner chosen, can be limiting on the size of the object you wish to scan. One of the great advantages of the structured light scanner, is that it

is relatively inexpensive, and in addition to this, it can be calibrated to scan objects of any size that you choose to calibrate for.

Microscribes unfortunately require the stylus to make contact with the object, which therefore involves the risk of damage. Additionally, unlike with structured light or CT scanning, the digital points which are captured are limited to where the researcher chooses, rather than the whole object.

1.42 Shape and Shape Space

To undertake a study of shape, one must first quantify exactly what shape is. It is something that we define intuitively, but it is difficult to describe exactly. Shape is defined (Kendall, 1977) not through what it is but rather what geometrical information is left when the location, scale and rotational effects are filtered from an object. As such, moving an object does not change its shape, nor does altering an object's size or orientation. In Geometric Morphometrics, we use techniques to remove these variables so that what remains is an analysis of the shape alone. The removed non-shape variables can then be factored in at a later stage when the results of the shape analysis are known, through conventional statistical analyses.

When non-shape variables are removed, the task is then to compare the shape data that remains. In order to do this, Geometric Morphometrics uses analysis of independent loci on the objects in question. These are known as landmarks, and are essentially the Cartesian coordinates of points on the object under study, and their relationships to each other are what form the basis of the analysis. In order to analyse shape independently, it must be removed from conventional space, as this is where the non-shape variables of location, size and orientation exist (Adams et al. 2004). This is achieved through Generalised Procrustes Analysis (Weber and Bookstein, 2011; Zelditch et al. 2012) (see Figure 1-1). This is then analysed in a constructed space without these variables, where shape alone can legitimately be compared. This 'shape space' (known as Kendall's Shape Space) provides a geometric setting for the comparison of landmark configurations across specimens (Kendall, 1977).

Figure 1-2: The Process of Procrustes Superimposition- removing size, location and orientation to compare shape
Taken from Klingenburg, (2015)

1.43 Landmarks and definitions

Distances in traditional morphometrics become replaced by configurations of coordinates in Geometric Morphometrics (Zelditch et al., 2012). When the coordinate data are collected on a number of specimens, they are referred to as corresponding landmarks. The reasons for this correspondence may be phylogenetic (these are sometimes called homologous points), structural, developmental, or biomechanical (Lele and Richtsmeier, 2001; Richtsmeier et al 2002). Corresponding landmarks should relate to each other in a biologically plausible way (O'Higgins, 2000). It is important to recognise, as Zelditch et al. (2012) point out, that landmarks are not shape variables in their own right. It is the configuration of all landmarks on the specimen that constitute the variable, as a single point does not satisfy a definition of shape. Nevertheless, these landmarks form the basis of shape analyses, and strict rules must be applied in their selection.

Characteristics of landmarks

There are some fundamental principles with regards to selecting landmarks (Zelditch et al. 2012). Importantly, landmarks must be homologous. This means that they must correspond between biological structures and be the same structure in all different

specimens. Landmarks cannot coincide- different landmarks must not be in the same place on any specimen under analysis, as this would imply that they are not homologous structures. Additionally, there must be adequate landmark coverage of an object, including in areas that are not the focus of study (Roth, 1993). This allows for unanticipated variation in shape to be studied and additionally allows the shape itself to be fully represented. Landmarks have to be reliably repeatable, and found on all objects under study, for if not, there is the risk of not comparing like with like and therefore making the foundations of the analysis unreliable. Furthermore, landmarks must not switch positions relative to each other, as this will skew the overall view of the shape.

Types of landmarks

Bookstein (1991) initially created definitions for three types of landmarks. These landmark classifications must satisfy the definitions above but have varying degrees of reliabilities within themselves.

Type I landmarks are those defined with respect to discrete juxtapositions of tissues, such as triple points of suture intersections. These are counted as the most reliable types of landmarks as they represent points which are supported by the strongest local evidence (O'Higgins, 2000)

Type II landmarks are curvature maxima associated with local structures usually with biomechanical implications. Type II landmarks include landmarks which are not homologous in a developmental or evolutionary sense but which share functionality (O'Higgins, 2000).

Type III landmarks are extremal points. These include start and end points of maximums such as length and breadth. They are defined with respect to a Type I or II landmark. As such, Type III landmarks are "deficient" in that they contain meaningful information only with respect to a remote defining structure (Slice, 2007). O'Higgins (2000) points out that most confidence can be placed in Type I landmarks and least in landmarks of Type III, and when using these types of landmarks there should be the expectation of greater variation due to error.

Semilandmarks

There are problems associated with the use of landmarks. This kind of data is not suitable for every type of investigation, but even for investigations in which landmark

data are appropriate, the Bookstein (1991) definitions are restrictive and can result in the removal of biologically meaningful information from the study.

With these landmark definitions, it is challenging to include information about curves and the surfaces between landmarks, as these correspond as whole structures rather than as distinct points (Gunz et al., 2005; Richtsmeier et al., 2002).

It is because of this that the notion of semilandmarks has been proposed (Gunz et al. 2005). This method maps structures known to correspond, using geometric curves. Each point on the curve is therefore not the corresponding structure, but rather, the entire selection of points on the curve represents the corresponding structure. The issue with this method arises from the fact that these points along a curve are still registered as Cartesian points in the analysis and the variation they show may be an indication of error in placement. When choosing semilandmarks, there must be some method in the selection of points that prevents them from being arbitrary, for instance ensuring that all points are equidistant, but this can still lead to inaccuracies. The concept of sliding semilandmarks attempts to address the arbitrary placement of these landmarks on curving structures by allowing these to 'slide' along directions of arbitrary variability (usually the tangent to the curve) to minimise either bending energy (the amount of non-uniform shape difference based on thin plate spline) or Procrustes distance (the sum of the squared distances between corresponding points) (Bookstein, 1997; Bookstein et al, 2002; Gunz et al. 2005, Slice 2007).

Since its beginning, palaeoanthropology has been dependent on comparison with extant species and the measurements available on fossil species to determine the phylogenetic relationships between ancestral and extant species. Linear measurements and ratios have been the backbone of the discipline, allowing us to make inferences for the behaviour and adaptations of fossil taxa, and ultimately, our own heritage. As the discipline of palaeoanthropology moves forward, however, it becomes increasingly important that the techniques we employ to extract the maximum information from a relatively sparse fossil record are enhanced. It is for this reason that palaeoanthropology is now becoming a digital subject where new techniques, such as 3D Geometric Morphometrics and simulation techniques, are being used to analyse our oldest ancestors. Although these techniques are used to tackle a variety of

questions regarding fossil hominoids, of particular interest to this study, are those that tackle questions relating to locomotion.

Australopithecines especially have been a focus of much of this research, and in particular, the largely complete skeleton of A.L. 288-1, an individual of the species *Australopithecus afarensis*- commonly known as Lucy. Australopithecines in general are very important, as they show clear bipedal traits but are near the origins of true terrestrial bipedalism in time. Further study into the locomotory styles of australopithecines serves to widen the picture of what was happening when our ancestors were becoming ground dwelling bipeds. Berge (1998) and Ward (2002) point out that various biomechanical studies of australopithecine bipedalism have suggested marked differences in the way in which australopithecines walked in comparison with modern humans. Their anatomy suggests that they perhaps moved with a waddling gait, involving large rotational movements of the pelvis and shoulders (Zihlman and Hunter, 1972; Berge, 1991, 1994; Rak, 1991). Others (Stern and Susman 1983, Susman et al. 1984, Hunt, 1994; Churchill et al., 2013; Da Silva e al. 2013) have demonstrated that the australopithecines are clearly adapted for exploitation of arboreal enviro^{nm}ents, particularly demonstrated in the morphology of the upper limb (McHenry & Berger, 1998; Green & Alemsegoed, 2012.)

Several studies have used computer simulation to assess the effectiveness of alternative gaits in *Australopithecus afarensis* (Kramer 1999; Sellers et al. 2003, 2004, 2005; Wang & Crompton 2004; Wang et al.2004 Nagano et al.2005; Crompton et al. 2010, 2012) and have demonstrated that Lucy could have been an energetically efficient biped.

A key problem regarding the determination of locomotory styles in fossil species is the paucity of information regarding musculature, as soft tissue information is rarely preserved in the fossil record. Although, through comparison to closely related extant species, we can sometimes infer some muscle attachment sites on the available osteology, a complete picture of the 'whole' can only be hypothesized. Equally, we can only hypothesize the effects such musculature would have had on the locomotory patterns that fossil species would be capable of.

To date, studies of fossil locomotion have largely focused on either comparisons of the bony morphology of the fossil species and extant species, or alternatively, on using

modelling and simulations based on either modern human or ape parameters to test hypotheses of their locomotory style. This study proposes a combined approach to the problem, using both Geometric Morphometrics to compare the bony elements, and forward dynamic modelling based on the results of the Geometric Morphometric analysis to propose a locomotory style.

In order to do this, a fundamental assumption must be made. This is that similarity in osteological shape equates to similarity in musculature (and conversely, that a difference in osteological shape equates to a difference in musculature). As the species under consideration are very closely related, and as their musculature does not vary hugely in the actual muscles within the lower limb, this is not an insurmountable problem (Ruff et al., 2006). A number of studies have demonstrated that closely related species display similarity in musculature and corresponding osteology. Scott, (1957) conducted a comprehensive review (at the time) of the impacts of muscle on bone, both through ontogeny, and in relation to sex and speciation. Ashton and Oxnard (1964) suggested that these similarities could be used to assess locomotor behaviours in fossil primates, through study of the fore- and hind-limbs of extant primates and the resultant impacts of their preferred locomotory pattern on the vertebral column. Oxnard (1967; 1968) then extended this work to focus on the primate and then mammalian shoulder girdle, looking particularly at the impacts of musculature on osteology in locomotion. Corruccini and Ciochon, (1976) undertook multivariate morphometric analyses of the primate shoulder girdle, and demonstrated that there was great similarity in myology and osteology within the extant apes, especially when allometry was accounted for. Further study on the *Papio* and *Maccaca* shoulder girdle by Kimes et al. (1981) emphasized that morphological study should by necessity be conducted on closely related groups as this would remove the possibility that structural differences observed were due to genetic or selective factors. This has become a fundamental principle in comparative anatomy and palaeoanthropological study.

This study aims to use 3D Geometric Morphometrics to explore the variability in the osteological shape in four key bones of the lower limb comprising the Os Coxa, the sacrum, the femur and the tibia across extant apes and modern humans, both between and within species groups. The affinity of the fossil specimen A.L. 288-1's osteological shape to the osteological shape of each species will then be assessed. Similarity in the shape of the bony morphology will then be used as a proxy for

similarity in muscle morphology and attachment. This information will then be translated into a hypothetical 3D muscular model for A.L. 288-1. This model will then be tested for reliability in a forward dynamic modelling program. The resultant locomotory style will then be compared to existing studies of locomotion in *Australopithecus afarensis*, to determine any commonalities.

It is hoped that this study will ultimately contribute to a greater understanding of locomotion in fossil species by establishing if this method could be used for future studies and other fossil species to assist in determining their locomotory styles.

1.5 Major aims and chapter structure

This study aims to use 3D Geometric Morphometrics to explore the variability in the osteological shape in four key bones of the lower limb comprising the Os Coxa, the sacrum, the femur and the tibia across extant apes and modern humans, both between and within species groups. The affinity of the fossil specimen A.L. 288-1's osteological shape to the osteological shape of each species will then be assessed. Similarity in the shape of the bony morphology will then be used as a proxy for similarity in muscle morphology and attachment. This information will then be translated into a hypothetical 3D muscular model for A.L. 288-1. This model will then be tested in a forward dynamic modelling program. The resultant locomotory style will then be compared to existing studies of locomotion in *Australopithecus afarensis*, to determine any commonalities.

As the focus of this study is to determine a theoretical muscular anatomy for a fossil species, and then to generate a functionally viable locomotory style using this hypothetical musculature, the methodology comprises two distinct parts. Initially, the musculature must be determined. This will be done using the comparative shape information obtained through Geometric Morphometric analyses. Chapter 2 outlines the materials and methods used to digitise the specimens, as well as the methods used in the Geometric Morphometric analysis. Chapter 3 then confirms the results of the Geometric morphometric study. The second phase of the project requires the use of this information in a forward dynamic modelling program and the testing of the theoretical musculature's viability for locomotion by the fossil specimen. This part of the study is explored in Chapter 4. Overall conclusions are presented in Chapter 5.

It is hoped that this study will ultimately contribute to a greater understanding of locomotion in fossil species by establishing if this method could be used for future studies and other fossil species to assist in determining their locomotory styles.

2. Materials and Methods of digitising

2.1 Materials

In order to conduct an analysis of shape in the fossil lower limb bones using Geometric Morphometrics, a comparative sample of ape bones was required. These needed to be similar enough in shape for a valid Geometric Morphometric analysis but also needed to represent the variation in species that practice a variety of locomotor techniques. As such, it was decided to use *Pan troglodytes* (chimpanzee), *Pan paniscus* (bonobo), *Gorilla gorilla* (Western Lowland gorilla), *Gorilla beringei* (Eastern Lowland gorilla), *Pongo pygmaeus* (orangutan) and *Homo sapiens* (human) for the comparative sample. These species share many morphological similarities and a close genetic relationship with the fossil species, *Australopithecus afarensis* (McHenry, 1978; Stern and Susman, 1983 etc.). Additionally, though each shares a repertoire of locomotor behaviours (Napier and Napier, 1985), they primarily practice differing locomotory styles (Prost, 1965; Rose 1973 etc; See Thorpe and Crompton, 2006 and Hunt, 2016 for comprehensive reviews). This means that, although apes are morphologically similar, there are enough differences in their morphology due these differing locomotory styles to make such an analysis both possible and worthwhile. *Australopithecus afarensis* has been shown to be bipedal (McHenry, 1974; McHenry 1978; Susman et al, 1984; Lovejoy, 1988, Rak, 1991; Berge, 1991; Berge, 1994; Crompton et al 2012, Nagano et al., 2005 etc.), but there is a great deal of debate as to the nature of this bipedalism (see Vaughn, 2003 for a review). It was decided to focus on the lower limb in this analysis, owing to its primary importance in bipedal locomotion. As such, the bones under study comprise the femur, tibia, and pelvic girdle (including Os Coxa and sacrum).

2.11 The collections

All specimens used were from dry bone skeletal collections. Specimens were chosen on the basis of having an example of each skeletal element required were possible, and where this was not possible, they were chosen on the basis of having the majority of elements required. All specimens were adult (classified as those with M_3 erupted for the purposes of this study). Where possible right hand elements were scanned, although occasionally, left hand elements were used where the right hand elements were either missing or badly damaged. Where left sided bones were used, the scans

were mirrored so as to be directly comparable with the majority of the specimens. This is because it is of primary importance when conducting a shape analysis using Geometric Morphometric techniques that one is comparing like with like and so it is a necessity that all the elements are from the same side (or at least, appear to be when the Geometric Morphometric analysis is conducted). Occasionally, elements were unavailable for a particular specimen (although this was only the case for 5 bones across the total of 312 possible). Only largely undamaged bones were used for the comparative analysis.

Several institutions provided the skeletal material under study. Visits to each collection were approximately a week long, and scans of each collection were taken in a single trip to each institution. The only exception to this was the data collection undertaken at the Natural History Museum in London, where two trips were taken due to equipment problems. Approximately 8-10 individuals could usually be scanned in a day, although this was variable depending on the condition of the osteological specimens, the ease of access to the specimens and the temperamental nature of the structured light scanner.

The specimens from the Powell-Cotton Museum, in Birchington, Kent, were collected by Major Percival Powell-Cotton during the period 1887 to 1939, and all were wild shot. The specimens from The Royal Museum for Central Africa in Tervuren, Belgium were all wild shot individuals from the Democratic Republic of Congo and collected in the early half of the 20th Century. The specimens from the University of Sheffield's osteological collections comprised individuals from the Barbican Collection, and the Carver Street Methodist Chapel collection and a single individual from the Black Gate Cemetery (BG170). Additionally, 2 known sex teaching skeletons were used (hereafter called Shef 1 and Shef 2). The individuals in the Barbican Collection derived from the site of All Saint's Church, Fishergate in York (a multi-period site with burials dating from the 11th-14th centuries B.C.) and the specimens are archaeological in nature (Bruce 2003; Bruce and McIntyre 2009). Those from the Carver Street collection derived from individuals excavated from the c.19th century Carver Street Methodist Chapel burial ground in Sheffield (McIntyre and Wilmott, 2003). These skeletons had been previously analysed by McIntyre using standard sex estimation techniques for the pelvis and cranium to determine their sex. The individual from the Black Gate derives from excavations conducted on the Black Gate Cemetery, Newcastle-Upon-Tyne, and archaeological site dating from the 8th-12th centuries,

between the 1980 and 1982 seasons (Swales, D. 2012). The *Pan troglodytes* sample was obtained in entirety from the Powell-Cotton collection. It comprised 10 male and 10 female individuals. Full details of the *Pan troglodytes* sample, including the specimens used, sex and the elements available for each specimen can be found in Table 2-1.

Table 2-1: The *Pan troglodytes* sample

Species	Specimen	Sex	Institution	sacrum	Os Coxa	femur	tibia
Pan troglodytes	m650	F	Powell-Cotton Museum	•	•	•	•
Pan troglodytes	m655	F	Powell-Cotton Museum	•	*	•	•
Pan troglodytes	m676	F	Powell-Cotton Museum	•	•	•	•
Pan troglodytes	m677	F	Powell-Cotton Museum	•	•	•	*
Pan troglodytes	m745	F	Powell-Cotton Museum	•	*	•	•
Pan troglodytes	m789	F	Powell-Cotton Museum	•	•	•	•
Pan troglodytes	m800	F	Powell-Cotton Museum	•	-	•	•
Pan troglodytes	m873	F	Powell-Cotton Museum	•	•	*	•
Pan troglodytes	m967	F	Powell-Cotton Museum	•	*	•	•
Pan troglodytes	m986	F	Powell-Cotton Museum	-	*	•	*
Pan troglodytes	cami206	M	Powell-Cotton Museum	•	•	•	•
Pan troglodytes	m254	M	Powell-Cotton Museum	•	•	*	*
Pan troglodytes	m272	M	Powell-Cotton Museum	•	*	•	•
Pan troglodytes	m347	M	Powell-Cotton Museum	•	*	*	*
Pan troglodytes	m401	M	Powell-Cotton Museum	-	*	•	•
Pan troglodytes	m440	M	Powell-Cotton Museum	•	*	•	*
Pan troglodytes	m712	M	Powell-Cotton Museum	•	*	*	*
Pan troglodytes	m724	M	Powell-Cotton Museum	•	•	•	•
Pan troglodytes	m984	M	Powell-Cotton Museum	•	*	•	*
Pan troglodytes	m998	M	Powell-Cotton Museum	•	*	*	•

• Indicates right hand element used; * indicates left hand element used; - indicates element unavailable

The gorilla sample (*Gorilla gorilla* and *Gorilla beringei)* was obtained from both the Powell-Cotton Museum (10 female and 3 male, all *Gorilla gorilla*) and the Royal Museum for Central Africa in Belgium (5 male, all *Gorilla beringei*). Full details of the *Gorilla* sample, including the specimens used, sex and the elements available for each specimen can be found in Table 2-2. The Royal Museum for Central Africa also supplied the sample of *Pan paniscus* (8 male and 9 female). Full details of the *Pan paniscus* sample, including the specimens used, sex and the elements available for each specimen can be found in Table 2-3.

Table 2-2: The *Gorilla sp.* sample

Species	Specimen	Sex	Institution	sacrum	Os Coxa	femur	tibia
Gorilla gorilla	m89	F	Powell-Cotton Museum	•	•	•	•
Gorilla gorilla	m96	F	Powell-Cotton Museum	•	•	•	•
Gorilla gorilla	m136	F	Powell-Cotton Museum	-	*	•	•
Gorilla gorilla	m150	F	Powell-Cotton Museum	•	•	•	•
Gorilla gorilla	m470	F	Powell-Cotton Museum	•	*	•	•
Gorilla gorilla	m856	F	Powell-Cotton Museum	•	•	•	•
Gorilla gorilla	mc95	F	Powell-Cotton Museum	•	•	•	•
Gorilla gorilla	mc174	F	Powell-Cotton Museum	•	•	•	•
Gorilla gorilla	mc799	F	Powell-Cotton Museum	•	•	•	•
Gorilla gorilla	mc878	F	Powell-Cotton Museum	•	•	•	•
Gorilla beringei	RMCA 994	M	Royal Museum of Central Africa	•	•	•	•
Gorilla beringei	RMCA 998	M	Royal Museum of Central Africa	-	•	•	•
Gorilla beringei	RMCA 999	M	Royal Museum of Central Africa	•	*	•	•
Gorilla beringei	RMCA 1001	M	Royal Museum of Central Africa	•	*	•	•
Gorilla beringei	RMCA 18739	M	Royal Museum of Central Africa	•	•	•	•
Gorilla gorilla	m879	M	Powell-Cotton Museum	•	*	•	•
Gorilla gorilla	mc206	M	Powell-Cotton Museum	•	•	•	•
Gorilla gorilla	mc717	M	Powell-Cotton Museum	•	*	•	•

• Indicates right hand element used; * indicates left hand element used; - indicates element unavailable

Table 2-3: The *Pan paniscus* sample

Species	Specimen	Sex	Institution	sacrum	Os Coxa	femur	tibia
Pan paniscus	13201	F	Royal Museum for Central Africa	•	•	•	•
Pan paniscus	15293	F	Royal Museum for Central Africa	•	•	•	•
Pan paniscus	15296	F	Royal Museum for Central Africa	•	•	•	•
Pan paniscus	27698	F	Royal Museum for Central Africa	•	•	•	•
Pan paniscus	29035	F	Royal Museum for Central Africa	•	•	•	•
Pan paniscus	29040	F	Royal Museum for Central Africa	•	•	•	•
Pan paniscus	29042	F	Royal Museum for Central Africa	•	•	*	*
Pan paniscus	29045	F	Royal Museum for Central Africa	•	•	•	•
Pan paniscus	84036m2	F	Royal Museum for Central Africa	•	•	•	•
Pan paniscus	13202	M	Royal Museum for Central Africa	•	•	*	*
Pan paniscus	15294	M	Royal Museum for Central Africa	•	•	•	•
Pan paniscus	15295	M	Royal Museum for Central Africa	•	•	•	•
Pan paniscus	27696	M	Royal Museum for Central Africa	•	•	•	•
Pan paniscus	27699	M	Royal Museum for Central Africa	•	*	•	•
Pan paniscus	29044	M	Royal Museum for Central Africa	•	•	•	•
Pan paniscus	29047	M	Royal Museum for Central Africa	•	•	•	•
Pan paniscus	29063	M	Royal Museum for Central Africa	•	*	•	•

• Indicates right hand element used; * indicates left hand element used; - indicates element unavailable

The *Pongo pygmaeus* sample was obtained from the Natural History Museum in London and comprised 7 male individuals. A wider sample of orang-utans would have been preferred, but unfortunately equipment problems prevented the collection of a larger sample in this species. Full details of the *Pongo pygmaeus* sample, including the specimens used, sex and the elements available for each specimen can be found in Table 2-4.

Table 2-2-4: The *Pongo pymaeus* Sample

Species	Specimen	Sex	Institution	sacrum	Os Coxa	femur	tibia
Pongo pygmaeus	1948992	M	Natural History Museum	•	•	•	•
Pongo pygmaeus	1976438	M	Natural History Museum	•	•	•	•
Pongo pygmaeus	18592102	M	Natural History Museum	•	*	•	•
Pongo pygmaeus	19731570	M	Natural History Museum	•	•	•	•
Pongo pygmaeus	19861114	M	Natural History Museum	•	•	•	•
Pongo pygmaeus	184510213a	M	Natural History Museum	•	*	•	•
Pongo pygmaeus	198610923c	M	Natural History Museum	•	•	•	•

• Indicates right hand element used; * indicates left hand element used; - indicates element unavailable

The human sample was acquired from the Barbican and Carver St collections at the University of Sheffield (7 male and 8 female). Full details of the *Homo sapiens* sample, including the specimens used, sex and the elements available for each specimen can be found in Table 2-5.

Table 2-5 The *Homo sapiens* sample

Species	Specimen	Sex	Institution	sacrum	Os Coxa	femur	tibia
Homo sapiens	bg170	F	University of Sheffield	•	•	•	•
Homo sapiens	shef1	F	University of Sheffield	•	*	*	*
Homo sapiens	shef2	F	University of Sheffield	•	•	•	•
Homo sapiens	sk203	F	University of Sheffield	•	•	•	•
Homo sapiens	sk302	F	University of Sheffield	•	*	*	*
Homo sapiens	sk947	F	University of Sheffield	-	•	•	*
Homo sapiens	sk974	F	University of Sheffield	•	•	•	•
Homo sapiens	y3743	F	University of Sheffield	•	*	•	-
Homo sapiens	sk1114	M	University of Sheffield	•	•	•	*
Homo sapiens	y2407	M	University of Sheffield	-	•	*	•
Homo sapiens	y2846	M	University of Sheffield	•	•	•	•
Homo sapiens	y2911	M	University of Sheffield	•	•	*	*
Homo sapiens	y3130	M	University of Sheffield	•	*	*	•
Homo sapiens	y3290	M	University of Sheffield	-	•	•	•
Homo sapiens	y3557	M	University of Sheffield	•	*	•	•

• Indicates right hand element used; * indicates left hand element used; - indicates element unavailable

2.12 The Fossil Specimen- A.L. 288-1

The fossil species under analysis is *Australopithecus afarensis*. As such, the relatively complete specimen A.L. 288-1 ('Lucy') (Johanson and Taieb, 1976) was used. Analysis was conducted on a high quality resinous cast held by the University of Sheffield.

2.2 Geometric Morphometrics

2.21 Digitisation of the specimens

The scans themselves were obtained using a custom built three dimensional structured light scanner comprising two Cannon light sensors and a standard high definition projector mounted upon a rigid frame, and interfaced with a computer. A software package (Flexscan 3D3 (2013, Copyright LMI Technologies)) was then used in order to digitise the osteological specimens. This package enables the projector to generate a sequence of reference patterns onto the surface of the specimen using white light. These patterns are distorted by the object's surface, and a series of pictures are taken by the two uEye (UI-1540LE) camera sensors. These cameras have a resolution of 1280x1024 pixels (1.3 megapixels), and a pixel size of 5.2µm. The software then translates the observed distortion into the object's depth and surface information. It then uses this information to create a three dimensional image of the original object using mesh geometry. This process is automated to a degree by the use of a rotary table which allows for the capture of several scans in sequence. These individual scans are then combined to create a single three dimensional digital object, using overlapping geometry.

The scanning unit was calibrated using 17mm calibration board owing to the size of the specimens. Calibration provides the software with a series of reference images which allow it to determine accurate size and shape information for the scanning area, and subsequently the specimens that are scanned. This in turn allows for accurate digital reproduction of the specimens, to approximately 30 µm.

The samples were positioned in front of the projector, and in the centre of the field of view of the two camera sensors, with a dark background to remove 'artefacts' created by additional objects. To complete a scan of the object, each surface must be presented to the sensors in turn, and then the scans of each surface be knitted together using the software. This 'knitting' process is largely automated, but does occasionally require

manual intervention, especially where there is not enough unique geometry (eg: flat surfaces), for the software to recognise.

There are, however, limitations to this type of scanning. In the first instance, the sensors will not detect surfaces that are too dark or alternately too shiny. Fortunately, the osteological specimens used were neither, although some areas (particularly holes, or where trabecular bone was exposed on the specimens) were more difficult to fully capture, resulting in areas of missing information.

2.22 Post-scan Processing

When the scanning process was complete the scans were then exported into a further software program, Geomagic Wrap 12 OEM (Geomagic, Incorporated, 2010). This program allows for small holes in the scans to be filled based on the surrounding geometry and allows the scans to be 'whole' for further analysis (Figure 2-1). This process was necessarily time consuming as accuracy in the filling of any holes was required. No hole greater than 5mm was considered acceptable to fill, and great care had to be taken to ensure that such holes did not occur during the initial scanning process. Additionally, holes in key areas where not accepted as these could have impacted the accuracy of future analyses on the scans by introducing the potential for error. As such, the time taken to repair the scans varied according to how much information was not captured in the original scan, but on average approximately 10 scans could be processed a day.

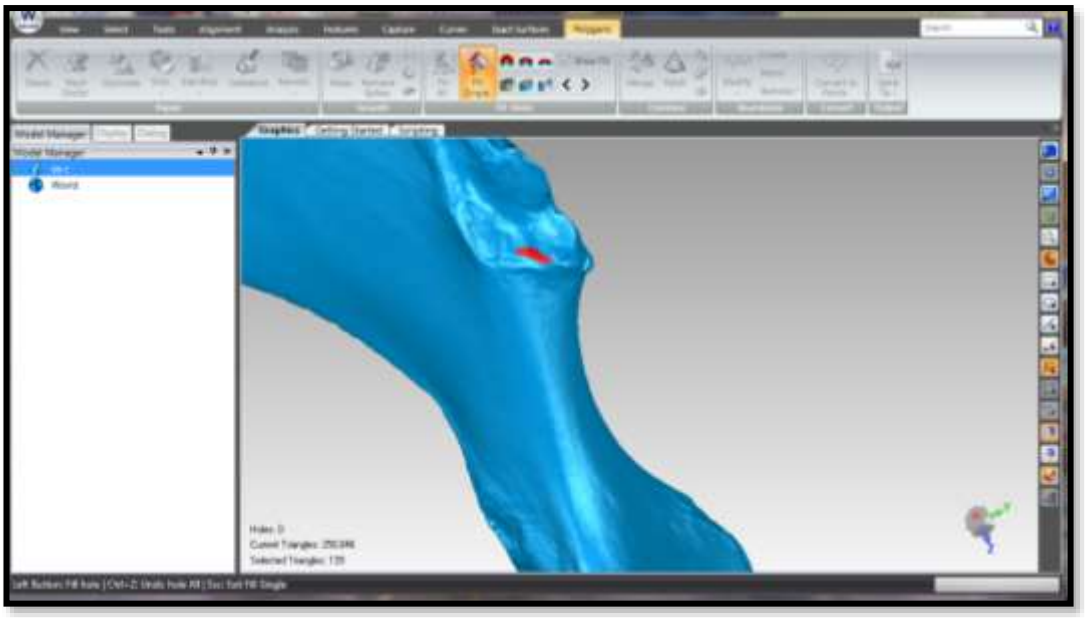

Figure 2-1: Hole filling in Geomagic Wrap

It is also in Geomagic Wrap 12 OEM where the mirroring of left hand side bones for Geometric Morphometric analysis was achieved. The scans were also decimated in Geomagic Wrap 12 OEM (Figure 2-2). This is a data reduction technique used to make the scans (now 3D objects) more compatible with the other computer programs used in later analysis. It was necessary to reduce the size of the 3D objects as the scanning process creates very large files, particularly due to the overlapping geometry data. Decimation reduces the polygon count of the 3D object with a minimal reduction in actual surface data, certainly with no discernible impact given the size of the features being used in the geometric morphometric analysis where accuracy of 30µ is excessive.

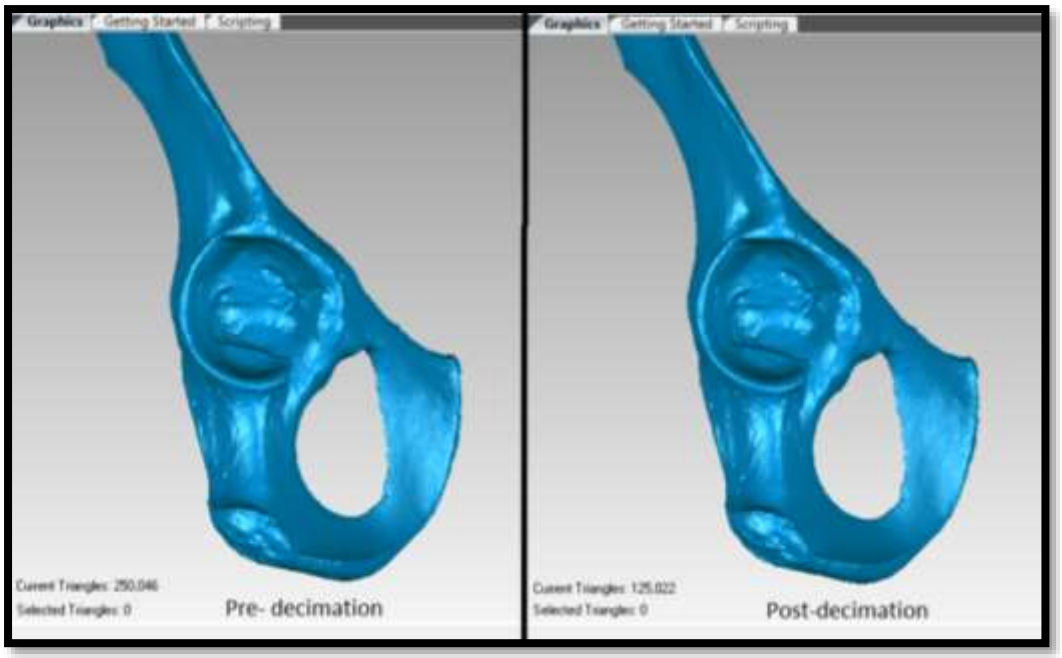

Figure 2-2: Decimation by 50% in Geomagic Wrap

2.3 Reconstruction

2.31 The reconstruction of the femur of A.L 288-1

The femur of A.L 288-1 was in several pieces. The damage on the femur was primarily concentrated on the distal end. There was a break in the femoral shaft about three-quarters down the length, and significant distortion and breakage on the femoral condyles.

The reconstruction was based on the work undertaken by Sylvester *et al.* (2008). They were able to use scans of A.L 129-1a, a distal femur attributed to *A. afarensis*, to complete the reconstruction of Lucy's femur. Unfortunately, as I did not have access to this specimen, I was unable to follow their method exactly, but instead used it as a basis for my own reconstruction.

Using the help of Mr Timothy Lister (BA), an independent 3D modeller, we were able to build the specimen's distal femur by modifying the distal femur of a *Pan paniscus*, in line with the distal femur of A.L129-1a, and combining this with what we had of Lucy's femur (Figure 2-3). This was undertaken in Maya (3D modelling software) (Autodesk, 2015). A *Pan paniscus* femur was chosen as it was decided that it required the least modification, but in truth any species could have been used as we were manipulating its shape in the software to match A.L129-1a.

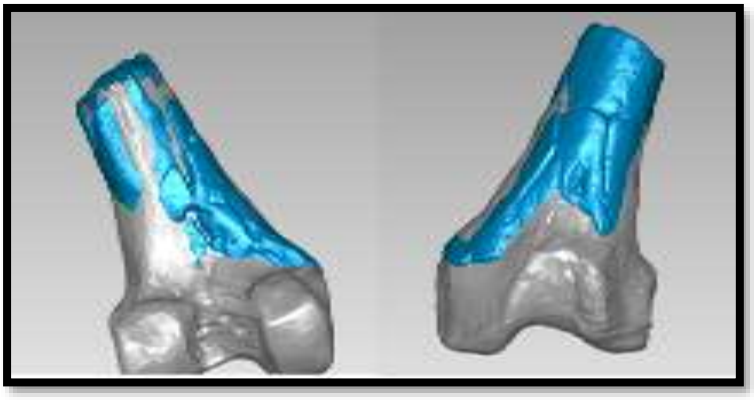

Figure 2-3: Reconstruction of the distal end of the femur of A.L. 288-1

When the modified distal end was attached to the proximal shaft (Figure 2-4), the linea aspera aligned perfectly on the reconstruction and the specimen, which came to light when the curves for the sliding semilandmarks were applied using the topographic modelling tool in Geomagic Wrap 12 OEM.

There have been a number of estimates as to the length of Lucy's femur (Johanson and Taieb, 1976; Johanson et al. 1976; Johanson et al., 1982; Jungers, 1982; Schmid, 1983)

clustering between 278 and 280mm. The reconstruction we undertook measured 279.086mm in length indicating that there is some merit to this method.

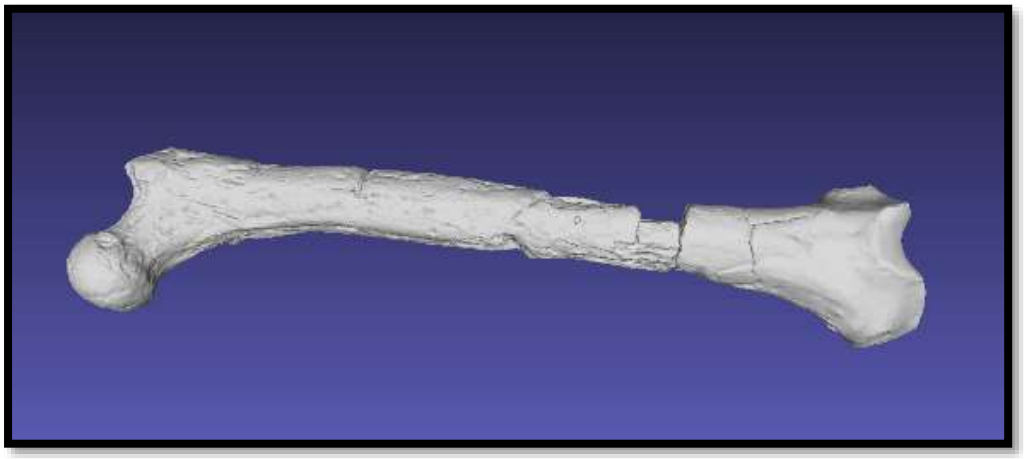

Figure 2-4: Reconstruction of full femur of A.L. 288-1

2.32 The reconstruction of the tibia of A.L. 288-1

The tibia of A.L. 288-1 was broken and the middle part of the shaft was missing. The proximal and distal ends were, however, fairly well preserved. To reconstruct the tibia, I modelled the shaft between the proximal and distal ends, following the estimated length of 241mm proposed by Schmidt (1983) (Figure 2-5). The length of the reconstruction in this study was 240.67mm.

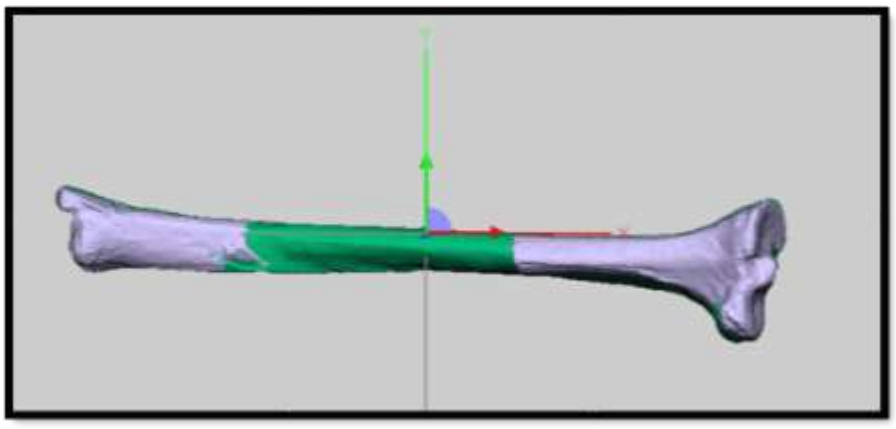

Figure 2-5: Reconstruction of the Tibia of A.L. 288-1
*Reconstruction shown in green

2.4 Landmark choice

Landmarks were chosen in line with the categorisations laid out in Bookstein (1991) for Type I, II and III Landmarks. Type I landmarks are those defined with respect to discrete juxtapositions of tissues, such as triple points of suture intersections. These are counted as the most reliable types of landmarks as they represent points which are supported by the strongest local evidence (O'Higgins, 2000). Type II landmarks are curvature maxima associated with local structures usually with biomechanical implications. Type II landmarks include landmarks which are not homologous in a developmental or evolutionary sense but which share functionality (O'Higgins, 2000). Type III landmarks are extremal points (points at the extreme ends of structures).

Landmarks were also selected using the criteria laid out in Zelditch et al. (2012). As such, all landmarks used across all specimens under study had to be determined to be homologous, meaning they correspond between biological structures and are the same structure in all different specimens. Additionally, none of the landmarks on a single specimen could coincide- no two landmarks are in the same place on any specimen under analysis in this study, as this would imply that they are not homologous structures. Furthermore, some landmarks were included despite not having a direct bearing on the study question, as suggested by Roth (1993). This was to ensure adequate landmark coverage and allow for the shape itself to be fully represented.

In addition to these true Landmarks, semilandmarks on curves were included in order to include information about curves and the surfaces between landmarks, as these correspond as whole structures rather than as distinct points (Gunz et al 2005; Richtsmeier et al 2002). These were chosen as lines of maximum curvature along particular structures of interest. In order to minimise error, the curved semilandmarks have been used in conjunction with true landmarks as these are fixed points. Additionally, in order to prevent the placement of each semilandmark within the curve from being arbitrary, sliding semilandmarks were used. The semilandmarks along the curves were allowed 'slide' along directions of arbitrary variability (usually the tangent to the curve) to minimise bending energy (Bookstein, 1997; Bookstein et al, 2002; Gunz et al. 2005, Slice 2007). A full description of all landmarks used for each bone can be found in Chapter 3.

2.41 Digitisation of Landmarks

Landmarks on each of the bones under study were digitised within two separate computer programs. Geomagic Wrap 12 OEM (Geomagic, Inc., 2010) was used to create the curves along which the sliding semilandmarks were to be added. The curves were drawn along lines of maximum curvature using a topographic shading tool within Geomagic Wrap 12 OEM (Geomagic, Inc. 2010). This allowed for accurate and repeatable determination of curved surfaces. The curves were always digitised in the same manner as each curve produced is made up of a series of discrete Cartesian points, which were then treated as homologous across specimens in further Geometric Morphometric analyses. See Figure 2-6 for an illustration of the digitisation of a curve in Geomagic Wrap 12 OEM.

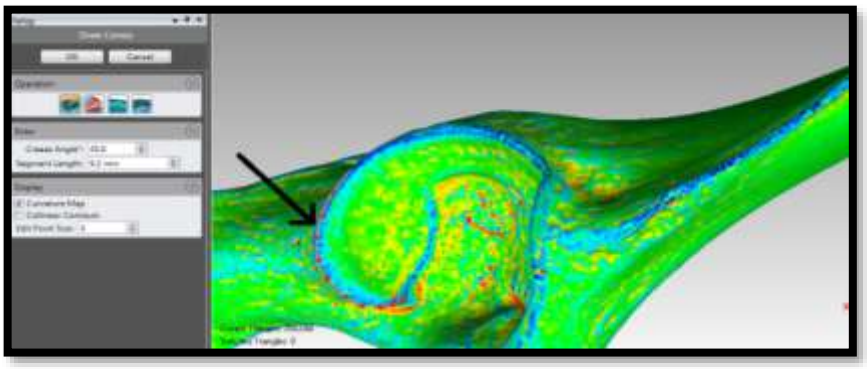

Figure 2-6 Drawing a curve in Geomagic Wrap

This curve data was then exported into Evan Toolbox (Phillips et al. 2010) and combined with the Landmark data for Geometric Morphometric analysis (Figures 2-7 and 2-8). Semilandmarks were digitised along the curves and then these semilandmarks were ‘slid’ along the curves using the warp and slide options within the program.

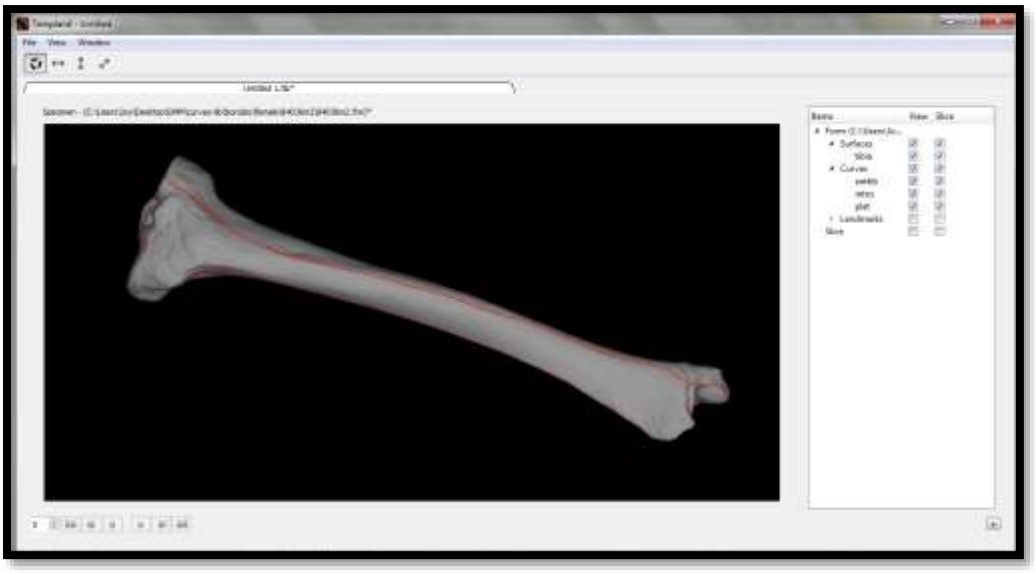

Figure 2-7: Evan Toolbox showing the curves imported from Geomagic

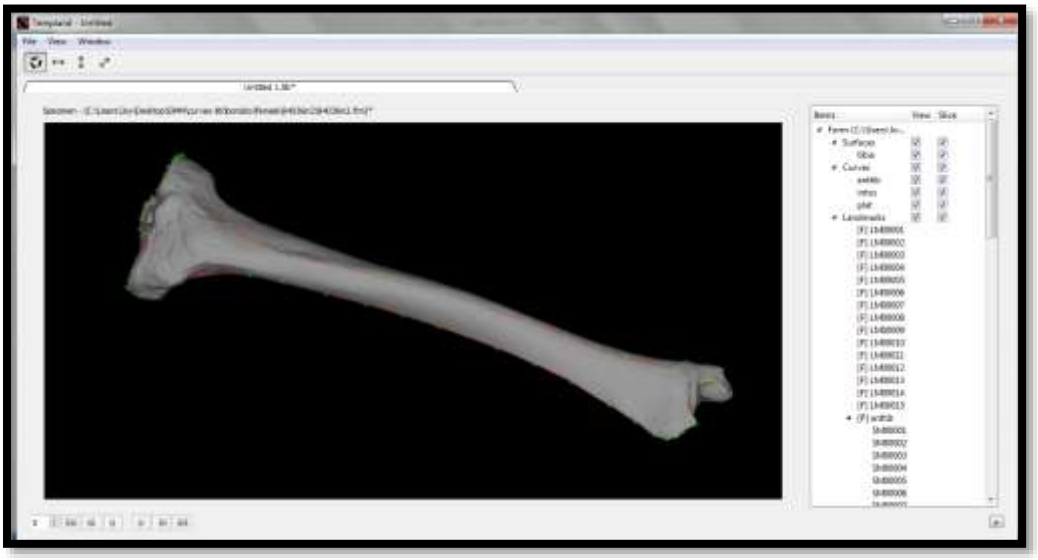

Figure 2-8: Evan Toolbox showing Landmarks and Semilandmarks on curves

2.42 Statistical methods

Geometric Morphometrics is primarily concerned with the study of shape and how this co-varies with other variables (Bookstein, 1991, Dryden and Mardia 1998, Adams et al. 2004). In order to isolate the variable of 'shape', the location, scale and rotational effects must be filtered from the specimens in question (Kendall, 1977).

As such, a Generalised Procrustes Analysis (GPA) was undertaken on the landmarks of the *Os Coxa*, femur, tibia and sacrum using Evan Toolbox (Phillips et al., 2010) on all specimens.

Through this process shape information was obtained by moving the landmark configurations on the specimens to a common position and scaling them to a standard centroid size. These were then rotated against each other until the 'best fit' of corresponding landmarks between specimens was achieved by achieving the minimal sum of squared distances between corresponding landmarks (Gower 1975; Rohlf and Slice 1990).

Shape differences among landmark and semilandmark configurations were measured by Procrustes distance. This is the Pythagorean distance between the two Procrustes superimposed landmark configurations (Bookstein, 1991, Weber and Bookstein, 2011), and is a measure of how closely related in location each landmark is to it homologous landmarks across specimens.

This process was then repeated for each individual species group, with the fossil species included.

A Principle Components Analysis (PCA) was then undertaken on the configuration of landmarks and semilandmarks of the skeletal elements across species as a data exploration exercise to both reduce the dimensionality of data and to visualize the main axes of variation (Dryden and Mardia 1998; Slice 2005, 2007) using the Procrustes coordinates. Visualization of these shape differences along principal components axes was achieved with the use of the EVAN toolbox (Philips et al 2010).

Between groups PCAs were also run taking into account both sex and species to assess whether these factors are informative in determining the differences in the shape of each of the skeletal elements.

Testing for normality in with Landmark data can be problematic, as the data are made of a series of 3D coordinates. As such, the Principle Components of each species and sex were tested for normality using a Shapiro-Wilk test (Shapiro and Wilk, 1965) for each landmark combination.

The Shapiro-Wilk test was chosen due to the small sample sizes used in this study. If the significance value of the Shapiro-Wilk Test is greater than 0.05, the data are normal. If it is below 0.05, the data significantly deviate from a normal distribution.

An Analysis of Variance (ANOVA) (Klingenberg & McIntyre 1998; Klingenberg et al. 2002) was then conducted within MorphoJ to determine if there was a statistically significant difference between the species groups, and where possible to determine if there was a significant difference between the sexes within species. This was also done for each landmark combination under study.

The results of the Principle Components Analyses were then used as a basis to hypothesize the thigh musculature of the fossil specimen. Where affinity in the shape of the skeletal element was observed, a similarity in musculature was inferred. This was repeated for each group of landmarks, including the complete landmark set (with landmarks and all semilandmarks) bone for each as well as for each semilandmark and landmark set individually (see Table 3-13 for associations of landmarks and semilandmarks with musculature). This was deemed valid given that the species in question are so closely related, and the differences in musculature are not extensive, but are potentially significant as the species practice very different forms of primary locomotion (Myatt *et al*. 2011). The arrangement and features of the musculature between the extant species vary in location of attachments, and the features of the muscle architecture such as fascicle length and physiological cross-sectional area (PCSA) (Payne *et al*. 2006). These differences were then used in the construction of the forward dynamic model.

Table 2-6: Muscles and Associated Landmarks and Semilandmarks

Muscle	Origin bone	Associated Landmarks	Insertion bone	Associated Landmarks
Adductor brevis	Os Coxa	15	Femur	SL 3
Adductor longus	Os Coxa	14	Femur	SL 3
Adductor magnus	Os Coxa	15, 9, SL 6	Femur	SL 3
Adductor magnus (Ham)	Os Coxa	SL6	Femur	SL 4
Biceps Femoris LH	Os Coxa	SL 6	Fibula	N/A
Biceps Femoris SH	Femur	SL 3	Fibula	N/A
Extensor Digitorum Brevis	Foot	N/A	Foot	N/A
Extensor Digitorum Longus	Tibia	-	Foot	N/A
Extensor Hallucis Brevis	Foot	N/A	Foot	N/A
Extensor Hallucis Longus	Fibula	N/A	Foot	N/A
Fibularis brevis	Fibula	N/A	Foot	N/A
Fibularis longus	Fibula	N/A	Foot	N/A
Fibularis tertius	Fibula	N/A	Foot	N/A
Flexor Digitorum Longus	Tibia	-	Foot	N/A
Flexor Hallucis Longus	Fibula	N/A	Foot	N/A
Gamellus inferior	Os Coxa	SL 6	Femur	SL 2
Gamellus superior	Os Coxa	18	Femur	SL 2
Gastrocnemius	Femur	SL 4	Foot	N/A
Gastrocnemius	Femur	SL 4	Foot	N/A
Gluteus Maximus	Os Coxa	SL 5	Femur	SL 2
Gluteus Maximus	Sacrum	All	Femur	SL 2
Gluteus Medius	Os Coxa	-	Femur	SL 2
Gluteus Minimus	Os Coxa	-	Femur	SL 2
Gracilis	Os Coxa	15	Tibia	5
Iliopsoas	Os Coxa	-	Femur	SL 2/ 10 11
Obturator externus	Os Coxa	16-19	Femur	SL 2
Obturator internus	Os Coxa	16-19	Femur	SL 2
Pectineus	Os Coxa	14	Femur	10 11
Piriformis	Sacrum	All	Femur	SL 2
Plantaris	Femur	SL 4 ?	Foot	N/A
Popliteus	Femur	SL 4	Tibia	
Quadratus femoris	Os Coxa	SL 6	Femur	SL 2
Rectus femoris	Os Coxa	SL 1, 3	Tibia	8
Sartorius	Os Coxa	2	Tibia	6
Semimembranosis	Os Coxa	SL 6	Tibia	6
Semitendinosis	Os Coxa	SL 6	Tibia	6
Soleus	Tibia	-	Foot	N/A
Tensor facia latae	Os Coxa	1,2	Tibia	6
Tibialis anterior	Tibia	SL 2	Foot	N/A
Tibilais posterior	Tibia	SL 3	Foot	N/A
Vastus Intermedius	Femur	SL 3	Tibia	8
Vastus Lateralis	Femur	SL 3	Tibia	8
Vastus Medialis	Femur	Shaft	Tibia	8

3. Geometric Morphometrics

The Geometric Morphometric analyses were conducted to explore the nature of the variation of shape between the extant groups, and also to determine which groups the australopithecine specimen was most closely aligned to, in terms of skeletal morphology. As such, various Geometric Morphometric techniques were used on each bone under study. A Generalised Procrustes Analysis was conducted initially. This was of primary importance as it removed the information not related to shape- it disregarded size, moved the sets of coordinates into alignment and rotated the sets of coordinates to the closest fit with each other, meaning that the comparison was solely of shape. This then formed the basis for further study regarding the shape of each bone. This exploration was conducted using a Principal Components Analysis, focussing on the overall shape of the bone across each species and for each sex, and then on specific areas of muscular importance, to determine how this may vary between the species. To ensure the robusticity of these results, ANOVA were conducted to confirm the results.

3.1 The Os Coxa

3.11 Definitions of the Landmarks of the Os Coxa

Landmarks of the Os Coxa

The Os Coxa is particularly difficult to define in terms of Type 1 or Type 2 landmarks (Bookstein, 1991). In adults, it lacks the sutures and discrete points that these landmark types require (Lewton, 2010). However, there are some points available (such as the anterior superior iliac spine) which are discrete, and from these, further landmarks can be devised. This study uses a combination of landmarks and curved semi-landmarks to fully define the shape of the Os Coxa. An illustration of the 'true' landmarks used can be seen in Figure 3-1, and their full definitions can be seen in Table 3-1. In total, 19 true landmarks were used, 13 of which were Type 2, and 6 of which were Type 3. No Type 1 landmarks were available.

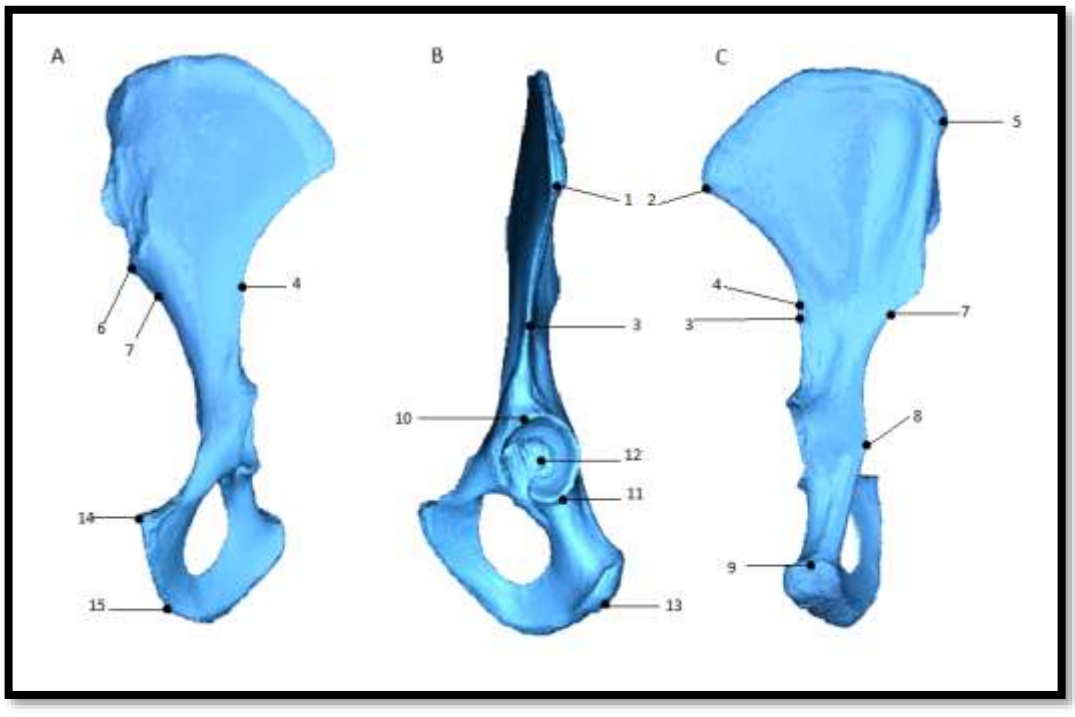

Figure 3-1: Anterior (A), Lateral (B) and Posterior (C) views of an Os Coxa depicting the 'true' landmarks used in this study
Semi-landmarks are shown in Fig. 3-2. Some of the landmarks are shown in multiple views. Full landmarks definitions can be found in Table 3-1.

Table 3-1:Three-Dimensional Landmarks of the Os Coxa

No.	Landmark	Definition	Type [a]
1	Lateral extent of the iliac crest	The most lateral extent of the iliac crest. In most cases, the same as ASIS	II
2	Anterior Superior Iliac Spine (ASIS)	The most anterior point of the iliac crest (ASIS)	II
3	Anterior Inferior Iliac Spine (AIIS)	The most anterior point on the AIIS. If only a bony roughening it is the centre of the AIIS rugosity	II
4	Lateral Ilium	The most lateral point on the lateral aspect of the iliac margin, above the AIIS, where the cross-section of the lower ilium is smallest	III
5	Posterior Superior Iliac Spine (PSIS)	The superomost medial point on the posterior iliac crest	II
6	Inferior extent of the auricular surface	The most inferior extent of the auricular surface, on the dorsal aspect of the Os Coxa	II
7	Dorsal ilium	The most dorsal point on the dorsal aspect of the lower ilium, where the cross-section of the lower ilium is smallest. Taken directly across from Landmark 4	III
8	Ischial Spine	The most dorsal projection of the spine located on the posterior ischium, medial to the acetabulum	II
9	Ischial tuberosity	The most dorsal point on the ischial tuberosity	II
10	Superior acetabulum	The point on the superior rim of the acetabulum that marks the intersection of the iliac margin and the acetabulum, which is defined as the extension of the line connecting ASIS and AIIS.	III
11	Inferior acetabulum	The point on the inferior rim of the acetabulum directly across from Landmark 10, along the long axis of the ischium	III
12	Centre acetabulum	The centre of the acetabulum, defined as the midpoint of the line between Landmarks 10 and 11	III
13	Ischium	The most distal point on the ischium that forms a line with the centre of the acetabulum (Landmark 12) that is parallel to the long axis of the ischium	III
14	Superior pubic symphysis	The most superior point on the pubic symphysis, taken on the most medial point of the pubis	II
15	Inferior pubic symphysis	The most inferior point of the pubic symphysis, taken on the most medial point of the pubis	II
16	Superior obturator foramen	The most superior point of the obturator foramen, where the foramen narrows along the long axis of the foramen, directly opposite from Landmark 17.	II
17	Inferior obturator foramen	The most inferior point on the obturator foramen, along the long axis of the foramen, directly opposite from Landmark 16	II
18	Posterolateral obturator foramen	The most posterior lateral point on the obturator foramen, where the foramen is widest. Perpendicular to the line formed between Landmarks 16 & 17. Directly opposite Landmark 19.	II
19	Anteromedial obturator foramen	The most anterior medial point on the obturator foramen, where the foramen is widest. Perpendicular to the line formed between Landmarks 16 & 17. Directly opposite Landmark 18.	II

Landmarks used taken from Lewton (2010). [a]As taken from Bookstein (1991).

Semilandmarks of the Os Coxa

These were determined as points of maximum curvature using the topographical feature available through Geomagic Wrap 12 OEM (Geomagic, Inc. 2010) and were also considered to be areas of interest owing to their statuses as muscle attachment sites and as areas of importance for locomotion. 6 curves were used for the purposes of this study (Figure 3-2). Each curve consisted of between 6 and 15 discrete semilandmark points (Table 3-2).

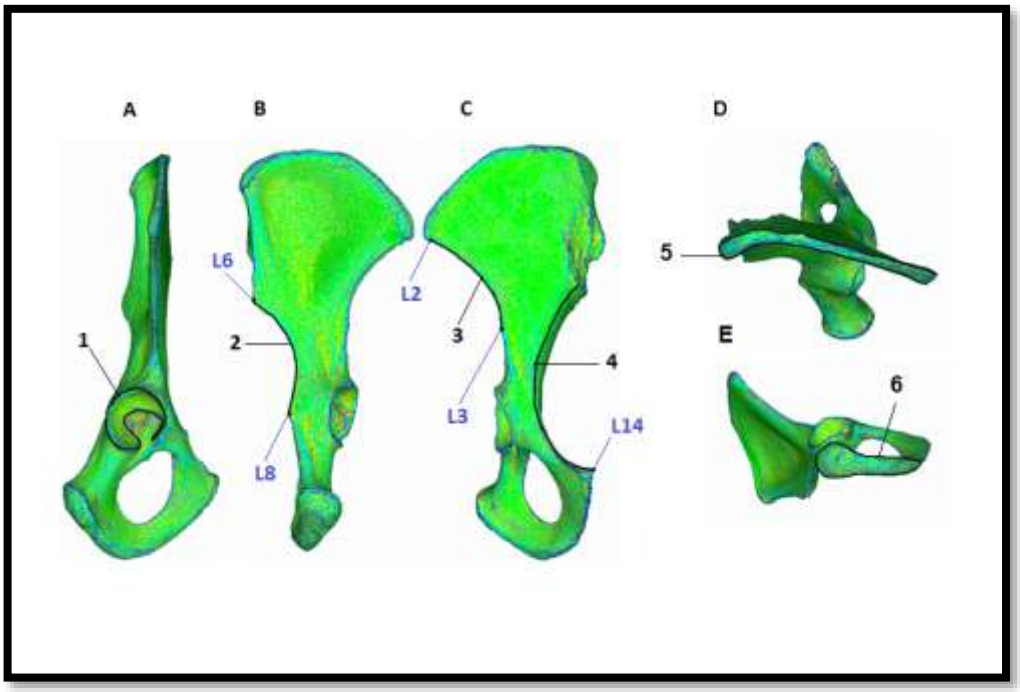

Figure 3-2: Lateral (A), Posterior (B), Anterior (C), Superior (D) and Postero-inferior (E) views of the Os Coxa depicting the curved semilandmarks used in this study.
Full definitions of these can be found in Table 3-2. Relevant landmarks are shown in blue

Table 3-2 Curved Semilandmarks of the Os Coxa

No.	Curve	Definition	No. of Points
1	Acetabulum	The curve formed by the outer margin of the acetabulum and continuing through to the lunate surface of the acetabulum. It is digitised from the point where the lunate surface and the acetabular margin meet posteriorly, around the acetabular margin (moving posteriorly and superiorly), and then anteriorly and inferiorly until meeting the lunate surface anteriorly. The curve then follows the lunate surface posteriorly until meeting the start point.	15
2	Greater Sciatic Notch	The curve formed by the greater sciatic notch, usually between Landmark 6 (Inferior Extent of the Auricular Surface) and Landmark 8 (Ischial Spine), along the line of maximum curvature. It is digitised from Landmark 6, and goes inferiorly to Landmark 8.	6
3	Lateral Iliac Border	The curve formed along the lateral border of the ilium, between Landmark 2 (Anterior Superior Iliac Spine) and Landmark 3 (Anterior Inferior Iliac Spine). It is digitised from Landmark 2, moving inferiorly to Landmark 3.	7
4	Pelvic Brim	The curve formed from the most anterior and most inferior point of the auricular surface, along the line of maximum curvature to Landmark 14 (Superior Pubic Symphysis). It is digitised from the point on the auricular surface, moving anteriorly and inferiorly along the line of maximum curvature to Landmark 14.	10
5	Iliac Crest	The curve formed by the anterior and posterior borders of the iliac crest. It is digitised from Landmark 2 (Anterior Superior Iliac Spine), along the line of maximum curvature which forms the anterior border of the iliac crest to Landmark 5 (Posterior Superior Iliac Spine), and then from Landmark 5 along the line of maximum curvature that forms the posterior border of the Iliac crest back to Landmark 2.	14
6	Ischial Tuberosity	The curve formed by the line of maximum curvature delineating the borders of the ischial tuberosity. It is digitised from the most medial point on the ischial tuberosity, moving laterally and posteriorly along the line of maximum curvature which forms the anterior border to the most posterior and lateral extent, then moving anteriorly and medially along the posterior border to the start point.	12

3.12 Results of the Geometric Morphometric Analysis in the Os Coxa

All Landmarks and Semilandmarks of the Os Coxa Across All Species

A Generalised Procrustes Analysis (GPA) was conducted on the Os Coxa, determining the Procrustes Distance within each species group. The Os Coxa was shown to be highly variable, with a Procrustes Distance of 1.90828 across the species (see Appendix for full results). This likely reflects the greater degree of morphological difference found in the pelvis relating to locomotory style. The *Homo sapiens* sample was the most variable in shape for the Os Coxa, with a Procrustes Distance of 0.10582. The *Pan troglodytes* and *Gorilla sp.* samples were very similar with Procrustes Distances of 0.09040 and 0.09024 respectively. The *Pan paniscus* sample had a slightly smaller Procrustes Distance of 0.06354, and the *Pongo pygmaeus* sample had the smallest with 0.03178.

A Principal Components Analysis was conducted on all species, including the *Australopithecus afarensis* sample, using all landmarks and semilandmarks. The first principal component explained 66.91% of the variance and the second explained 11.74% of the variance- a cumulative amount of 78.65% (see Appendix for full results).

A bi-plot of the first two principal components (Figure 3-3) shows the *Homo sapiens* sample was clearly differentiated from the other groups along Principal Component 1. The *Gorilla sp.* group were clearly differentiated along Principal Component 2, but clustered with the *Pongo pygmaeus* along Principal Component 1. The *Pan paniscus* sample clustered most closely with the *Pan troglodytes* group, although they showed some differentiation along Principal Component 2. The *Australopithecus afarensis* individual did not form part of any species cluster, but was most closely aligned with *Homo sapiens* along Principal Component 1, and with the extant apes, with the exception of the *Gorilla sp.* along Principal Component 2.

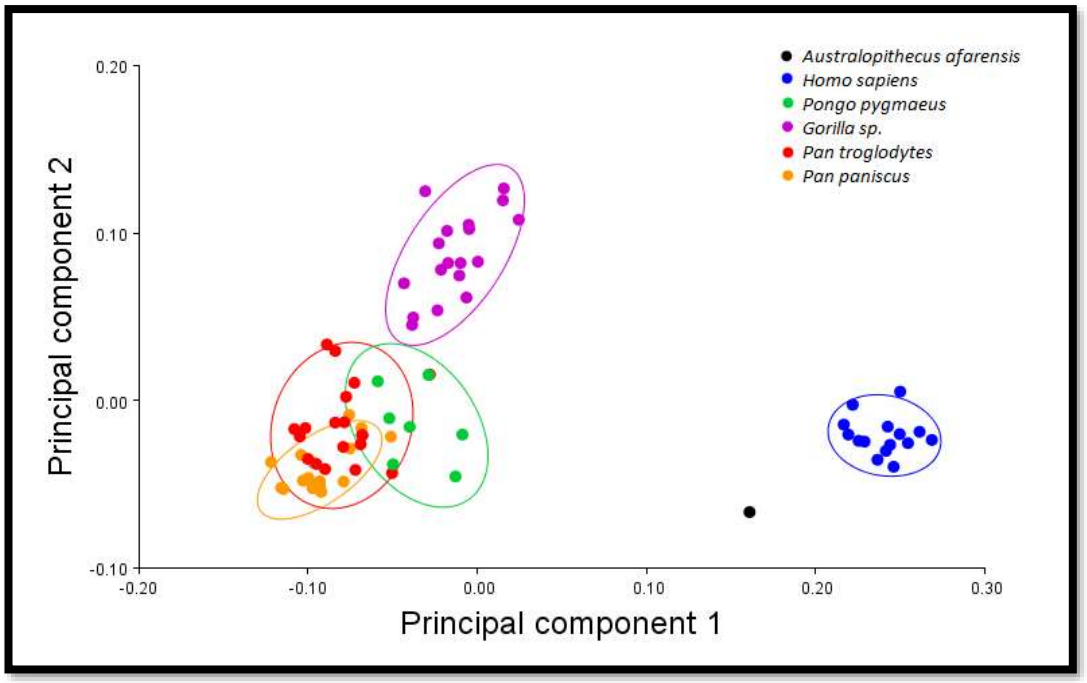

Figure 3-3: Plot of Principal Component 1 against Principal Component 2 for All Landmarks and Semilandmarks Across All Species' Os Coxa

Shapiro-Wilk tests showed the data to be normally distributed (see Appendix) and Levene's Tests were conducted to determine whether there was homogeneity of variance for Principal Components 1 and 2. The Levene's tests were not significant; PC1 $F(4, 73) = 0.285$, $p = 0.887$ – at the .05 alpha level and PC2 $F(4,73)=3.424$, $p=0.53$. As such, ANOVAs were conducted (see Appendix).

The ANOVA (see Appendix) showed that there was a significant difference at the $p<0.005$ level for both Principal Component 1 and Principal Component 2, indicating that there were significant differences between the groups along both principal components. A Tukey post hoc test was undertaken to determine the nature of these significant differences (see Appendix).

As was shown in Figure 3-3, the Tukey post hoc tests showed the *Pan paniscus* and *Pan troglodytes* groups clustered together along Principal Component 1. The remaining groups were significantly different from each other. Principal Component 2 showed that *Pan paniscus* grouped most closely with *Homo sapiens*, which in turn grouped with *Pan troglodytes* and *Pongo pygmaeus.* The *Gorilla sp.* group were significantly different from all other species groups on the second principal component.

Shape changes indicated by the Principal Components

There were changes in shape in the Os Coxa along Principal Components 1 and 2 (Figure 3-4). The anterior view showed a changed in the shape of the pelvic brim to a more rounded shape along Principal Component 1. The angle of the pubis and ischium became more laterally and inferiorly oriented. The width of the ilium increases and the iliac crest became longer and more noticeably curved.

In the lateral view, the overall size of the acetabulum increased along Principal Component 1. It can also be seen that the ischium became less curved, with the ischial tuberosity becoming more superiorly oriented. The iliac crest also became more posteriorly oriented. The juncture between the ilium and the pubis developed a more acute angle along Principal Component 1.

The medial view showed a broad increase in robusticity along Principal Component 1. The Auricular surface became wider, and the iliac blade more bowl shaped. The Obturator foramen became more triangular in shape.

Posteriorly, the greater sciatic notch became more curved. The ischial tuberosity became wider and more superiorly oriented. The iliac pillar also became wider.

Principal Component 2 contributed less considerably to the overall variation than Principal Component 1, but its contribution was still significant. The anterior view showed that along Principal Component 1 the iliac blade became more flared. The

iliac pillar became much shorter. Additionally, the orientation of the pubic symphysis became more superior, and the pubis more gracile overall.

The lateral view showed an increase in the curvature of the lateral iliac border. This also became more superiorly oriented. The ischium was shown to become more laterally oriented.

In the medial view, the iliac pillar shortened, and the orientation of the iliac blade became more superiorly oriented, and the auricular surface became more gracile along Principal Component 2.

The posterior view showed the flaring of the iliac blade, as well as the shortening of the iliac pillar seen in the other views along Principal Component 2. The change in the orientation of the ischium was also reflected, and the ischial tuberosity was shown to become more inferiorly oriented.

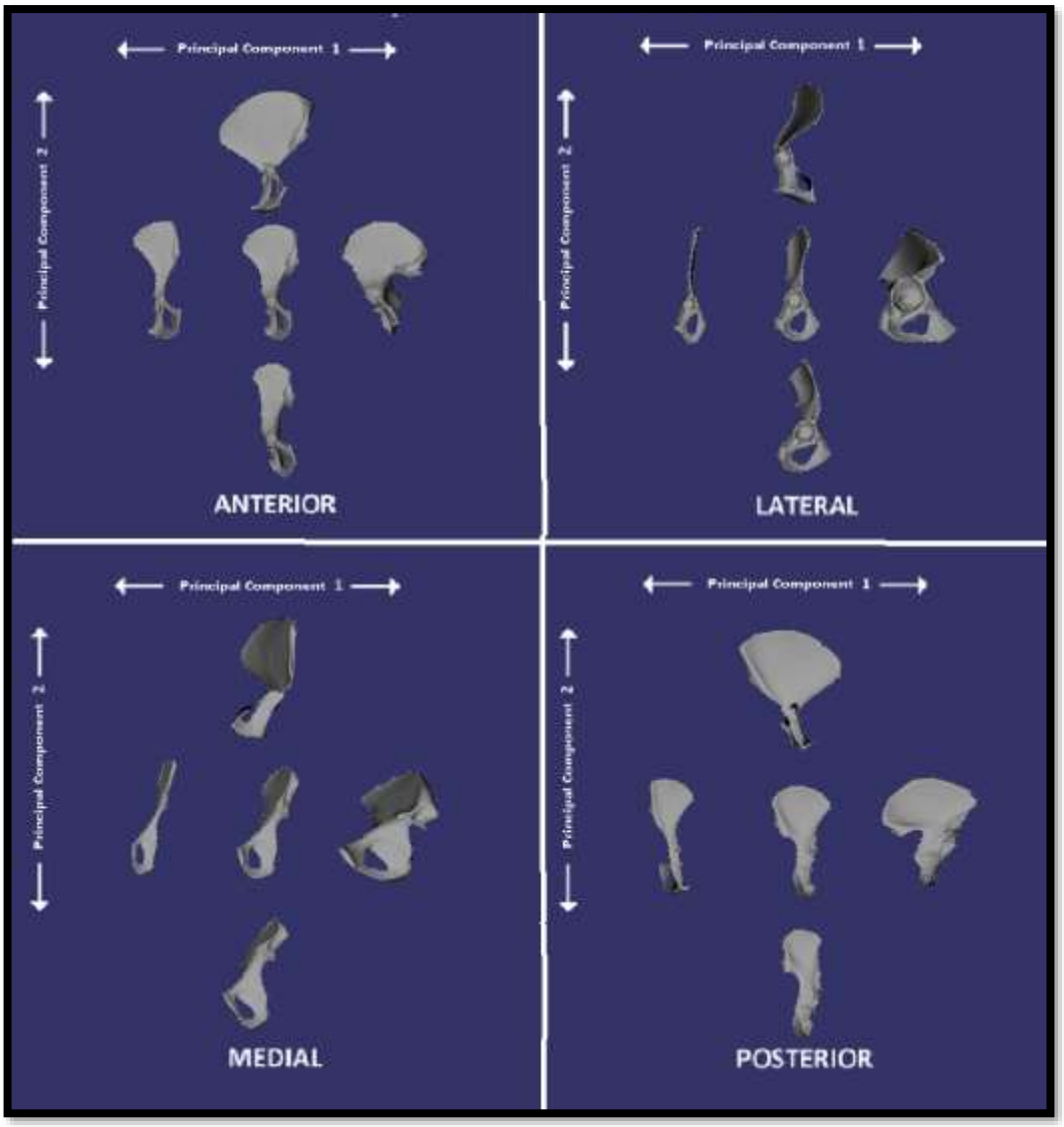

Figure 3-4 Changes in Os Coxa Shape Along Principal Components 1& 2, shown in Anterior, Lateral, Medial and Posterior Views

Mean Os Coxa Shape shown centrally and the extremes of each Principal Component surrounding this

Shape changes across the species groups

Figure 3-5 shows how these changes in shape were reflected in each species subset. As shown by the Tukey post hoc tests (see Appendix), Principal Component 1 showed that the *Pan paniscus* and *Pan troglodytes* subsets were grouped together along the first principal component. The other species groups were all significantly different from each other.

This was reflected in the shape changes seen in the species means- the *Pan paniscus* and *Pan troglodytes* Os Coxae were shown to be very similar in shape, with the *Pan troglodytes* Os Coxa marginally more robust overall in comparison to the *Pan paniscus* mean. The *Pongo pygmaeus* mean was shown to have a relatively wider ilium than the *Pan paniscus* and *Pan troglodytes* subsets, with a more curved lateral iliac border. The *Pongo pygmaeus* acetabulum was slightly larger relative to the *Pan* groups. The ischium was marginally more robust than the *Pan* subsets, and displayed slightly less curvature along its inferior border. The ischial tuberosity was oriented more superiorly than in the *Pan* subsets.

The *Gorilla sp.* Os Coxa was relatively larger and more robust than the other non-human apes. It displayed a more inferiorly oriented and longer ischial tuberosity. The obturator foramen was oriented more sagitally than in the other non-human ape groups, and the pubis was longer. In addition to this, the pelvic brim was rounder than that of the other non-human ape groups, and the iliac pillar shorter.

The *Homo sapiens* group differed most substantially from the other Os Coxa. The iliac crest was longer and more curved in the *Homo sapiens* group. The acetabulum was relatively much larger, and the ischium much less curved. The height of the iliac blade was relatively much reduced in comparison to the other groups. The auricular surface was relatively wider. The greater sciatic notch was more pronounced and the ischial tuberosity more superiorly oriented than all the non-human ape groups. The *Homo sapiens* Os Coxa is also more robust than that of the other groups.

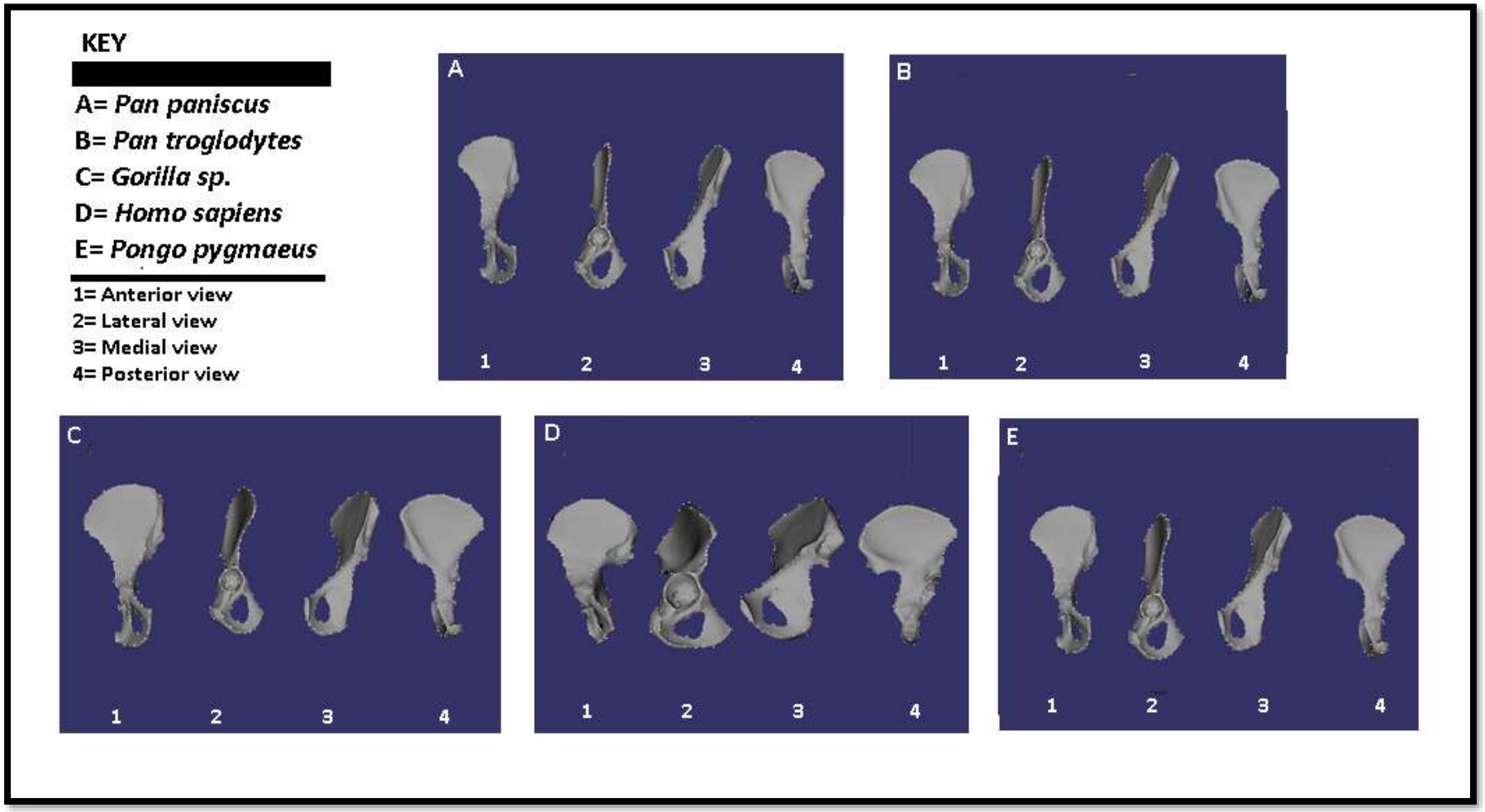

Figure 3-5: Mean Os Coxa shape for each species subset

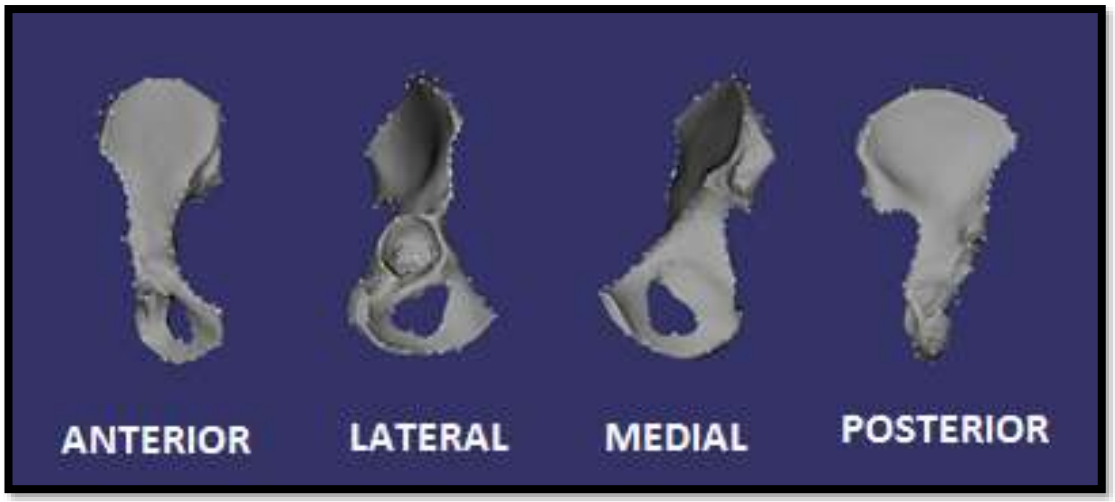

Figure 3-6: The Shape of the *Australopithecus afarensis* Os Coxa shown in Anterior, Lateral, Medial and Posterior Views

The *Australopithecus afarensis* Os Coxa showed a mixture of features (Figure 3-6). The iliac blade was less flared than the *Homo sapiens* iliac blade, and the pelvic brim was similar in shape to that of the non-human apes. The lateral view of the *Australopithecus afarensis* Os Coxa was very similar in shape to the *Homo sapiens* mean. The iliac blade was more anteriorly oriented and is longer sagitally in the australopithecine than in the *Homo sapiens* group. However, the ischial tuberosity and orientation of the ischium was similar in *Australopithecus afarensis* and the *Homo sapiens* mean.

Overall Musculature of the Os Coxa

The Os Coxae serve as the attachment points for muscles connecting the trunk to the lower limb, as well as for muscles that then cross the hip and allow for movement of the thigh (including flexion, extension, adduction, abduction and medial and lateral rotation). As the scope of this study only encompasses the lower limb, it is these muscles which will be examined further (Table 3-3). These muscles take their origin on the Os Coxa and insert on the lower limb- either on the femur, tibia or fibula. In all cases, the shape of the A.L. 288-1 Os Coxa showed the greatest affinity with the *Homo sapiens* group.

Table 3-3: Muscles with their origin on the Os Coxa and the affinity of A.L. 288-1 based on Geometric Morphometric results

Muscle	Associated Landmarks	Affinity of A.L. 288-1
Adductor brevis	15	*Homo sapiens*
Adductor longus	14	*Homo sapiens*
Adductor magnus (Add)	15, 9, SL 6	*Homo sapiens*
Adductor magnus (Ham)	SL 6	*Homo sapiens*
Biceps Femoris LH	SL 6	*Homo sapiens*
Gemellus inferior	SL 6	*Homo sapiens*
Gemellus superior	8	*Homo sapiens*
Gluteus Maximus	SL 5	*Homo sapiens*
Gluteus Medius	SL 5	*Homo sapiens*
Gluteus Minimus	SL 3	*Homo sapiens*
Gracilis	15	*Homo sapiens*
Iliopsoas	SL 3, SL 4, SL 5	*Homo sapiens*
Obturator externus	16-19	*Homo sapiens*
Obturator internus	16-19	*Homo sapiens*
Pectineus	14	*Homo sapiens*
Quadratus femoris	SL 6	*Homo sapiens*
Rectus femoris	SL 1, 3	*Homo sapiens*
Sartorius	2	*Homo sapiens*
Semimembranosus	SL 6	*Homo sapiens*
Semitendinosus	SL 6	*Homo sapiens*
Tensor fasciae latae	1,2	*Homo sapiens*

In order to explore each semilandmark set independently, and to confirm what any likely affiliation there may have been between the *Australopithecus afarensis* specimen and any of the species groups, Principal Components Analyses were conducted on each semilandmark set. The 'True Landmarks' were included along with each semilandmark set as these provided a reference for the semilandmarks in terms of shape. See the Appendix for the percentage of variance explained by each principal component for each semilandmark set.

The first two principal components in each Semilandmark set were plotted against each other (Figure 3-7). The resultant plots largely reflected what was found when all landmarks and semilandmarks were considered together, but to ensure that this was in fact the case, it was determined that ANOVAs should be conducted on each semilandmark set, and Tukey post hoc tests undertaken.

Before this could be done, each principal component had to be normally distributed and meet the assumption of Homogeneity of Variance required by the ANOVA. As such Shapiro-Wilk test of normality were undertaken, and Homogeneity of Variance tested.

The Shapiro-Wilk tests showed all the data to be largely normally distributed, and to largely display Homogeneity of Variance (see Appendix). This being the case, it was decided that an ANOVA could be conducted. The ANOVA showed a significant difference in all Semilandmark sets (see Appendix).

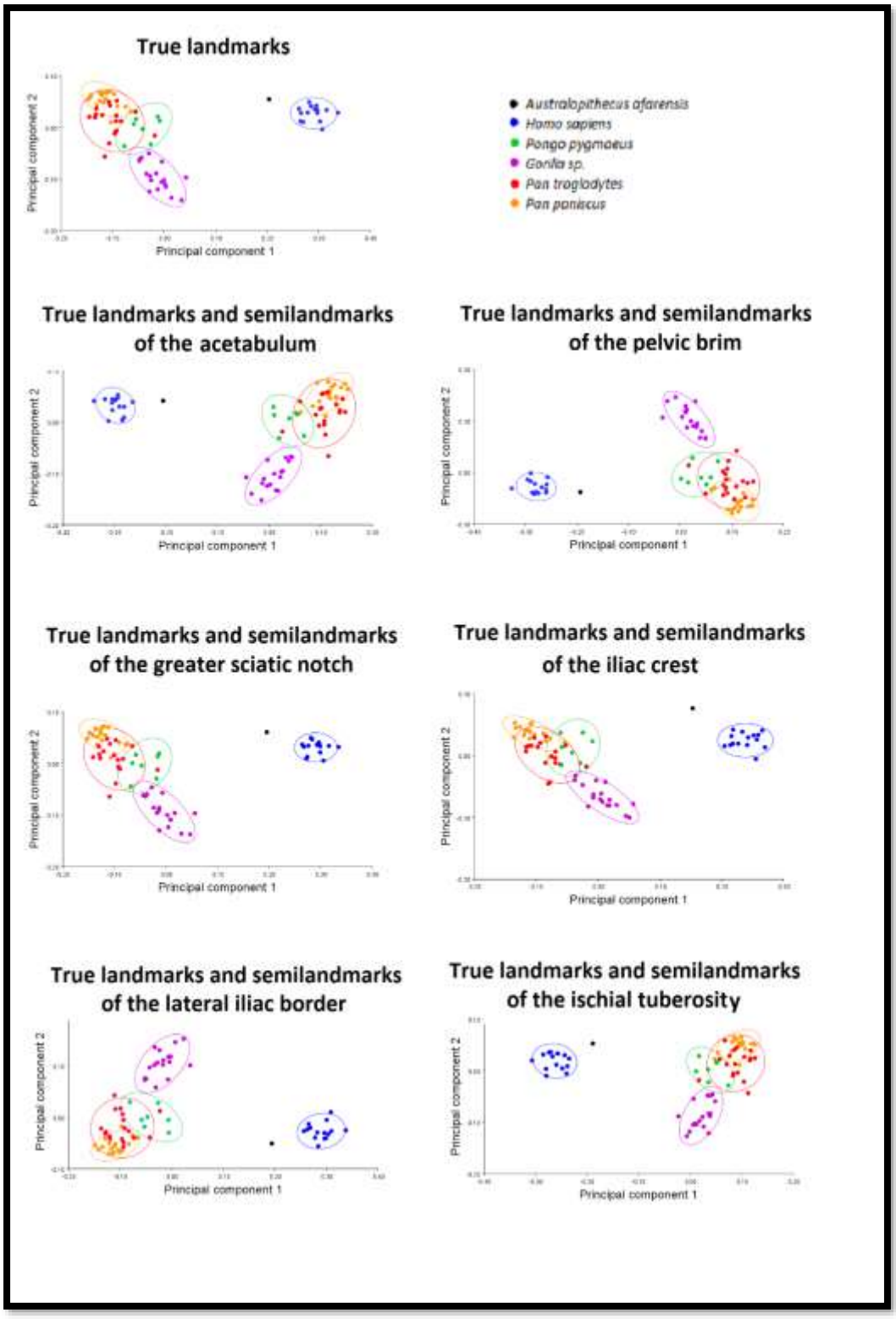

Figure 3-7: Plots of Principal Component 1 against Principal Component 2 for Each Semilandmark Set of the Os Coxa Across All Species Groups

True landmarks

For the True Landmarks, the first principal component explained 67.99% of the variance in shape, and the second explained 10.46% a cumulative amount of 78.46%. The Tukey post hoc test (Appendix) showed that for the True Landmarks along Principal Component 1, the *Pan paniscus* and *Pan troglodytes* subsets group together, as do the *Pongo pygmaeus* and *Gorilla sp.* groups. *Homo sapiens* did not group with any other species group.

Along Principal Component 2, the Tukey post hoc showed that the True Landmarks of the Os Coxa are divisible into four groups- the *Gorilla sp.* and the *Homo sapiens* subsets do not group with other species and the *Pan troglodytes* subset can group with *Pongo pygmaeus* subset or with the *Pan paniscus* subset. The shape changes this reflected are shown in Figure 3-8.

Shape changes indicated by the Principal Components

The shape changes visible when just the True Landmarks were used in the Principal Components Analysis in many ways reflected those shown when all the landmarks and semilandmarks were used in the analysis. The Anterior view showed a widening of the iliac blade between the Anterior Superior Iliac Spine and the auricular surface along Principal Component 1. There was also an increase in the width of the iliac pillar and an increase in the curvature of the pelvic brim. There was also a change in the orientation of the ischium towards a more sagittal axis.

In the lateral view, it was shown that Principal Component 1 was also responsible for a decrease in the curvature of the ischium, with an accompanying increase in relative length. The acetabulum also increased in its relative size.

Medially, these changes were also visible, as well as a clear indication that the pubis increased in length along the first principal component.

The posterior view reflected the widening of the iliac blade as seen in the anterior view, and also the change in orientation of the ischium along Principal Component 1. It could also be seen that the ischial tuberosity became more superiorly oriented and that the greater sciatic notch became more curved along the first principal component.

Principal Component 2 showed both a widening of the iliac blade, and a decrease in the relative length of the iliac pillar in the anterior view.

Laterally, Principal Component 2 shows a change in orientation of the ischial tuberosity from superiorly to inferiorly oriented, as well as a flattening between the tuberosity and the rest of the ischium. The acetabulum also became slightly more posteriorly oriented.

A decrease in the robusticity of the pubis is shown in the medial view along Principal Component 2, as well as an increase in the acuteness of the angle of the junction between the ilium and the pubis.

Posteriorly, Principal Component 2 showed a decrease in the thickness of the iliac pillar, as well as the aforementioned change in the orientation of the ischium. The widening of the iliac blade along Principal Component 2 is also visible.

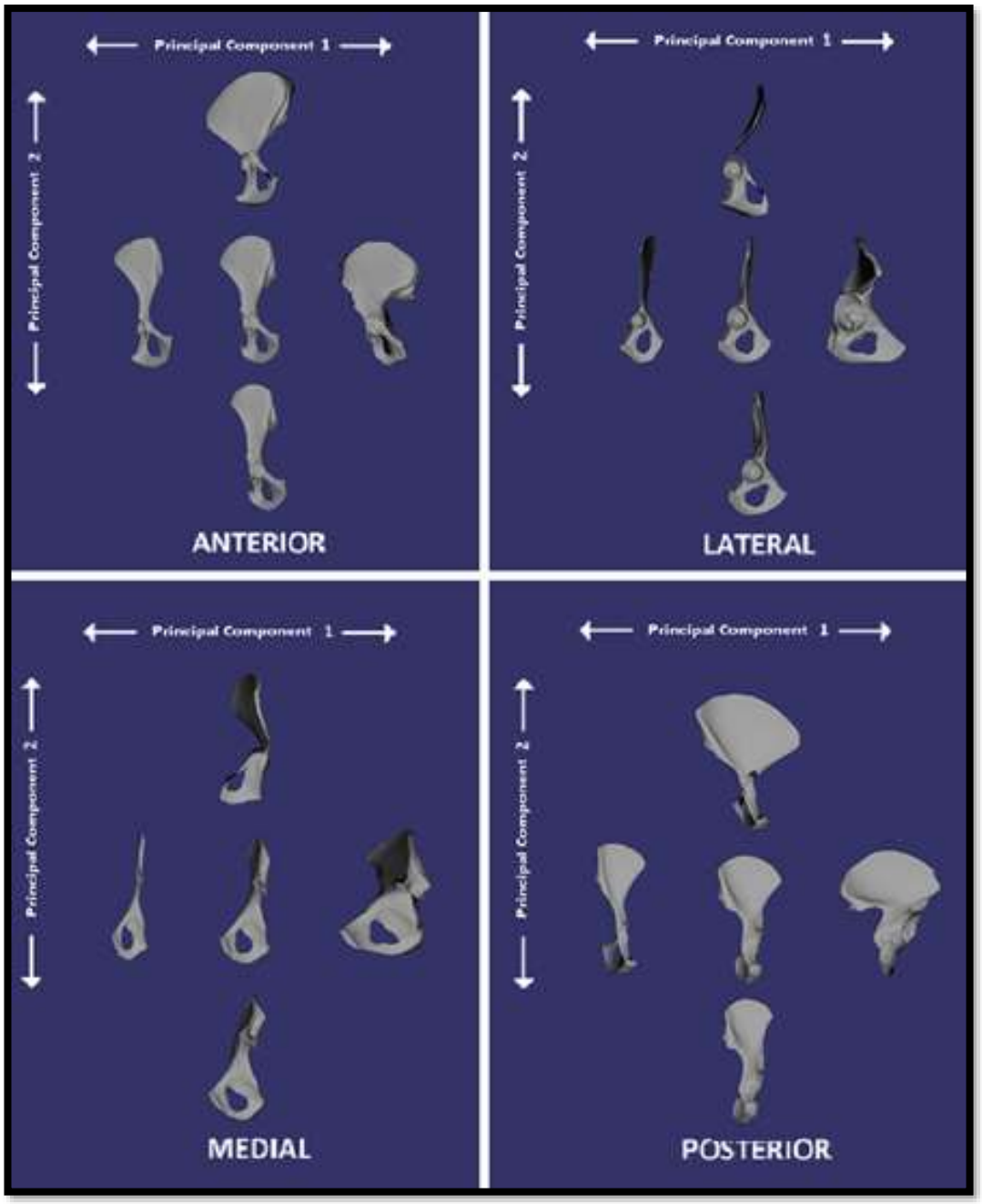

Figure 3-8: Changes in Os Coxa Shape Along Principal Components 1& 2, shown in Anterior, Lateral, Medial and Posterior Views

Mean Os Coxa Shape shown centrally and the extremes of each Principal Component surrounding this

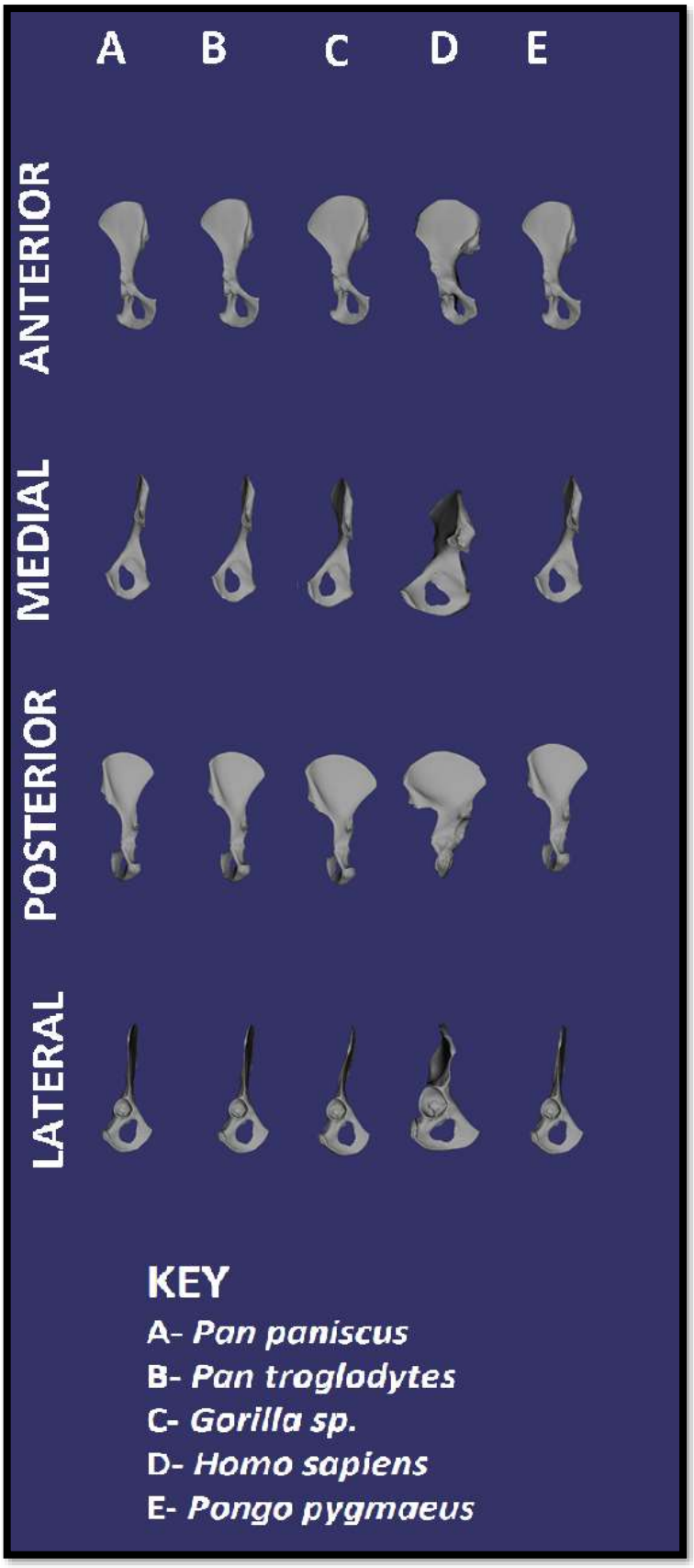

Figure 3-9: Mean Shape of the Os Coxa, using True Landmarks Across Species Groups showing Anterior, Medial, Lateral and Posterior Views

Shape changes across the species groups

The differences in the mean shape of the Os Coxa, across each species group, as shown when only the True Landmarks were used is shown in Figure 3-9.

In the anterior view, the *Pan paniscus* and *Pan troglodytes* mean Os Coxa shapes were very similar, although the *Pan troglodytes* Os Coxa showed a marginally wider iliac blade, and a moderately more curved pelvic brim, and was slightly more robust overall than the *Pan paniscus* Os Coxa. The *Pongo pygmaeus* Os Coxa shows a rounder pelvic brim and a more flared iliac blade than the *Pan paniscus* subset. The *Homo sapiens* Os Coxa showed a more antero-posteriorly oriented ischium than the other species groups, and the most curved pelvic brim of all the species. It also displayed a relatively wide iliac blade, with the most acutely angled lateral iliac border.

The medial view illustrated that the *Gorilla sp.* displayed the most superiorly oriented ilium. It also showed a more moderately curved ischium than the *Pan* and *Pongo pygmaeus* groups. The *Homo sapiens* group showed the least curvature of the ischium. The *Homo sapiens* mean also showed that the ilium in this group possesses a more anterior lateral edge than the other species.

Posteriorly, the *Pan paniscus* and *Pan troglodytes* groups are very similar. The *Pongo pygmaeus* group was shown to be more robust than the *Pan* groups, with a wider iliac blade and also a greater curvature to the greater sciatic notch. The *Gorilla sp.* Os Coxa displayed a wider iliac blade than the other non-human ape groups. The *Homo sapiens* Os Coxa was the most different from the other groups, with an extremely curved greater sciatic notch, relatively shorter and broader ilium and a superiorly oriented ischial tuberosity. It also displayed a relatively wide iliac pillar in comparison to the other groups.

In the lateral view, the *Homo sapiens* Os Coxa showed the largest acetabulum relative to the other groups. It also displayed the longest and least curved ischium of all the groups. The *Gorilla sp.* ilium curves anteriorly compared to the other non-human ape groups.

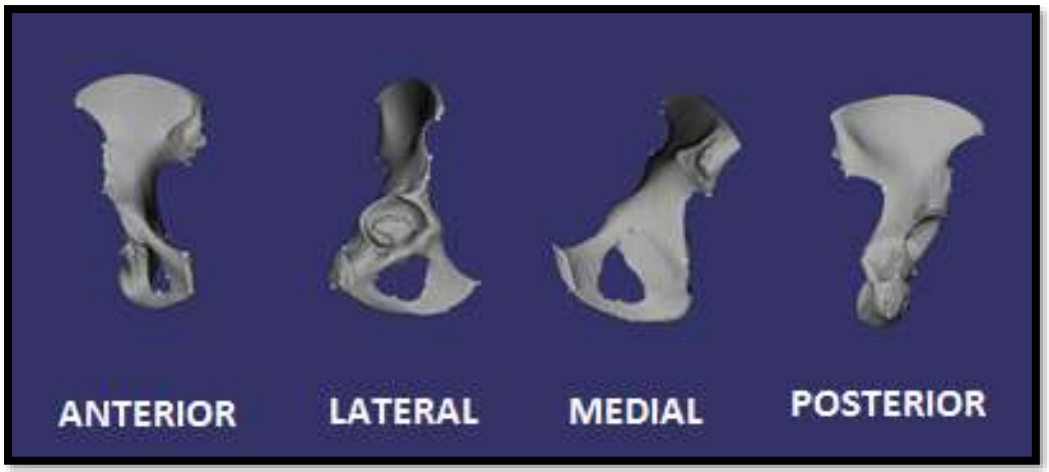

Figure 3-10: Shape of the *Australopithecus afarensis* Os Coxa as Determined by the True Landmarks, Shown in Anterior, Lateral, Medial and Posterior Views

When only the True Landmarks were used to analyse the shape of the Os Coxa, the shape of the australopithecine Os Coxa plotted most closely to the *Homo sapiens* group (Figure 3-10). It showed a similar orientation of the ischium and relative enlargement of the acetabulum. The ischial tuberosity was superiorly oriented as in the *Homo sapiens* sample. The ilium showed a similar curvature to that seen in the *Homo sapiens* group, and the ischium less curved than that of the other non-human ape groups. The ilium is shown to be relatively shorter than the non-human ape groups, and the auricular surface wider than those groups. The greater sciatic notch displayed a greater curvature than the non-human ape groups. The *Australopithecus afarensis* Os Coxa showed a similar level of robusticity to the *Homo sapiens* group.

Musculature associated with the True Landmarks

As alluded to above, when only true landmarks were considered, *Australopithecus afarensis* was shown to group most closely with *Homo sapiens*. This indicated that the basic shape of the Os Coxa in A.L. 288-1 was most similar to that of the *Homo sapiens* group overall.

Additionally, some muscles had specific landmark correlates- the point at which the muscle attached was a specific bony point which was associated with a landmark used in this study. These included: *m. gemellus superior* (Landmark 8, ischial spine), *m. sartorius* (Landmark 2, anterior superior iliac spine), *m.* Tensor fasciae latae (Landmark 1, lateral extent of the iliac crest and Landmark 2, anterior superior iliac crest), the anterior head of *m. rectus femoris* (Landmark 3, anterior inferior iliac spine) and *m. obturator internus* and *m. obturator externus* (Landmarks 16-19, landmarks of the obturator foramen).

M. adductor brevis, *m. adductor longus* and *m. pectineus* did not have exact landmark correlates, but were closely associated with the landmarks on the pubis (Landmark 14, superior pubic symphysis, and Landmark 15, inferior pubic symphysis).

True landmarks and semilandmarks of the acetabulum

For the True Landmarks and semilandmarks of the acetabulum, the first principal component explained 65.65% of the variance in shape, and the second explained 11.07% a cumulative amount of 76.72% (see Appendix).

The Tukey post hoc test (see Appendix) showed that for the True Landmarks and semilandmarks of the acetabulum along Principal Component 1, the *Pan paniscus* and *Pan troglodytes* subsets grouped together, but all other groups could be separated from each other. Along Principal Component 2 there was less clear separation. The *Gorilla sp.* group were not closely associated with any other species group, and the *Homo sapiens* group had commonalities with both the *Pan* subsets. *Pongo pygmaeus* and *Pan troglodytes* could also be grouped together. The second principal component did, however, contribute significantly less to the overall variation.

Shape changes indicated by the Principal Components

Along Principal Component 1 there was a decrease in size in the acetabulum, and a narrowing of the lower portion of the lunate surface. The lunate surface also became more right angled. The shape of the acetabulum became relatively narrower along the diagonal axis, and simultaneously wider supero-inferiorly. There was also a shift in the orientation of the acetabulum from a slightly more posterior position to a more lateral position.

On Principal Component 2, the shape of the acetabulum shifted from being wider along its inferior margin, to a more rounded overall shape. There was also a change in its relative position to the ilium, with the iliac blade becoming more superiorly oriented relative to the acetabulum. This change was reflected in the axis of the ischium, which became more inferior relative to the acetabulum (see Figure 3-11).

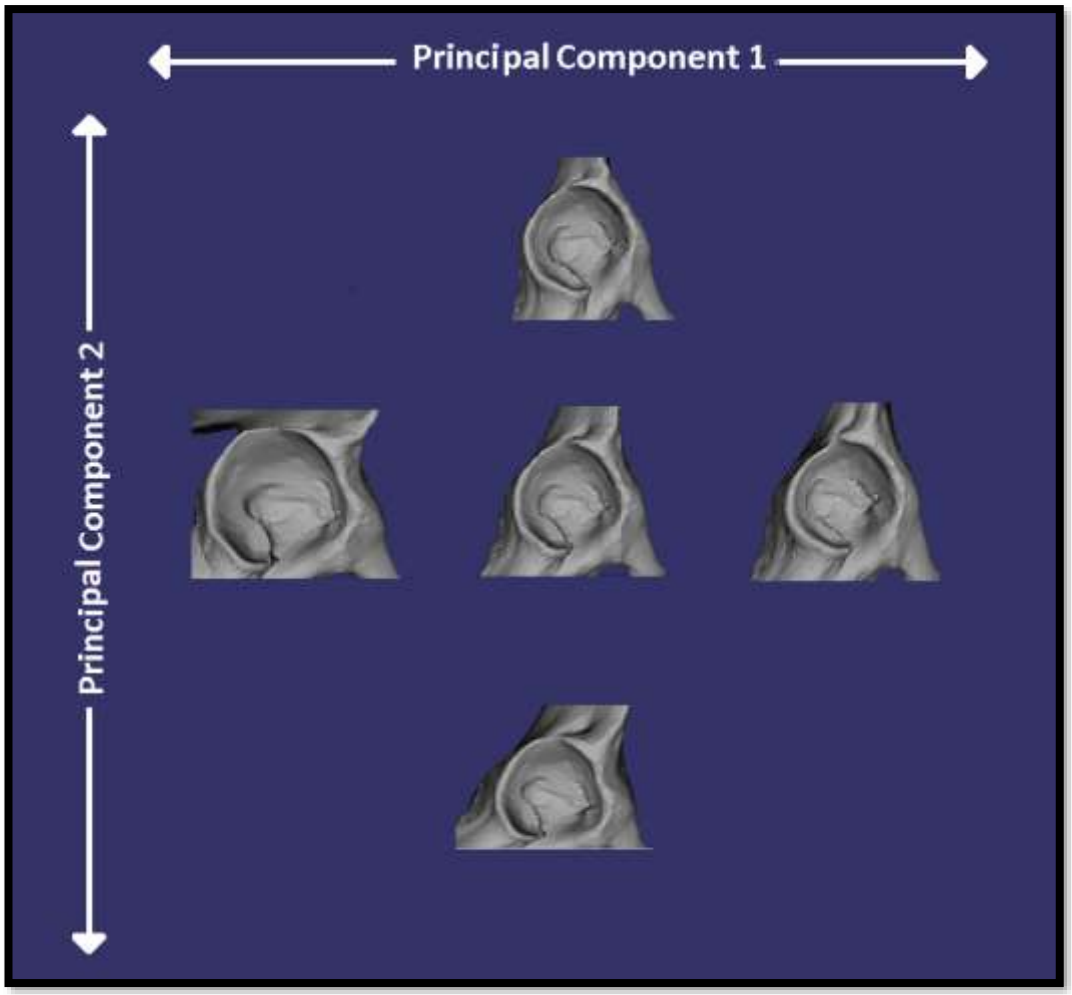

Figure 3-11: Changes in Acetabular Shape along Principal Components 1 and 2, with the Mean Acetabular Shape shown in the Centre

Shape changes across species groups

The shapes of the acetabulum in each species group were primarily attributable to changes along the first principal component, with a smaller contribution from Principal Component 2. (Figure 3-12). As the Tukey post hoc test (see Appendix) showed, the *Pan paniscus* and *Pan troglodytes* were very similar in shape, with the *Pan troglodytes* acetabulum marginally wider in the antero-posterior axis across its centre than the *Pan paniscus* subset. The *Gorilla sp.* acetabulum was relatively larger than the *Pan* groups, and also wider in the supero-inferior axis. The *Homo sapiens* Os Coxa was relatively larger than all the other species groups. The lunate surface was also less rounded. The acetabular rim showed a slight expansion along the inferior border. The *Pongo pygmaeus* acetabulum is relatively larger than the *Pan* acetabulum, and is relatively wider antero-posteriorly in the centre.

Figure 3-12: Mean Shape of the Acetabulum across species groups

The *Australopithecus afarensis* acetabulum (Figure 3-13) shows slightly less widening of inferior border of the acetabulum than the *Homo sapiens* group. The lower portion of the lunate surface was also marginally narrower. It was relatively larger than the *Pan* and *Pongo pygmaeus* subsets and was most similar overall to the *Homo sapiens* group.

Figure 3-13: The Shape of the *Australopithecus afarensis* Acetabulum

Musculature associated with the True Landmarks and the Semilandmarks of the Acetabulum

In true landmarks and semilandmarks of the Acetabulum, *Australopithecus afarensis* was shown to group most closely with *Homo sapiens.* The acetabulum is key in the origin of the posterior head of the *m. rectus femoris.*

True landmarks and semilandmarks of the pelvic brim

For the True Landmarks and semilandmarks of the pelvic brim, the first principal component explained 64.25% of the variance in shape, and the second explained 11.80% a cumulative amount of 76.05% (see Appendix). The Tukey post hoc test (see Appendix) showed that for the True Landmarks and semilandmarks of the pelvic brim along Principal Component 1, the *Pan paniscus* and *Pan troglodytes* subsets grouped together, as did the *Pongo pygmaeus* and *Gorilla sp.* groups. The *Homo sapiens* subset did not group with any other species group along Principal Component 1. Along Principal Component 2, the *Pan paniscus* and *Gorilla sp.* subsets did not group with any other species subset. The *Pan troglodytes* subset grouped with both the *Homo sapiens* and *Pongo pygmaeus* subsets, but they did not group with each other.

Shape changes indicated by the Principal Components

The shape of the pelvic brim was largely dependent on Principal Component 1. Figure 3-14 illustrates that along PC1, the pubis became shorter and the angle that the angle that the pubis joined to the ilium was increased. The iliac portion of the pelvic brim became more superiorly oriented. Along Principal Component 2, the shape of the pelvic brim changed from relatively round (a 'c' shape) to a narrower curve, with a widening inferiorly, and a straighter and diagonal superior portion.

Shape changes across the species groups

The shape changes of the mean species pelvic brim shape are shown in Figure 3-15. This showed that the *Pan paniscus* pelvic brim had a longer iliac portion, with an inferior curvature and relatively short pubic portion. The *Pan troglodytes* pelvic brim was similar, but the point of curve was closer to the centre due to a slightly longer pubic portion. The *Gorilla sp.* mean showed a rounder pelvic brim, with a relatively shorter iliac portion. The *Homo sapiens* pelvic brim is the most 'c' shaped, with the shortest pubis, which formed a near right angle with the iliac portion. Additionally, the auricular surface forms a matching curve superiorly. The *Pongo pygmaeus* pelvic brim had a marginally more superior point of curve than the *Pan paniscus* subset and a relatively longer pubis.

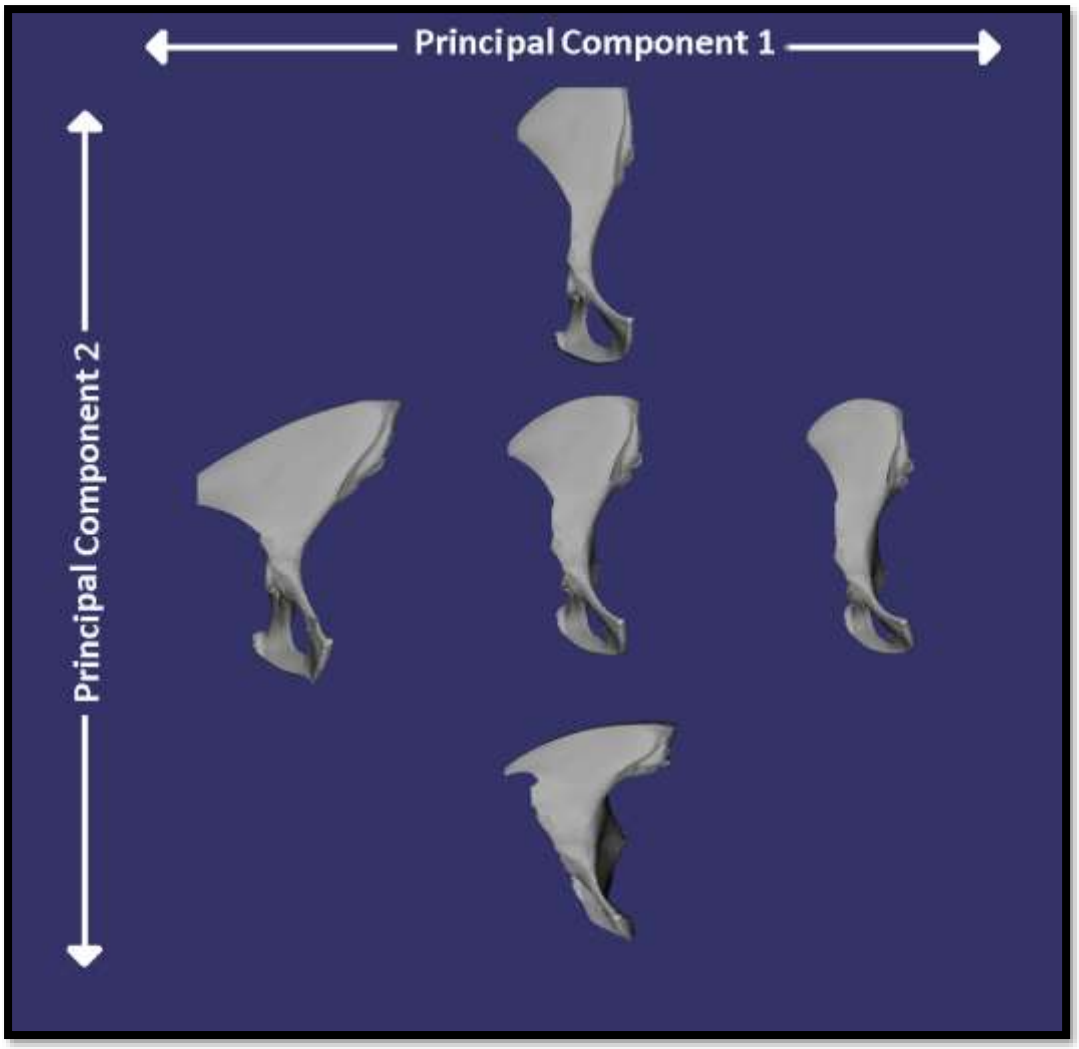

Figure 3-14: Changes in the Shape of the Pelvic Brim along Principal Components 1 and 2, with the Mean Pelvic Brim Shape shown in the Centre

Figure 3-15: Mean Shape of the Pelvic Brim across species groups

The *Australopithecus afarensis* pelvic brim (Figure 3-16) was most similar in shape to that of the *Homo sapiens* group, although the point of maximum curvature was more inferior. It was broadly 'c' shaped but did exhibit a longer pubis, as seen in the non-human ape groups.

Figure 3-16: The Shape of the *Australopithecus afarensis* Pelvic Brim

Musculature associated with the True Landmarks and the Semilandmarks of the Pelvic Brim

In all landmarks and semilandmarks of the pelvic brim *Australopithecus afarensis* was shown to group most closely with *Homo sapiens.* In terms of locomotion, the pelvic brim forms part of the transmission of load from the sacroiliac joint to the hip joint. It is also indicative of the inferior extent of the origin of *m. iliopsoas*.

True landmarks and semilandmarks of the greater sciatic notch

For the True Landmarks and semilandmarks of the greater sciatic notch, the first principal component explained 67.55% of the variance in shape, and the second explained 9.89%, a cumulative amount of 77.44% (see Appendix). The Tukey post hoc test (see Appendix) showed that for the True Landmarks and semilandmarks of the greater sciatic notch, the *Pan paniscus* and *Pan troglodytes* subsets grouped together, but all other species groups were independent. Along Principal Component 2, the *Gorilla sp.* group were clearly separate, but separation amongst the other groups was less clear, with *Pan paniscus* grouping with both *Pongo pygmaeus* and *Homo sapiens*. *Homo sapiens* also grouped with the *Pan paniscus* subset.

Shape changes indicated by the Principal Components

The changes in shape of the greater sciatic notch were greatest along Principal Component 1, with a much smaller contribution from Principal Component 2. These changes in shape can be seen in Figure 3-17. Along Principal Component 1, the shape of the greater sciatic notch became more acutely angled. Along Principal Component 2, the greater sciatic notch became less rounded, and the angle of the ischium less laterally oriented.

Shape changes across the species groups

The greater sciatic notch varies between the species groups (Figure 3-18). The *Pan paniscus* and *Pan troglodytes* subsets were very similar in shape to each other, however, the point of curve of the greater sciatic notch in the *Pan paniscus* subset was slightly more inferior, and the curve itself marginally less acute than that of the *Pan troglodytes* subset. The *Gorilla sp.* subset exhibited greater curvature of the greater sciatic notch than the *Pan* groups. The *Homo sapiens* group displayed the greatest curvature of the greater sciatic notch, with a relatively short ischial portion in relation to the other species groups. The *Pongo pygmaeus* subset showed a similar amount of curvature to the *Gorilla sp.* group, but showed a relatively longer ischial portion to the greater sciatic notch.

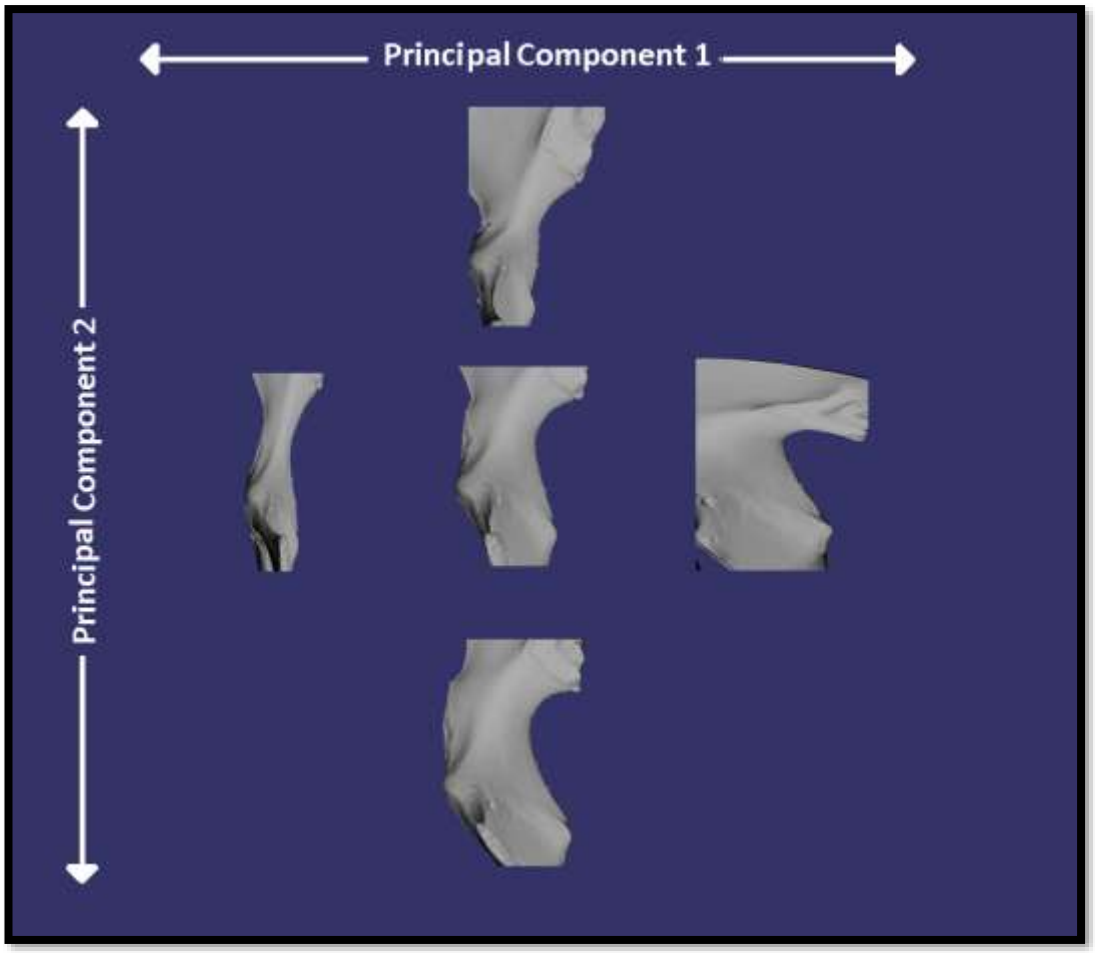

Figure 3-17: Changes in the Shape of the Greater Sciatic Notch along Principal Components 1 and 2, with the Mean Greater Sciatic Notch Shape shown in the Centre

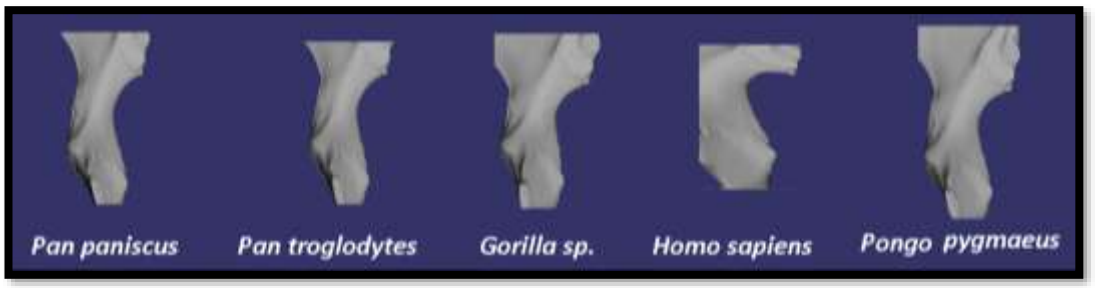

Figure 3-18: Mean Shape of the Greater Sciatic Notch across species groups

The australopithecine greater sciatic notch (Figure 3-19) showed the greatest similarity to that of the *Homo sapiens* subset, with a high degree of curvature, and a point of curvature located superiorly in comparison to the non-human apes. However, the angle of the ischial portion of the notch in *Australopithecus afarensis* was less medially

oriented than in the *Homo sapiens* subset. It was, however, more medially oriented than the non-human ape subsets.

Figure 3-19: The Shape of the *Australopithecus afarensis* Greater Sciatic Notch

Musculature associated with True Landmarks and the Semilandmarks of the Greater Sciatic Notch

In true landmarks and semilandmarks of the greater sciatic notch *Australopithecus afarensis* was shown to group most closely with *Homo sapiens.* Whilst none of the muscles took an origin or insertion on the greater sciatic notch, it is worth noting that *m. piriformis* passes through this structure in *Homo sapiens*.

True landmarks and semilandmarks of the iliac crest

For the True Landmarks and semilandmarks of the iliac crest, the first principal component explained 71.93% of the variance in shape, and the second explained 8.17%, a cumulative amount of 80.10% (see Appendix). The Tukey post hoc test (see Appendix) showed that for the True Landmarks and semilandmarks of the greater sciatic notch, the *Pan paniscus* and *Pan troglodytes* subsets grouped together, but all other species groups were independent. The *Gorilla sp.* group were clearly separate along Principal Component 2. *Homo sapiens* grouped with both *Pan paniscus* and *Pongo pygmaeus. Pongo pygmaeus* also grouped with the *Pan troglodytes* subset.

Shape changes indicated by the Principal Components

The shape of the iliac crest along Principal Component 1 changed from a single centrally located anterior curve, to a sigmoid curve along the iliac crest. The relative length of the iliac crest increased along Principal Component 1, as did its robusticity. Along Principal Component 2, there was a change from a sigmoid curve along the iliac crest, with an anterior facing medial curve to a reverse of this, where the medial curve facing posteriorly. There was also a decrease in the robusticity of the iliac crest along Principal Component 2. These changes are illustrated in Figure 3-20.

Shape changes across the species groups

The changes in the shape of the iliac crest in each species are illustrated in Figure 3-21. This shows that the *Pan paniscus* iliac crest was the shortest relative to all other species groups, but still very similar in shape to the *Pan troglodytes* subset, which displayed a slightly more centrally located point of curve. The *Gorilla sp.* iliac crest was relatively straight in comparison to the other species groups. It also displayed a relatively long iliac crest in comparison to both the *Pan* and *Pongo pygmaeus* groups. The *Homo sapiens* group possessed a sigmoid curve not visible in any other species group and was the most robust overall. The *Pongo pygmaeus* subset seemed to be intermediate in shape between the *Pan troglodytes* and *Gorilla sp.* subsets, with a relatively longer and flatter iliac crest than the *Pan* group.

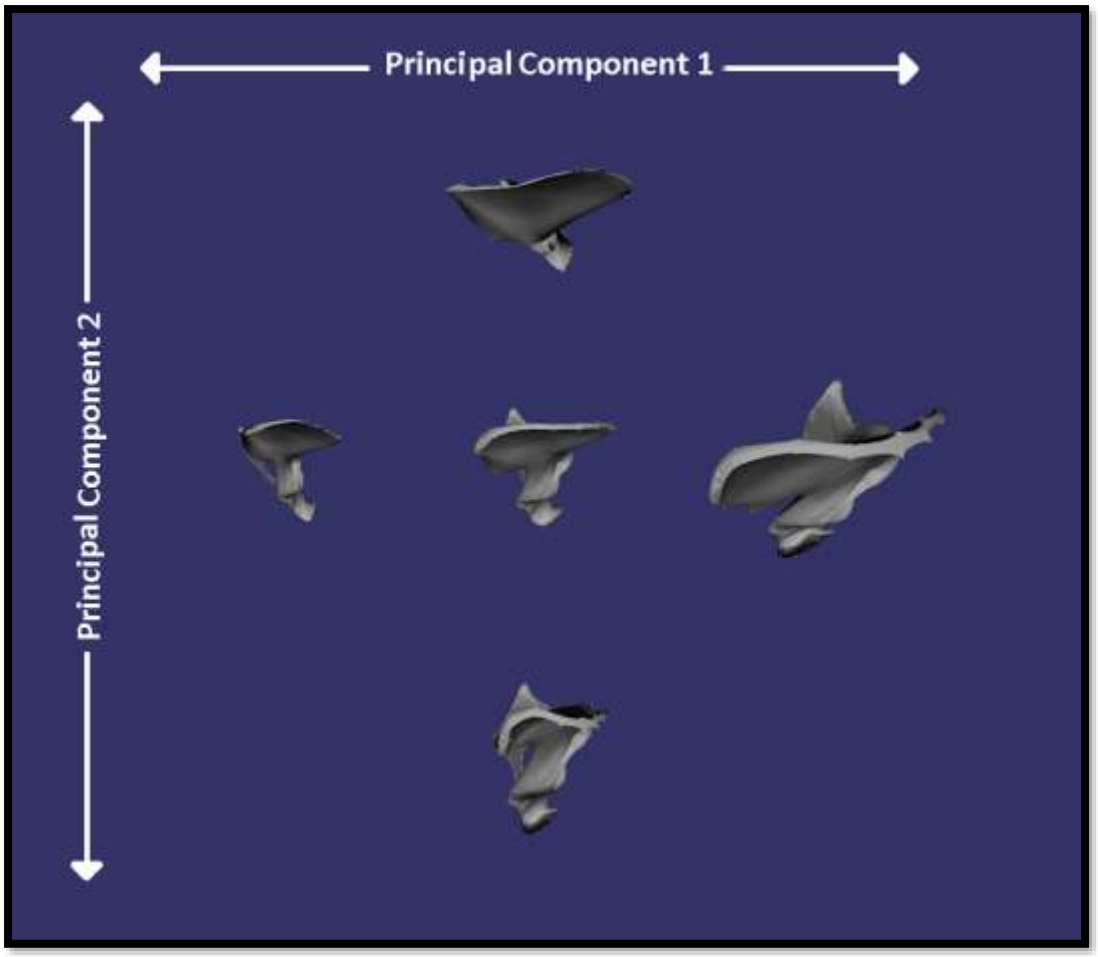

Figure 3-20: Changes in the Shape of the Iliac Crest along Principal Components 1 and 2, with the Mean Iliac Crest Shape shown in the Centre

Figure 3-21: Mean Shape of the Iliac Crest across Species Groups

The shape of the *Australopithecus afarensis* iliac crest was near identical to that of the *Homo sapiens* mean, although this was oriented slightly differently to the rest of the Os Coxa, with the lateral edge less anteriorly located than in the *Homo sapiens* subset.

Figure 3-22: The Shape of the *Australopithecus afarensis* Iliac Crest

Musculature associated with the True Landmarks and the Semilandmarks of the Iliac Crest

In true landmarks and semilandmarks of the iliac crest, *Australopithecus afarensis* was shown to group most closely with *Homo sapiens.* The iliac crest serves as on origin for *m. gluteus maximus, m. gluteus medius* and *m. iliopsoas.*

True landmarks and semilandmarks of the ischial tuberosity

For the True Landmarks and semilandmarks of the ischial tuberosity, the first principal component explained 66.38% of the variance in shape, and the second explained 10.52%, a cumulative amount of 76.91% (see Appendix). The Tukey post hoc tests of each principal component (see Appendix) showed that along Principal Component 1 *Homo sapiens* did not group with any other subset. The *Pongo pygmaeus* and *Gorilla sp.* subsets grouped together, as did the *Pan paniscus* and *Pan troglodytes* subsets.Along Principal Component 2, the *Gorilla sp.* and *Pan paniscus* subsets did not group with any other species. All other species groups grouped together.

Shape changes indicated by the Principal Components

Along Principal Component 1, the shape changes were largely to do with the orientation of the ischial tuberosity and it relative length. Along the first principal component, the ischial tuberosity became more perpendicular relative to the ilium and increased in length. Along Principal Component 2, there was an increase in robusticity (see Figure 3-23).

Shape changes across the species groups

The differences in the shape of the ischial tuberosity across the species groups is illustrated in Figure 3-24. The *Pan paniscus* and *Pan troglodytes* subsets were very similar. The *Gorilla sp.* ischial tuberosity was shown to be slightly more perpendicular relative to the ilium than that of the *Pan* subsets. The *Pongo pygmaeus* subset was marginally less robust than the *Gorilla sp.* subset, but was very similar in its orientation to the *Gorilla sp.* subset. The *Homo sapiens* subset was both relatively longer, than the other species groups and oriented past the point of being perpendicular to the ilium, whereas the other groups were not.

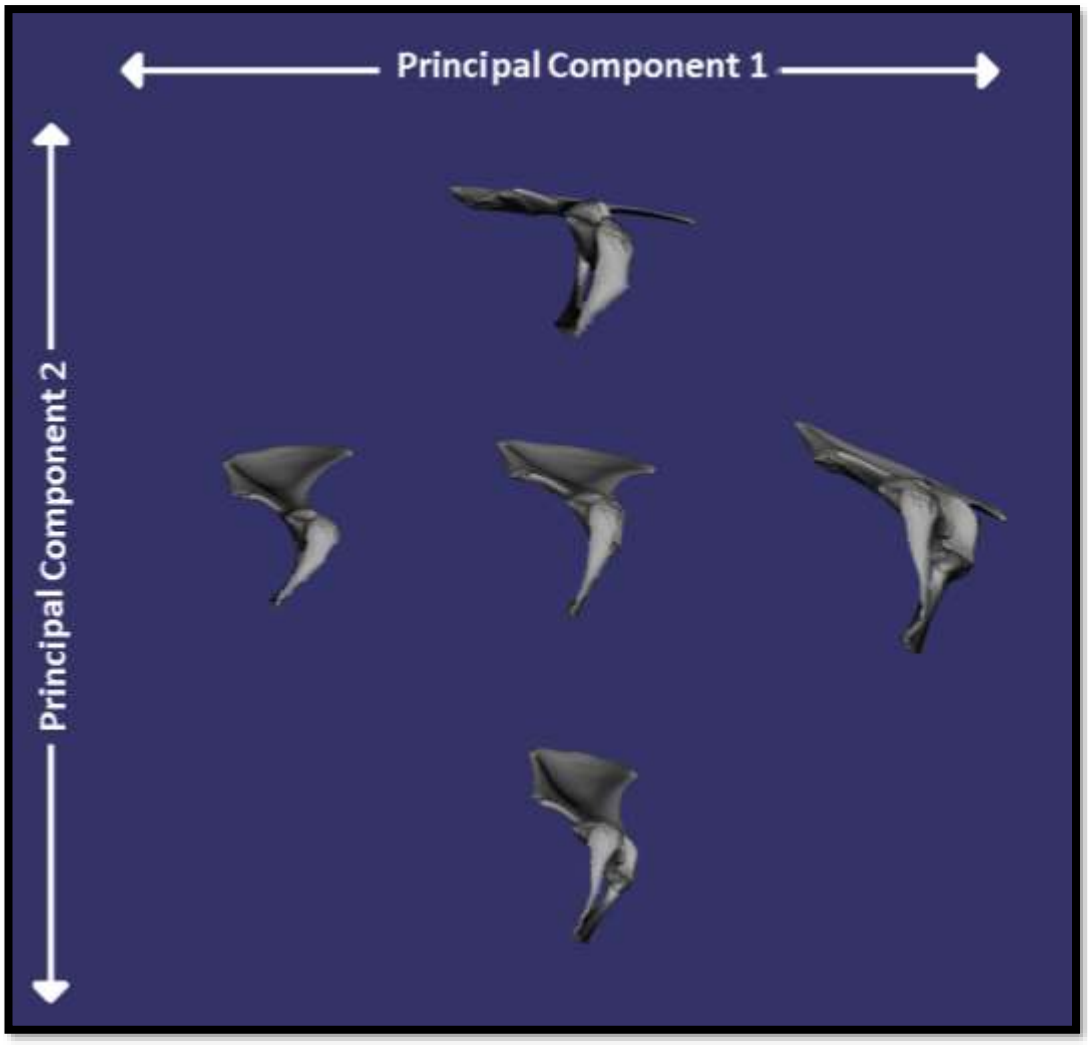

Figure 3-23: Changes in the Shape of the Ischial Tuberosity along Principal Components 1 and 2, with the Mean Ischial Tuberosity Shape shown in the Centre

Figure 3-24: Mean Shape of the Ischial Tuberosity across Species Groups

The *Australopithecus afarensis* ischial tuberosity (Figure 4-30) was similar in both its relative robusticity and length to that of the *Homo sapiens* subset. Its orientation, however was intermediate between the *Homo sapiens* group and the non-human ape groups and was reasonably perpendicular to the ilium.

Figure 3-25: The Shape of the *Australopithecus afarensis* Ischial Tuberosity

Musculature Associated with the True Landmarks and the Semilandmarks of the Ischial Tuberosity

In true landmarks and semilandmarks of the ischial tuberosity, *Australopithecus afarensis* was shown to group most closely with *Homo sapiens.* The ischial tuberosity was an origin for the *m. adductor magnus, m. biceps femoris* and *m. gemellus inferior.*

True landmarks and the semi landmarks of the lateral iliac border

For the True Landmarks and semilandmarks of the lateral iliac border, the first principal component explained 68.15% of the variance in shape, and the second explained 11.99%, a cumulative amount of 80.14% (see Appendix). The Tukey post hoc tests (see Appendix) showed that the *Pan paniscus* and *Pan troglodytes* subsets grouped together along Principal Component 1, as did the *Pongo pygmaeus* and *Gorilla sp.* subsets. The *Homo sapiens* subset did not group with any other species group.

Along Principal Component 2, the *Pan paniscus* and *Gorilla sp.* subsets did not group with any other species group, and all other subsets grouped together.

Shape changes indicated by the Principal Components

The changes in shape along the first two principal components are illustrated in Figure 3-26. Along the first principal component, the length of the lateral iliac border decreased relative to the rest of the Os Coxa. Along the second principal component, the length of the lateral iliac border also decreased, but this was accompanied by a medial rotation of the border.

Shape changes across the species groups

The shape of the lateral iliac border varied across the species groups (Figure 3-27). In the *Pan paniscus* and *Pan troglodytes* groups, it was much the same shape although in the *Pan troglodytes* group, the lateral iliac border was relatively longer. In the *Gorilla sp.* and *Pongo pygmaeus* groups, the lateral iliac border shape was very similar, with both being longer than that of the *Pan groups.* The *Homo sapiens* group showed a remarkably shorter lateral iliac border than the non-human ape groups.

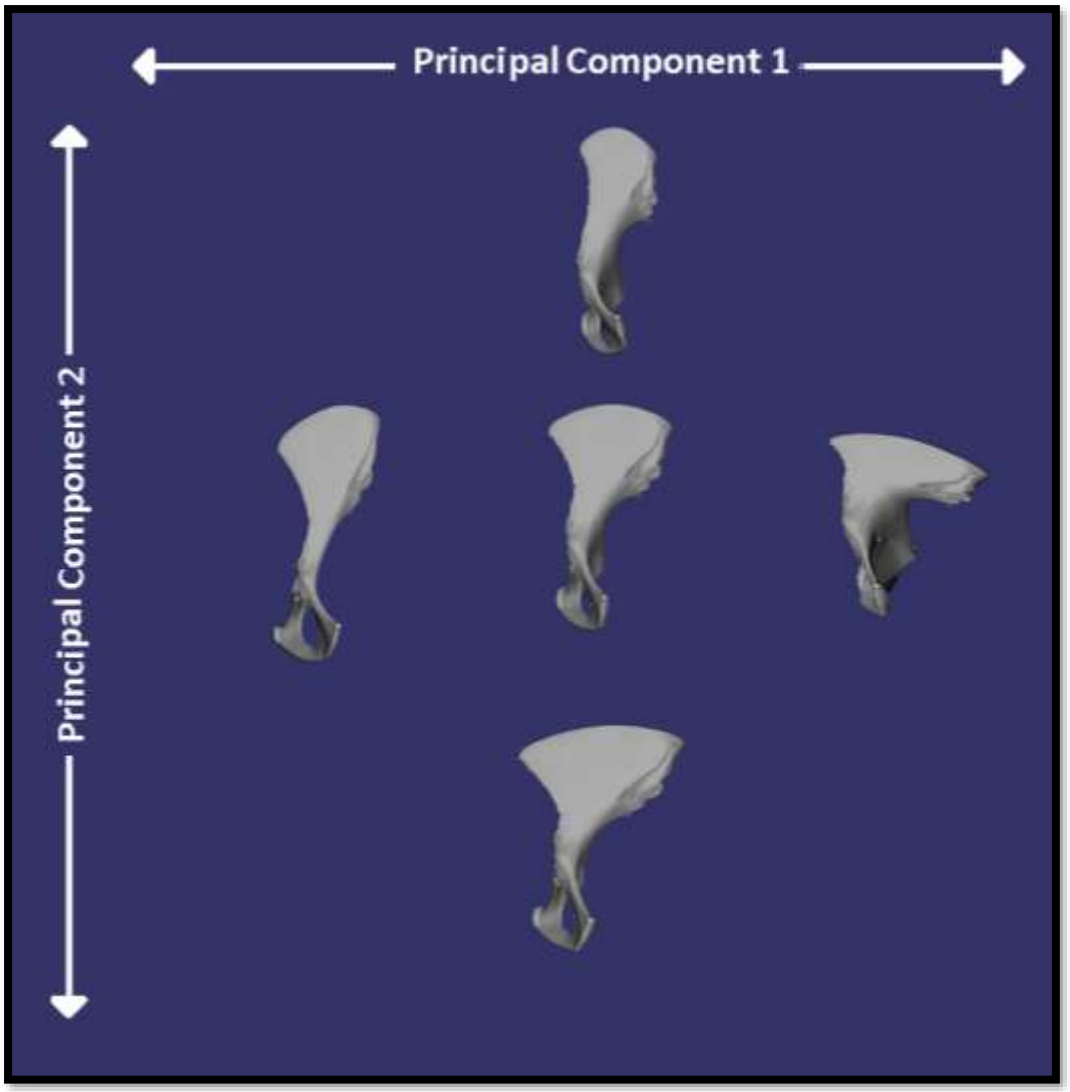

Figure 3-26: Changes in the Shape of the Lateral Iliac Border along Principal Components 1 and 2, with the Mean Lateral Iliac Border Shape shown in the Centre

Figure 3-27: Mean Shape of the Lateral Iliac Border Across Species Groups

Figure 3-28: The Shape of the *Australopithecus afarensis* Lateral Iliac Border

The *Australopithecus afarensis* lateral iliac border (Figure 4-33) was relatively shorter than that of the non-human ape subsets, but relatively longer than that of the *Homo sapiens* subset. Overall, however, it was nearer in length to the *Homo* group.

Musculature associated with the True Landmarks and the Semilandmarks of the Lateral Iliac Border

In true landmarks and semilandmarks of the lateral iliac border *Australopithecus afarensis* was shown to group most closely with *Homo sapiens.* Whilst the lateral iliac border was not a direct origin for any of the muscles, it formed a reference for both *m. gluteus minimus* and *m. iliopsoas.*

3.13 Summary of the shape and musculature of the Os Coxa

The shape of the Os Coxa was shown to vary between the species groups. This is in accordance with previous studies on the Os Coxa (i.e.: Arsuaga, 1981, 1985; Ashton and Oxnard 1964, Ashton et al., 1981; Berge, 1984, 1990, 1993; Berge & Kazmierczak, 1986; Berge & Ponge, 1983; ; Marchal 1997; 2000; Orban, 1982; Reynolds, 1931; Schultz, 1930; Sigmon & Farslow, 1986; Steudel, 1981; Straus, 1929; Waterman, 1929; Zuckerman et al., 1973). This is likely due to a combination of factors such as positional and locomotory behaviours (Berge, 1984; Berge and Kazmierczak, 1986; MacLatchy and Bossert, 1996; Reynolds, 1931; Reynolds and Hooton, 1936; Schultz, 1936; Steudel, 1981; Straus, 1929; Ward, 2002; Waterman, 1929; Yirga, 1987; Zuckerman et al., 1973 etc.), obstetric differences (DeSilva, 2011; Hager, 1996; Rosenberg and Trevathan, 2002) and factors of size (allometry) (Fleagle, 1999; Lycett and Von Cramon-Taubadel, 2013).

The Os Coxa in Pan

The Os Coxae in *Pan paniscus* and *Pan troglodytes* were shown to be very similar in their overall shape in all tested iterations. This is in accordance Payne et al. (2006) who noted the similarity in the muscle architecture of these two species. The *Pan* groups also proved to be the most intermediate in shape amongst the species groups.

The *Pan troglodytes* Os Coxa was marginally thicker overall in comparison to that of *Pan paniscus*, possibly an indication of the fact that *Pan troglodytes* is generally larger than *Pan paniscus* (Coolidge, 1933; Zihlman and Cramer, 1978) and this increased robusticity may be a factor of the enlargement of the Os Coxa as a response to increased weight bearing (Fleagle, 1999). The *Pan paniscus* iliac crest was the shortest relative to all other species groups, indicating the smallest relative attachments for *m. latissimus dorsi*, but was still very similar in shape to the *Pan troglodytes* subset, which displayed a slightly more centrally located point of curve. This possibly reflects the increased mobility (especially adduction at the hip) required for the increased arboreality seen in *Pan paniscus* relative to *Pan troglodytes* (Doran, 1992, 1993; Payne at al. 2006; Sugardjito and van Hooff, 1986; Thorpe & Crompton, 2004).

Pan troglodytes showed a marginally relatively wider iliac blade than *Pan paniscus*, indicating potentially larger origins for the gluteal muscles -*m. gluteus medius* and *m.*

gluteus minimus (abductors at the hip) - and *m. iliacus* (flexor at the hip). In the *Pan troglodytes* group, the lateral iliac border was relatively longer, indicating a relatively greater origin for *m. sartorius* (flexor at the hip and knee, abductor and lateral rotator at the hip).

The point of curve of the greater sciatic notch in the *Pan paniscus* subset was slightly more inferior, and the curve itself marginally less acute than that of the *Pan troglodytes* subset. The *Pan troglodytes* pelvic brim was similar to that of *Pan paniscus*, but the point of curve was closer to the centre due to a slightly longer pubic portion. This area forms the part of the origin for *m. gluteus minimus* in *Pan*. The *Pan troglodytes* acetabulum marginally wider in the antero-posterior axis across its centre than the *Pan paniscus* subset, perhaps indicating greater movement antero-posteriorly in *Pan troglodytes* or supero-inferiorly in *Pan paniscus*. The *Pan paniscus* and *Pan troglodytes* ischial tuberosity was shown to be slightly less perpendicular relative to the ilium than that of the *Gorilla sp*. subset. As this forms the origin of the hamstring muscles and *m. gluteus maximus*, all important extensors, this likely reflects a difference in extensor capability between these groups. As *Pan* are more arboreal (Ashton and Oxnard, 1964; Fleagle, 1999), this may indicate the degree of climbing behaviour.

The Os Coxa in Gorilla

The *Gorilla sp.* Os Coxa was relatively larger and more robust than the other non-human apes, probably a function of the species' greater overall size (as per Fleagle, 1999; Lycett and Von Cramon-Taubadel, 2013). This meant that all muscles attaching to the Os Coxa had relatively larger attachments.

The *Gorilla sp.* iliac crest was relatively straight in comparison to the other species groups, perhaps due to the ilium curving anteriorly compared to the other non-human ape groups. It also displayed a relatively long iliac crest in comparison to both the *Pan* and *Pongo pygmaeus* groups, providing greater attachment for the *m. latissimus dorsi.* The *Gorilla* trunk is relatively larger than the other species groups, and increased attachment for the *m. latissimus dorsi* may indicate the use of this muscle in climbing and lifting the great body weight of the *Gorilla.* There was greater curvature of the greater sciatic notch than the *Pan* groups. The *Gorilla sp.* Os Coxa displayed a

wider iliac and more superiorly oriented iliac blade than the other non-human ape groups, reflecting its muscular hind limb (Zihlman et al. 2011), with large attachments for the *m. iliacus* ventrally, and *m. gluteus maximus* and *m. gluteus minimus* dorsally. The iliac pillar shorter was also shorter. In the *Gorilla sp.* the lateral iliac border shape was longer than that of the *Pan groups* indicating a greater origin for *m. sartorius.*

The obturator foramen was oriented more sagitally than in the other non-human ape groups, and the pubis was longer. In addition to this, the pelvic brim was rounder than that of the other non-human ape groups, The *Gorilla sp.* mean showed a rounder pelvic brim, with a relatively shorter iliac portion. As this structure is important for weight transfer across the pelvis to the hip joint, this is probably a reflection of the greater weight of *Gorilla sp.*

The *Gorilla sp.* acetabulum was relatively larger than the *Pan* groups, and also wider in the supero-inferior axis. This was probably also a factor of the *Gorilla's* massive size, and transfer of this weight into the femur.

The ischial tuberosity was longer and more inferiorly oriented, and more perpendicular to the ilium when compared to the other groups. It was also more moderately curved than the *Pan* and *Pongo pygmaeus* groups. It serves as the origin for the extensors of the thigh at the hip, including *m. ischiofemoralis, m. semimembranosus, m. semitendinosus* and *m. biceps femoris* and its large size reflects the importance of these muscles in climbing and particularly extension. These results may also reflect the *Gorilla sp.'s* need for stability at the hip during quadrupedal locomotion (Zihlman et al. 2011), including reduced flexibility and the need for weight bearing and propulsion in the hind limb.

The Os Coxa in Pongo

The *Pongo pygmaeus* group was shown to be more robust than the *Pan* groups- a possible indication of this species greater overall size. *Pongo pygmaeus* was also shown to have a relatively wider ilium than the *Pan* subsets possibly an indication that the *m. gluteus maximus* has a superior origin on the posterior ilium in *Pongo* (Sigmon 1974; 1975; Zihlman et al. 2011) and that there is a wide origin for *m. gluteus medius*. *Pongo* also exhibits a more curved lateral iliac border- the origin for *m. scansorius* (important for flexion, medial rotation and abduction) (Sigmon, 1974) and a greater

curvature to the greater sciatic notch. This configuration in the gluteal musculature has been suggested (Harmon, 2007; Payne et al, 2006; Sigmon; 1974; Thorpe and Crompton, 2004; Zihlman et al. 2011) to reflect the greater need for circumduction of the thigh in *Pongo* due to its increased arboreality in comparison to the other groups.

The *Pongo pygmaeus* iliac crest seemed to be intermediate in shape between the *Pan troglodytes* and *Gorilla sp.* subsets, being relatively longer and flatter than in *Pan* but with less anterior curvature than *Gorilla.* This could indicate that in *Pongo* the attachment for *m. latissimus dorsi* shows a compromise between the increased body mass that *Pongo* shares with *Gorilla* but also the greater arboreality it shares with *Pan.* The *Pongo pygmaeus* acetabulum was relatively larger than the *Pan* acetabulum, and was relatively wider antero-posteriorly.

The *Pongo pygmaeus* Os Coxa showed a rounder pelvic brim with a marginally more superior point of curve than the *Pan paniscus* subset and a relatively longer pubis, indicating greater origins for the adductors of the thigh.

The ischial tuberosity was oriented more superiorly than in the *Pan* subsets and was more robust also displaying slightly less curvature along its inferior border. This is the attachment for *m. ischiofemoralis* an important extensor of the thigh, useful in climbing.

The Os Coxa in Homo

The *Homo sapiens* Os Coxa differed most substantially from the groups. It was the most robust of all the groups, likely indicating its importance in weight bearing-supporting the trunk habitually erect posture (McHenry, 1974). The iliac crest was longer, thicker and had a sigmoid curve in the *Homo sapiens* group, reflecting the attachment of the *m. gluteus maximus* and its importance in extension in bipedal locomotion. The height of the iliac blade was relatively much reduced in comparison to the other groups, with a relatively shorter and broader ilium. The ilium was also more mediolaterally oriented than in the other species groups, meaning *m. gluteus minimus* and *m. gluteus medius* are in a position at side of pelvis allowing abduction of the thigh and support of the body during locomotion (Waterman, 1929; Ward, 1993).

It also displayed a relatively wide iliac pillar in comparison to the other groups- likely important in weight transmission through the pelvis and toward the lower limb. The *Homo sapiens* group showed a remarkably shorter lateral iliac border than the non-human ape groups. The auricular surface was relatively wider, also a feature of weight transmission from trunk to lower limb (Leutenegger, 1974.) The prominent greater sciatic notch, which develops as a function of the shortening of the ischium and orientation of the ilium as well as the proximity of the acetabular and sacroiliac joints and expansion of the ischial spine likely reflects bipedal adaptions (Hager, 1996) within the *Homo sapiens* Os Coxa.

The *Homo sapiens* pelvic brim is the most 'c' shaped and the most curved, with the shortest pubis, which formed a near right angle with the iliac portion. This is a function of the change in orientation of the ilia as well as the reduction in distance between the sacroiliac and acetabular joints (Lovejoy, 2005).

The *Homo sapiens* acetabulum was relatively larger than all the other species groups (Lovejoy, 2005). The lunate surface was also less rounded.

The ischial tuberosity was more superiorly oriented than all the non-human ape groups, was relatively longer, and the ischium as a whole much less curved. This difference in orientation indicated its importance as an attachment for *m. gluteus maximus* for extension in bipedal walking (Sigmon, 1974).

The Os Coxa of A.L. 288-1

The *Australopithecus afarensis* Os Coxa showed a similar level of robusticity to the *Homo sapiens* group.

The iliac blade was less flared than the *Homo sapiens* iliac blade, and more laterally oriented. It was also relatively longer sagitally than in the *Homo sapiens* group but showed a similar degree of curvature. The shape of the *Australopithecus afarensis* iliac crest was near identical to that of the *Homo sapiens* mean, although this was oriented slightly differently to the rest of the Os Coxa, with the lateral edge less anteriorly located than in the *Homo sapiens* subset. The ilium was relatively shorter than the non-human ape groups, and the auricular surface wider than those groups signifying (as per McHenry, 1974) the role of the sacroiliac joint in transferring the weight of the trunk onto the limbs, as expected in a modern biped. The *Australopithecus afarensis*

lateral iliac border was relatively shorter than that of the non-human ape subsets, but relatively longer than that of the *Homo sapiens* subset. Overall, however, it was nearer in relative length to the *Homo* group.

The *Australopithecus afarensis* pelvic brim was most similar in shape to that of the *Homo sapiens* group, although the point of maximum curvature was more inferior. It was broadly 'c' shaped but did exhibit a longer pubis, as seen in the non-human ape groups.

The greater sciatic notch displayed a greater curvature than the non-human ape groups. The angle of the ischial portion of the notch in *Australopithecus afarensis* was less medially oriented than in the *Homo sapiens* subset. It was, however, more medially oriented than the non-human ape subsets.

There was similar relative enlargement of the acetabulum as in *Homo sapiens*. The *Australopithecus afarensis* acetabulum shows slightly less widening of inferior border of the acetabulum than the *Homo sapiens* group. The lower portion of the lunate surface was also marginally narrower. It was relatively larger than the *Pan* and *Pongo pygmaeus* subsets and was most similar overall to the *Homo sapiens* group.

The ischial tuberosity and orientation of the ischium is similar in *Australopithecus afarensis* and the *Homo sapiens* mean. The ischial tuberosity was superiorly oriented as in the *Homo sapiens* sample, and the ischium less curved than that of the other non-human ape groups. It was similar in both its relative robusticity and length to that of the *Homo sapiens* subset. Its orientation, however was intermediate between the *Homo sapiens* group and the non-human ape groups and was reasonably perpendicular to the ilium.

These features show that the pelvis of *A. afarensis* was intermediate in many ways between *Homo sapiens* and the extant non-human apes. Whilst it exhibits some features associated with bipedalism in our own species (as per Lovejoy, 1979: 1980), with the exception of the shape of the iliac crest, these are not in the exact form as seen in *Homo sapiens.* This perhaps suggests that the species retained an arboreal component to its locomotor repertoire (as per Tuttle, 1981; Stern and Susman, 1981; 1983; 1991; 1993; Stern and Larson, 1993) and probably practiced a form of bipedalism different to that seen in *Homo sapiens* (as per Berge, 1991; 1993; 1994; Hunt, 1994).

3.2 The Sacrum

3.21 Definitions of the Landmarks of the Sacrum

Fourteen ‘true’ landmarks were used to determine the shape of the sacrum. Figure 3-29 illustrates these, and their full definitions can be found within Table 3-4.
Like the Os Coxa, the sacrum in the main lacks the discrete juxtaposition of tissues required for Type 1 landmarks. As such, the majority of the landmarks used to define its shape are Type 2. In total, a single Type 1 landmark, ten Type 2 landmarks and three Type 3 landmarks were defined. No semilandmarks were used on the sacrum.

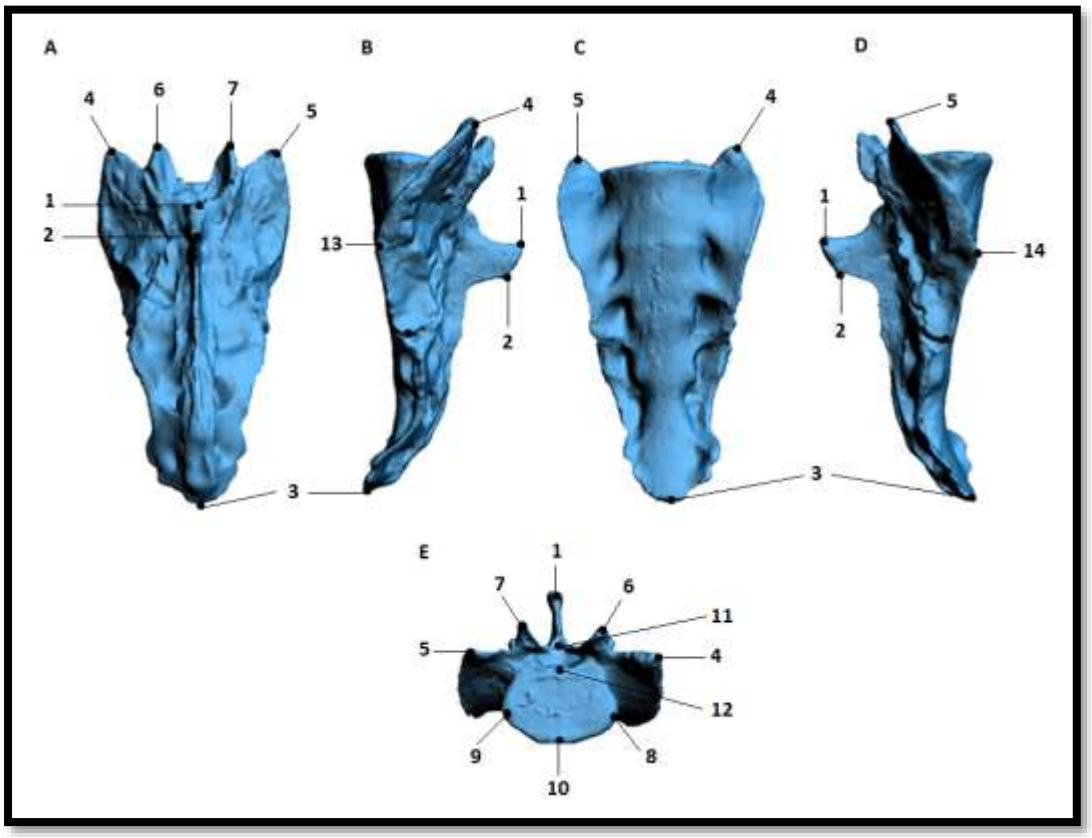

Figure 3-29: Posterior (A), Left (B), Anterior (C) , Right (D) and Superior (E) views of a sacrum depicting the ‘true’ landmarks used in this study.
Some of the landmarks are shown in multiple views. Full landmark definitions can be found in Table 3-4.

Table 3-4: The Three-Dimensional Landmarks of the Sacrum

No.	Landmark	Definition	Type
1	Superior spinous process	The most superior point of the tip of the most superior spinous process on the sacrum	II
2	Inferior spinous process	The most inferior point of the tip of the most superior spinous process of the sacrum	II
3	Distal sacrum	The most distal point on the sacrum	II
4	Superior sacral ala (right)	The most superior point of the sacral ala on the right hand side of the sacrum	II
5	Superior sacral ala (left)	The most superior point of the sacral ala on the left hand side of the sacrum	II
6	Superior articular process (right)	The most superior point of the articular process on the right hand articular surface of the sacrum	II
7	Superior articular process (left)	The most superior point of the articular process on the left hand articular surface of the sacrum	II
8	Lateral sacral plateau (right)	The most lateral extent of the sacral plateau on the right hand side	II
9	Lateral sacral plateau (left)	The most lateral extent of the sacral plateau on the left hand side	II
10	Sacral promontory	The tip of the sacral promontory	I
11	Base of spinous process	The centre of the lower-most point of the most superior spinous process of the sacrum, where it meets the sacral body	II
12	Posterior sacral plateau	The point on the posterior border of the sacral plateau directly opposite landmark 10	III
13	Maximum anterior extent sacral ala (right)	The most anterior point of the sacral ala on the right hand side	III
14	Maximum anterior extent sacral ala (left)	The most anterior point of the sacral ala on the left hand side	III

[a]As taken from Bookstein (1991)

3.22 Results of the Geometric Morphometric Analysis of the Sacrum

A Generalised Procrustes Analysis (GPA) was conducted on the sacrum, determining the Procrustes Distance within each species group. The Procrustes Distances confirmed that across the species, the sacrum was the most variable bone with a Procrustes Distance of 2.25542, and this was borne out in my personal observations. The Procrustes Distances in the sacrum showed it to be the most variable in shape within each species. The *Pongo pygmaeus* sample showed the greatest similarity in shape with a Procrustes distance of 0.14199, followed closely by the *Homo sapiens* sample and *Pan paniscus* samples with Procrustes Distances of 0.17680 and 0.19697 respectively. The *Gorilla sp.* and *Pan troglodytes* samples showed the least consistency in shape across the sacrum with Procrustes Distances of 0.29439 and 0.34413 in that order. Full details of these tests can be found in the Appendix.

The Principal Components Analysis conducted on all species, including the *Australopithecus afarensis* sample, using all landmarks and semilandmarks showed that the first principal component explained 23.07% of the variance and the second explained 17.42% of the variance- a cumulative amount of 40.49% (see Appendix).

When the first two principal components were plotted against each other (Figure 3-30), the sacrum is shown to be relatively variable across species groups, although there did appear to be some separation of the groups. The *Gorilla sp.* and *Pongo pygmaeus* subsets appeared to be the most variable, with the *Homo sapiens, Pan paniscus* and *Pan troglodytes* being more tightly grouped. The *Australopithecus afarensis* individual was most closely associated with the *Homo sapiens* subset.

The data was normally distributed (see Appendix). The Levene's tests showed that PC1 $F(4, 65) = 3.188$, $p = 0.019$ – at the .05 alpha level and PC2 $F(4,65)=1.238$, $p=0.304$. As the data were normally distributed and the assumption of Homogeneity of Variance was only met on Principal Component 2, a Welch test for equality of means was undertaken. This showed a significant difference in the means with PC1 $F(4;24.58)=47.86$, $p=0.000$ and PC2 $F(4;25.89)=3.97$, $p=0.12$. As such, an ANOVA was conducted further explore the nature of the variance between the species groups (see Appendix).

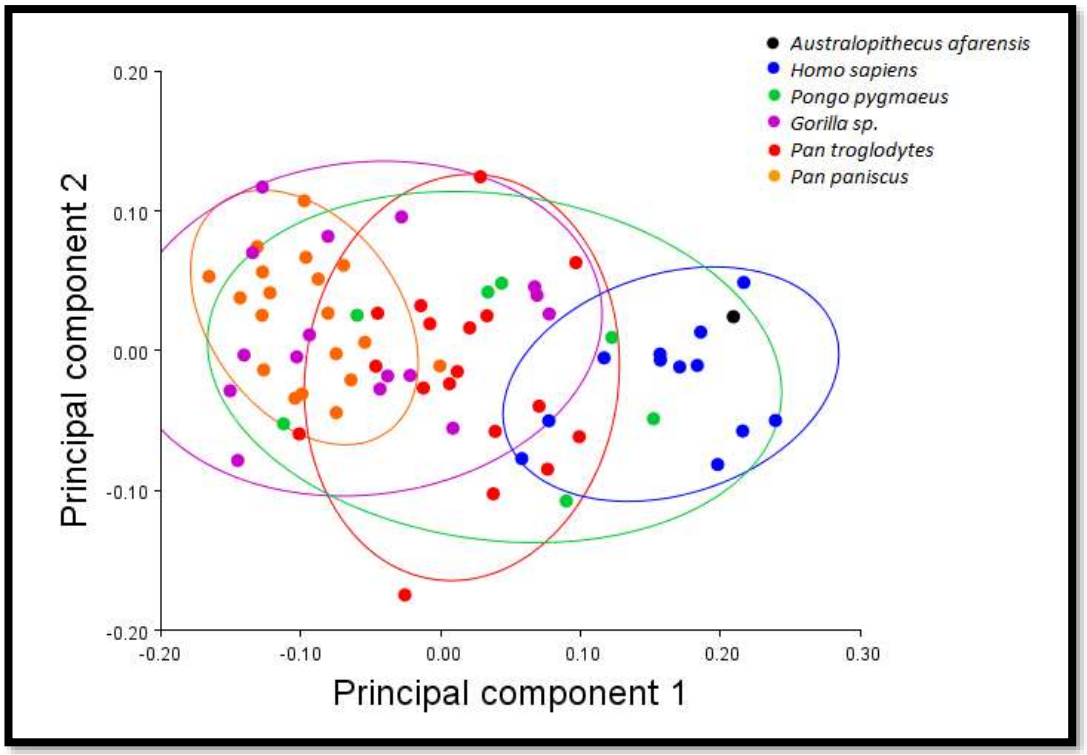

Figure 3-30: Plot of Principal Component 1 against Principal Component 2 for All Landmarks and Semilandmarks Across All Species' Sacrum

The ANOVA showed that there was a significant difference in the species groups at a $p<0.05$ level along both principal components. As equal variances were not assumed, a Games-Howell post hoc test was used, instead of a Tukey post hoc test, to assess how the species groups varied.

The Games-Howell post hoc test along Principal Component1 (see Appendix) showed that there was no significant difference between the *Pan paniscus* and *Gorilla sp.* subsets. The *Pan troglodytes* and *Gorilla sp.* subsets did not differ significantly from the *Pongo pygmaeus* subset. The *Homo sapiens* group also did not differ significantly from the *Pongo pygmaeus* subset and, in fact, the *Pongo pygmaeus* subset only differed significantly from the *Pan paniscus* group. Along Principal Component 2, only the *Pan paniscus* and *Homo sapiens* groups differed significantly from each other.

Shape changes indicated by the Principal Components

The changes in the shape of the sacrum along Principal Components 1 and 2 are illustrated in Figure 3-31. The anterior and posterior views showed a decrease in width coronally along Principal Component 1. With this decrease in width, a corresponding increase in length was seen. When viewed from the side, an overall decrease in robusticity was evident, along with the change in length. The angle of sacral tilt was increased along the first Principal component, and the curvature of the lower sacral vertebrae decreased. In the superior view, a decrease in both the relative size of the sacral alae and sacral plateau was visible along Principal Component1.

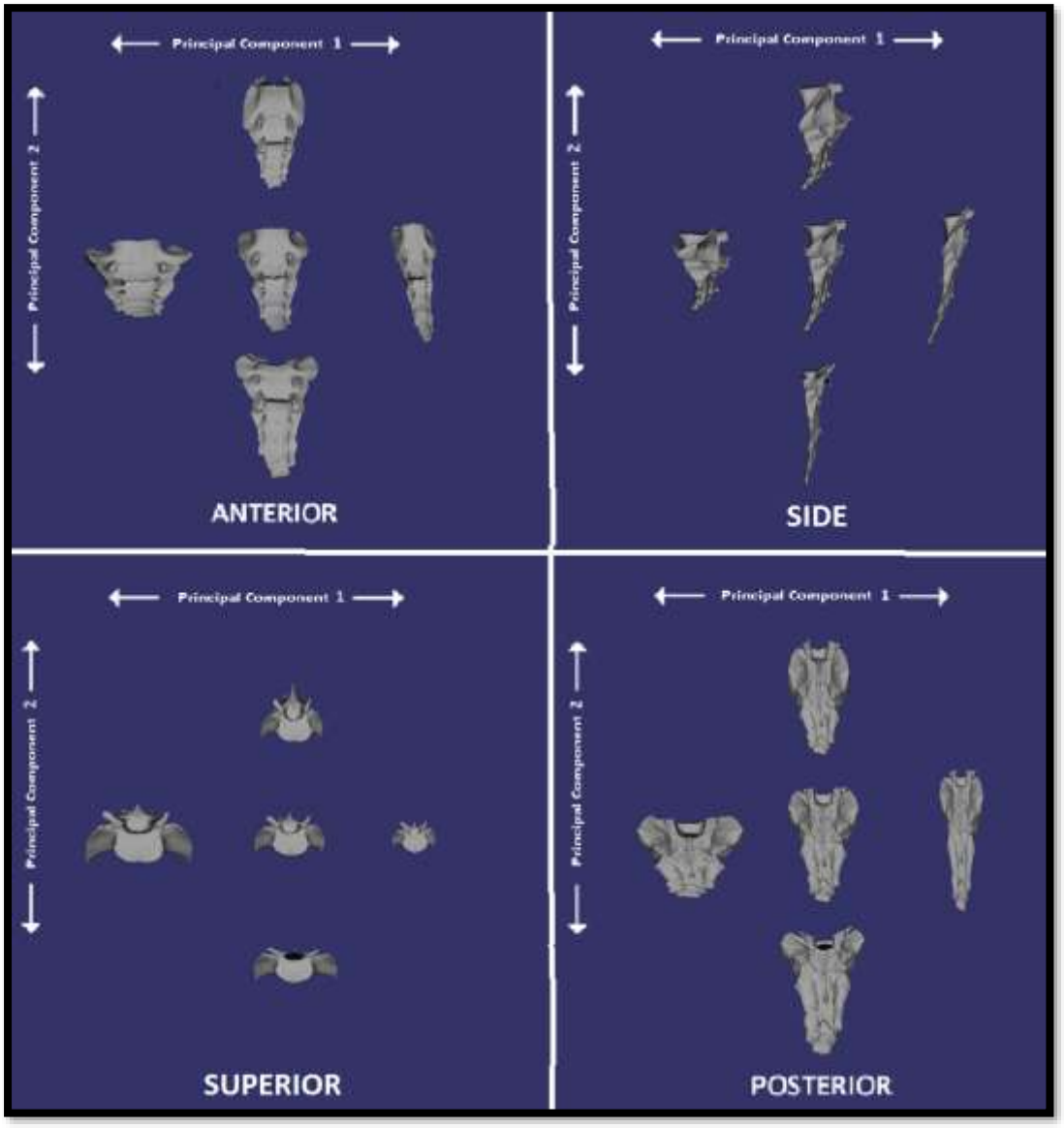

Figure 3-31: Changes in Sacrum Shape along Principal Components 1& 2, shown in Anterior, Side, Superior and Posterior Views
Mean Sacrum Shape shown centrally and the Extremes of each Principal Component surrounding this

Principal Component 2 showed a change from a more broad triangular shape, with widely flaring alae, to a near rectangular shape, with alae that were far less flared. Additionally, the alae were much shorter in length relative to the rest of the sacrum. There was also shown to be an increase in the antero-posterior width of the sacral body. There was also an increase in the relative length of the spine of the first sacral vertebra.

Shape changes across the species groups

The changes along each Principal Component were reflected in the shape of the sacrum in each species (Figure 3-33). The *Pan paniscus* mean sacral shape was the most gracile of the species groups, and was narrower than the others in the antero-posterior plane. It was also the longest relative to the others. The *Gorilla sp.* subset, although relatively more robust than the *Pan paniscus* group was very similar in shape. The *Pan troglodytes* group was both shorter and wider than the *Pan paniscus* and *Gorilla sp.* subsets, with much wider flaring alae and a relatively larger sacral plateau. The *Homo sapiens* group were shown to be the most robust overall, with the shortest relative length and widest relative width. This group had the largest sacral plateau relative to the rest of the sacrum and also the largest and widest flaring alae. It also displayed the smallest angle of sacral tilt. The *Pongo pygmaeus* group was most different from the *Pan paniscus* group, being relatively shorter, broader and more robust, with a lesser angle of sacral tilt and much larger and more flared alae.

Figure 3-32: The Sacral Shape of *Australopithecus afarensis*

The shape of the *Australopithecus afarensis* sacrum (Figure 3-32) was most similar to that of the *Homo sapiens* group, although slightly longer and less robust. It displayed a relatively large sacral plateau in comparison to the other groups, and relatively wide, flaring alae. There was also a relatively low angle of sacral tilt, compared to the other groups.

Musculature associated with the Sacrum

The sacrum forms an origin for muscles which attach to the femur (Table 3-5). The sacrum was not considered with semilandmarks and only true landmarks were used. As such, all landmarks were used in judging the placement of *m. gluteus maximus* and *m. piriformis*.

Table 3-5: Muscles with their origin on the Sacrum and the affinity of A.L. 288-1 based on Geometric Morphometric results

Muscle	Associated Landmarks	Affinity of A.L. 288-1
Gluteus Maximus	All	*Homo sapiens*
Piriformis	All	*Homo sapiens*

As the *Australopithecus afarensis* sample grouped most closely with the *Homo sapiens* subset, *m. gluteus maximus* and *m. piriformis* were placed on the model as in *Homo sapiens.*

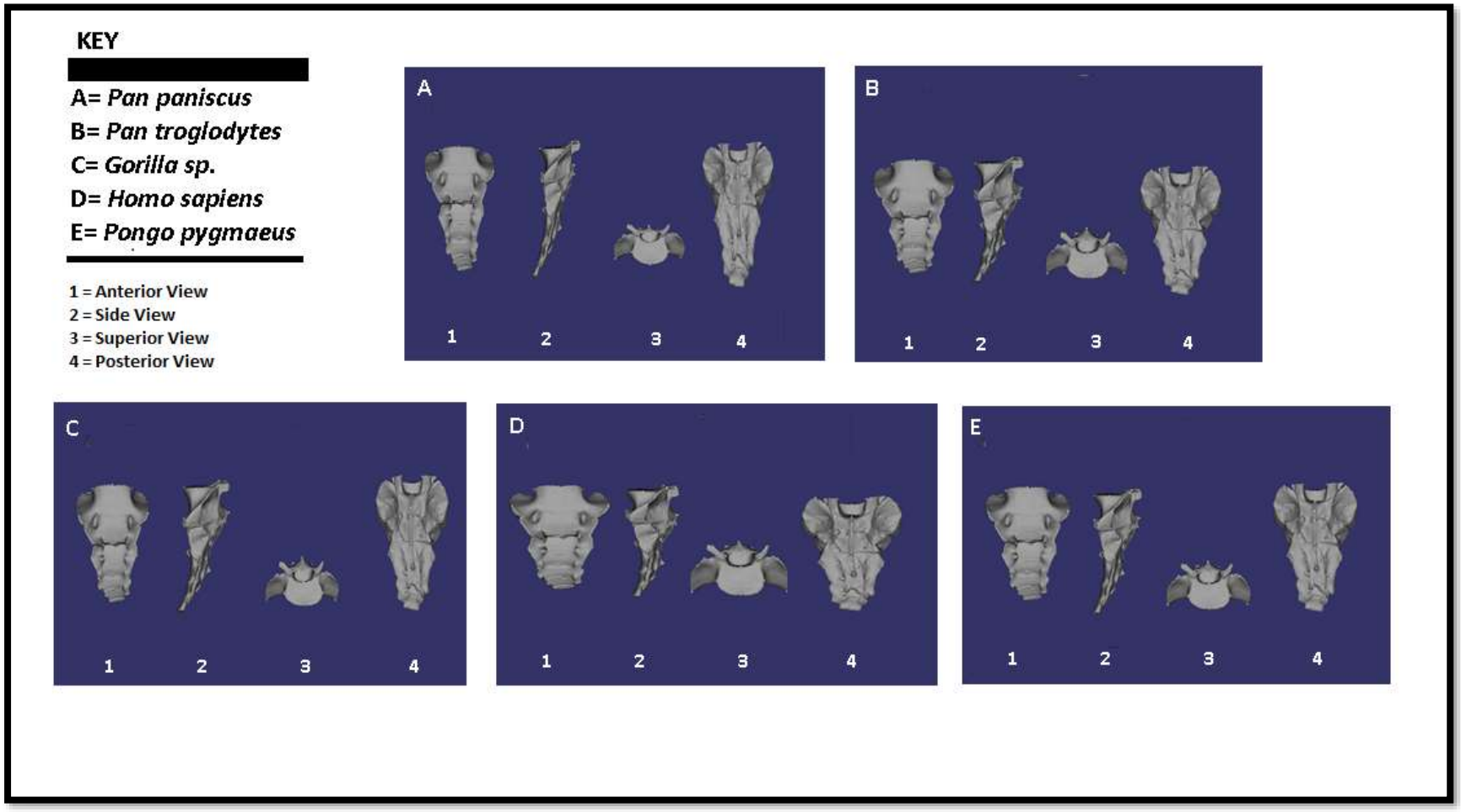

Figure 3-33: Mean Sacrum shape for each species subset, shown in Anterior, Side, Superior and Posterior views

3.23 Summary of the Shape and Musculature of the Sacrum

The sacrum was variable across all species. The *Pan paniscus* mean sacral shape was the most gracile of the species groups, and was relatively longer and narrower than the other groups. The *Gorilla sp.* subset, although relatively more robust than the *Pan paniscus* group was very similar in shape. The *Pan troglodytes* group was both shorter and wider than the *Pan paniscus* and *Gorilla sp.* subsets, with much wider flaring alae and a relatively larger sacral plateau. The *Pongo pygmaeus* group was most different from the *Pan paniscus* group, being relatively shorter, broader and more robust, with a lesser angle of sacral tilt and much larger and more flared alae. The *Homo sapiens* sacrum was the most robust overall, with the shortest relative length and widest relative width. This group had the largest sacral plateau relative to the rest of the sacrum and also the largest and widest flaring alae. It also displayed the smallest angle of sacral tilt. The broadening and shortening of the sacrum are indicative of two major differences between the extant non-human apes, and the *Homo sapiens.* Firstly, the change in the orientation of the ilia combined with the need to transmit the weight of the trunk into the lower limb for bipeds, means that the sacrum needs to broader in bipeds. Secondly, the relative shortening of the ilia leads to a relative shortening of the sacrum (Lovejoy, 2005).

The sacrum of A.L. 288-1

The shape of the *Australopithecus afarensis* sacrum was most similar to that of the *Homo sapiens* group, although slightly longer and less robust. It displayed a relatively large sacral plateau in comparison to the non-human apes, and relatively wide, flaring alae, as seen in *Homo sapiens*. There was also a relatively low angle of sacral tilt. This configuration, as in modern bipeds is indicative of the weight transmission from the trunk to the lower limb, and the re-orientation and shortening of the ilia.

3.3 The Femur

3.31 Definitions of the Landmarks of the Femur

Landmarks of the Femur

There were 20 landmarks of the femur. As with the landmarks of the sacrum, the majority of these were Type 2. These are illustrated in Figure 3-34, and full definitions can be found in Table 3-6. Of the landmarks, 15 were considered to be Type 2, and 5 were considered to be Type 3. There were no Type 1 Landmarks. Curved Semilandmarks were also used. These are illustrated in Figure 3-35, and fully defined in Table 3-7.

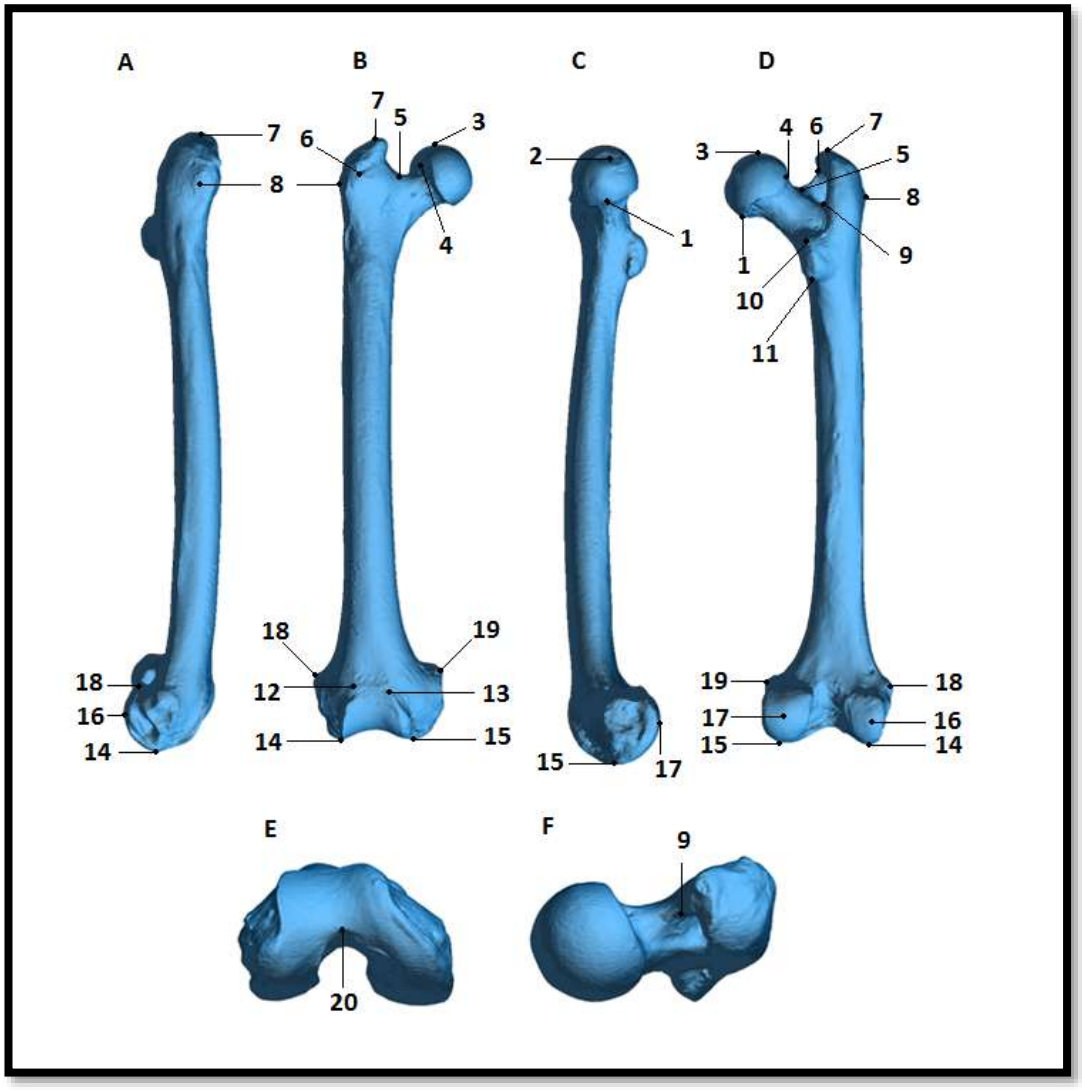

Figure 3-34: Lateral (A), Anterior (B), Medial (C), Posterior (D), Inferior (E) and Superior (F) views of a femur depicting the landmarks used in this study.
Full definitions can be found in Table 3-6. Some landmarks pictured in multiple views

Table 3-6: The Landmarks of the Femur

No.	Landmark	Definition	Type[a]
1	Inferior head/neck border	The most inferior point on the femoral head/neck border at the midline of the neck on the medial aspect.	III
2	Fovea capitis	The centre of the fovea capitis. Where this is absent, it is the centre of the femoral head on the medial aspect.	II
3	Superior head	The most superior point on the head, along the midline.	III
4	Superior head/neck border	The most superior point on the femoral head/neck border at the midline of the neck on the lateral aspect.	III
5	Neck midpoint	The midpoint on the femoral neck between Landmark 1 (Inferior head/neck border) and Landmark 7 (Superior greater trochanter).	III
6	Neck/greater trochanter border	The most anterior point on the border between the neck and the greater trochanter.	II
7	Superior greater trochanter	The most superior point on the greater trochanter.	II
8	Lateral greater trochanter	The most lateral point on the greater trochanter.	II
9	Trochanteric fossa	The deepest point on the trochanteric fossa.	III
10	Superior lesser trochanter	The most superior point on the plateau of the lesser trochanter.	II
11	Inferior lesser trochanter	The most inferior point on the plateau of the lesser trochanter.	II
12	Anterior lateral condyle	The most superior point on the anterior aspect of the lateral femoral condyle/patella surface.	II
13	Anterior medial condyle	The most superior point on the anterior aspect of the medial femoral condyle/patella surface.	II
14	Inferior lateral condyle	The most inferior point on the lateral femoral condyle.	II
15	Inferior medial condyle	The most inferior point on the medial femoral condyle.	II
16	Posterior Lateral condyle	The most posterior point on the lateral femoral condyle.	II
17	Posterior medial condyle	The most posterior point on the medial femoral condyle.	II
18	Superior lateral condyle	The most superior point on the lateral border of the lateral femoral condyle.	II
19	Superior medial condyle	The most superior point on the lateral border of the medial femoral condyle.	II
20	Anterior intercondylar notch	The most anterior point on the intercondylar notch.	II

[a] As taken from Bookstein (1991). Landmarks 1-10 adapted from Harmon (2007)

Semilandmarks of the Femur

Four curves were created on the femur for this study. These are illustrated in Figure 3-35 and full definitions can be found in Table 3-7. They were chosen as areas important to muscle attachment and as areas with important functional roles in locomotion. Each curve was composed of between 22 and 57 discrete semilandmark points.

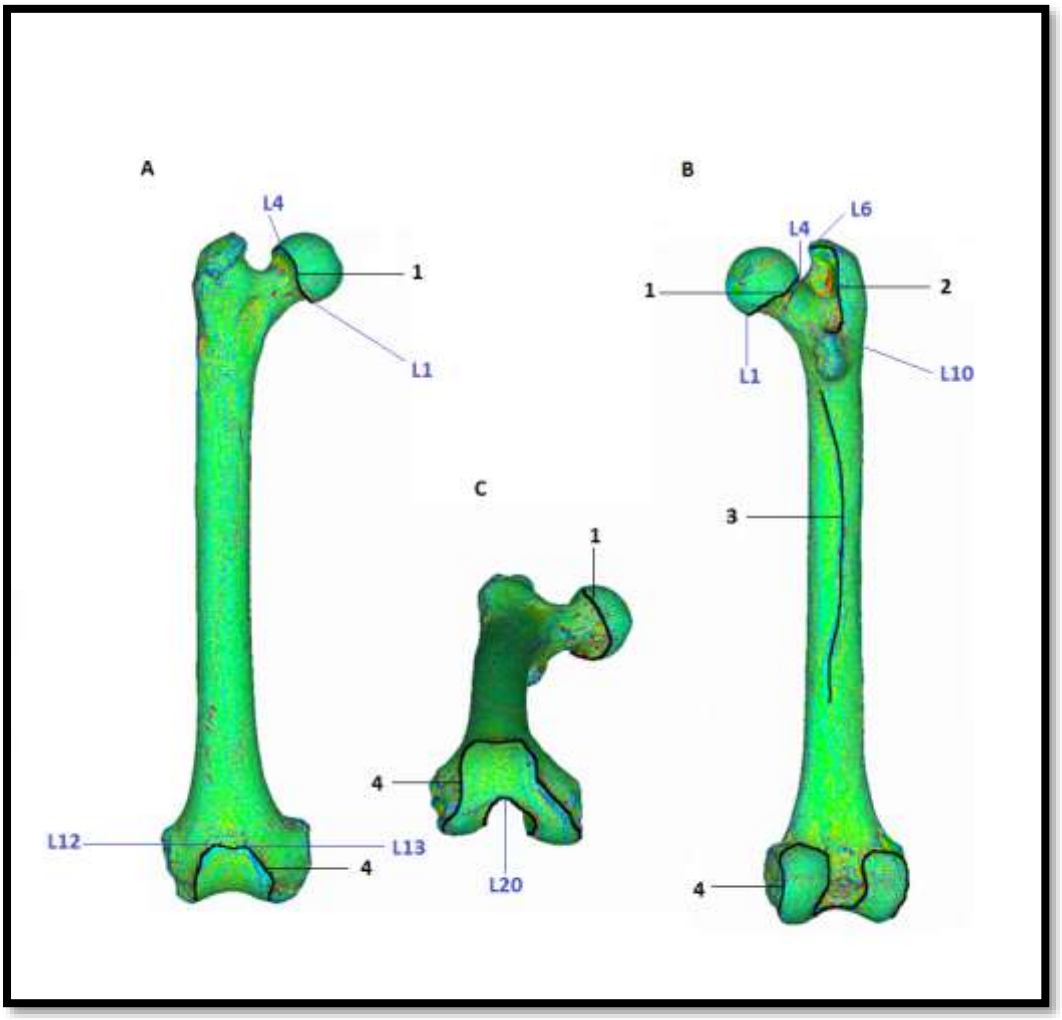

Figure 3-35: Anterior (A), Posterior (B) and Antero-inferior (C) views of a femur depicting the semilandmark curves used in this study.

See Table 3-7 for full definitions. Relevant landmarks are shown in blue.

Table 3-7: The Curved Semilandmarks of the Femur

No.	Curve	Definition	No. of Points
1	Margin of femoral head	The curve formed along the line of maximum curvature along the margin of the femoral head passing through Landmark 1 (Inferior head/neck border) and Landmark 4 (Superior head/neck border). It is digitised from Landmark 4 and moving posteriorly and inferiorly to Landmark 1, and then anteriorly and superiorly back to Landmark 4 along the line of maximum curvature.	25
2	Greater trochanter and intertrochanteric crest	The curve formed along the line of maximum curvature from Landmark 6 (Neck/greater trochanter border) to Landmark 10 (Superior Lesser trochanter). It is digitised from Landmark 6 and moving posteriorly and inferiorly along the line of maximum curvature to Landmark 10.	22
3	Linea aspera	The curve formed along the line of maximum curvature which denotes the linea aspera on the posterior/posterolateral surface of the femur. It is digitised from its most superior point beneath the lesser trochanter along the line of maximum curvature inferiorly until the point that it terminates.	57
4	Femoral condyles	The curve formed along the line of maximum curvature denoting the femoral condyles and patella surface of the femur, and passing through Landmark 12 (Anterior lateral condyle), Landmark 13 (Anterior medial condyle) and Landmark 20 (Anterior intercondylar notch). It is digitised along the line of maximum curvature from Landmark 12 and moving medially to Landmark 13, then inferiorly and medially, before moving posteriorly and superiorly. The line of maximum curvature is followed laterally and then anteriorly and laterally to Landmark 20, before moving posteriorly and laterally. It then moves superiorly to join with Landmark 12, where it terminates.	51

3.32 Results of the Geometric Morphometric Analysis of the Femur

All Landmarks and Semilandmarks of the Femur Across All Species

A Generalised Procrustes Analysis (GPA) was conducted on the femur, determining the Procrustes Distance within each species group. The femur showed the least variability in shape across the species, with a Procrustes Distance of 0.17216. The shape of the femur was shown to be relatively consistent within each species, with the least variation in shape found in the *Pongo pygmaeus* sample with a Procrustes Distance of 0.00870. *Pan paniscus* showed slightly more variation within the sample with a Procrustes Distance of 0.00905, followed closely by the *Homo sapiens* sample with a Procrustes Distance of 0.01182. There was a marginally greater variation in shape within the *Pan troglodytes* sample, and the largest variability was found within the *Gorilla sp.* sample (see Appendix).

A Principal Components Analysis was conducted on all Landmarks and Semilandmarks of the femur across all species groups. The first principal component explained 42.64% of the variance and the second explained 15.96%, cumulatively 58.60% (see Appendix). When the first two principal components are plotted against each other (Figure 3-36), clear differentiations between the species groups were revealed. The *Pongo pygmaeus* cluster were clearly separated along Principal Component 2, but grouped with the other extant apes on Principal Component 1. The *Pan troglodytes* group and the *Pan paniscus* group also clustered together, although within the *Pan troglodytes* group, the *Pan paniscus* group could be distinguished as they clustered within a smaller range. A.L. 288-1 was very clearly grouped with the *Homo sapiens* sample.

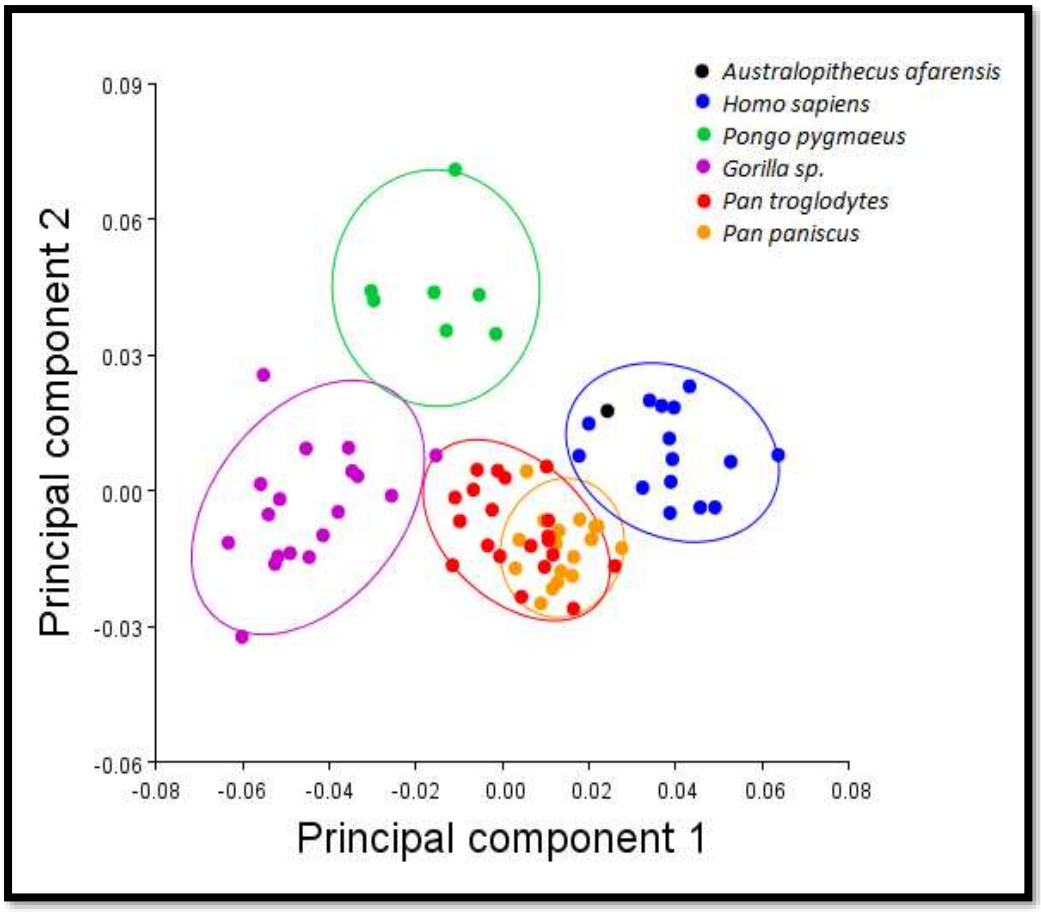

Figure 3-36: Principal Components Analysis of all Landmarks and Semilandmarks of the femur showing PC1 and PC2

A Shapiro-Wilk test was conducted on the first two principal components to determine if these were normally distributed (see Appendix), as abnormal distribution could have skewed the results. The significance values for each species on Principal Component 1 were greater than 0.05, indicating that the data on PC1 were normally distributed. Along Principal Component 2, the data for the *Pan paniscus*, *Pan troglodytes*, *Gorilla sp.* and *Homo sapiens* were normally distributed. The *Pongo pygmaeus* data for Principal Component 2 were not normally distributed, with a significance value of 0.009. This was not necessarily surprising as the *Pongo pygmaeus* group had a very small sample size, all of whom were male. As such, the *Pongo pygmaeus* results should be treated with a measure of caution.

A Levene's Test was conducted to determine whether there was homogeneity of variance for the principal component groups. The Levene's tests were not significant; PC1 $F(4, 72) = 1.349$, $p = .260$ – at the .05 alpha level and PC2 $F(4,72)=1.227$, $p=.307$.

Thus, both the assumptions of homogeneity of variance and normality were met, and an ANOVA could be conducted. A between groups ANOVA was conducted to determine whether there was a significant difference between the species groups (see Appendix). The significance level is 0.000 (p = .000), which is below 0.05 and, therefore, there is a statistically significant difference between the groups.

Groups that could be reliably separated indicated that the overall shape as determined by all the landmarks and semilandmarks was different enough between species to warrant further analysis. As the assumption of homogeneity of variance was met, a Tukey post hoc test was used to determine which groups were significantly different from each other (see Appendix). These showed that there were significant differences between the species groups in Principal Component 1, with the exception of *Pan paniscus* and *Pan troglodytes* which did not differ significantly. In Principal Component 2, *Pongo pygmaeus* and *Homo sapiens* were clearly distinct from each other and the other groups.

Shape changes indicated by the Principal Components

Along Principal Component 1 the relative length of the femoral shaft was shown to decrease (Figure 3-37). The shaft was also shown to increase in its circumference. Both the femoral head and the femoral condyles were shown to become relatively larger along the first principal component. In the lateral view, an increase in the antero-posterior curvature of the shaft was noted- particularly in the posterior of the supra-condylar area. In the medial view, Principal Component 1 showed a shift in the position of the femoral head and greater trochanter anteriorly and the shape of the medial femoral condyle became more rounded. Posteriorly, Principal Component 1 showed that there was a change in the size of the femoral condyles relative to each other (i.e.: the negative extreme of Principal Component 1 showed a larger lateral femoral condyle, and at the extreme positive end of Principal Component 1 the medial femoral condyle was relatively larger). The femoral condyles overall are also much increased in their relative size at the extreme positive end of Principal Component 1. The intertrochanteric crest both lengthened and became more sagitally oriented along the first principal component.

Principal Component 2 showed a change in the curvature of the landmarks along the femoral shaft from medially concave to medially convex. There was also a change in the size and the orientation of the femoral head.

Shape changes across the species groups

In order to determine what this meant in terms of shape, the shape of the femur for each species mean was compared (Figure 3-38).

The shape of the femur in the *Pan paniscus* and *Pan troglodytes* groups were very similar, with the *Pan paniscus* mean marginally more gracile than that of the *Pan troglodytes* group. The *Gorilla sp.* group were shown to be the most robust overall, with a shorter shaft in relation to the femoral head and condyles. These were also shown to be relatively larger in comparison to the other groups. The *Homo sapiens* group had the longest femoral shaft in comparison to the other species groups. The femoral condyles in the *Homo sapiens* group were also noticeably laterally inclined, a trait which was shared by the *Pongo pygmaeus* group. The *Pongo pygmaeus* group also had relatively large femoral condyles and head, and relatively large and laterally leaning greater trochanter in comparison to the other groups.

The *Australopithecus afarensis* femur (Figure 3-39) was very similar to the *Homo sapiens* mean shape, with a relatively long femoral shaft, and laterally inclined femoral condyles.

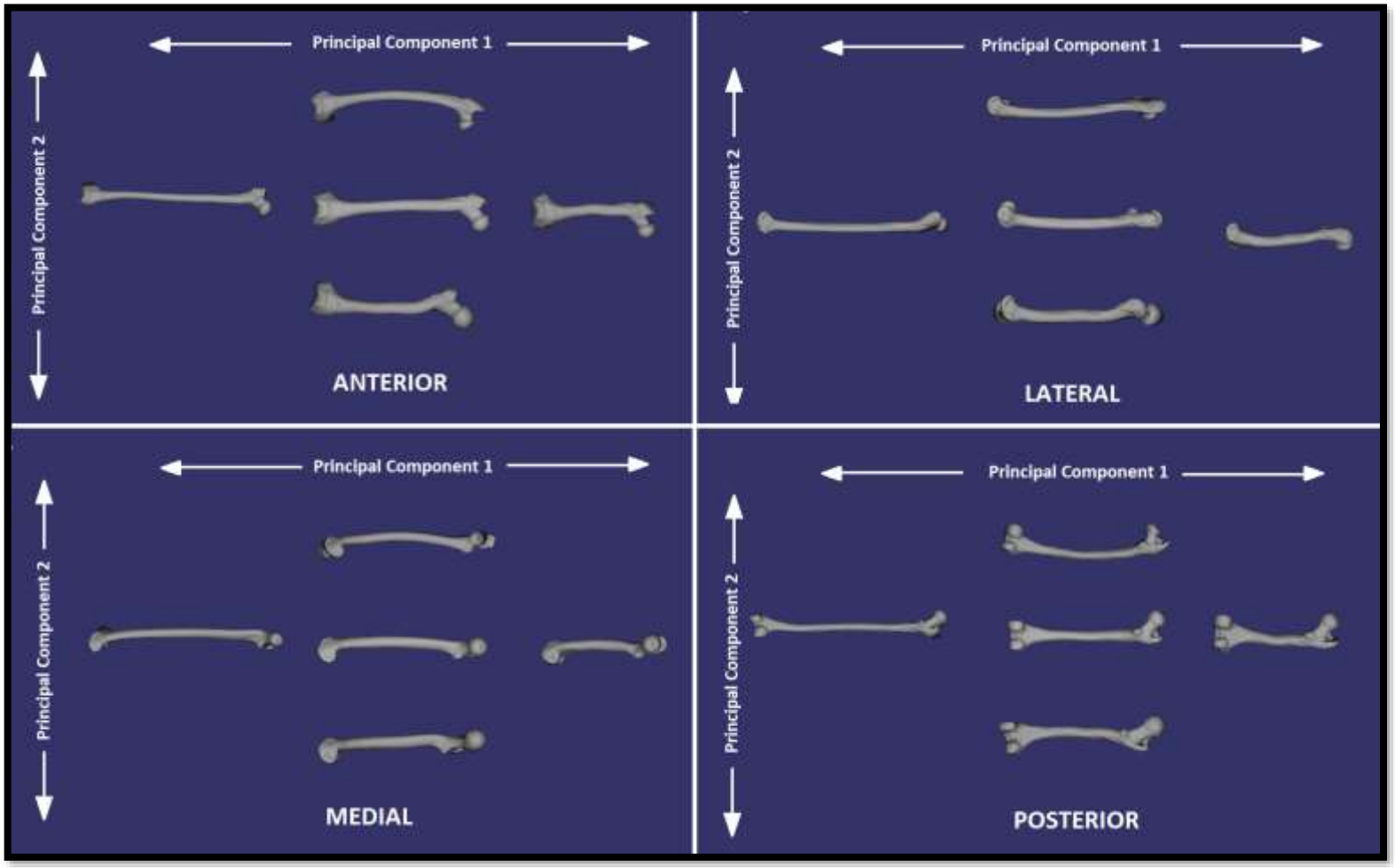

Figure 3-37: Changes in Femur Shape along Principal Components 1& 2, shown in Anterior, Lateral, Medial and Posterior Views
Mean Femur Shape shown centrally and the Extremes of each Principal Component surrounding this

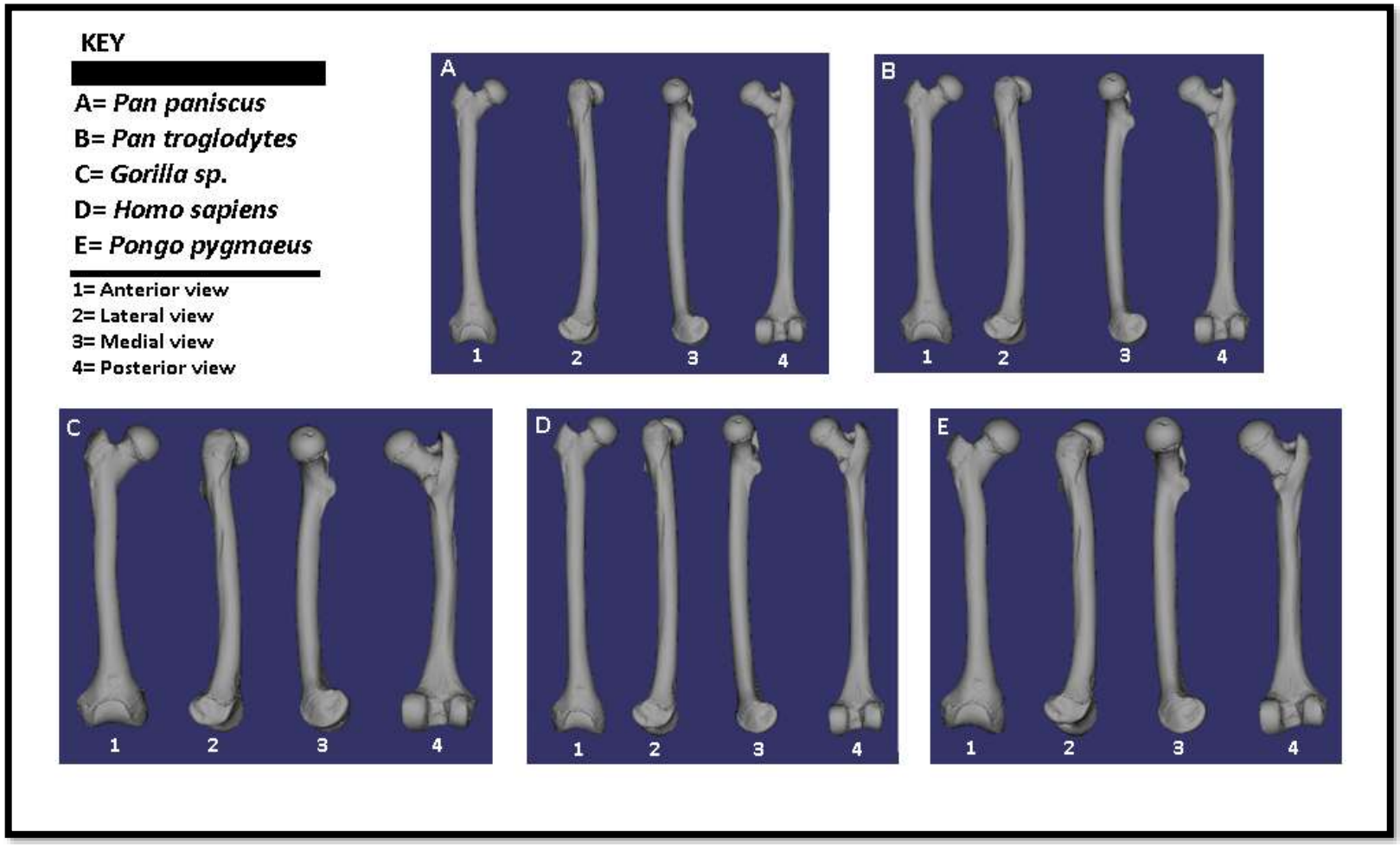

Figure 3-38: Mean Femur shape for each species subset, shown in Anterior, Lateral, Medial and Posterior views

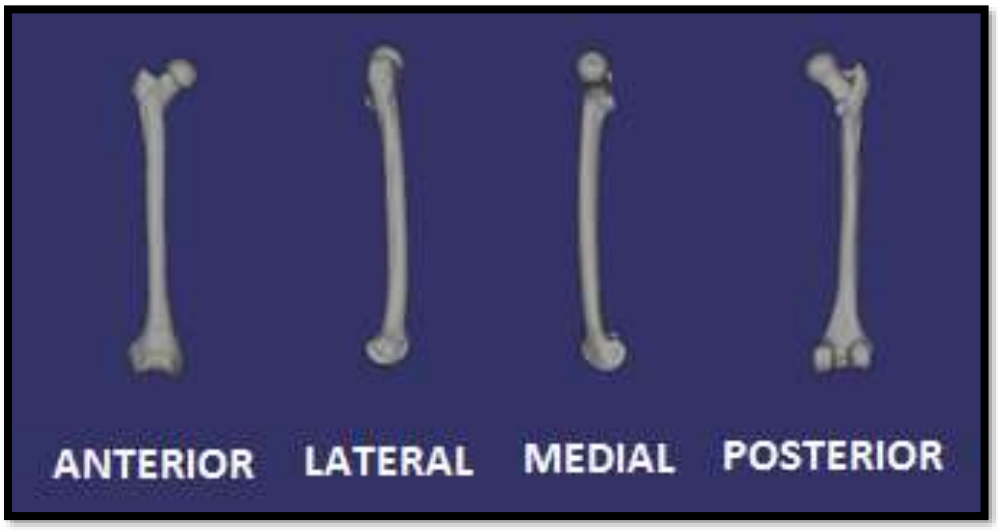

Figure 3-39: The shape of the *Australopithecus afarensis* femur using all Landmarks and Semilandmarks

Overall Musculature of the Femur

The femur serves as both an origin for muscles which cross the knee and as an insertion for muscles which cross the hip. The muscles which originate on the femur (Table 3-8) and cross the knee allow for movement of the leg- including flexion and extension and medial and lateral rotation of the leg. The muscles which insert on the femur (Table 3-9) allow for movement of the thigh at the hip and take their origin from the sacrum and the Os Coxa. In all cases, the landmarks and semilandmarks of the femur in *Australopithecus afarensis* showed an affinity with the *Homo sapiens* sample.

Table 3-8: Muscles with their origin on the Femur and the affinity of A.L. 288-1 based on Geometric Morphometric results

Muscle	Associated Landmarks	Affinity of A.L. 288-1
Biceps Femoris SH	SL 3	*Homo sapiens*
Gastrocnemius	SL 4	*Homo sapiens*
Plantaris	SL 4 ?	*Homo sapiens*
Popliteus	SL 4	*Homo sapiens*
Vastus Medialis	SL 3	*Homo sapiens*
Vastus Lateralis	SL 3	*Homo sapiens*
Vastus Intermedius	Shaft	*Homo sapiens*

Table 3-9: Muscles with their insertion on the Femur and the affinity of A.L. 288-1 based on Geometric Morphometric results

Muscle	Associated Landmarks	Affinity of A.L. 288-1
Adductor brevis	SL 3	*Homo sapiens*
Adductor longus	SL 3	*Homo sapiens*
Adductor magnus	SL 3	*Homo sapiens*
Adductor magnus (Ham)	SL 4	*Homo sapiens*
Gemellus inferior	SL 2	*Homo sapiens*
Gemellus superior	SL 2	*Homo sapiens*
Gluteus Maximus	SL 2	*Homo sapiens*
Gluteus Maximus	SL 2	*Homo sapiens*
Gluteus Medius	SL 2	*Homo sapiens*
Gluteus Minimus	SL 2	*Homo sapiens*
Iliopsoas	SL 2/ 10 11	*Homo sapiens*
Obturator externus	SL 2	*Homo sapiens*
Obturator internus	SL 2	*Homo sapiens*
Pectineus	10 11	*Homo sapiens*
Piriformis	SL 2	*Homo sapiens*
Quadratus femoris	SL 2	*Homo sapiens*

Landmarks and Semilandmarks

In order to determine the changes in shape for specific areas of the femur, Principal Component Analyses were conducted on the 'True Landmarks' and each subset of Semilandmarks across all species groups.

The Principal Component Analysis conducted on just the True Landmarks of the femur across all species groups showed that the first Principal Component explained 38.60% of the variance and the second explained 14.82%, cumulatively 53.42%. When conducted on the Landmarks and Semilandmarks of the femoral head across all species groups, the first Principal Component explained 37.47% of the variance and the second explained 13.46%, totalling 50.93%. The first two principal components when the True Landmarks and the Semilandmarks of the greater trochanter and intertrochanteric crest were examined explained 40.15% and 13.07% respectively, totalling 53.22%. For the True Landmarks and the Semilandmarks of the medial linea aspera, the first Principal Component explained 44.70% of the variance and the second

explained 16.19%, cumulatively 60.89%. On all Landmarks and Semilandmarks of the femoral condyles across all species groups, the first two principal components explained 46.59% and 12.89% of the variance respectively, for a total of 59.49% (see Appendix). In all cases, as expected, the first principal component contributed most significantly to the overall shape, with between 37.47% and 46.59% of the variance, whereas the second principal component only explained between 12.89% and 16.89%. In all cases, the combined variance explained by the first two principal components was over 50%.

The first two principal components in each Semilandmark set were plotted against each other (Figure 3-40). The resultant plots showed that in each Semilandmark set largely showed clear differentiation between the species groups. The *Pan paniscus* and *Pan troglodytes* groups showed the greatest overlap, and the *Australopithecus afarensis* specimen plotted clearly with the *Homo sapiens* group in every case. The *Pongo pygmaeus* and *Gorilla sp.* plotted closely along the first principal component. There was the greatest separation in the groups along the first principal component, although the *Gorilla sp.* group was differentiated along the second principal component in the majority of cases. ANOVAs were conducted, each semilandmark set having largely met the assumptions of normality and Homogeneity of Variance, with each showing a significant difference in all Semilandmark sets for both principal components (see Appendix).

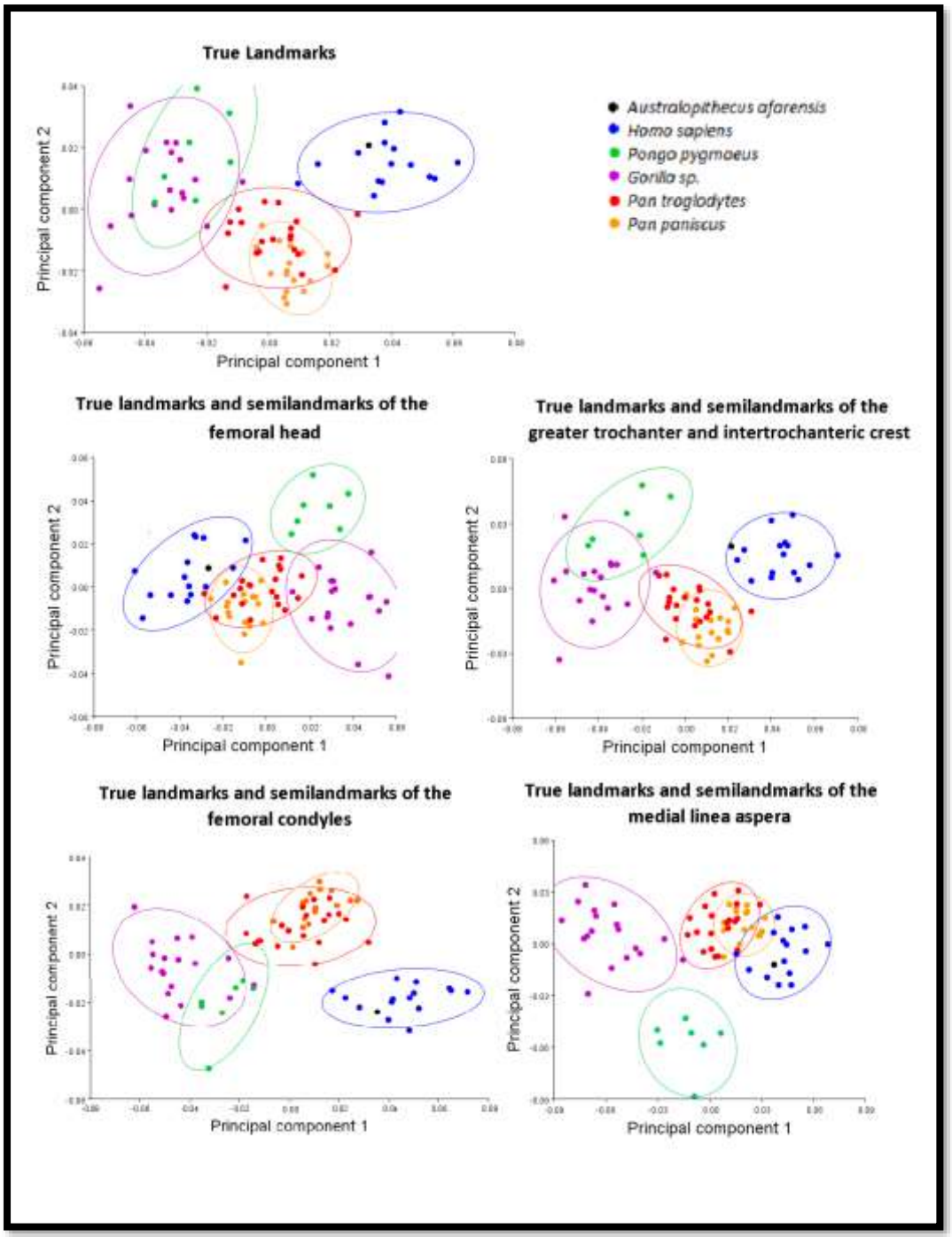

Figure 3-40: Plots of Principal Component 1 against Principal Component 2 for Each Semilandmark Set of the Femur across All Species Groups

True landmarks

When the first Principal Component was plotted against the second Principal Component, there was a clear separation between the extant apes and the *Homo sapiens* sample (Figure 3-40). There was overlap with between the *Gorilla sp.* group and the *Pongo pygmaeus* group. There was also a clear overlap between the *Pan paniscus* and *Pan troglodytes* groups. AL 288-1 fitted clearly into the *Homo sapiens* group. The majority of the variation between the groups was seen along Principal Component 1. An ANOVA there were significant differences along both Principal Component 1 and 2 and Tukey post hocs (see Appendix) showed that along Principal Component 1, the *Gorilla sp.* and *Pongo pygmaeus* subsets grouped together, as did the *Pan troglodytes* and *Pan paniscus* subsets. The *Homo sapiens* subset did not group with any other extant group. Along Principal Component 2, the *Pan paniscus* and *Pan troglodytes* subsets grouped together, as did the *Gorilla sp, Homo sapiens* and *Pongo pygmaeus* subsets.

Shape changes indicated by the Principal Components

The first principal component showed a decrease in shaft length, and an increase in the relative size of the femoral head and femoral condyles. The relative height of the greater trochanter also increased. Additionally, along Principal Component 1, there was an increase in the size of the medial femoral condyle relative to the lateral femoral condyle. In the medial and lateral views, it could be seen that the proximal femur relative to the condyles became more posteriorly oriented. The condyles also showed a change from a medially inferior angle of articulation, to one that was more perpendicular to the axis of the femoral shaft.

The second principal component showed a change in the orientation of the greater trochanter from a more lateral to a more medial position. The greater trochanter also showed an increase in relative height. The femoral neck decreased in relative length and its orientation changed from a more superior alignment to one that was more perpendicular to the axis of the shaft. The shaft length also increased along the second principal component and the femoral condyles rotated medially relative to the rest of the femur. The femoral head changed from having an oval shape with the long axis' superior edge on the anterior side, to an oval with the superior edge on the posterior side. The lesser trochanter also migrated from a medial position on the femoral shaft

to one that was more laterally placed. These changes in shape are illustrated in Figure 3-41.

Shape changes across the species groups

Each species group showed a combination of features from each principal component (Figure 3-42). The *Pan paniscus* and *Pan troglodytes* mean femoral shapes were very similar, with the *Pan paniscus* mean showing a slightly longer greater trochanter and slightly larger femoral condyles, as well as a slightly shorter femoral shaft.

The *Gorilla sp.* mean had the relatively shortest femoral shaft of all the species groups as well as the largest femoral head and neck. The femoral condyles were the widest medio-laterally in comparison to the other groups. The *Gorilla sp.* mean greater trochanter was also the shortest of all the species groups.

The *Homo sapiens* mean showed the relatively longest femoral shaft of all the species groups. The femoral condyles were the narrowest of all the species groups, and also displayed the most medially inferior angle of articulation. The femoral neck was also the longest proportional to the size of the femoral head among the species groups and was also oriented the most superiorly of the species groups. The femoral condyles were the widest antero-posteriorly of all the species groups.

The *Pongo pygmaeus* mean femoral shape had a relatively short femoral shaft in comparison to the other species groups and the greater trochanter was relatively tall. In other respects, the mean femoral shape for the *Pongo pygmaeus* group was most similar to the *Gorilla sp.* mean, with relatively large condyles and femoral head and neck. The femoral neck was slightly more superiorly oriented than the *Gorilla sp.* group, and the condyles slightly wider antero-posteriorly.

The *Australopithecus afarensis* femoral shape (Figure 3-43) largely echoed that of the *Homo sapiens* subset, with a long femoral shaft, relatively narrow femoral condyles medio-laterally, and medially inclined angle of articulation. A relatively long and more superiorly oriented femoral neck also featured, as well as femoral condyles which were wider antero-posteriorly than the non-human apes.

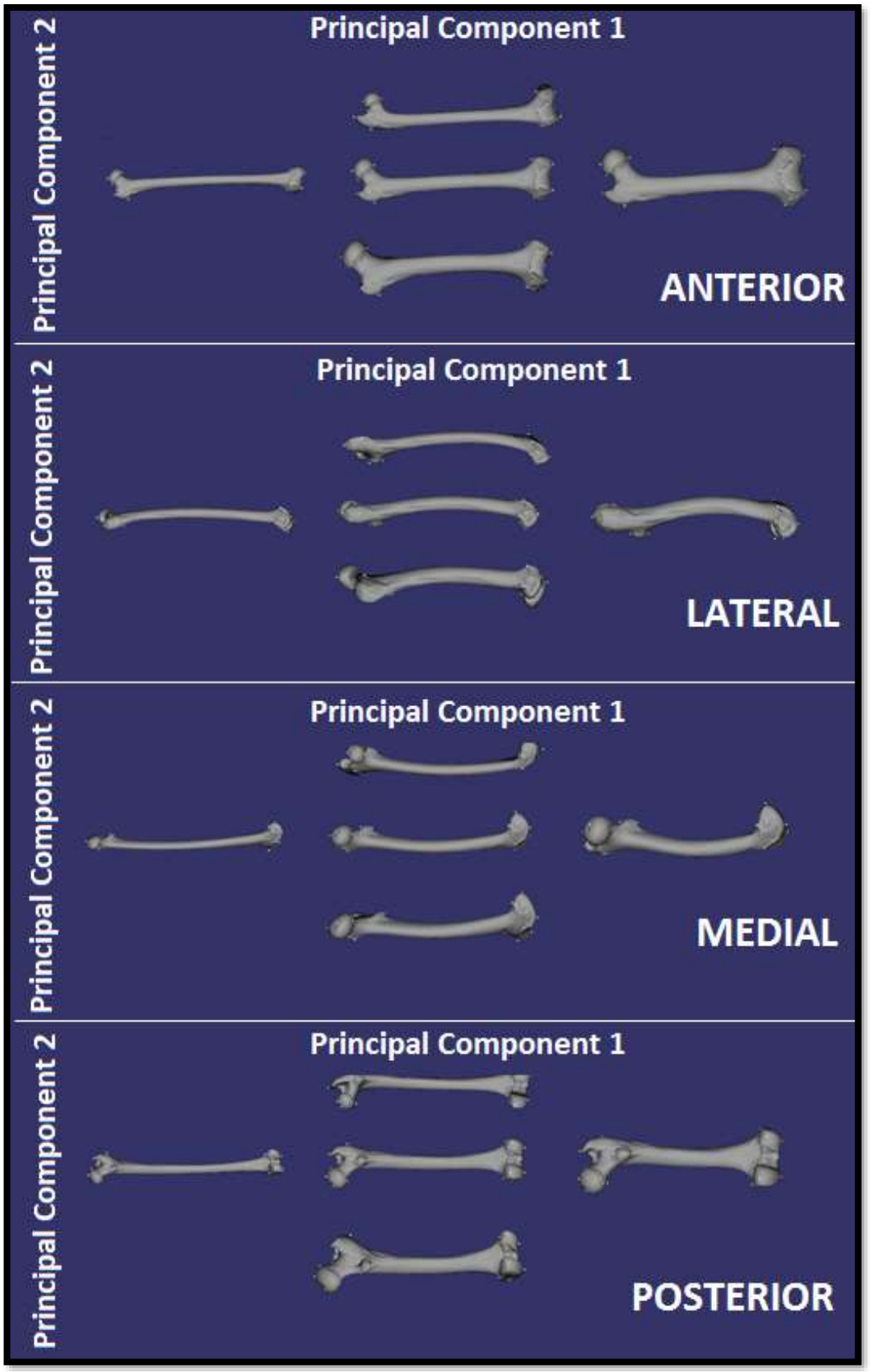

Figure 3-41: Changes in Femur Shape Along Principal Components 1& 2, shown in Anterior, Lateral, Medial and Posterior Views as determined by the True Landmarks

Mean Femur Shape shown centrally and the extremes of each Principal Component surrounding this

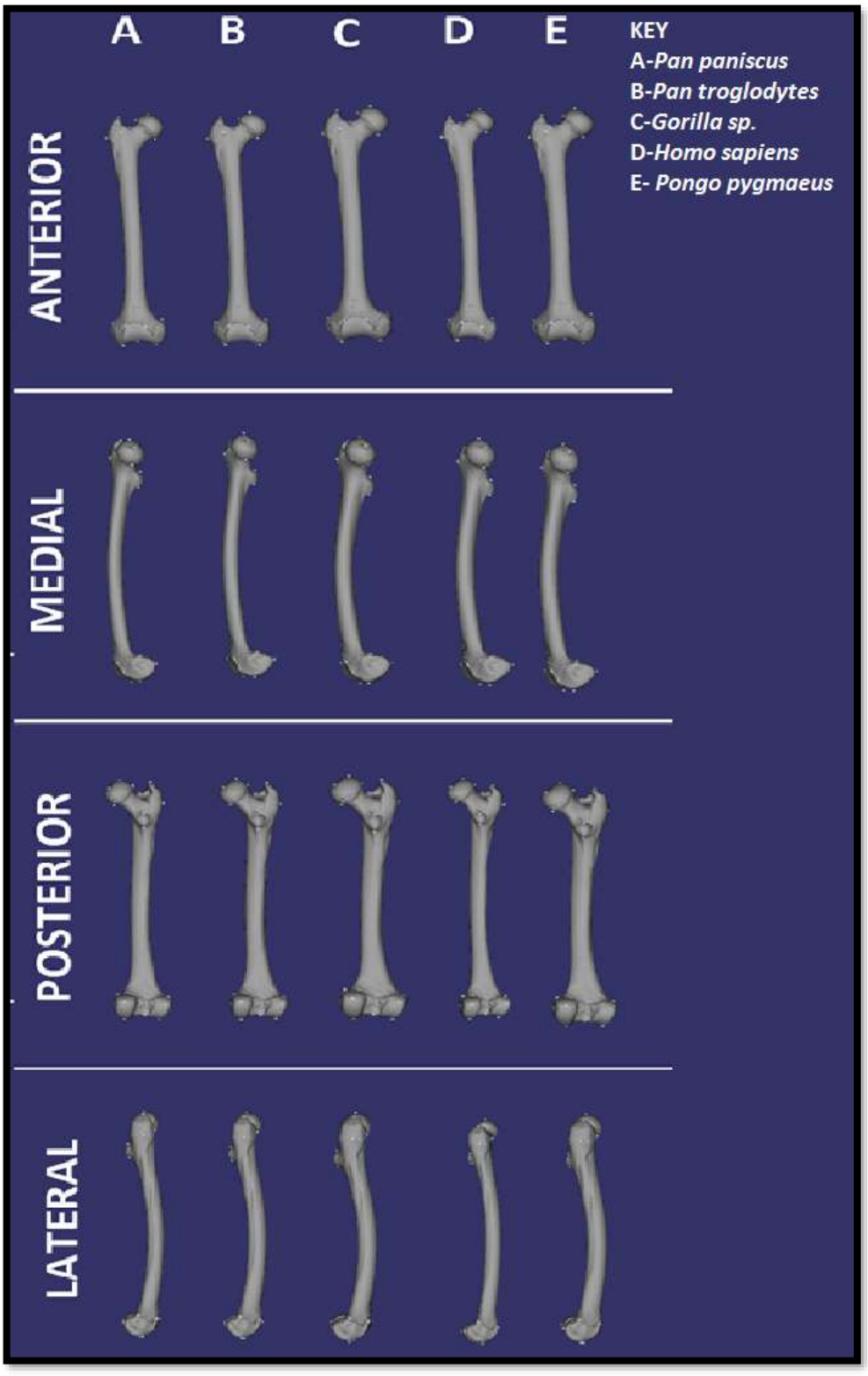

Figure 3-42: Mean Shape of the Femur, using True Landmarks across Species Groups showing Anterior, Medial, Lateral and Posterior Views

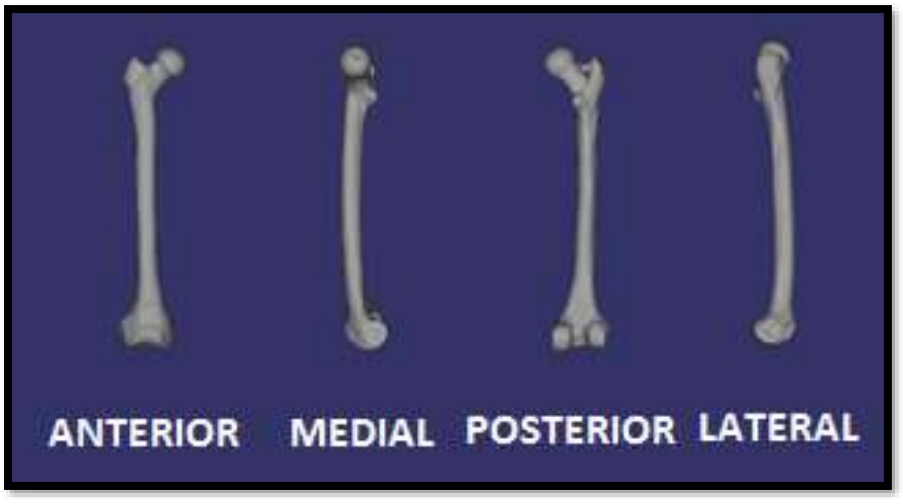

Figure 3-43: Shape of the *Australopithecus afarensis* Femur as Determined by the True Landmarks, Shown in Anterior, Medial, Posterior and Lateral Views

Musculature associated with the True landmarks of the femur

When only true landmarks were considered, *Australopithecus afarensis* was shown to group most closely with *Homo sapiens*. This indicated that the basic shape of the femur in A.L. 288-1 was most similar to that of the *Homo sapiens* group overall.

There were muscles which had specific landmark correlates on the femur. These included: *m. iliopsoas* (Landmark 10- Superior lesser trochanter; and Landmark 11- Inferior lesser trochanter) and *m. pectineus* (Landmark 10 and 11 also).

When the first Principal Component was plotted against the second Principal Component, there was a broad separation of the groups (Figure 3-40). There was significant overlap between the *Pan paniscus* and *Pan troglodytes* groups. A.L 288-1 clustered within the *Homo sapiens* subset, although there was overlap between the *Homo sapiens* group with the *Pan paniscus* and *Pan troglodytes* groups. The *Pongo pygmaeus* group was distinct and there was some overlap between the *Pan troglodytes* and *Gorilla sp.* groups. The Tukey post-hoc tests (see Appendix) showed that along Principal Component 1, whilst the *Pan* groups clustered together, all other groups were distinct from each other. Along the second principal component the *Pan pansicus, Gorilla sp.* and *Pan troglodytes* groups were not significantly different from each other. Additionally, the *Pan troglodytes* and *Homo sapiens* groups were not reliably differentiable. The *Pongo pygmaeus* subset did not group with any other subset.

Shape changes indicated by the Principal Components

Along Principal Component 1, the shape of the femoral head became relatively larger and the long axis shifted from posteriorly to anteriorly superior (Figure 3-44). Principal Component 2 showed a shift in the orientation of the head relative to the shaft, with it becoming more inferiorly oriented. The fovea capitus also became more inferiorly oriented along the second principal component, and the shape of the head less rounded.

Shape changes across the species groups

Each species mean showed a combination of traits from each principal component (Figure 3-45). The *Pongo pygmaeus* mean was distinct from the other groups with the femoral head being the largest relative to the other groups, and also with the fovea capitus being the most centrally located on the femoral head. The *Pongo* pygmaeus femoral head was also the roundest of all the groups. The *Pan paniscus* and *Pan troglodytes* groups were very similar, although the *Pan paniscus* mean femoral head was slightly smaller than that of the *Pan troglodytes* mean. The *Homo sapiens* group had a relatively larger femoral head than the *Pan* species, although was quite similar in shape. The *Gorilla sp.* had a relatively larger femoral head than the *Homo sapiens*

group. The fovea capitus was slightly more centrally located, and the femoral head was wider on the antero-posterior axis than the other groups. The *Australopithecus afarensis* femoral head showed some affinity in its orientation to the *Pan* species, but was most similar overall to the *Homo sapiens* group (Figure 3-46).

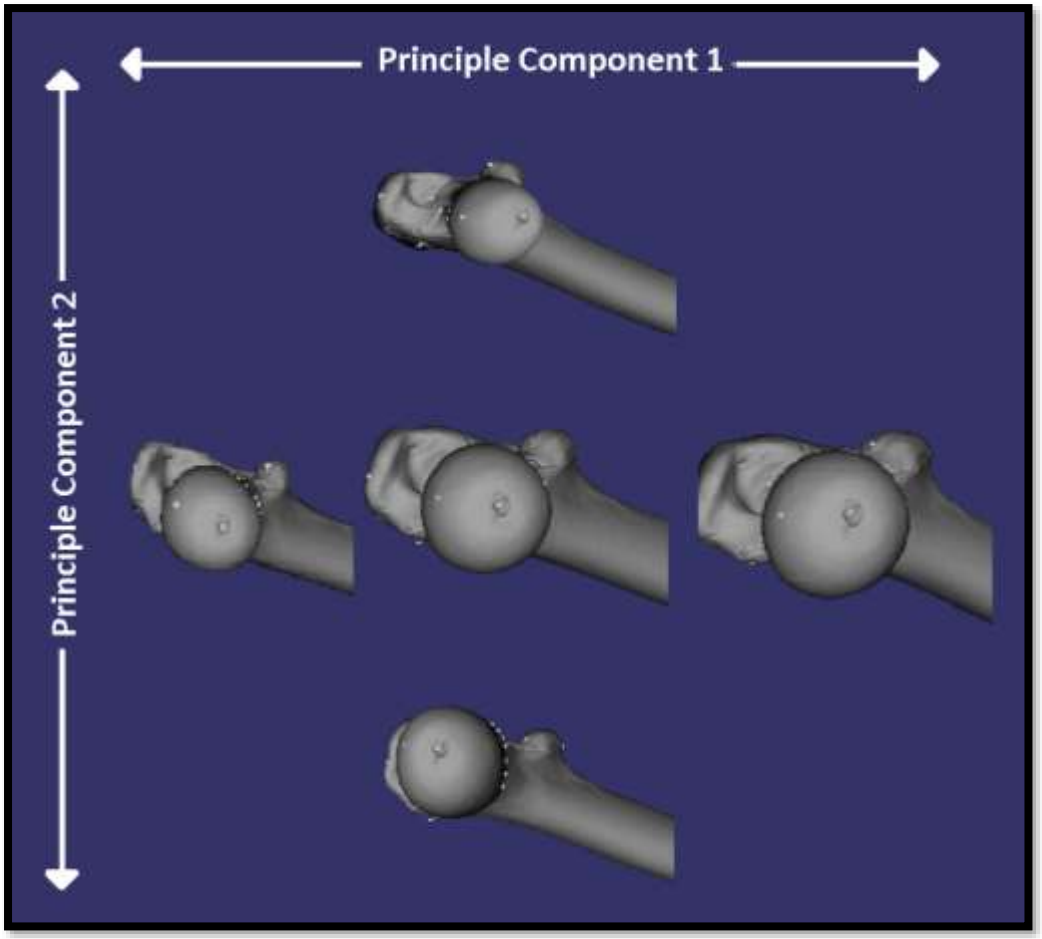

Figure 3-44: Changes in Femoral Head Shape along Principal Components 1 and 2, with the Mean Acetabular Shape shown in the Centre

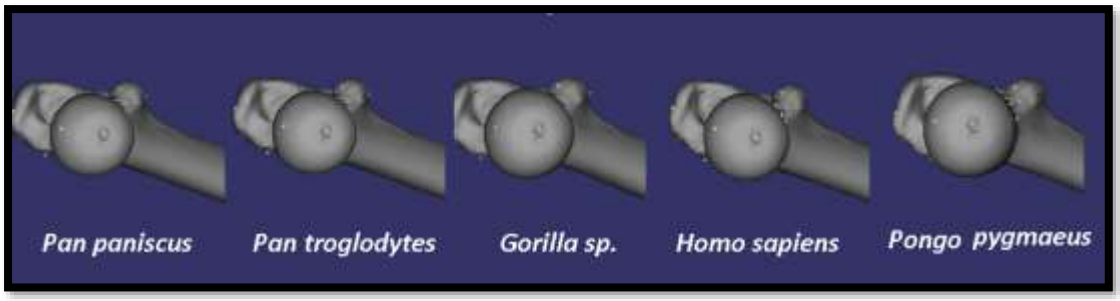

Figure 3-45: Mean Shape of the Femoral Head across species groups

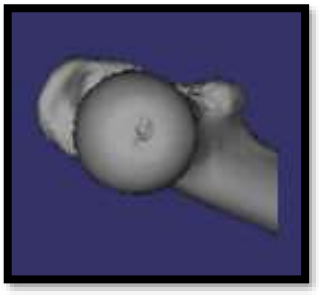

Figure 3-46: The Shape of the *Australopithecus afarensis* Femoral Head

Musculature associated with the True landmarks and semilandmarks of the femoral head

In true landmarks and semilandmarks of the femoral head *Australopithecus afarensis* was shown to group most closely with *Homo sapiens*. There are no muscles which attach to the femoral head but it is, however, a key anatomical structure in locomotion as it is key in the transmission of load from the pelvis and trunk into the femur.

A bi-plot of the first and second principal components showed there was clear separation of the groups (Figure 3-40). The *Pongo pygmaeus* and *Gorilla sp.* groups overlapped, as did the *Pan troglodytes* and *Pan paniscus* subsets. The *Pan paniscus* group remained tightly clustered within the larger *Pan troglodytes* sample. The *Homo sapiens* cluster was distinct, and A.L. 288-1, fell within the *Homo sapiens* range.

The Tukey post-hoc tests (see Appendix) showed that along Principal Component 1, only the *Pan paniscus* and *Pan troglodytes* grouped together- all other species groups were distinguishable from each other. Along Principal Component 2, the *Pan paniscus* and *Pan troglodytes* subsets grouped together, although the *Pan troglodytes* subset also could be grouped with the *Gorilla sp.* subset. The *Homo sapiens* and *Pongo pygmaeus* groups were distinct from all other groups.

Shape changes indicated by the Principal Components

As seen in Figure 3-47, along the first principal component, the superior portion of the greater trochanter became more anteriorly oriented, and also lengthened. The intertrochanteric crest became more sigmoid in shape. There was also an increase in relative size.

The second principal component, showed the greater trochanter became less rounded, and developed a ‘v’ shape along its medial edge. The intertrochanteric crest became shorter in its relative length along the second principal component.

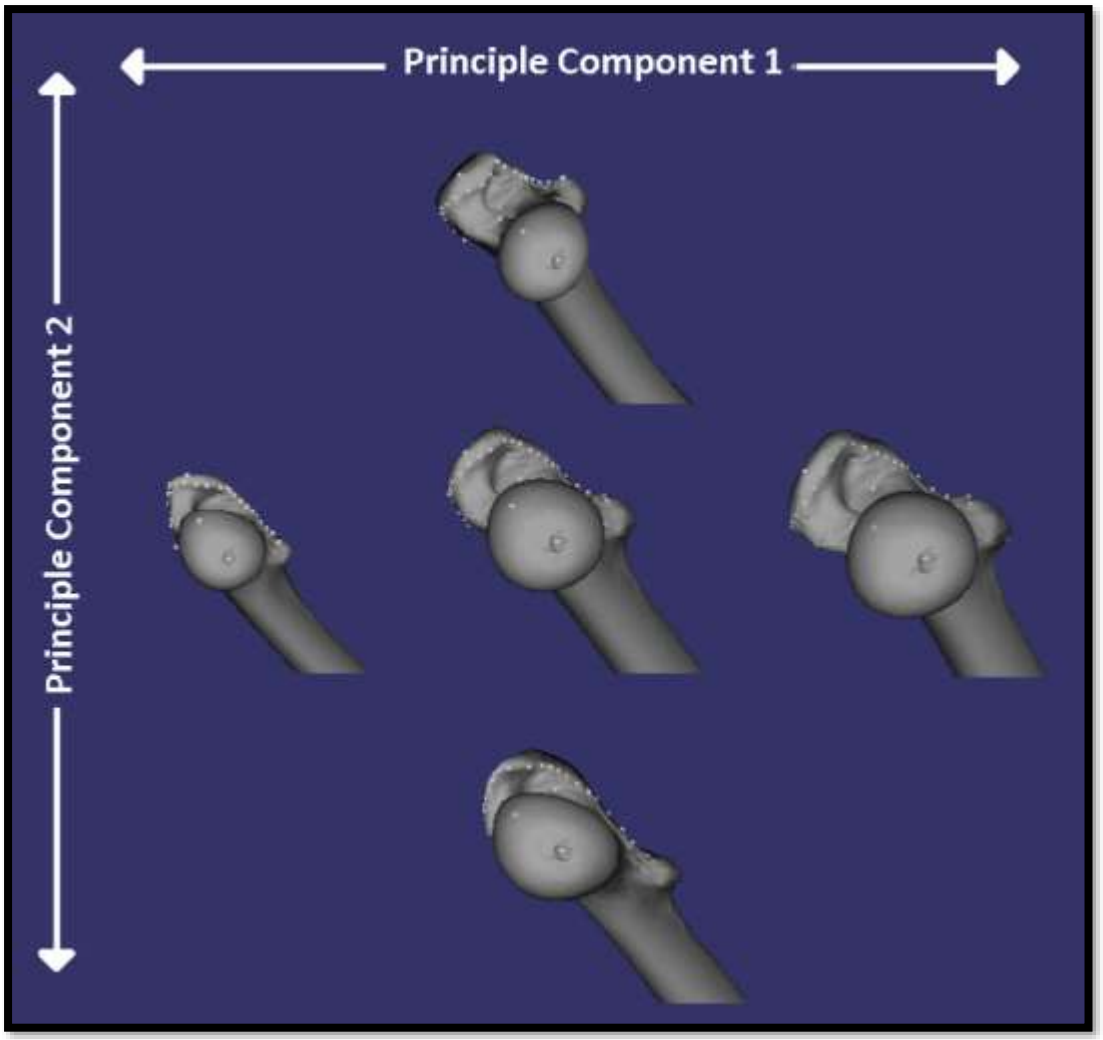

Figure 3-47: Changes in Greater trochanter and Intertrochanteric Crest Shape along Principal Components 1 and 2, with the Mean Acetabular Shape shown in the Centre

Shape changes across the species groups

The species groups showed a combination of the changes along each principal component (Figure 3-48). The *Pan paniscus* superior greater trochanter was slightly longer than that of the *Pan troglodytes* group. The *Gorilla sp.* greater trochanter was angled more anteriorly than in the *Pan* groups, but was of a similar relative size. The greater trochanter of the *Homo sapiens* was less highly angled than that of the *Pan* and *Gorilla sp.* groups. In the *Pongo pygmaeus* group, the greater trochanter was rounded, like that of the *Homo sapiens* group but more similar in relative size to the *Pan* and *Gorilla sp.* groups. The intertrochanteric crest of the *Homo sapiens* group was relatively straight in comparison to the other groups. The *Pan paniscus, Pan troglodytes* and *Gorilla sp.* groups showed a similar amount of curvature along the

intertrochanteric crest, although the *Gorilla sp.* group was slightly shorter, relative to the greater trochanter. The *Pongo pygmaeus* group showed the widest curvature along the intertrochanteric crest of all the species groups.

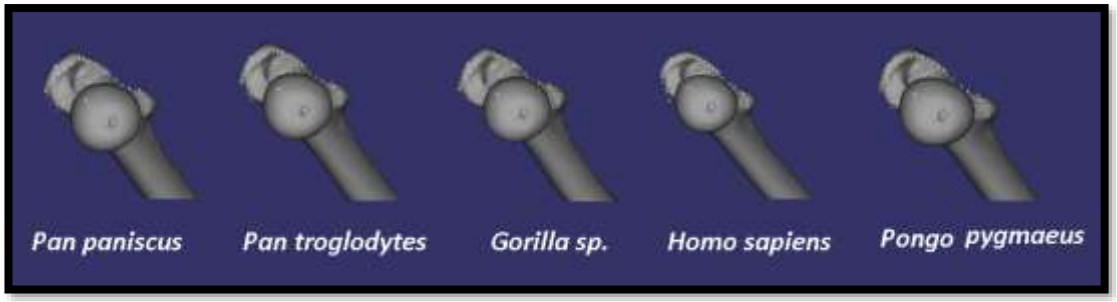

Figure 3-48: Mean Shape of the Greater Trochanter and Intertrochanteric Crest across species groups

The shape of the *Australopithecus afarensis* greater trochanter and intertrochanteric crest was very similar to that of the *Homo sapiens* group, although the intertrochanteric crest was slightly smaller than that of the *Homo sapiens* group (Figure 3-49).

Figure 3-49: The Shape of the *Australopithecus afarensis* Greater Trochanter and Intertrochanteric Crest

Musculature associated with the True landmarks and semilandmarks of the greater trochanter and intertrochanteric crest

In true landmarks and semilandmarks of the greater trochanter and intertrochanteric crest *Australopithecus afarensis* was shown to group most closely with *Homo sapiens.* Many muscles insert onto the greater trochanter and the intertrochanteric crest including *m.* gemellus *inferior, m.* gemellus *superior, m. gluteus maximus, m. gluteus medius, m. gluteus minimus, m. iliopsoas, m. obturator internus, m. obturator internus, m. piriformis* and *m. quadratus femoris,* indicating that these would have had a similar configuration in *Australopithecus afarensis* to *Homo sapiens.*

True Landmarks and Semilandmarks of the Femoral Condyles

A bi-plot of the first two Principal Components showed clear differentiation between the *Homo sapiens* group and the extant apes (Figure 3-40). The A.L. 288-1 specimen grouped within the *Homo sapiens* subset. The *Pan paniscus* and *Pan troglodytes* samples clustered together, but the *Pan paniscus* sample remained discrete within the group. There was also overlap between the *Gorilla sp.* and the *Pongo pygmaeus* sample.

The Tukey post-hoc tests (see Appendix) showed that along Principal Component 1, the *Pan paniscus* and *Pan troglodytes* subsets grouped together, but all other species groups were significantly different from each other. Along Principal Component 2, the *Pongo pygmaeus* and *Homo sapiens* subsets were not significantly different from each other, nor were the *Pan paniscus* and *Pan troglodytes* subsets. The *Gorilla sp.* group was distinct from the other groups.

Shape changes indicated by the Principal Components

As illustrated in Figure 3-50, the first principal component showed a narrowing of the femoral condyles medio-laterally. This was primarily a factor of a narrowing of the medial femoral condyle. Additionally, the intercondylar fossa narrowed along the first principal component. The patellar surface shifts from having a rounded superior surface, to one that is more m-shaped. The medial condyle also decreased in length along Principal Component 1.

Principal Component 2 showed an increase in height of the patella surface and also a widening of the posterior femoral condyles. Combined with this was a narrowing of the patella surface along the second principal component and a narrowing of the lateral femoral condyle. Additionally, the curvature along the edge of the medial condyle went from convex to concave along Principal Component 2.

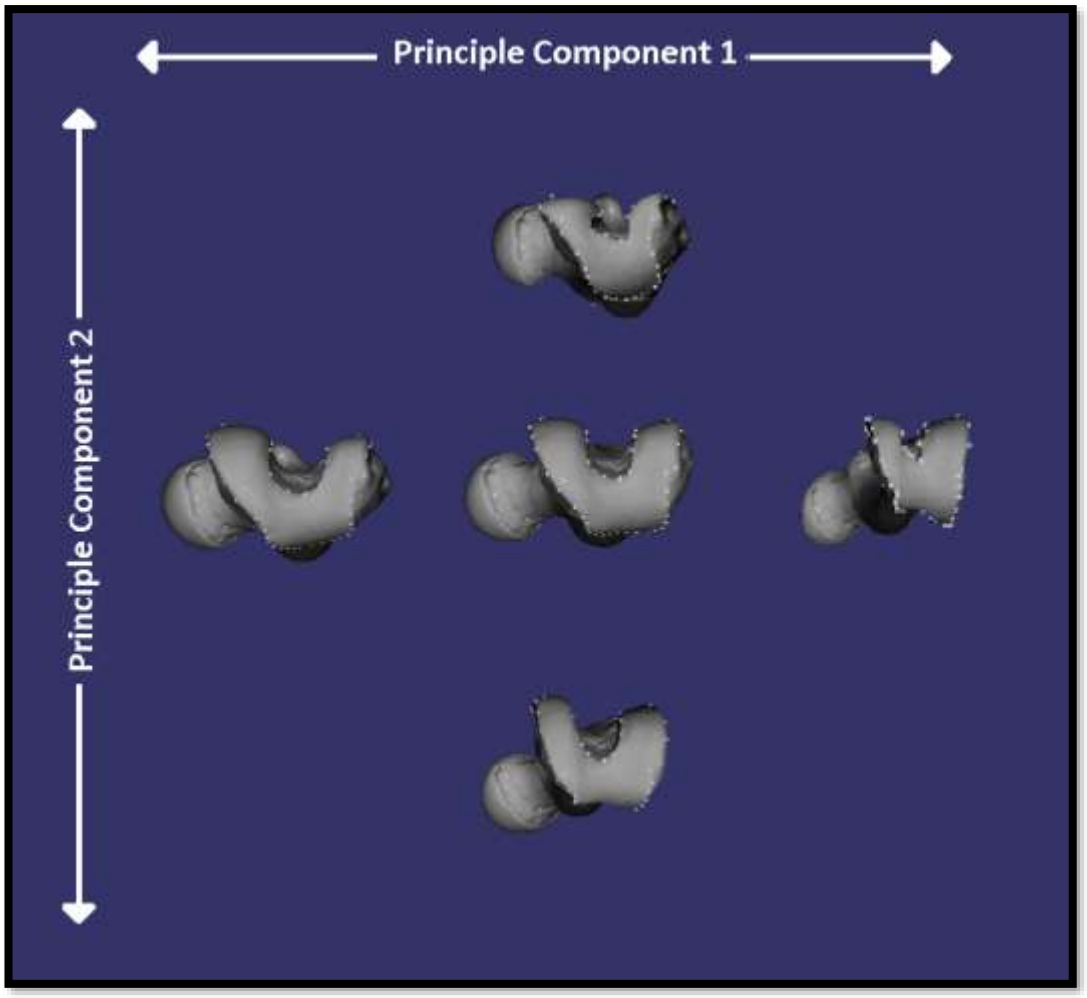

Figure 3-50: Changes in Femoral Condyle Shape along Principal Components 1 and 2, with the Mean Femoral Condyle Shape shown in the Centre

Shape changes across the species groups

The species groups showed a combination of features from each principal component (Figure 3-51). The *Pan paniscus* femoral condyles were very similar to those of the *Pan troglodytes* group, although the condyles of the *Pan troglodytes* group were slightly longer along the inferior surface. The *Gorilla sp.* femoral condyles were relatively wider than all the other species groups, with the medial condyle in particular forming a greater angle. The intercondylar notch was also the widest of all the species groups, and the medial condyle of the *Gorilla sp.* group was significantly longer than the lateral condyle. The *Homo sapiens* condyles were the smallest and narrowest in relation to the other species groups, although the lateral condyle was relatively wide in comparison to the medial condyle. The intercondylar notch was narrower than that of the other groups, and the patella surface formed more of an m-shape. The *Pongo*

pygmaeus femoral condyles were similar to those of the *Gorilla sp.* group, although they were slightly narrower and the medial condyle formed less of an angle.

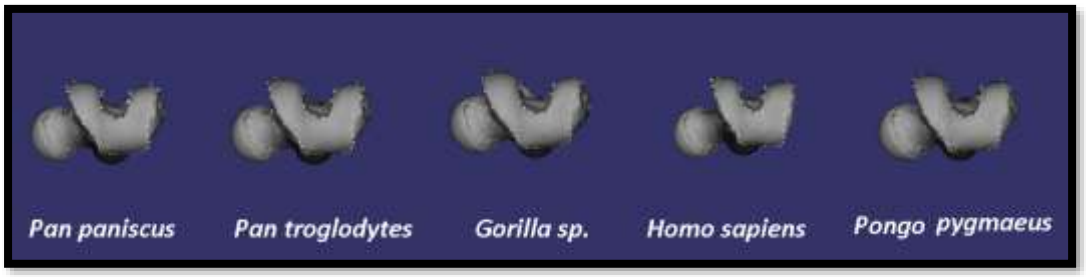

Figure 3-51: Mean Shape of the Femoral Condyles across species groups

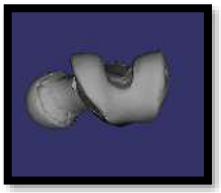

Figure 3-52: The Shape of the *Australopithecus afarensis* Femoral Condyles

The *Australopithecus afarensis* femoral condyles (Figure 3-52) were similar in shape to that of the *Homo sapiens*, although slightly wider medio-laterally. Additionally, the patella surface had the same m-shape as seen in the *Homo sapiens* group. The condyles were similar in size, and, as in the *Homo sapiens* group, the lateral condyle was slightly wider than the medial condyle.

Musculature associated with the True landmarks and semilandmarks of the femoral condyles

In true landmarks and semilandmarks of the femoral condyles *Australopithecus afarensis* was shown to group most closely with *Homo sapiens.* The femoral condyles and surrounding area serve as origins for *m. gastrocnemius, m. plantaris* and *m. popliteus.* This area also serves as an insertion for the *m. adductor magnus.*

A plot of the first two Principal Components, as shown in Figure 3-40, showed that there was a distinction between the species groups. The *Gorilla sp.* and the *Pongo pygmaeus* groups were discrete. The *Pan paniscus* group overlapped with both the *Pan troglodytes* and the *Homo sapiens* subsets. A.L. 288-1 fell within the range of the *Homo sapiens* group.

The Tukey post-hoc tests (see Appendix) showed that all the species groups were significantly different along the first principal component. Along the second principal component, the *Pongo pygmaeus* group was significantly different from all the other groups. The *Homo sapiens* and *Gorilla sp.* subsets could be grouped together along the second principal component, but the *Gorilla sp.* could also be grouped with both the *Pan paniscus* and *Pan troglodytes* subsets.

Shape changes indicated by the Principal Components

Each principal component showed different effects in the shape of the linea aspera (Figure 3-53). The first principal component showed a decrease in the overall length of the linea aspera, and also the transition from a double curve along the length of the shaft, to a single more rounded curve. The second principal component showed a decrease in the curvature of the linea aspera, from bow shaped to relatively straight along the femoral shaft.

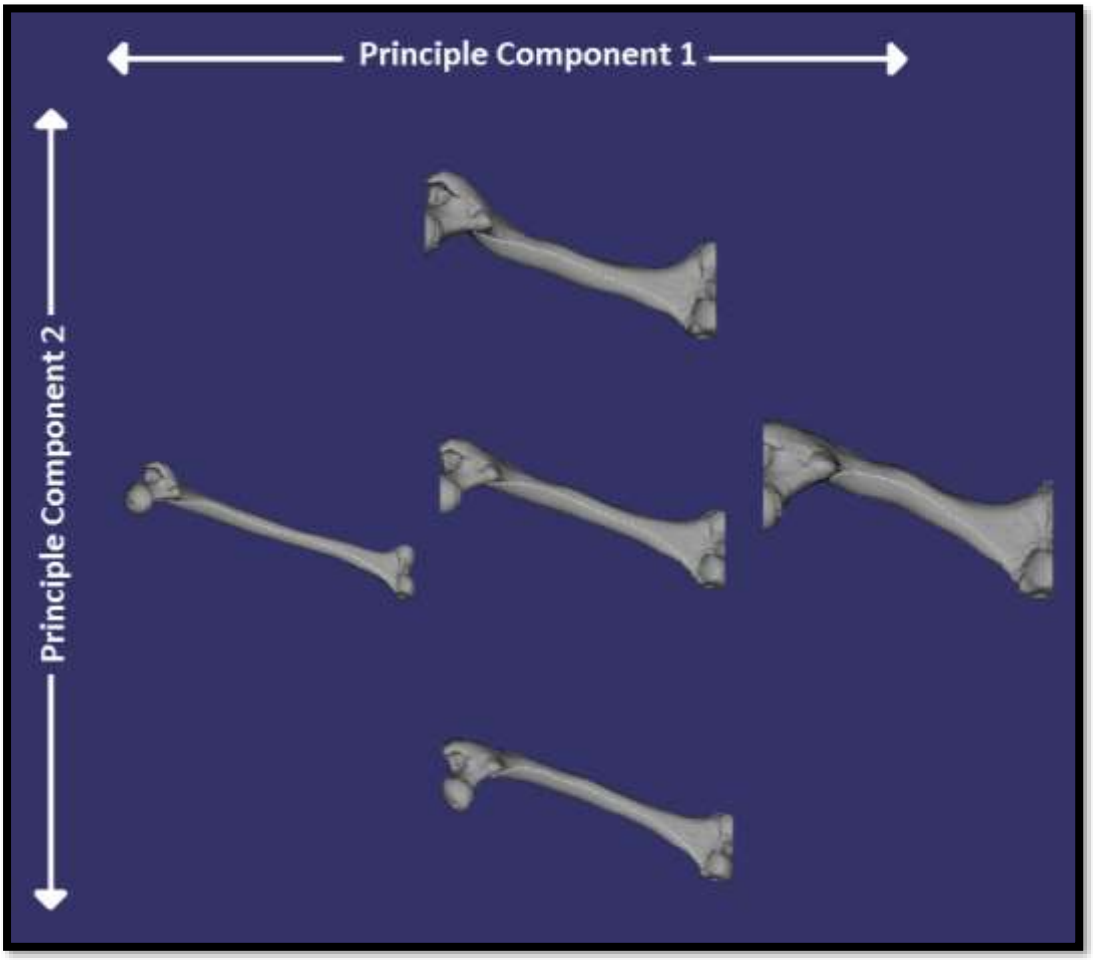

Figure 3-53: Changes in Medial Linea Aspera Shape along Principal Components 1 and 2, with the Mean Acetabular Shape shown in the Centre

Shape changes across the species groups

The linea aspera of each species group showed a combination of traits from each principal component (Figure 4-71). The *Pan paniscus* linea aspera was most similar to that of the *Pan troglodytes* group, although the superior portion of the *Pan troglodytes* linea aspera was slightly shorter, with a slightly more superior point of curvature than that of the *Pan paniscus* group. The *Gorilla sp.* linea aspera was the shortest relative to the other species groups and also showed the greatest amount of curvature. The *Homo sapiens* linea aspera was both the longest and straightest in its middle portion of all the species groups, with a very medial superior portion. The *Pongo pygmaeus* linea had the most inferior point of curvature, and a relatively medial superior portion.

Figure 3-54: Mean Shape of the Medial Linea Aspera across species groups

Figure 3-55: The Shape of the *Australopithecus afarensis* Medial Linea Aspera

The *Australopithecus afarensis* linea aspera (Figure 4-72) was almost identical to that of the *Homo sapiens* group, although it was very slightly shorter.

Musculature associated with the True landmarks and semilandmarks of the medial linea aspera

In true landmarks and semilandmarks of the medial linea aspera *Australopithecus afarensis* was shown to group most closely with *Homo sapiens.* Several muscles take their origin along the linea aspera including the short head of *m. biceps femoris, m. vastus medialis* and *m. vastus lateralis*. Whilst *M. vastus intermedius* does not directly take its origin on the linea aspera, it has a very close association with the other muscles which do.

3.33 Summary of the Shape and Musculature of the Femur

The femur was shown to vary across the species groups, in accordance with previous studies (i.e.: Doran, 1992; 1993; Gebo, 1996; Harcourt-Smith, 2007; Harmon 2007; Lovejoy,1988; 2007; MacLatchy, 1996; MacLatchy & Bossert, 1996; Payne at al. 2006; Ruff, 2003; Sugardjito and van Hooff, 1986; Thorpe & Crompton, 2004; Zihlman et al. 2011), showing variations due to relative mass in primates as well as locomotory function.

The femur in Pan

The shape of the femur in the *Pan paniscus* and *Pan troglodytes* groups were very similar, with the *Pan paniscus* mean marginally more gracile than that of the *Pan troglodytes* group.

The *Pan paniscus* mean femoral head was slightly smaller than that of the *Pan troglodytes* mean. Both quite similar in shape to the *Homo sapiens* group but relatively smaller. The relative size of the femoral head in *Pan* has been linked to increased capability for abduction at the hip (MacLatchy & Bossert, 1996; MacLatchy, 1996; Harmon 2007).

The *Pan paniscus* showed a slightly longer superior greater trochanter than *Pan troglodytes.* The greater trochanter was angled more posteriorly in *Pan* than in the *Gorilla sp.* group, but was of a similar relative size, and there was a similar amount of curvature along the intertrochanteric crest. This has been attributed to relatively large insertions for the lateral rotators of the thigh (Aiello and Dean, 2002; Harmon, 2007).

Pan paniscus had a slightly shorter femoral shaft than that of the *Pan troglodytes* group and the linea aspera in *P. paniscus* had a slightly more inferior origin than that of *Pan troglodytes.* This shortening of the femoral shaft may be indicative that *Pan paniscus* are slightly more arboreal than *Pan troglodytes* (Doran, 1992, 1993; Payne at al. 2006; Sugardjito and van Hooff, 1986; Thorpe & Crompton, 2004), and a slightly different configuration of the quadriceps muscles of the thigh which are important flexors of the thigh and extensors of the knee.

The *Pan paniscus* femoral condyles were very similar to those of the *Pan troglodytes* group, although the condyles of the *Pan troglodytes* group were slightly longer along the inferior surface, perhaps indicating a slightly greater range of motion at the knee.

The femur in Gorilla

Overall, the femur in the *Gorilla sp.* group was the most robust of the species groups.

The *Gorilla sp.* had a relatively larger femoral head than the *Homo sapiens* group. The fovea capitus was slightly more centrally located, and the femoral head was wider on the antero-posterior axis than the other groups, suggesting a more limited capacity for abduction (Gebo, 1996; Harmon, 2007).

The *Gorilla sp.* greater trochanter was also the shortest of all the species groups and was angled more anteriorly than in the *Pan*, indicating a relatively smaller attachment for the lateral rotators of the thigh, and their decreased importance in climbing in this species (Harmon, 2007). The increased robusticity in the proximal femur indicates a concentration of musculature proximally, reflective of the stability required around the joints due to the gorilla's heavy body (Zihlman et al. 2011)

Gorilla sp. had the shortest femoral shaft relative to the size of the femoral head and neck, and as a consequence, the shortest and most curved linea aspera, which serves as attachment for the quadriceps. Zihlman et al. (2011) point out that these muscles are relatively massive in the gorilla, correlating with propulsive power and joint stability.

The *Gorilla sp.* femoral condyles were relatively wider than all the other species groups, with a medial condyle that was significantly longer than the lateral condyle, indicating the importance of lateral rotation of the leg in this group.

The femur in Pongo

The *Pongo pygmaeus* group had a relatively large femoral head, and relatively large and laterally leaning greater trochanter in comparison to the other groups. The femoral neck was slightly more superiorly oriented than the *Gorilla sp.* group. This is consistent with previous analyses (Godfrey et al., 1995; Harmon, 2007 and Ruff, 2002) stating that in more arboreal primates, there are increased hindlimb joint surface areas. The femoral head was also the roundest of the species groups, indicating the greatest range of motion at the hip in this species.

In the *Pongo pygmaeus* group, the greater trochanter was rounded, like that of the *Homo sapiens* group but more similar in relative size to the *Pan* and *Gorilla sp.* groups.

In *Pongo*, the rotators of the thigh are prominent (Zihlman et al., 2011) indicative of their increased arboreality. The relatively long femoral neck means that the femoral head is more superiorly oriented than the greater trochanter and this in turn could be an adaptation for greater rotation at the hip as *m. scansorius* and gluteals attach lower down, allowing a greater range of motion in climbing (Sigmon, 1974; Harmon, 2007)

In concert with this, *Pongo pygmaeus* had a relatively short femoral shaft in comparison to the other species groups and the linea aspera had the most inferior point of curvature, and a relatively medial superior portion. This indicates the relative importance of the *m. rectus femoris* in flexion at the hip, but the reduced importance of the quadriceps group for power in extension at the knee in arboreal locomotion (Zihlman et al. 2011).

The *Pongo pygmaeus* femoral condyles were similar to those of the *Gorilla sp.* group, although they were slightly narrower and the medial condyle formed less of an angle to the shaft. As in *Gorilla sp.* this is indicative of the importance in lateral rotation of the leg at the knee, but also, the narrowing of the condyles may indicate the reduced weight of *Pongo* in comparison.

The femur in Homo

The femoral neck in *Homo sapiens* was the longest proportional to the size of the femoral head and was oriented the most superiorly of the species groups. The *Homo sapiens* group had a relatively larger femoral head than the *Pan* species. The greater trochanter of the *Homo sapiens* was less highly angled than that of the *Pan* and *Gorilla sp.* groups. The intertrochanteric crest of the *Homo sapiens* group was relatively straight in comparison to the other groups. These features have been associated with less prominent *M. gluteus minimus* and *m. gluteus medius* in *Homo sapiens Homo* (Harmon, 2007; Stern, 1972; Sigmon, 1974; Stern & Susman, 1983). Additionally, the orientation of the femoral head and long neck have been suggested to be a result of the valgus knee joint in bipeds (Tardieu & Preuschoft, 1996; Harmon, 2007) and enhances the action of the abductors of the hip (Lovejoy, 2002).

The *Homo sapiens* group had the longest femoral shaft in comparison to the other species groups and the linea aspera was both the longest and straightest in its middle

portion of all the species groups, with a very medial superior portion. This indicates the importance of extension at the knee in bipedal locomotion in modern humans (Ruff, 2003).

The *Homo sapiens* condyles were the relatively narrowest mediolaterally, but widest anteroposteriorly of the species groups, and the lateral condyle was relatively wide in comparison to the medial condyle. The intercondylar notch was narrower than that of the other groups, and the patella surface formed more of an m-shape. The femoral condyles in the *Homo sapiens* group were also noticeably laterally inclined. These features relate to the distinct valgus position of the knee seen in modern human bipeds (Lovejoy, 2007).

The femur of A.L. 288-1

The *Australopithecus afarensis* femoral head was relatively round, but similar in relative size to that of the *Homo sapiens* mean. The fovea capitus was also similarly located, indicating a similar attachment for the *ligamentum teres.* A relatively long and more superiorly oriented femoral neck, as in *Homo sapiens*, indicated enhanced action of abductors at the hip (Lovejoy, 2002). The shape of the *Australopithecus afarensis* greater trochanter and intertrochanteric crest was very similar to that of the *Homo sapiens* group, although the intertrochanteric crest was slightly smaller than that of the *Homo sapiens* group.

The femoral shaft was relatively long (although shorter than *Homo sapiens*), and the linea aspera, although slightly shorter was almost identical to that of the *Homo sapiens* group.

The *Australopithecus afarensis* femoral condyles (Figure 4-69) were similar in shape to that of the *Homo sapiens*, although slightly wider medio-laterally as in the extant non-human apes. Additionally, the patella surface had the same m-shape as seen in the *Homo sapiens* group. As in the *Homo sapiens* group, the lateral condyle was slightly wider than the medial condyle, and there was a distinct valgus angle at the knee. Tardieu (1979a; 1979b;1983; 1986a, 1986b) and Tardieu and Preuschoft, (1996) suggest that these features represent an early stage in hominid bipedalism, with adaptations to arboreal activity and an enhanced range of rotation of the leg, without the locking mechanism of the knee found in modern humans.

3.4 The Tibia

3.41 Definitions of the Landmarks of the Tibia

Landmarks of the Tibia

Fifteen landmarks were chosen on the tibia, based on their ability to best represent overall shape. Of these 12 were Type 2 landmarks and 3 were Type 1. These landmarks are illustrated in Figure 3-56 and their full definitions can be found in Table 3-10. Curved Semilandmarks are shown separately in Figure 3-57 and defined in Table 3-11.

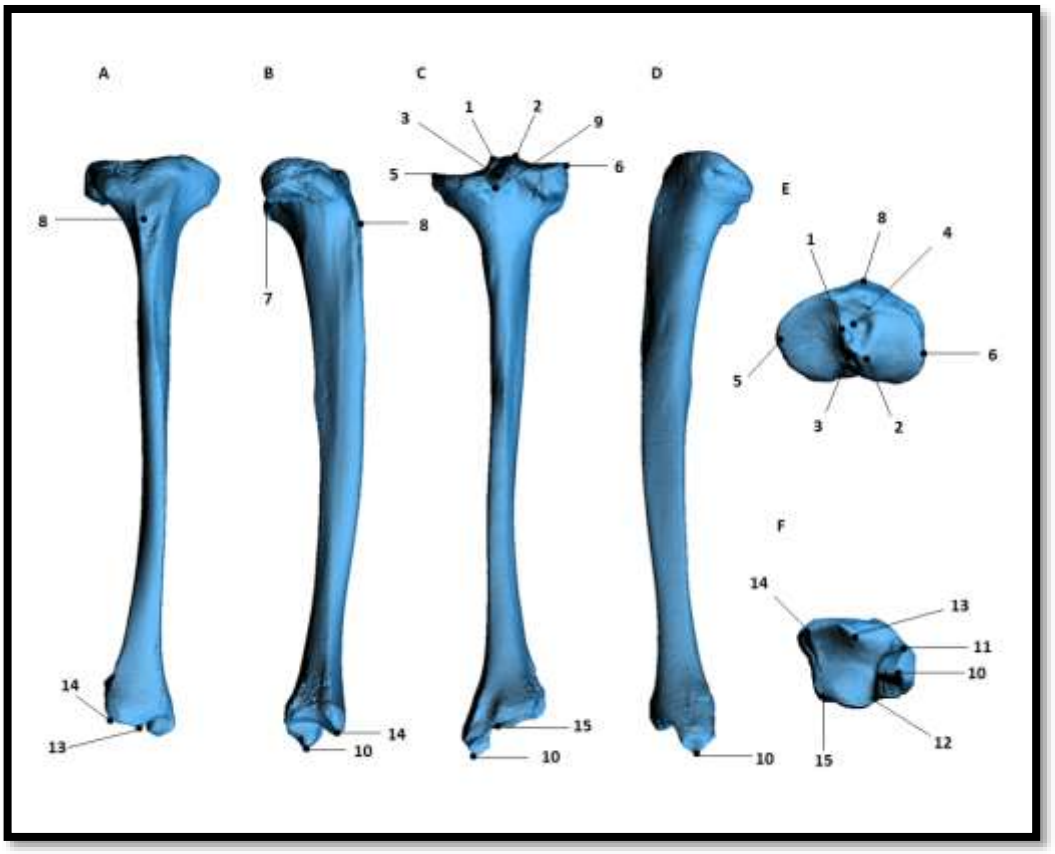

Figure 3-56: Anterior (A), Lateral (B), Posterior (C) , Medial (D), Superior (E) and Inferior (F) views of a tibia depicting the landmarks used in this study.
Full definitions can be found in Table 3-10. Some landmarks pictured in multiple views

Table 3-10 The Landmarks of the Tibia

No.	Landmark	Definition	Typea
1	Medial intercondylar tubercle	The most superior point on the medial intercondylar tubercle of the tibia.	I
2	Lateral intercondylar tubercle	The most superior point on the lateral intercondylar tubercle of the tibia.	I
3	Posterior intercondylar area	The most anterior point on the posterior intercondylar area.	II
4	Anterior intercondylar area	The most posterior point on the anterior intercondylar area.	II
5	Medial tibial plateau	The most medial point of the tibial plateau.	II
6	Lateral tibial plateau	The most lateral point of the tibial plateau.	II
7	Superior fibular articular facet	The most anterior and most superior point of the superior fibular articular facet on the tibia (postero-lateral surface).	II
8	Tibial tuberosity	The most anterior point on the tibial tuberosity.	II
9	Popliteal notch	The most inferior point of the popliteal notch on the posterior surface of the tibia.	II
10	Tip of the medial malleolus	The most inferior point on the tip of the medial malleolus of the tibia	I
11	Anterior trochlear facet medial malleolar junction	The most anterior point at which the medial malleolus borders the trochlear facet of the tibia.	II
12	Posterior trochlear facet medial malleolar junction	The most posterior point at which the medial malleolus borders the trochlear facet of the tibia.	II
13	Distal anterior tibia	The most distal point on the anterior surface of the tibia	II
14	Distal lateral tibia (anterior)	The most distal point on the anterior of the lateral border of the tibial trochlear facet.	II
15	Distal lateral tibia (posterior)	The most distal point on the posterior of the lateral border of the tibial trochlear facet.	II

[a] As taken from Bookstein (1991). Landmarks 11 & 12 adapted from Turley et al. (2011)

Semilandmarks of the Tibia

The semilandmarks of the tibia were digitised in 3 curves, and consisted of between 16 and 31 individual semilandmark points. These are illustrated in Figure 3-15 and full definitions can be found in Table 3-12. They were chosen as suitable as they both describe muscle attachment and important locomotory features of the tibia.

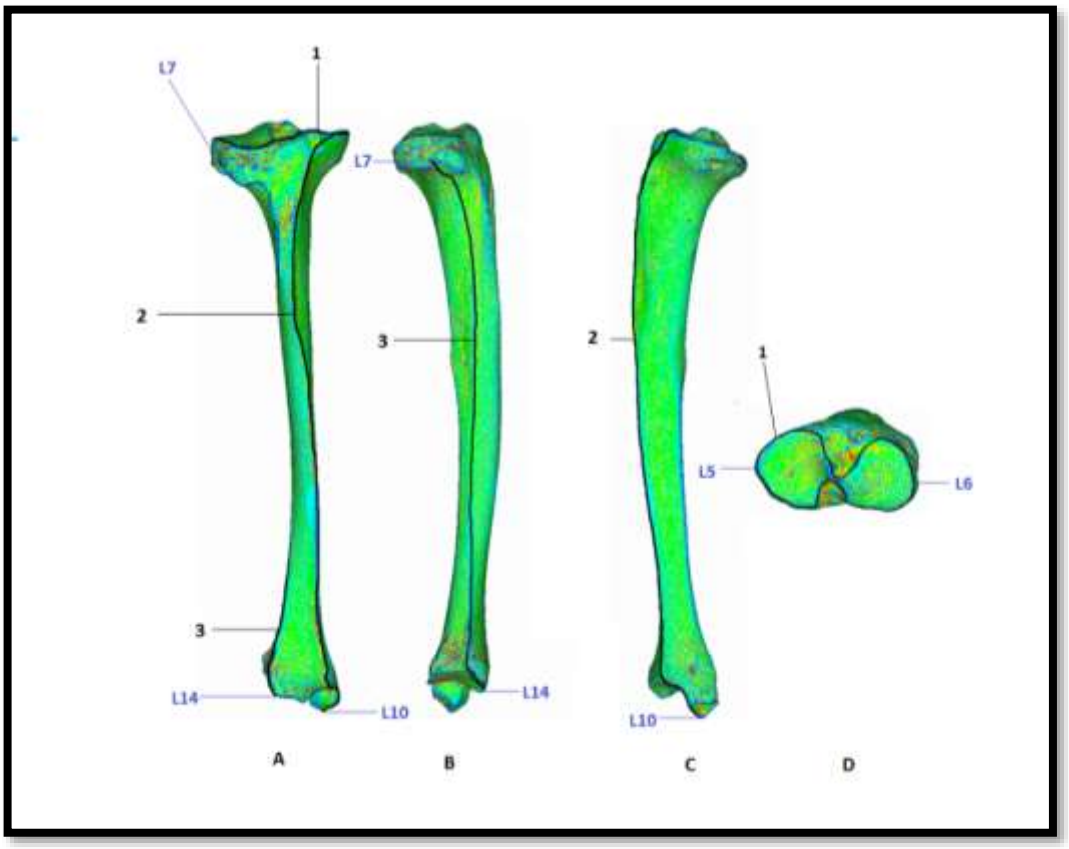

Figure 3-57: Anterior (A), Lateral (B), Medial (C) and Superior (E) views of a tibia depicting the curved semilandmarks used in this study.
Full definitions can be found in Table 3-11. Relevant landmarks are shown in blue.

Table 3-11 The Curved Semilandmarks of the Tibia

No.	Curve	Definition	No. of points
1	Tibial plateau	The line of maximum curvature around the external border of the tibial plateau passing through Landmark 5 (Medial tibial plateau) and Landmark 6 (Lateral tibial plateau). It is digitised from Landmark 5, anteriorly and laterally to the point where the border curves posteriorly, then along the border anteriorly and the posteriorly and laterally to Landmark 6. It then curves posteriorly and medially to the point where the border curves anteriorly, then moves posteriorly and finally anteriorly and laterally to Landmark 5 along the line of maximum curvature.	31
2	Anterior tibial crest	The line of maximum curvature that forms the anterior crest on the tibia, from the medial border of the tibial plateau along the anterior tibial shaft and continuing medially to Landmark 10 (Tip of the medial malleolus). It is digitised from the anterior border of the tibial tuberosity where it meets the border of the tibial plateau, along the line of maximum curvature inferiorly to the point that it meets the trochlear facet on the distal end of the tibia. It then moves medially to Landmark 10 where it terminates.	20
3	Interosseous crest	The line of maximum curvature that forms the interosseous crest, beginning from Landmark 7 (Superior fibular articular facet) on the lateral tibial shaft and then continuing medially to Landmark 14 (Distal lateral tibia [anterior]). It is digitised from landmark 7 and moves inferiorly along the line of maximum curvature to the point where this meets the border of the trochlear facet on the distal tibia. It then moves medially along the line of maximum curvature to Landmark 14 where it terminates.	16

3.42 Results of Geometric Morphometric Analysis of the Tibia

All Landmarks and Semilandmarks Across Species

A Generalised Procrustes Analysis (GPA) was conducted on the tibia determining the Procrustes Distance within each species group. The tibia showed a similarly low amount of variability in shape across the species to the femur, with Procrustes Distance of 0.17720. The tibia was also shown to be of a relatively consistent shape within the species groups. The greatest variation within the samples was shown by the *Gorilla sp.* group, with a Procrustes Distance of 0.01859. The smallest variation in shape was across the *Pongo pygmaeus* group, with a Procrustes Distance of 0.00555. The *Pan paniscus* and *Pan troglodytes* samples, as well as the *Homo sapiens* sample were all very similar with Procrustes Distances ranging from 0.0117 to 0.01663 (see Appendix)

The Principal Components Analysis conducted on all species, including the *Australopithecus afarensis* sample, using all landmarks and semilandmarks showed that the first principal component explained 21.57% of the variance and the second explained 13.60% of the variance- a cumulative amount of 35.17% (see Appendix).

A bi-plot of the first two principal components (Figure 3-58), showed clear differentiations between the *Homo sapiens* group and the other groups along Principal Component 1. The *Pan paniscus*, *Pan troglodytes* and *Pongo pygmaeus* groups were indistinguishable along the first principal component but showed some separation along Principal Component 2. The *Gorilla sp.* group was distinct along the first principal component, although along Principal Component 2 showed affinities with both the *Pongo pygmaeus* group and the *Homo sapiens* group.

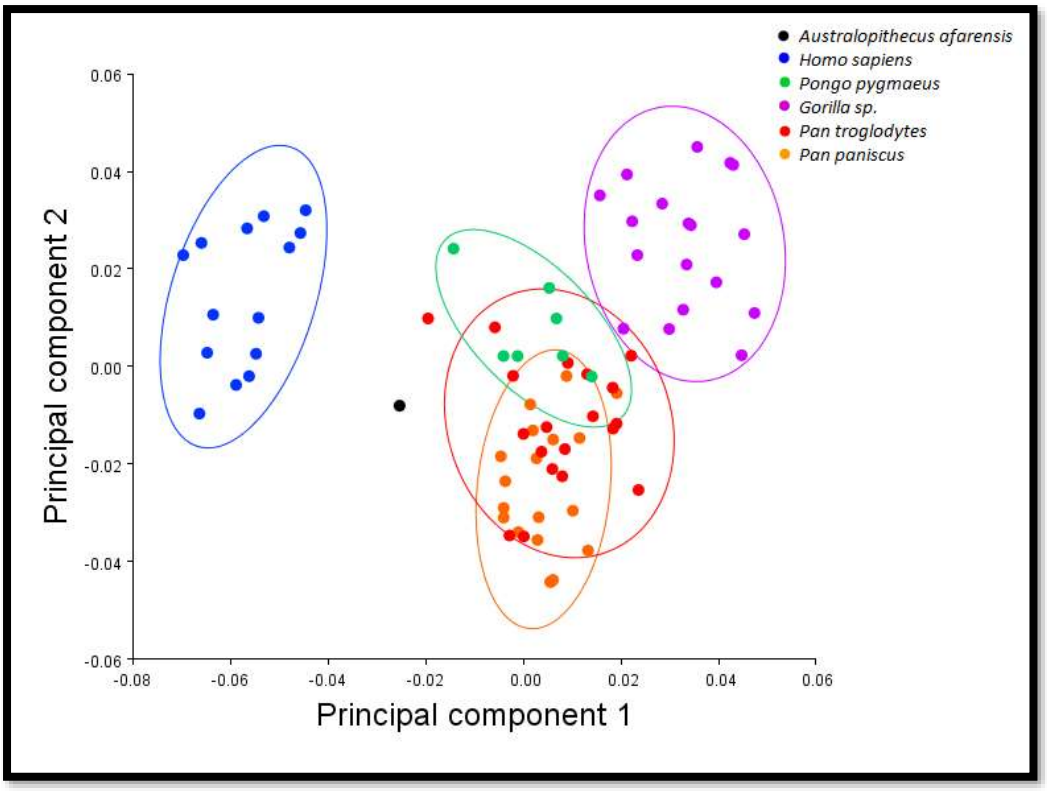

Figure 3-58: Principal Components Analysis of all Landmarks and Semilandmarks of the femur showing PC1 and PC2

A Shapiro-Wilk test conducted on the principal components showed that they were normally distributed (Table 4-42). The Levene's tests were not significant; PC1 $F(4, 70) = 0.936$, $p = 0.448$ – at the .05 alpha level and PC2 $F(4,70)=0.882$, $p=0.479$.

The ANOVA (see Appendix) showed that there were significant differences in the species groups across both principal components, at a $p> 0.005$ level and Tukey post-hoc tests showed that along the first principal component, the *Homo sapiens* and *Gorilla sp.* groups were distinct, and the other subsets grouped together. Along the second principal component, the *Pan paniscus* and *Pan troglodytes* subsets grouped together. The *Homo sapiens* subset could group with either the *Pongo pygmaeus* or *Gorilla sp.* subsets.

Shape changes indicated by the Principal Components

The shape of the tibia as determined by all landmarks and semilandmarks in the tibia varied along each principal component (Figure 3-59). Along the first principal component the relative size of the proximal and distal tibia decreased. The tibial plateau became more superiorly oriented along Principal Component 1, and the tibial shaft became straighter along its long axis. The tibial plateau became shorter and the shaft became wider in the antero-posterior axis. The tibial tuberosity became shorter and less pronounced. In the posterior view, the tibial shaft became thinner. The medial malleolus also became shorter and the distal articular surface of the tibia became less posteriorly oriented and oriented more inferiorly.

Along the second principal component the tibial shaft became longer and thinner, and also became more curved. Both the proximal and distal tibia reduced in relative size along Principal Component 2. The distal articular surface became more inferiorly oriented and the tibial plateau became more posteriorly oriented and angled more laterally. The tibial tuberosity reduced in relative size.

Shape changes across the species groups

The shape changes along each principal component were reflected in the shapes of the species means (Figure 4-3-61). The *Pan paniscus* and *Pan troglodytes* tibia were similar but the *Pan troglodytes* tibia showed a slightly larger tibial tuberosity and the tibial shaft was marginally wider antero-posteriorly.

The *Gorilla sp.* mean showed that both the proximal and distal tibia were the largest relative the shaft of all the species groups. The shaft also showed the greatest amount of curvature. The tibial tuberosity was the most pronounced of all the groups. The distal articulation of the tibia was also the most highly angled of all the species groups.

The *Homo sapiens* tibia had the straightest tibial shaft of all the species groups. Both the proximal and distal tibia were the narrowest medio-laterally of all the species groups. The tibial plateau was the most superiorly oriented, and the distal articulation the most inferiorly oriented of all the species groups.

The *Pongo pygmaeus* tibia was very similar to the tibiae of the *Pan* groups, although the shaft was slightly more curved, and both the proximal and distal articulation were relatively larger.

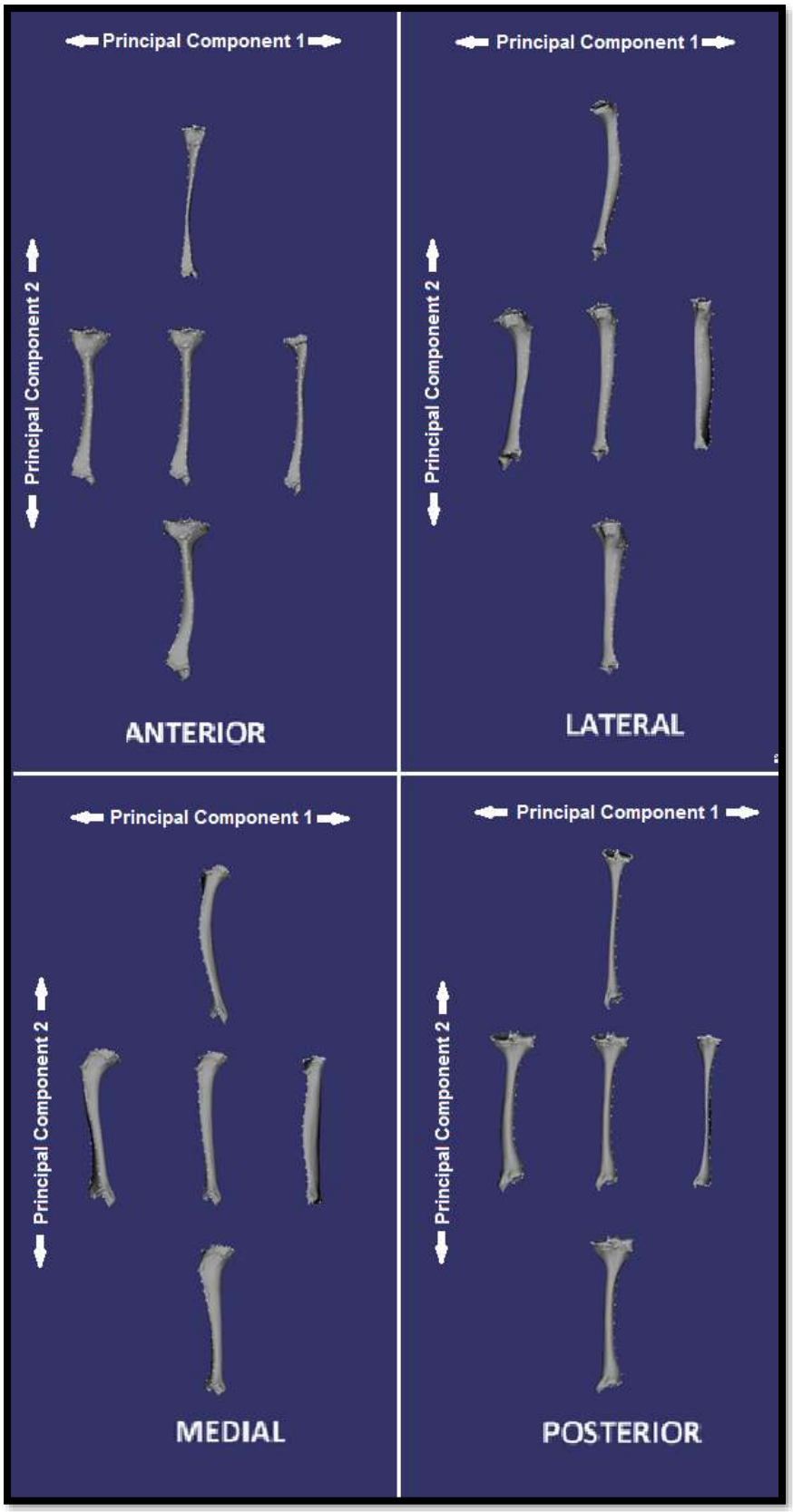

Figure 3-59: Changes in Tibia Shape along Principal Components 1 & 2 using all Landmarks and Semilandmarks.

Mean shown centrally with the extremes of each principal component surrounding this

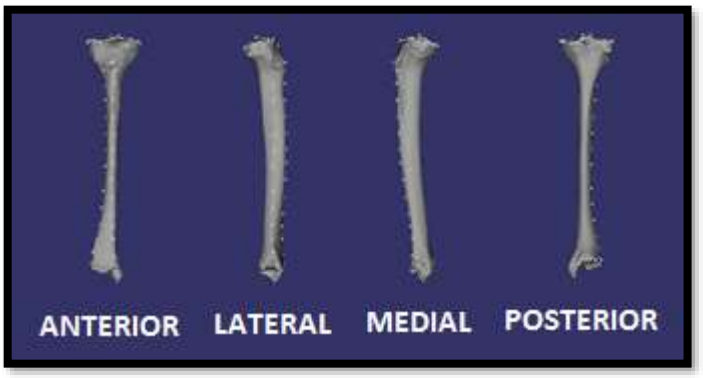

Figure 3-60: The Shape of the *Australopithecus afarensis* Tibia using all Landmarks and Semilandmarks

The *Australopithecus afarensis* tibia (Figure 3-60) was intermediate in shape between the *Pan* and *Homo sapiens* tibiae.

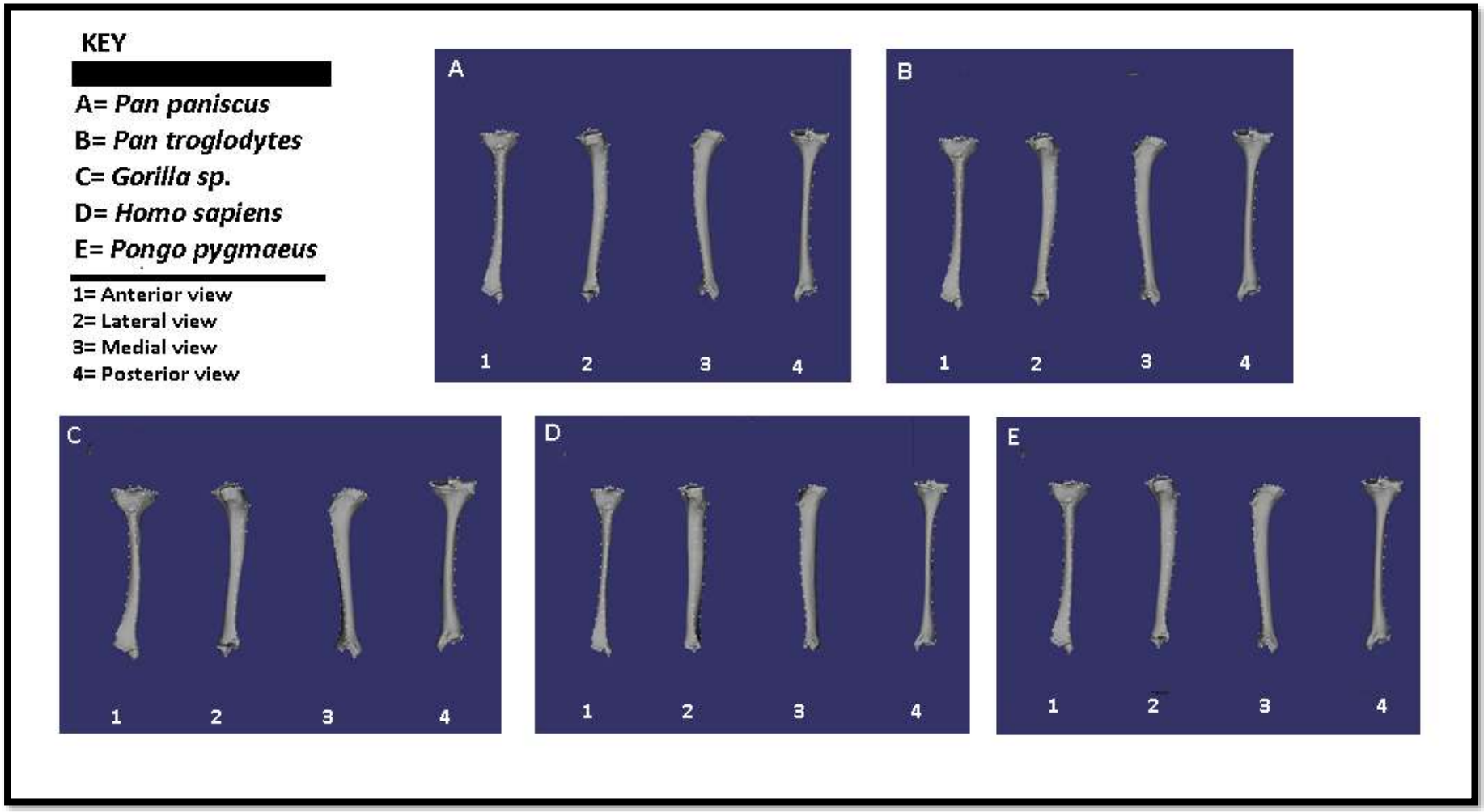

Figure 3-61: Mean Tibial shape for each species subset using all Landmarks and Semilandmarks

The Overall Musculature of the Tibia

The tibia serves as both an origin for muscles which cross the ankle and as an insertion for muscles which cross the knee. The muscles which originate on the tibia (Table 3-12) and cross the ankle allow for movement of the foot- including plantarflexion, dorsiflexion, inversion and eversion of the foot, and flexion and extension of the toes. The muscles which insert onto the tibia (Table 3-13) allow for movement of the leg at the knee and take their origin from the Os Coxa and the femur. The landmarks and semilandmarks of the tibia largely showed that the *Australopithecus afarensis* tibia was intermediate in shape between the *Homo sapiens* tibia and that of the *Pan* groups.

For muscles without a direct association with the available landmarks and semilandmarks, the overall shape using all landmarks and semilandmarks was used to determine the placement of muscles on the model. These included *m. popliteus* and *m. soleus.* Also, as the fibula was not used in this study, the nearest spot available on the tibia was used for *m. flexor digitorum longus.*

Table 3-12: Muscles with their origin on the Tibia and the affinity of A.L. 288-1 based on Geometric Morphometric results

Muscle	Associated Landmarks	Affinity of A.L. 288-1
Extensor Digitorum Longus	5	*Homo sapiens/ Pan*
Flexor Digitorum Longus	-	*Homo sapiens/ Pan*
Soleus	-	*Homo sapiens/ Pan*
Tibialis anterior	SL 2	*Pan*
Tibialis posterior	SL 3	*Pongo pygmaeus*

Table 3-13: Muscles with their insertion on the Tibia and the affinity of A.L. 288-1 based on Geometric Morphometric results

Muscle	Associated Landmarks	Affinity of A.L. 288-1
Gracilis	5	*Pan troglodytes*
Popliteus	-	*Homo sapiens/ Pan*
Rectus femoris	8	*Pan troglodytes*
Sartorius	6	*Pan troglodytes*
Semimembranosus	6	*Pan troglodytes*
Semitendinosus	6	*Pan troglodytes*
Tensor fasciae latae	6	*Pan troglodytes*
Vastus Intermedius	8	*Pan troglodytes*
Vastus Lateralis	8	*Pan troglodytes*
Vastus Medialis	8	*Pan troglodytes*

Landmarks and Semilandmarks

In order to determine the changes in shape for specific areas of the tibia, Principal Component Analyses were conducted on the 'True Landmarks' and each subset of Semilandmarks across all species groups.

The Principal Component Analysis conducted on just the True Landmarks of the tibia across all species groups showed that the first Principal Component explained 20.59% of the variance and the second explained 15.24%, cumulatively 35.83%. For the True Landmarks and the Semilandmarks of the Anterior Crest, the first principal component explained 23.78%, the second explained 15.75% for a total of 39.53% (see Appendix). When the Ture Landmarks and the Semilandmarks of the Interosseous Crest were considered, Principal Component 1 explained 22.45% of the total variance, and Principal Component 2 explained 13.15%, cumulatively 35.60%. The Principal Components Analysis of the True Landmarks and the Semilandmarks of the tibial plateau showed the first principal component explained 22.20% and the second explained 11.74%, a total of 33.94% (see Appendix).

Bi-plots of the first two principal components in each Semilandmark set (Figure 3-62) that each Semilandmark set largely showed a similar pattern, with the *Homo sapiens* and *Gorilla sp.* groups clearly separate from the other groups. There was a great deal of overlap between the *Pan paniscus, Pan troglodytes* and *Pongo pygmaeus* groups.

ANOVAs were conducted, each semilandmark set having largely met the assumptions of normality and Homogeneity of Variance (see Appendix), and each showed a significant difference in all Semilandmark sets for both principal components.

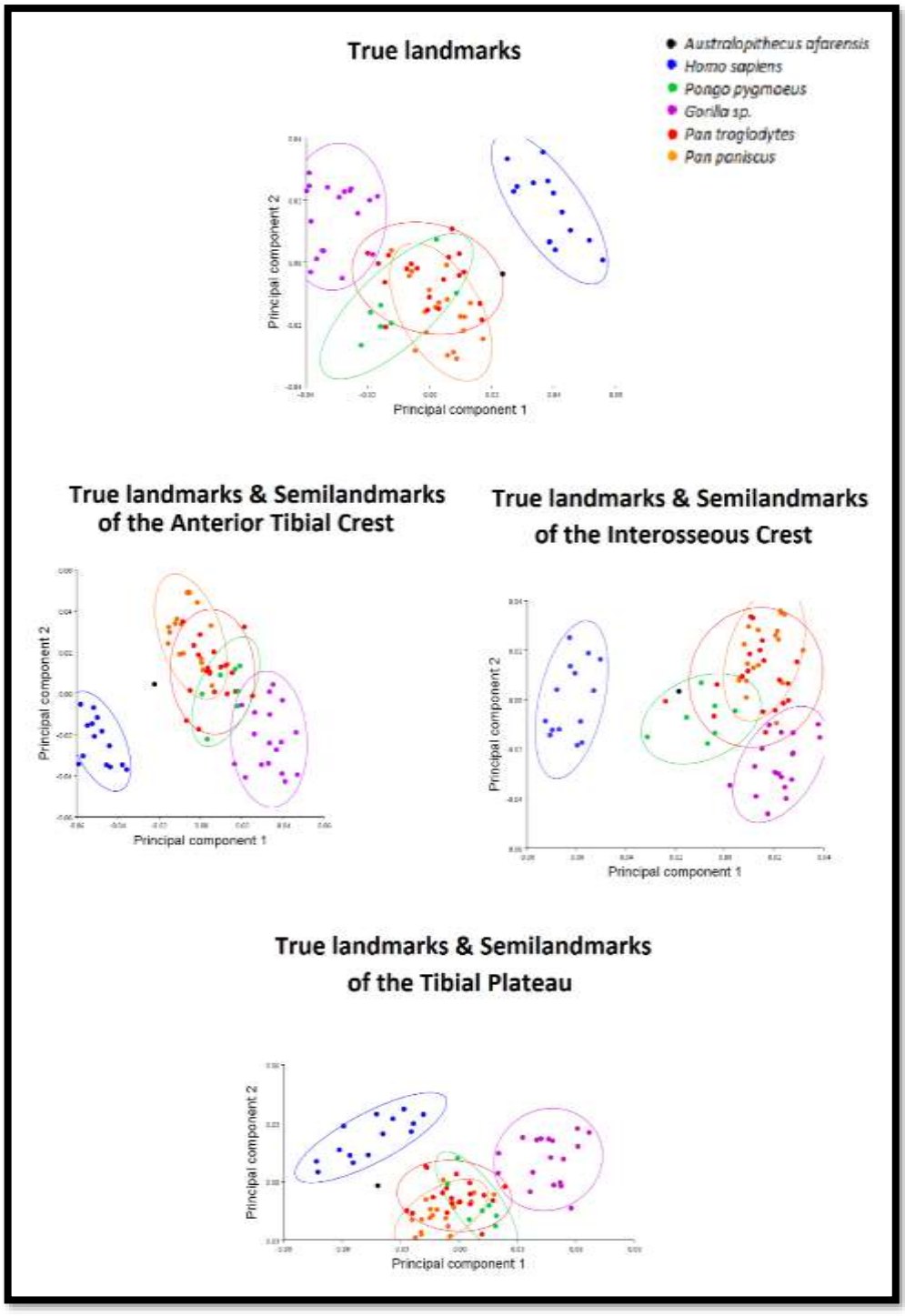

Figure 3-62: Plots of Principal Component 1 against Principal Component 2 for Each Semilandmark Set of the Tibia across All Species Groups

True landmarks

When the first Principal Component was plotted against the second Principal Component (Figure 3-62) the *Homo sapiens* and *Gorilla sp.* groups were distinct from the other groups. The *Pan paniscus, Pan troglodytes* and *Pongo pygmaeus* groups were less distinct, and clustered together. There was some separation of the *Pongo pygmaeus* group and the *Pan paniscus* group along the first principal component, and of the *Pan troglodytes* group along the second. The *Homo sapiens* group and the *Gorilla sp.* group were not distinct along the second principal component. The *Australopithecus afarensis* sample was closest to the *Pan troglodytes* group when plotted, though broadly fell between the *Pan* specimens and the *Homo sapiens* group.

The Tukey post-hocs (see Appendix) showed that along Principal Component 1, the *Gorilla sp.* group was distinct, as was the *Homo sapiens* group. The *Pan troglodytes* sample could group with either the *Pan paniscus* or *Pongo pygmaeus* samples along the first principal component. Along the second principal component the *Gorilla sp.* and *Homo sapiens* samples grouped together, as did the *Pan paniscus, Pan troglodytes* and *Pongo pygmaeus* samples.

Shape changes indicated by the Principal Components

The first two principal components when the true landmarks were considered were responsible for the majority of the shape variation within the tibia across the species groups (Figure 3-63). The shape changes along Principal Component 1 showed a general increase in width both medio-laterally and antero-posteriorly. The tibial plateau became more medially oriented and the intercondylar eminences became both wider and more pronounced. The medial condyle and articular surface increased in size. The tibial tuberosity became larger in relation to the shaft. The medial malleolus became more pronounced along Principal Component 1, and moved more posteriorly. The inferior articular surface became more laterally oriented along the first principal component. The tibial shaft became more curved along Principal Component 1and relatively shorter in comparison to the proximal and distal articular surfaces.

The second principal component showed a shortening of the tibial tuberosity and the tibial plateau shifted to a more posterior orientation. The inferior articular surface widened medio-laterally and the medial malleolus became more inferiorly oriented

along the second principal component. In addition to this, the tibial shaft became wider antero-posteriorly and also more curved along Principal Component 2.

Shape changes across the species groups

The shape changes along each principal component were reflected in the species groups (Figure 3-64). The *Pan paniscus* and the *Pan troglodytes* groups were very similar, although the medial malleolus in *Pan paniscus* was slightly more posteriorly placed than that of the *Pan troglodytes* group, and also slightly longer. The *Pan troglodytes* intercondylar eminences were slightly more pronounced than that of the *Pan paniscus* group and the tibial shaft showed marginally more curvature in the antero-posterior axis. The *Gorilla sp.* tibia was the most robust of the species groups, with increased thickness of the shaft, increased prominence of both the intercondylar eminences and the tibial tuberosity, and increased surface area of both the proximal and distal articular surfaces. The medial malleolus was less inferiorly oriented than the other species groups. The tibial shaft showed the greatest amount of curvature antero-posteriorly of all the species groups, and was relatively short in comparison to the other species groups. The tibial plateau was the most anteriorly angled of the groups.

The *Homo sapiens* group was the narrowest medio-laterally of all the species groups, with the greatest ratio of tibial shaft to proximal/distal tibia. The shaft was also the straightest of all the species groups. The inferior articular surface was perpendicular to the shaft, unlike all the other groups which showed a more angled surface. The *Pongo pygmaeus* tibia was similar in shape to the *Pan* groups, although showed a greater relative size of the inferior articulation, and a less inferiorly angled medial malleolus. The tibial shaft also showed a greater amount of curvature in the antero-posterior axis than that of the *Pan* groups.

The *Australopithecus afarensis* tibia (Figure 3-65) was most similar in shape to that of the *Pan troglodytes* group, although showed a relatively straighter tibial shaft similar to that of the *Homo sapiens* group. The inferior articular surface was angled similarly to the *Pongo pygmaeus* group, and the medial malleolus was of a similar proportion to this group also.

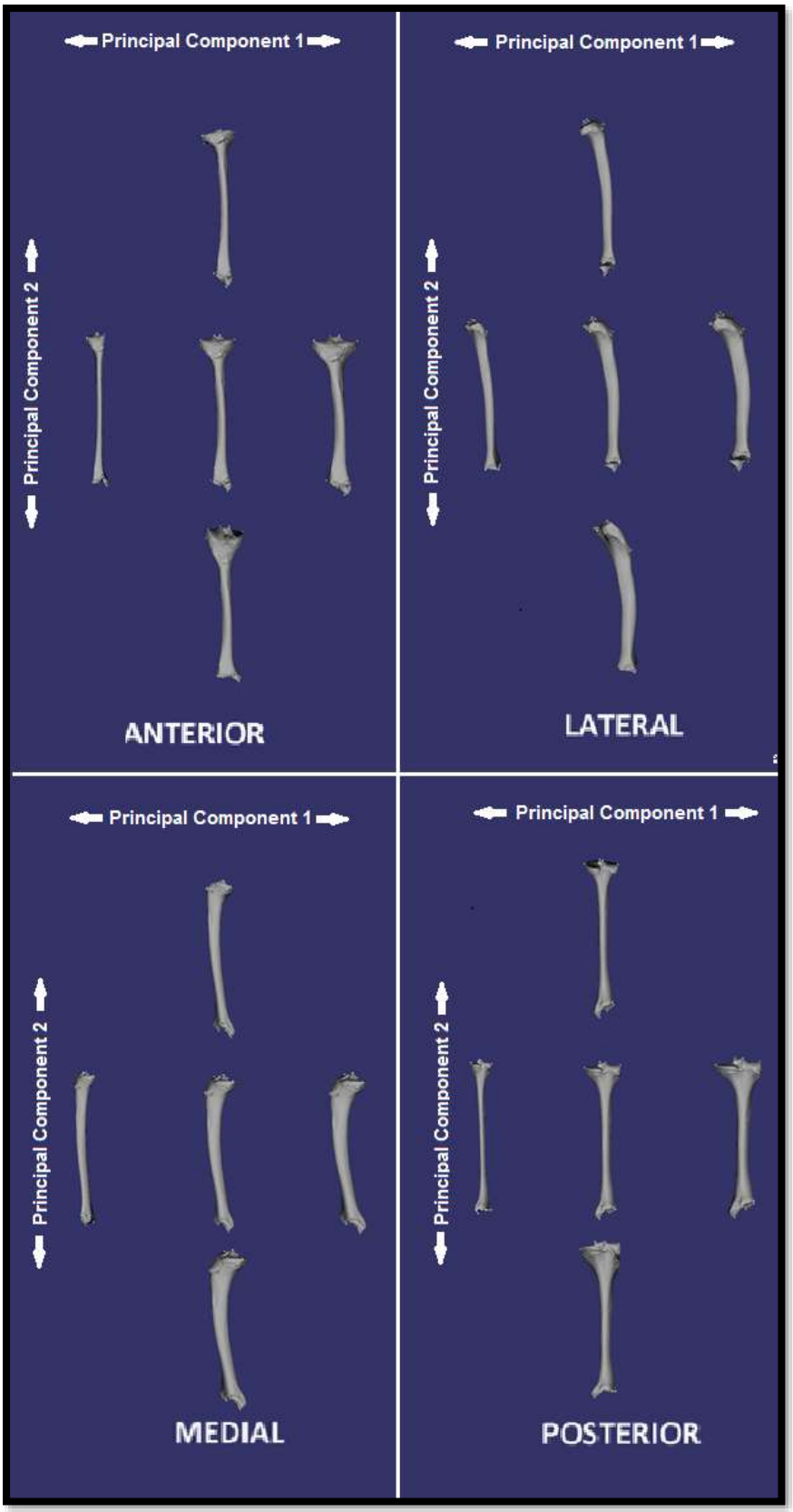

Figure 3-63: Changes in Tibia Shape Along Principal Components 1& 2, shown in Anterior, Lateral, Medial and Posterior Views as determined by the True Landmarks

Mean Tibia Shape shown centrally and the extremes of each Principal Component surrounding this

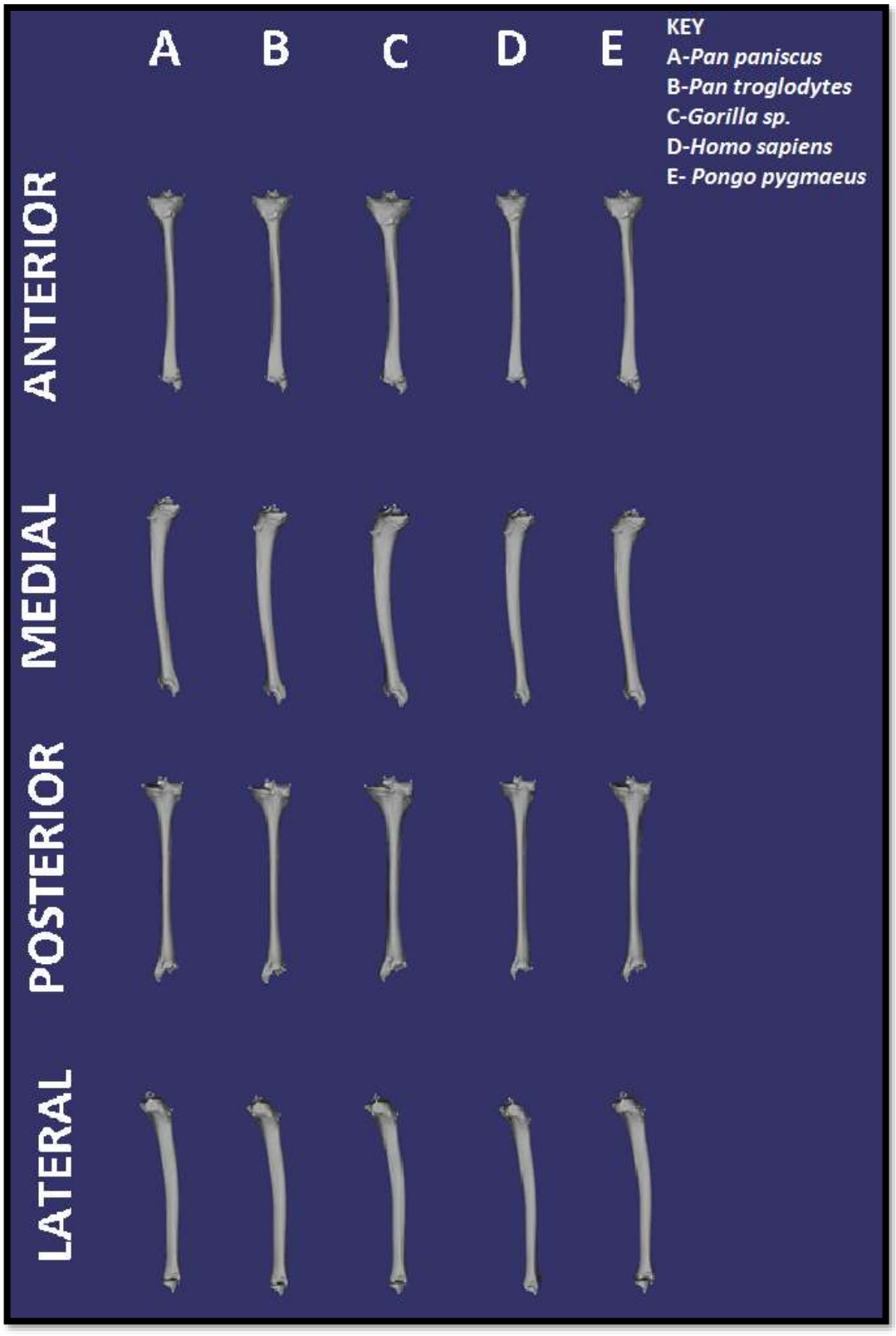

Figure 3-64: Mean Tibial shape for each species subset using True landmarks

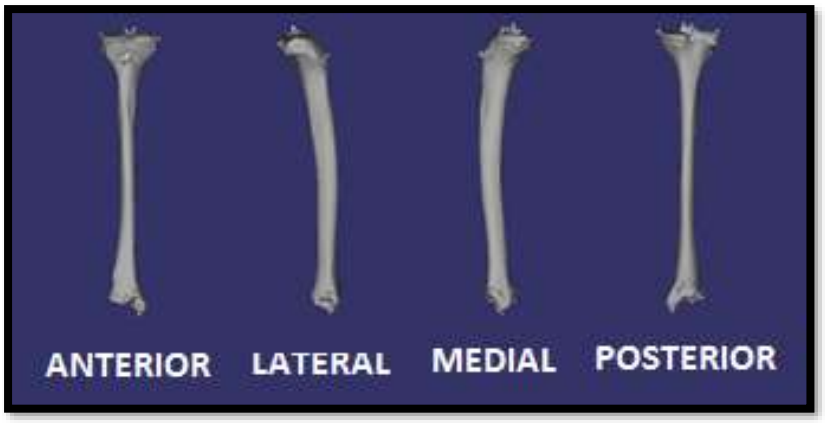

Figure 3-65: The shape of *Australopithecus afarensis* tibia using True Landmarks

Musculature associated with the True landmarks of the Tibia

When only the true landmarks were considered, the basic shape of the tibia in *Australopithecus afarensis* was closest to the *Pan troglodytes* group. The muscles associated with the True Landmarks of the tibia included *m. gracilis* (Landmark 5- Medial tibial plateau); *m. rectus femoris, m. vastus intermedius, m. vastus lateralis* and *m. vastus medialis* (Landmark 8- Tibial tuberosity); and *m. sartorius, m. semitendinosus, m. semimembranosus,* and *m. tensor fasciae latae* (Landmark 6- Lateral tibial plateau) which insert onto the tibia and *m. extensor digitorum longus* (Landmark 6) which originates on the tibia.

A bi-plot of the first two principal components (Figure 3-62) showed that the *Homo sapiens* group was most distinct from the other species groups. The *Gorilla sp.* was also largely distinct from the other groups. The *Pan paniscus, Pan troglodytes* and the *Pongo pygmaeus* groups showed were overlapping but the *Pan paniscus* and *Pongo pygmaeus* groups could largely be separated from each other, although both grouped with the *Pan troglodytes* sample. The *Homo sapiens* and *Gorilla sp.* samples grouped with each other along Principal Component 2. The *Australopithecus afarensis* sample plotted closest to the *Pan* groups.

The Tukey post-hoc tests (see Appendix) showed that along Principal Component 1, the species groups were largely distinct from each other, with the exception of the *Pan troglodytes* and *Pongo pygmaeus* groups which could be grouped together. Along Principal Component 2, the *Homo sapiens* and *Gorilla sp.* samples grouped together, and the *Pan troglodytes* sample could group both the *Pan paniscus* and *Pongo pygmaeus* groups.

Shape changes indicated by the Principal Components

Along each principal component, there was variation in the shape of the Anterior Tibial Crest (Figure 3-66). Along the first principal component, the crest changed from medially concave and largely bow shaped, to a more sigmoid shape, with the largest distal portion becoming medially convex. Along the second principal component, the anterior tibial crest shifted from a more medial position to one that was more anteriorly placed. The point of curvature in the superior portion of the crest also moved proximally along the second principal component.

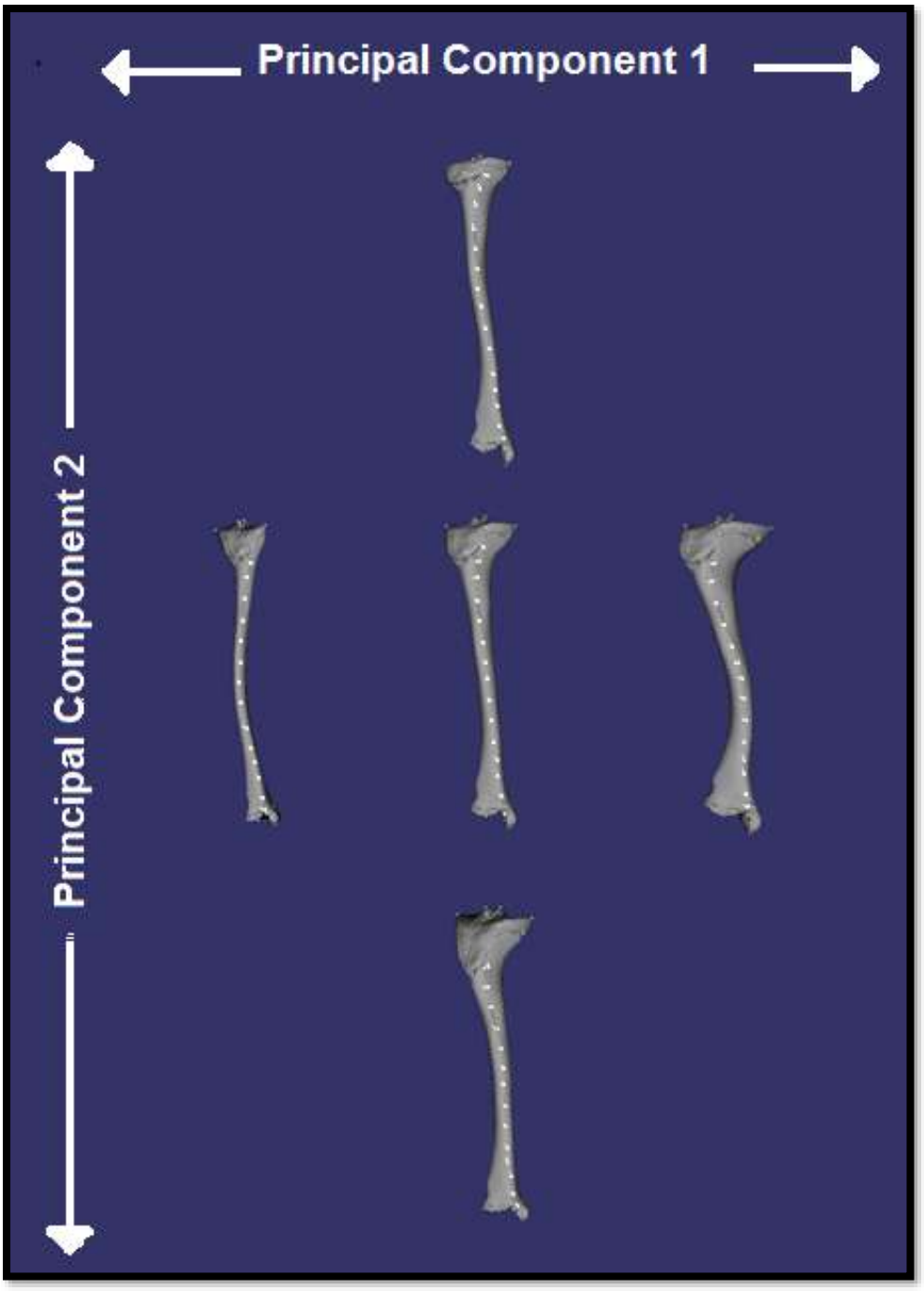

Figure 3-66: Changes in the Shape of the Anterior Tibial Crest along Principal Components 1 and 2, with the Mean Shape shown in the Centre

Shape changes across the species groups

The shape of the anterior tibial crest across the species groups showed a combination of the features seen along each principal component (Figure 3-67). The *Pan paniscus*, *Pan troglodytes* and *Pongo pygmaeus* anterior tibial crests were all broadly similar in shape, but showed an increasing amount of curvature in the distal portion of the crest.

The anterior tibial crest in the *Homo sapiens* group showed the least amount of curvature overall, resulting in a relatively straight crest along the shaft. The *Gorilla sp.* mean showed the most sigmoid shaped curvature of all the groups, with both pronounced proximal and distal curves.

Figure 3-67: Mean Shape of the Anterior Tibial Crest across species groups

The *Australopithecus afarensis* specimen (Figure 3-68) showed a relatively straighter anterior tibial crest than the *Pan* groups. This was not as straight as that of the *Homo sapiens* group, with a more pronounced curve on the distal portion of the crest.

Figure 3-68: The Shape of the *Australopithecus afarensis* Anterior Tibial Crest

Musculature associated with the True landmarks and semilandmarks of the anterior tibial crest

When only the true landmarks and the semilandmarks of the anterior tibial crest were considered, the *Australopithecus afarensis* specimen showed the greatest affinity with the *Pan* groups. As such, the origin for the *m. tibialis anterior* was assumed to be similar to the *Pan* condition.

True landmarks and Semilandmarks of the Interosseous Crest

A bi-plot of the first two principal components (Figure 3-62) showed that the *Homo sapiens* group was most distinct from the other species groups along the first principal component. The *Pongo pygmaeus* group was also separable along Principal Component 1. The *Pan paniscus*, *Pongo pygmaeus* and *Gorilla sp.* were largely distinct from each other but the *Pan troglodytes* group overlapped with all of them to some degree. The *Australopithecus afarensis* specimen grouped clearly with the *Pongo pygmaeus* subset.

The Tukey post-hoc tests (Table 4-50) showed that along the first principal component, the *Homo sapiens* group and the *Pongo pygmaeus* group were distinct from the other groups. Along the second principal component, the *Gorilla sp.* subset was distinct from all the other species subsets. The *Homo sapiens* subset could group with both the *Pongo pygmaeus* and *Pan troglodytes* subsets, and the *Pan troglodytes* Subset could also group with the *Pan paniscus* subset.

Shape changes indicated by the Principal Components

Along each principal component there were changes in the shape of the interosseous crest (Figure 3-69). Along Principal Component 1 the interosseous crest shifted from a diagonal orientation to one that was straighter. The change in shape along the second principal component was primarily due to a change in the relative length of the interosseous crest.

Shape changes across the species groups

The interosseous crest of each species showed a combination of features from Principal Components 1 and 2 (Figure 3-70). The *Pan paniscus*, *Pan troglodytes* and *Pongo pygmaeus* interosseous crests were all very similar, although the *Pongo pygmaeus* crest was the most diagonally oriented of the three groups. The *Homo sapiens* group had the most diagonally oriented interosseous crest of all the groups, and also, along with the *Pan paniscus* group had the relatively longest length along the shaft of the species groups. The *Gorilla sp.* interosseous crest was the straightest of all of the groups and also had the relatively shortest length along the shaft.

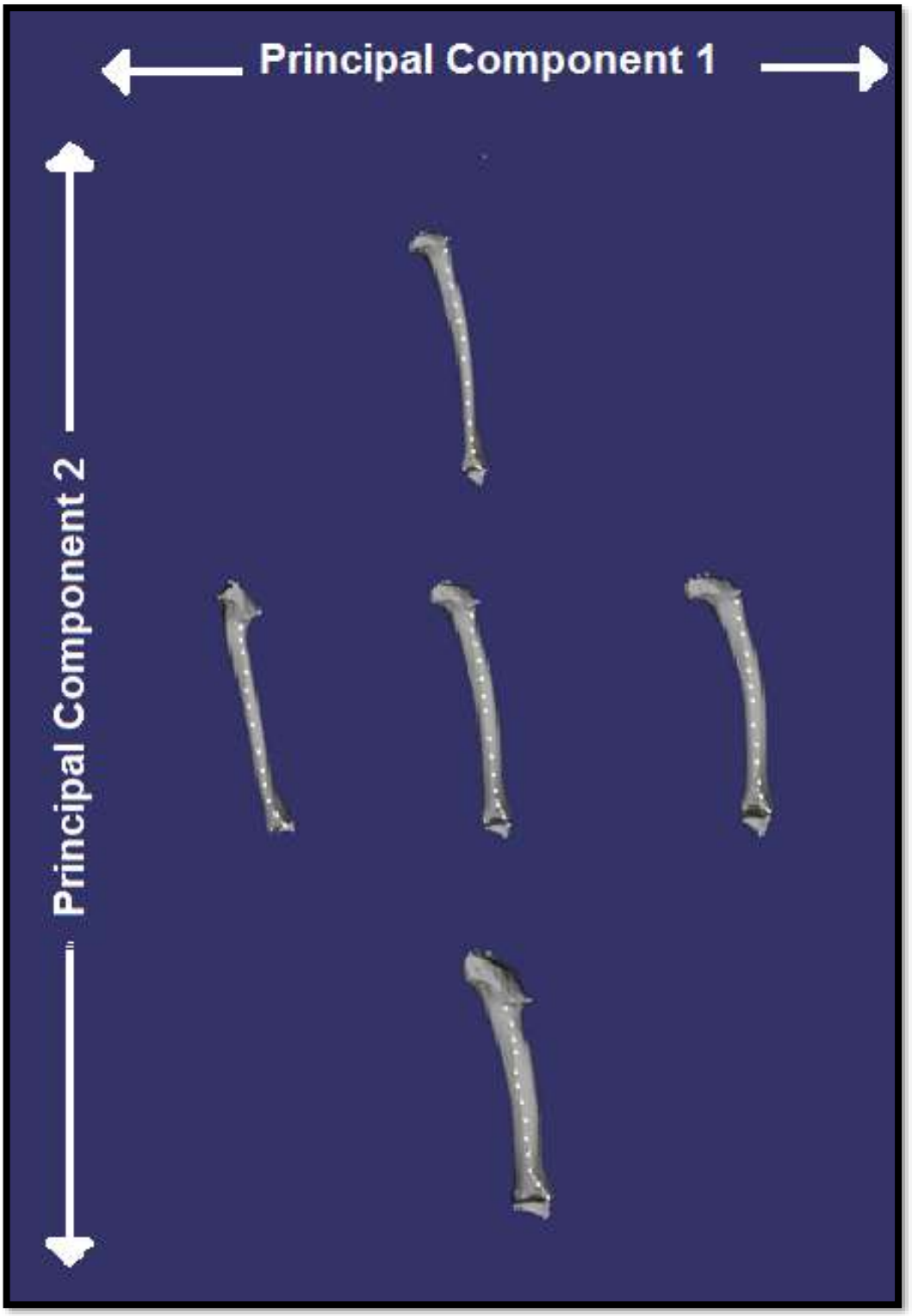

Figure 3-69: Changes in Tibial Interosseous Crest Shape along Principal Components 1 and 2, with the Mean Shape shown in the Centre

Figure 3-70: Mean Shape of the Interosseous Crest across species groups

The *Australopithecus afarensis* interosseous crest was most similar to the *Pongo pygmaeus* group, with a similar degree of diagonal orientation along the shaft. The length of the crest along the tibial shaft was intermediate between the species groups (Figure 3-71).

Figure 3-71: The Shape of the *Australopithecus afarensis* Interosseous Crest

Musculature associated with the True landmarks and semilandmarks of the interosseous crest

When only the true landmarks and semilandmarks of the interosseous crest were considered, the *Australopithecus afarensis* specimen showed the greatest affinity with *Pongo pygmaeus*. As such, the origin of the *m. tibialis posterior* was assumed to reflect the condition in *Pongo pygmaeus.*

True landmarks and Semilandmarks of the Tibial Plateau

The bi-plot of the first two principal components (Figure 3-62) showed a clear separation of the *Homo sapiens* group and also the *Gorilla sp.* group. There was some separation of the *Pan paniscus* and *Pongo pygmaeus* groups, but the *Pan troglodytes* group was not separable from either of these groups. The greatest differentiation between the groups was along the first principal component, although there was differentiation of the *Homo sapiens* and *Gorilla sp.* groups along the second principal component. The *Australopithecus afarensis* specimen did not group directly with any species group, and was largely intermediate between the *Homo sapiens* group and the *Pan* groups. Along Principal Component 1, the australopithecine specimen grouped with the *Homo sapiens* subset, but along Principal Component 2, could group with any of the non-human ape groups.

The Tukey post-hoc tests (see Appendix) showed that the *Homo sapiens* and *Gorilla sp.* groups were distinct from the other groups along both Principal Components 1 and 2. Along Principal Component 1, the *Pan troglodytes* subset could group with either the *Pan paniscus* or *Pongo pygmaeus* subsets, and along Principal Component 2, the three subsets grouped together.

Shape changes indicated by the Principal Components

Along each principal component, there were changes to the shape of the tibial plateau (Figure 3-72). Along the first principal component there was a decrease in the medio-lateral width of the plateau. This was largely as a result of the medial articular surface decreasing in size. The lateral articular surface also decreased in size, but to a much lesser degree, resulting in the articular surfaces becoming more equally sized along the first principal component. Along the second principal component, there was a decrease in medio-lateral width, with a corresponding increase in antero-posterior width.

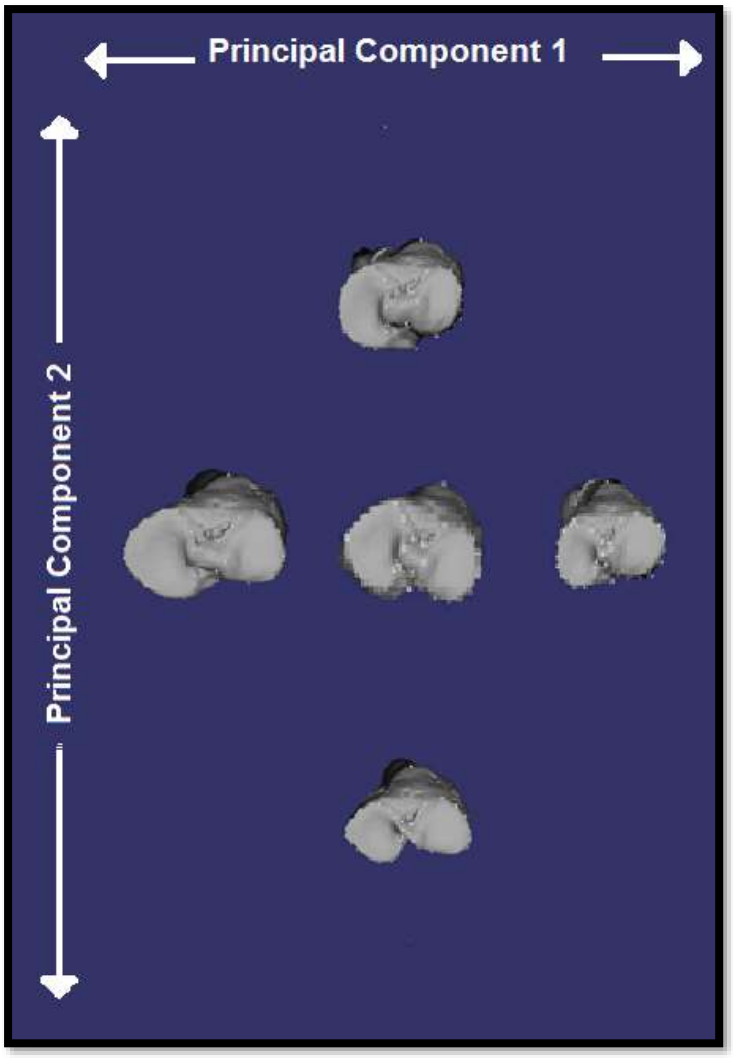

Figure 3-72: Changes in Tibial Plateau Shape along Principal Components 1 and 2, with the Mean Shape shown in the Centre

Shape changes across the species groups

The changes in the shape of the tibial plateau along each principal component were reflected in the shapes of the tibial plateau across the species groups (Figure 3-73). The *Pan paniscus* mean tibial plateau was very similar to that of the *Pan troglodytes* group, although the *Pan troglodytes* mean was slightly medio-laterally wider than that of the *Pan paniscus* group. The *Pongo pygmaeus* mean was also very similar to that of the *Pan troglodytes* group but showed marginally greater width medio-laterally. The *Gorilla sp.* mean tibial plateau was the widest medio-laterally of all the groups, but also showed greater width antero-posteriorly. The *Homo sapiens* mean showed the narrowest medio-lateral width, but also the relatively greatest antero-posterior width.

Figure 3-73: Mean Shape of the Tibial Plateau across species groups

The *Australopithecus afarensis* tibial plateau (Figure 3-74) had a rounder medial articular surface than any of the extant groups. This was a consequence of being medio-laterally narrower than the *Pan* groups, but also having relatively longer articular surfaces antero-posteriorly.

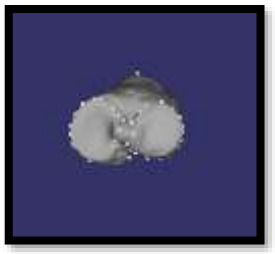

Figure 3-74: The Shape of the *Australopithecus afarensis* Tibial Plateau

Musculature associated with the True landmarks and tibial plateau

In true landmarks and semilandmarks of the tibial plateau *Australopithecus afarensis* was shown to be intermediate between the *Homo sapiens* and *Pan* groups. There are no muscles which attach to the tibial plateau, and so this didn't have an impact on the placement of muscles on the model. The tibial plateau is, however, a key anatomical structure in locomotion as it is key in the transmission of load from the thigh into the leg, and serves as the articulation with the femur at the knee.

3.43 Summary of the Shape and Musculature of the Tibia

The tibia in Pan

As in all bones under study, the *Pan paniscus* and *Pan troglodytes* tibiae were similar.

The *Pan paniscus* tibial plateau was very similar to that of the *Pan troglodytes* group, although the *Pan troglodytes* plateau was slightly medio-laterally wider than that of the *Pan paniscus* group. The *Pan troglodytes* intercondylar eminences were also slightly more pronounced than that of the *Pan paniscus* group, indicating slightly less rotational capability at the knee.

The *Pan troglodytes* tibia showed a slightly larger tibial tuberosity than the *Pan paniscus* group, indicating a stronger attachment for the quadriceps group in *Pan troglodytes*

The *Pan troglodytes* tibial shaft was marginally wider antero-posteriorly, but the *Pan paniscus* group shaft was longer than in *Pan troglodytes*, in accordance with Zihlman and Cramer (1978).

The *Pan troglodytes* anterior tibial crest showed more of curvature in the distal portion of the crest, indicating a marginally different configuration of *m. tibialis anterior*- important for dorsiflexion and inversion of the foot, and perhaps indicative of the increased arboreality in *Pan paniscus*.

Further to this, the medial malleolus in *Pan paniscus* was slightly more posteriorly placed than that of the *Pan troglodytes* group, and also slightly longer indicating flexibility of the ankle and stability in dorsiflexion and inversion when vertically climbing (DeSilva, 2009).

The tibia in Gorilla

The *Gorilla sp.* tibia was the most robust of the species groups, with the greatest relative size of the proximal and distal articulations, as well as the thickest and shortest shaft.

The tibial plateau was the widest medio-laterally of all the groups, but also showed greater width antero-posteriorly. There was also increased prominence of the intercondylar eminences, indicating greater stability at the knee (Zihlman et al. 2011) and less rotational capability than in *Pan.*

The tibial tuberosity was the most pronounced of all the groups, indicating the relatively largest quadriceps, demonstrating the propulsive power required in *Gorilla*.

The tibial shaft showed the greatest amount of curvature antero-posteriorly of all the species groups, and was relatively short in comparison to the other species groups.

Gorilla sp. showed the relatively shortest shaft of all the species groups. The anterior tibial crest had pronounced proximal and distal curves, but the interosseous crest was the straightest of all of the groups, indicating the significant propulsive action required at the ankle due to the *Gorilla's* increased size (Zihlman et al. 2011).

The medial malleolus was less inferiorly oriented than the other species groups, which could suggest the need for stability at this joint due to the increased body mass of *Gorilla* (De Silva, 2009).

The tibia in Pongo

The *Pongo pygmaeus* tibia was very similar to the tibiae of the *Pan* groups, although the shaft was slightly more curved, and both the proximal and distal articulations were relatively larger- a possible indication of *Pongo's* greater relative size or greater arboreality.
The tibial shaft also showed a greater amount of curvature in the antero-posterior axis than that of the *Pan* groups and an increased amount of curvature in the distal portion of the anterior tibial crest than in the *Pan* groups, the origin for the *m. tibialis anterior*.

The *Pongo pygmaeus* interosseous crest was more diagonally oriented than in *Pan*- the origin of the *m. tibialis posterior*- primarily an inverter of the foot. Additionally, *Pongo pygmaeus* also showed a less inferiorly angled medial malleolus than *Pan*.

These features reflect the grasping foot and joint mobility required by a highly arboreal species (Payne et al., 2006). Greater rotational capability at the knee and ankle (Zihlman et al. 2011) combine with in inverted foot (Grand, 1967) to allow stable propulsion through an arboreal environment.

The tibia in Homo

The *Homo sapiens* tibial plateau mean showed the narrowest medio-lateral width, but also the relatively greatest antero-posterior width and was the most superiorly oriented of the species groups. This likely reflects the reduced medial and lateral rotation found in the modern human biped's knee (Sylvester, 2013).

The tibial shaft was the longest and straightest of all the species groups.
The anterior tibial crest in the *Homo sapiens* group showed the least amount of curvature overall, resulting in a relatively straight crest along the shaft. Additionally, the *Homo sapiens* group had the most diagonally oriented interosseous crest of all the groups.

The inferior articular surface was perpendicular to the shaft, unlike all the other groups which showed a more angled surface. This angled surface allows for the non-human apes to have a greater degree of ankle mobility- required for successful arboreal locomotion (Sigmon, 1974).
In contrast to this, the modern human biped's ankle and knee show significantly reduced mobility in comparison, with the greatest amount of movement occurring only in the mid-sagital plane. The knee and the ankle are therefore more stable.

The tibia of A.L. 288-1

The *Australopithecus afarensis* tibia was broadly intermediate in shape between the *Pan* and *Homo sapiens* tibiae but most similar in shape to that of the *Pan troglodytes* group overall.
The *Australopithecus afarensis* tibial plateau had a rounder medial articular surface than any of the extant groups. This was a consequence of being medio-laterally narrower than the *Pan* groups, but also having relatively longer articular surfaces antero-posteriorly than in *Homo sapiens.*

The tibial shaft was relatively straight, as in the *Homo sapiens* group, however, the anterior tibial crest had a more pronounced curve on the distal portion of the crest. The

interosseous crest was most similar to the *Pongo pygmaeus* group, with a similar degree of diagonal orientation along the shaft.
The inferior articular surface was angled similarly to the *Pongo pygmaeus* group, and the medial malleolus was of a similar proportion to this group also.

This would seem to suggest a knee intermediate in its capabilities between *Homo sapiens* and *Pan* as argued by Tardieu (1979a; 1979b; 1983; 1986a, 1986b) and Tardieu and Preuschoft, (1996) but an ankle with increased mobility, and potentially grasping capabilities (Christie, 1977; Deloison, 1991 and Gomsberg, 1985).

As the distal lower limb seems to become more like the distal limb in the more arboreal extant non-human apes, it could be inferred that, as in these apes, the limb tapers less than in *Homo sapiens.* This has been suggested (Payne et al. 2006) to be indicative of the use of the feet for grasping.

4. Modelling the Musculature of *Australopithecus afarensis*

4.1 Forward Dynamic Model

In order to construct the model for the locomotion of the fossil species within the forward dynamic modelling program GaitSym (Sellers, 2014), an XML configuration file had to initially be created. This file needed to contain all the musculature information, as well as the information required by the program to determine the mechanical properties of the simulation.

4.11 The Configuration file

The basic format of the configuration file was as follows:

```
<?xml version="1.0"?>
<GAITSYMODE>
<STATE options />
<IOCONTROL options />
<GLOBAL options />
<ENVIRONMENT options />
<BODY options />
<JOINT options />
<GEOM options />
<MUSCLE options />
<DRIVER options />
</GAITSYMODE>
```

The file was created following the recommended workflow set out in the GaitSym 2013 Manual (Sellers, 2013).

4.12 Anatomical Capture

The previously scanned skeletal elements from the fossil specimen used for the Geometric Morphometric analyses were used to create a complete model of the lower limb. This was done in Maya (Autodesk, 2015). Elements from the complete side were mirrored to produce the full skeleton. Additionally, a basic model of the foot was

created using human-like proportions (as suggested by Nagano et al., 2005). The required end result was a representation of the complete lower skeleton on *Australopithecus afarensis* as OBJ surfaces in their relative positions using a right handed coordinate system with Z up as this is the default for GaitSym. This model can be seen in Figure 4-1.

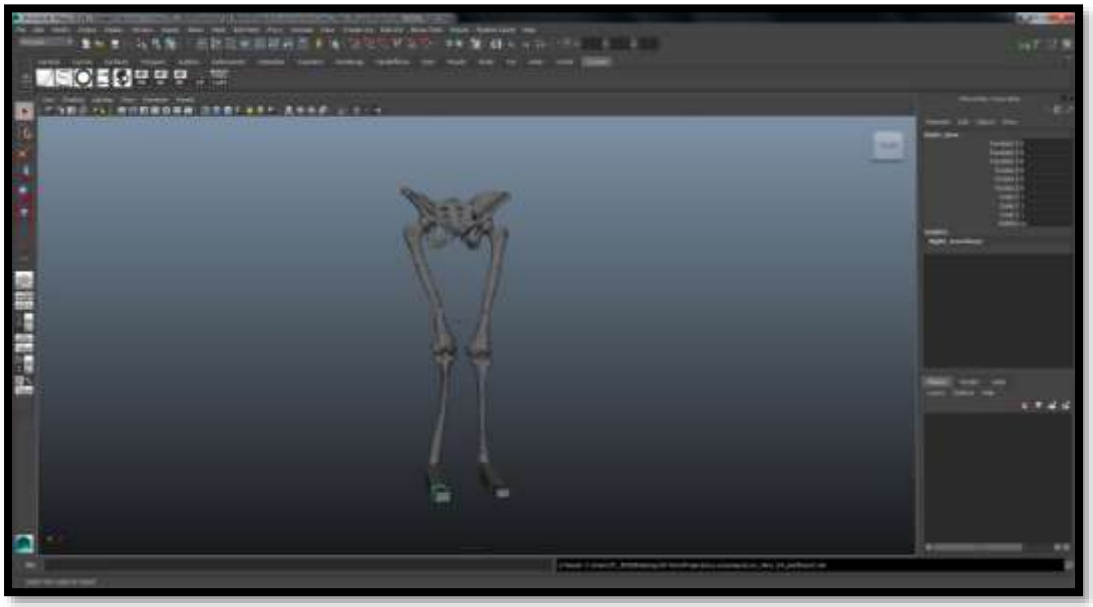

Figure 4-1: Complete Lower Skeleton of A.L. 288-1 Reconstructed in Maya (Autodesk, 2015)

Each element was then exported as separate triangulated OBJ surfaces using these global coordinates.

4.13 Initial Configuration File Creation

A basic configuration file was created to allow the skeletal form to be interpreted by the GaitSym program. This was done in order to create the basic model on which the final model was constructed (Figure 4-2).

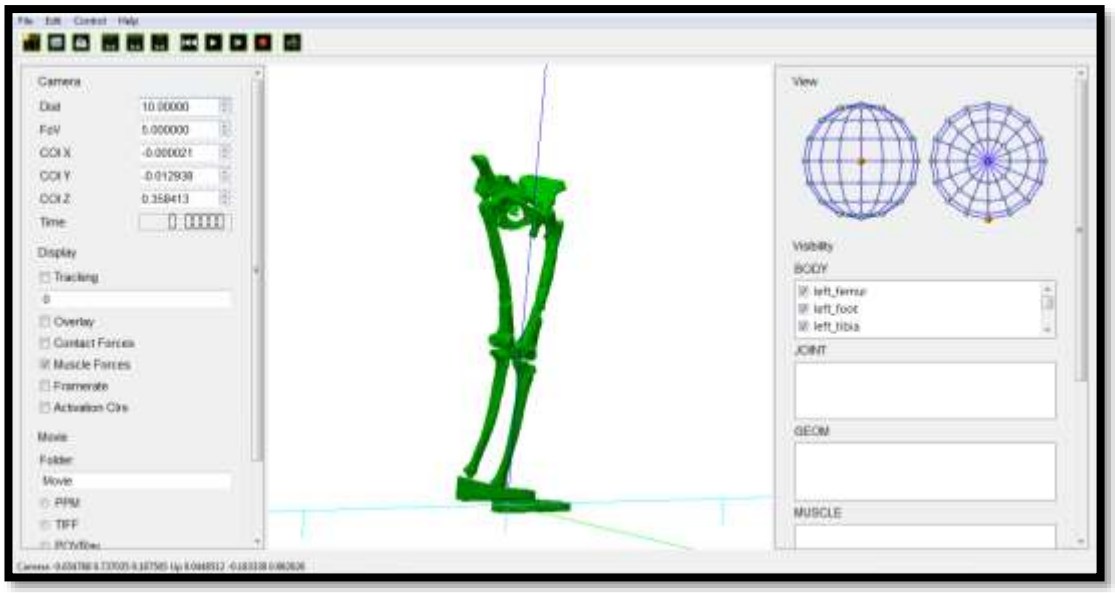

Figure 4-2 Basic Configuration file uploaded into GaitSym

4.14 Joints, Contact Points and Muscles

Once the model was imported into GaitSym, the 3D cursor function within GaitSym was used to specify the coordinates of all the joints, contact points and muscle paths (Figure 4-3). The cursor provides the 3D coordinates for any point on the model, so each point was placed on the model in turn. These were then copied into Microsoft Excel for use in the construction of the more complete final model.

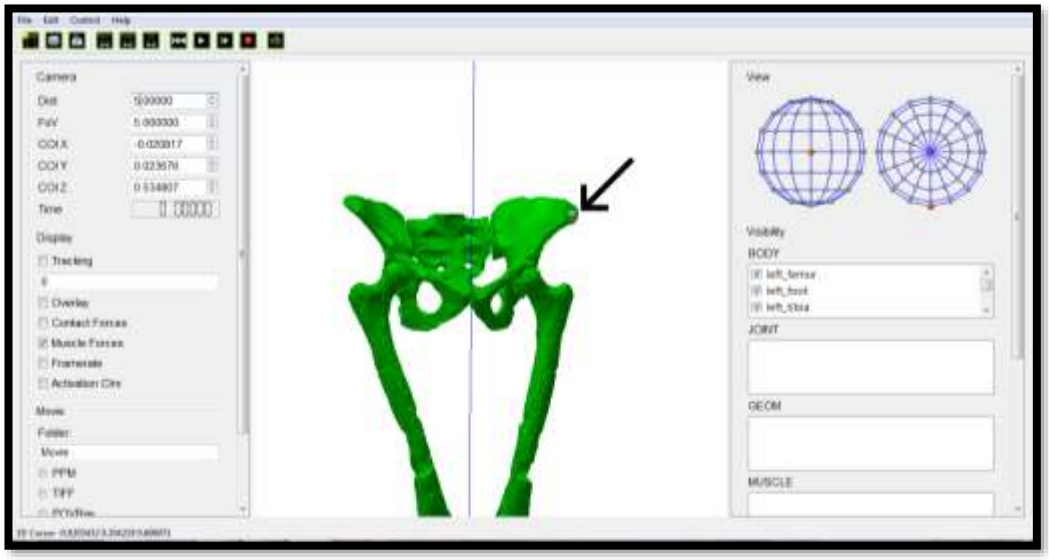

Figure 4-3: The 3D Cursor Tool In GaitSym
(Coordinates are displayed in the Lower Left Corner of the figure)

4.15 Creation of the Complete Configuration File

In order to create the complete configuration file, the parameters of each skeletal element (body), each joint, each contact point and each muscle had to be input. The drivers to run the simulation also had to be input.

The Joints

For the joints, the configuration file required a name for each joint (Joint ID) and the type of joint also had to be specified. In addition to this, the maximum allowable movements at each joint had to be set. In order to do this, the ParamLoStop and ParamHiStop had to be specified in degrees with a "d" suffix, relative to the reference pose. The Hinge Anchor and Hinge Axis positions also had to be specified. These specify the positions on the skeletal elements that form the basis of the joints and also the axis around which the joint pivots respectively. These were obtained using the 3D Cursor function in GaitSym. An illustration of a typical joint configuration can be seen in Figure 4-4.

```
<JOINT ID="left_ankle"
Type="Hinge"
Body1ID="left_tibia"
Body2ID="left_foot"
ParamLoStop="-10d"
ParamHiStop="10d"
HingeAnchor="left_tibia    -0.172012    0.134363    0.0952053"
HingeAxis="left_tibia      0      1      0"
Body2HingeAnchor="left_foot    -0.167647    0.143809    0.0814813"
Body2HingeAxis="left_foot 0      1      0"
StartAngleReference="0"/>
```

Figure 4-4: An Example of the Configuration for a Joint

The Contact Points

The position of the contact points (GEOMs) were specified using the 3D cursor. As with the joints, a name for each contact point had to be specified (GEOM ID). These were set to be spherical in shape. Each contact node also had to be attached to a body on the model (Body ID), and given a size (Radius). The position of each contact point had to be above ground level as if they were below the ground level, the model would generate extreme forces. Figure 4-5 shows a typical configuration for a contact point.

The values not specified above were kept as recommended by the GaitSym manual (Sellers, 2013).

```
<GEOM ID="left_foot.HeelContactNode"
Type="Sphere"
BodyID="left_foot"
Radius="0.01"
SpringConstant="1e5"
DampingConstant="1e4"
Mu="1.0"
Abort="false"
Position="left_foot  -0.172112    0.146723     0.00000304406"
Quaternion="left_foot       0.5    -0.5    0.5     0.50000000000000011"/>
```

Figure 4-5: An Example of the Configuration of a Contact Point

The Muscles

The basis for the positioning of the muscles was determined as a result of the Geometric Morphometric analysis previously conducted. Where similarity in shape of the skeletal elements of A.L. 288-1 and an extant species was determined, it was assumed that there was similarity in the position and construction of the muscles in this area (as per Scott, 1957; Ashton and Oxnard, 1964; Oxnard, 1967; 1968; Bryden and Felts,1974; Corruccini and Ciochon, 1976; Kimes et al. 1981;Diogo, 2004; Ruff et al., 2006; Diogo et al. 2012).In the construction of the model, the Minetti Alexander Extended model (Minetti and Alexander, 1997) was used as it was a stable forward dynamic modelling system available within the GaitSym options. Each separate muscle was identified using an individual Muscle ID.

```
<MUSCLE ID="Rectus femoris L"
Type="MinettiAlexanderExtended"
OriginBodyID="pelvis"
InsertionBodyID="left_tibia"
ForcePerUnitArea="300000"
PCA="0.001584485"
FibreLength="0.03492764"
VMaxFactor="8.4000000000000004"
SerialStrainAtFmax="0.052999999999999999"
ParallelStrainAtFmax="0.5"
ActivationK="0.17"
ActivationKinetics="false"
Strap="NPoint"
ViaPointBody0="left_femur"
TendonLength="-1"
Origin="pelvis        -0.0212834   0.135859      1.13995"
Insertion="left_tibia  -0.0309049   0.11025       0.485472"
ViaPoint0="left_femur       -0.0139065   0.147199      0.84674"/>
```

Figure 4-6: An Example of the Configuration of a Muscle

The Origin and Insertion positions were obtained using the 3D Cursor, as were any additional contact points for the muscles (ViaPoints or MidPoints depending on the muscle parameters). These were described in the model depending on the parameters of each muscle. The muscles used were specified as 'Strap', although obviously not every muscle is a strap muscle. It is important to note here that when building the musculature for the model, it is not necessarily the exact configuration of the muscle, as is seen in real life anatomy that is used, but a configuration that is appropriate to obtain an equivalent movement result. For example- the Gluteus Maximus muscle was divided into 3 separate 'straps', although in reality it is one muscle. Where there were multiple parts of the same muscle, these were identified as *Muscle Name 1, Muscle name 2* etc.

As with the previous parts of the model, the muscle information also needed to refer to the bodies which it made contact with, thus the origin body and insertion body had to be specified for each muscle, as well as the bodies for ViaPoints and MidPoints).

Force per unit area was chosen to be 300 000Nm^{-2} as per Hutchinson (2004), however other values have been used in previous studies ranging from 250 000Nm^{-2} (Umberger et al., 2003) to 400 000Nm^{-2} (Zheng et al., 1998). Alexander (2003) reports in vitro maximum values of between 330 000Nm^{-2} and 360 000Nm^{-2}, and Pierrynowski (1995) recommends 350 000Nm^{-2}. Hutchison's value was chosen as this was intermediate between the recommendations.

Muscle fibre lengths are often problematic to estimate in fossil species as direct measurements are not available. However, Payne *et al* (2006) demonstrated that this scales to body mass in closely related species relatively successfully (see also Sellers *et al.* 2005; Nagano *et al.* 2005). As such, the fibre lengths for each muscle were scaled from known fibre lengths taken from Friedrich and Brand (1990) for the muscles with an assumed association with humans, and from Payne *et al.* (2006) for the muscles associated with the other comparative species. Scaling was done according to body mass estimates following Kramer (1999), under the assumption that AL 288-1 had a body mass of approximately 33kg.

Calculating the Physiological Cross Sectional Area (usually referred to as PCSA, but known as PCA within the GaitSym program) was done using the formula:

$$PCSA = m/\rho l$$

where m is muscle belly mass in kilograms, ρ is muscle density (1.06 g $cm^{-3,}$ Mendez & Keys, 1960) and l is muscle fibre length in metres (Payne *et al.*, 2006). This was calculated for each individual muscle based on its affinity as suggested by the Geometric Morphometric analysis, and scaled to *Australopithecus afarensis* proportions, assuming a body mass of 33kg as per Kramer (1999).

The ratio of the individual muscle mass to total body mass of the affinitive species was calculated, and then this proportion of muscle mass to body mass was applied to the fossil specimen and used in the above calculation of PCSA for each muscle predicted for AL 288-1. This of course relies on the assumption that the specimens used in Payne *et al.* (2006) and Friedrich and Brand (1990) are typical in their ratios of muscle mass to body mass, and that this can be assumed to correlate in the fossil species.

A maximum contraction speed (VMaxFactor) of $8.4s^{-1}$ was chosen to represent a mixed fibred muscle as suggested by Sellers *et al* (2013). This represents a midpoint between the values suggested in Umberger et al. (2003) - $12s^{-1}$ for fast twitch muscle fibres and $4.8s^{-1}$ for slow twitch muscle fibres in humans.

The Activation K (ActivationK) value was set to 0.17 as recommended by the model used (Minetti & Alexander, 1997). This value is a constant determined by the maximum moment, and allowing for the calculation of the metabolic power for a muscle (Minetti & Alexander, 1997).

The TendonLength was set to -1 as this allowed the value to be calculated so that the muscle was slack in the original reference pose. The values not specified above were kept as recommended by the GaitSym manual (Sellers, 2013). Figure 4-6 illustrates a typical configuration for a muscle.

Drivers

In order to produce a walking model, the muscular elements needed to be activated in an appropriate sequence. In order to do this, 'drivers' had to be added to the model. These supplied a time dependent value change to each muscle. The typical configuration of a driver is shown in Figure 4-7.

In order to create a working driver, the driver itself initially needed to be named and the object (muscle) it was driving, identified. The type of driver also needed to be determined. A cyclic driver was chosen for all the muscles in this study. A cyclic driver

stipulated that the muscles would activate at a specified level for a specified time, and then, when the cycle of activation was complete, repeat the cycle.

The "DurationValuePairs" element of the driver represented the duration and the activation level of each activation of the muscle.

A full step cycle was estimated to take approximately 1.118 seconds. This was then separated into 20 individual activation periods of approximately 0.056 seconds.

```
<DRIVER      Type="Cyclic"   ID="Tibilais posterior R"
Target="Tibilais posterior R"   DurationValuePairs=
"0.05591937466307250        0.055919375   0.3
0.055919375   0.5     0.055919375   0.8
0.055919375   1       0.055919375   1
0.055919375   1       0.055919375   0.8
0.055919375   0.5     0.055919375   0.3
0.055919375   0       0.055919375   0
0.055919375   0       0.055919375   0
0.055919375   0       0.055919375   0
0.055919375   0       0.055919375   0
0.055919375   0       0.055919375   0"/>
```

Figure 4-7: An Example of the Configuration of a Driver

The pattern of activation for the muscle drivers was then determined using the muscle activation pattern as described in Tao *et al.* (2012), who used wearable sensors on human subjects to determine a normal muscle activation pattern during bipedal walking. A smooth curve of activation was used for each muscle. Where the activation for a particular muscle was not available, the pattern for its nearest synergist was used. Table 4-1 shows the muscle activation pattern adapted from Tao *et al.* (2012), and Table 4-2 shows the activation levels used in the simulation for the muscles of the right-hand side. The activation patterns for the left-hand side were the same as that of the right-hand side, but at half a phase out of sync.

Table 4-1: Muscle Activation by Percentage of Bipedal Stride (Taken from Tao *et al.* 2012)

Muscle	Percentage of stride that muscle is activated		
Biceps Femoris Long Head	0-10	88-100	
Biceps Femoris Short Head	0-3	79-100	
Extensor Digitorum Longus	0-12	50-100	
Extensor Hallucis Longus	0-18	57-100	
Gemellus Inferior	0-12	95-100	
Gemellus Superior	0-12	95-100	
Gluteus Maximus	0-12	95-100	
Gluteus Medius	0-40	88-100	
Gluteus Minimus	0-38		
Gracilis	0-3	79-100	
Obturator Externus	0-12	95-100	
Obturator Internus	0-12	95-100	
Pectineus	0-12	95-100	
Piriformis	0-12	95-100	
Popliteus	0-53	91-100	
Quadratus Femoris	0-12	95-100	
Rectus Femoris	0-12	46-70	91-100
Semimembranosus	0-4	87-100	
Semitendinosus	0-5	85-100	
Tibialis Anterior	0-13	58-100	
Vastus Intermedius	0-29	55-61	87-100
Vastus Lateralis	0-23	88-100	
Vastus Medialis	0-25	86-100	
Extensor Digitorum Brevis	6-12	50-75	
Extensor Hallucis Brevis	6-12	57-75	
Tibialis Posterior	8-52		
Fibularis Longus	10-53		
Soleus	11-48		
Plantaris	12-49		
Tensor Fascia Latae	13-43		
Gastrocnemius	14-50		
Flexor Digitorum Longus	18-50		
Fibularis Brevis	19-50		
Fibularis Tertius	19-50		
Flexor Hallucis Longus	22-50		
Adductor Longus	42-61		
Adductor Magnus	48-61		
Adductor Brevis	50-61		
Iliopsoas	60-80		
Sartorius	61-78		

Table 4-2: Muscle Activation During Simulation

Muscle	Activation (where 0 is inactive, and 1 is active)																			
Adductor Brevis	0	0	0	0	0	0	0	0	0	0	1	1	0	0	0	0	0	0	0	0
Adductor Longus	0	0	0	0	0	0	0	0	.	1	1	.	0	0	0	0	0	0	0	0
Adductor Magnus	1	.	0	0	0	0	0	0	0	0	0	0	0	0	0	0	0	0	0	.
Biceps Femoris Long	0	0	0	0	0	0	0	0	.	1	1	.	0	0	0	0	0	0	0	0
Biceps Femoris Short	0	0	0	0	0	.	1	1	1	.	0	0	0	0	0	0	0	0	0	0
Extensor Digitorum	0	1	0	0	0	0	0	0	0	.	.	1	1	.	.	0	0	0	0	0
Extensor Digitorum	.	.	.	0	0	0	0	0	0	0	.	.	.	1	1	1	1	1	1	1
Extensor Hallucis	0	1	0	0	0	0	0	0	0	.	.	1	1	.	.	0	0	0	0	0
Extensor Hallucis	1	.	.	.	0	0	0	0	0	0	0	0	.	.	.	1	1	1	1	1
Fibularis Brevis	0	0	0	.	.	1	1	1	.	.	0	0	0	0	0	0	0	0	0	0
Fibularis Longus	0	.	.	.	1	1	1	1	.	.	.	0	0	0	0	0	0	0	0	0
Fibularis Tertius	0	0	0	.	.	1	1	1	.	.	0	0	0	0	0	0	0	0	0	0
Flexor Digitorum	0	0	0	.	.	1	1	1	.	.	0	0	0	0	0	0	0	0	0	0
Flexor Hallucis	0	0	0	.	.	1	1	1	.	.	0	0	0	0	0	0	0	0	0	0
Gemellus Inferior	0	0	0	0	0	0	0	0	0	.	1	1	.	0	0	0	0	0	0	0
Gemellus Superior	0	0	0	0	0	0	0	0	0	.	1	.	0	0	0	0	0	0	0	0
Gastrocnemius	0	0	.	.	1	1	1	1	.	.	0	0	0	0	0	0	0	0	0	0
Gluteus Maximus	1	1	.	0	0	0	0	0	0	0	0	0	0	0	0	0	0	0	0	.
Gluteus Medius	0	0	0	0	0	0	0	0	.	.	.	1	1	1	1	.	.	.	0	0
Gluteus Minimus	0	0	0	0	0	0	0	0	0	0	.	.	1	1	1	1	.	.	0	0
Gracilis	.	0	0	0	0	0	0	0	0	0	0	0	0	0	0	0	.	1	1	1
Iliopsoas	0	0	0	0	0	0	0	0	0	0	0	.	1	1	1	.	0	0	0	0
Obturator Externus	0	0	0	0	0	0	0	0	0	.	1	.	0	0	0	0	0	0	0	0
Obturator Internus	0	0	0	0	0	0	0	0	0	.	1	.	0	0	0	0	0	0	0	0
Pectineus	0	0	0	0	0	0	0	0	0	.	1	.	0	0	0	0	0	0	0	0
Piriformis	0	0	0	0	0	0	0	0	0	.	1	.	0	0	0	0	0	0	0	0
Plantaris	0	.	.	.	1	1	1	.	.	.	0	0	0	0	0	0	0	0	0	0
Popliteus	.	1	1	1	1	1	1	1	.	.	.	0	0	0	0	0	0	0	.	.
Quadratus Femoris	0	0	0	0	0	0	0	0	0	.	1	.	0	0	0	0	0	0	0	0
Rectus Femoris	1	.	0	0	0	0	0	0	0	.	1	1	1	.	0	0	0	0	.	1
Sartorius	0	.	1	1	1	.	0	0	0	0	0	0	0	0	0	0	0	0	0	0
Semimembranosus	.	0	0	0	0	0	0	0	0	0	0	0	0	0	0	0	0	.	1	1
Semitendinosus	.	0	0	0	0	0	0	0	0	0	0	0	0	0	0	0	0	.	1	1
Soleus	0	.	.	.	1	1	1	.	.	.	0	0	0	0	0	0	0	0	0	0
Tensor Fascia Latae	0	0	0	0	0	0	0	0	0	0	0	0	.	.	1	1	.	.	0	0
Tibialis Anterior	0	0	.	.	.	1	1	1	1	1	.	.	.	0	0	0	0	0	0	0
Tibiialis Posterior	0	.	.	.	1	1	1	.	.	.	0	0	0	0	0	0	0	0	0	0
Vastus Intermedius	0	1	0	0	0	0	0	.	.	.	1	1	1	.	.	.	0	0	0	0
Vastus Lateralis	0	0	0	0	0	0	0	.	.	.	1	1	.	.	.	0	0	0	0	0
Vastus Medialis	0	0	0	0	0	0	.	.	.	1	1	1	.	.	.	0	0	0	0	0

4.16 Muscle properties

Once the affiliation of each muscle was known, the muscle properties of each muscle were calculated, including fibre length and physiological cross-sectional area were

calculated (Table 4-3) and scaled for the body size of A.L. 288-1. This information was then also entered into the model's configuration file, along with the information for the joints, contact points and the drivers for the model (See Supplementary Info 1 for the complete model file).

Once the configuration file was completed, it was uploaded into GaitSym. The simulation was then played and the resultant gait qualitatively assessed and compared to the existing theories for the locomotory style of Australopithecus afarensis.

Table 4-3: Calculation of muscle fibre length and physiological cross-sectional area in A.L. 288-1 based on affiliated extant group as determined by Geometric Morphometric analysis

Muscle	Affiliation	Affiliate Fibre length (m)	Affiliate mass (kg)	A.L.288-1 mass (kg)	A.L.288-1 Fibre length (m)	A.L.288-1 PCA
Adductor brevis 1	*Homo*	0.12 [1]	0.0546 [3]	0.023738988	0.064284	0.001439658
Adductor brevis 2	*Homo*	0.117 [1]	0.0546 [3]	0.023738988	0.0626769	0.001403666
Adductor brevis 3	*Homo*	0.118 [1]	0.0546 [3]	0.023738988	0.0632126	0.001415663
Adductor longus 1	*Homo*	0.1056 [1]	0.0747 [3]	0.032478066	0.05656992	0.001733285
Adductor magnus 1	*Homo*	0.077 [1]	0.3247 [3]	0.141173066	0.0412489	0.005493617
Adductor magnus 2	*Homo*	0.1205 [1]	0.3247 [3]	0.141173066	0.06455185	0.008597153
Adductor magnus 3	*Homo*	0.1416 [1]	0.3247 [3]	0.141173066	0.07585512	0.010102547
Biceps femoris LH	*Homo**	0.0658 [1]	0.1134 [3]	0.049304052	0.03524906	0.001639549
Biceps femoris SH	*Homo**	0.1108 [1]	0.0598 [3]	0.025999844	0.05935556	0.001455882
Extensor Digitorum B.	*Pan* *	0.023 [2]	0.0109 [2]	0.00883772	0.0186484	0.000155481
Extensor Digitorum L.	*Pan*	0.09 [2]	0.0432 [2]	0.03502656	0.072972	0.002411281
Extensor Hallucis B.	*Pan*	0.083 [2]	0.0115 [2]	0.0093242	0.0672964	0.000591967
Extensor Hallucis L.	*Pan*	0.083 [2]	0.0121 [2]	0.00981068	0.0672964	0.000622852
Fibularis brevis	*Pan*	0.062 [2]	0.0314 [2]	0.02545912	0.0502696	0.001207377
Fibularis longus	*Pan*	0.062 [2]	0.0706 [2]	0.05724248	0.0502696	0.002714676
Fibularis tertius	*Pan*	0.062 [2]	0.0415 [2]	0.0336482	0.0502696	0.001595737
Flexor Digitorum L.	*Pan*	0.023 [2]	0.0121 [2]	0.00981068	0.0186484	0.000172598
Flexor Hallucis L.	*Pan*	0.02 [2]	0.0121 [2]	0.00981068	0.016216	0.000150085
Gemellus inf.	*Homo*	0.0265 [1]	0.0131 [4]	0.005695618	0.01419605	7.62786E-05
Gemellus sup.	*Homo*	0.0275 [1]	0.0131 [4]	0.005695618	0.01473175	7.9157E-05
Gastrocnemius	*Pan* *	0.096 [2]	0.2467 [2]	0.20002436	0.0778368	0.014687977
Gluteus Max. 1	*Homo*	0.0747 [1]	0.5472 [3]	0.237911616	0.04001679	0.008981565
Gluteus Max. 2	*Homo*	0.1136 [1]	0.5472 [3]	0.237911616	0.06085552	0.013658712
Gluteus Max. 3	*Homo*	0.1345 [1]	0.5472 [3]	0.237911616	0.07205165	0.016171627
Gluteus Med. 1	*Homo*	0.0405 [1]	0.2735 [3]	0.11891233	0.02169585	0.002433872
Gluteus Med. 2	*Homo*	0.0508 [1]	0.2735 [3]	0.11891233	0.02721356	0.003052856
Gluteus Med. 3	*Homo*	0.055 [1]	0.2735 [3]	0.11891233	0.0294635	0.003305258
Gluteus Min. 1	*Homo*	0.0322 [1]	0.1134 [4]	0.049304052	0.01724954	0.000802332
Gluteus Min. 2	*Homo*	0.0274 [1]	0.1134 [4]	0.049304052	0.01467818	0.00068273
Gluteus Min. 3	*Homo*	0.0301 [1]	0.1134 [4]	0.049304052	0.01612457	0.000750006
Gracilis	*Homo**	0.2543 [1]	0.0525 [3]	0.02282595	0.13622851	0.002933533
Iliopsoas 1	*Homo*	0.0964 [1]	0.1137 [3]	0.049434486	0.05164148	0.002408368
Obturator ext.	*Homo*	0.0492 [1]	0.0131 [5]	0.005695618	0.02635644	0.000141619
Obturator int.	*Homo*	0.0344 [1]	0.025 [5]	0.0108695	0.01842808	0.000188966
Pectineus	*Homo*	0.1047 [1]	0.0525 [4]	0.02282595	0.05608779	0.00120779
Piriformis	*Homo*	0.0415 [1]	0.00656 [4]	0.002852157	0.02223155	5.98187E-05
Plantaris	*Pan* *	0.018 [2]	0.0087 [2]	0.00705396	0.0145944	9.71211E-05
Popliteus	*Pan* *	0.031 [2]	0.0322 [2]	0.02610776	0.0251348	0.000619069
Quadratus femoris	*Homo*	0.0538 [1]	0.0584 [4]	0.025391152	0.02882066	0.000690368
Rectus femoris	*Homo*	0.0652 [1]	0.1106 [3]	0.048086668	0.03492764	0.001584485
Sartorius	*Homo*	0.3911 [1]	0.0785 [3]	0.03413023	0.20951227	0.006745945
Semimembranosus	*Homo*	0.0536 [1]	0.1343 [3]	0.058390954	0.02871352	0.001581707
Semitendinosus	*Homo*	0.0885 [1]	0.0997 [3]	0.043347566	0.04740945	0.001938759
Soleus	*Pan*	0.06 [2]	0.2202 [2]	0.17853816	0.048648	0.008193891
Tensor fasciae latae	*Homo*	0.1015 [1]	0.0598 [4]	0.025999844	0.05437355	0.001333683
Tibialis anterior	*Pan*	0.095 [2]	0.1012 [2]	0.08205296	0.077026	0.005962463
Tibialis posterior	*Pongo*	0.021 [2]	0.015 [2]	0.00703125	0.00984375	6.52961E-05
Vastus Int.	*Homo*	0.0785 [1]	0.1719 [3]	0.074738682	0.04205245	0.002965042
Vastus Lat.	*Homo*	0.0807 [1]	0.3759 [3]	0.163433802	0.04323099	0.006665476
Vastus Med.	*Homo*	0.079 [1]	0.2394 [3]	0.104086332	0.0423203	0.004155627

[1] Friedrich & Brand, 1990; [2] Payne *et al.*, 2006; [3] Ward *et al.*, 2009; [4] Handsfield *et al.*, 2014. *Closest affiliate

4.17 The locomotion of the A.L. 288-1 model

The model was run in the GaitSym, and a locomotory pattern produced. This unfortunately was backwards, but this was believed to be an artefact of the way the drivers must be configured in GaitSym. The drivers must be configured in a cyclical pattern which meant that the initial step of the model was confused, which in turn resulted in a backwards momentum for the model (see Figure 4-8 but for Full video- Supplementary info. 2). For comparative purposes, the video was reversed (Supplementary info. 3), and this showed the overall pattern was similar to a modern bipedal stride, and certainly not a waddling bent hip bent knee gait (Figure 4-9).

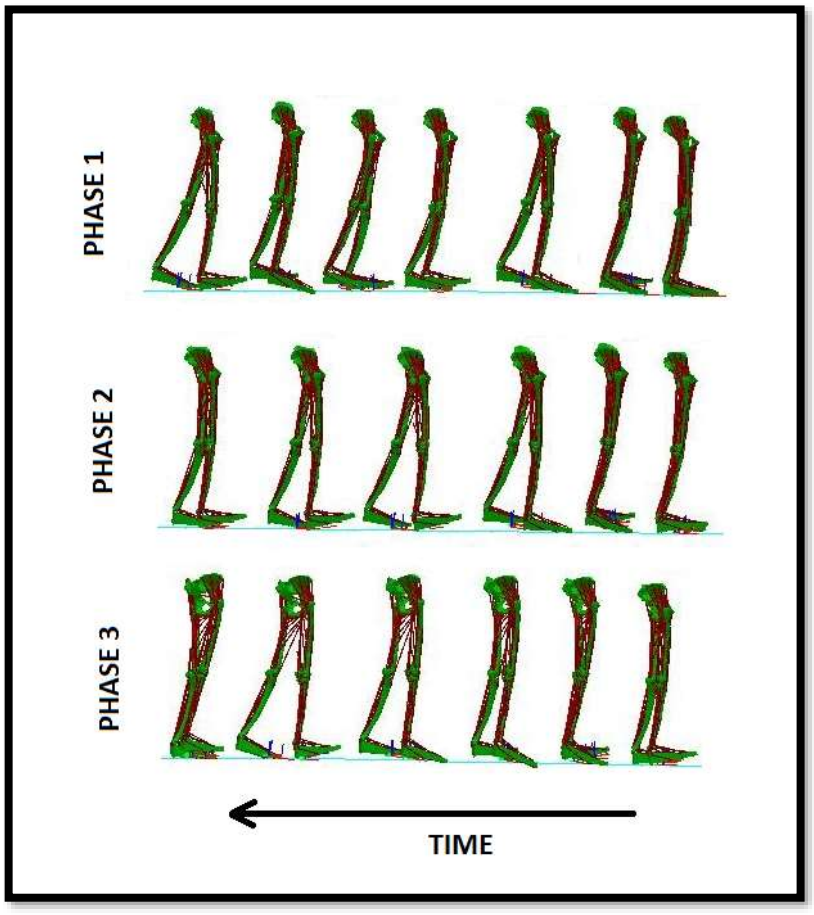

Figure 4-8- Motion produced for Al 288-1 in GaitSym.
Phase 1 indicates the initial confused step; Phase 2 the backwards step with the left leg, and Phase 3 the backwards step with the right leg

A classic bipedal gait can be described in various phases, as previously discussed. Examining the model with these same parameters showed that the gait of *Australopithecus afarensis* followed this pattern:-

1. Heel strike/initial contact

The model showed flexion of the thigh at the hip and extension of the leg at the knee in the dominant leg. The foot was dorsiflexed. The knee began to flex.

2. Foot Flat/ loading response phase

The thigh at the hip became less flexed and moved into extension, the leg began to flex at the knee, and the foot began to plantarflex.

3. Midstance

The thigh continued to extend at the hip. The knee began to extend. The foot became slightly dorsiflexed at the ankle and the whole body was supported by the limb.

4. Heel Off

The dominant heel left the floor and the foot began to move from dorsiflexion to plantarflexion. The leg was extended at the knee, and the thigh was hyperextended.

5. Toe Off

The thigh at the hip became less extended. The knee was flexed and the plantarflexion of the foot at the ankle increased.

6. Acceleration/Early Swing

The thigh and hip continued to flex and the foot moved into dorsiflexion. Throughout the swing phase, the limb is not in contact with the substrate and is not weight bearing.

7. Mid Swing

The thigh continued to flex at the hip, and the knee also was flexed, shortening the limb to clear the substrate.

8. Late Swing

The thigh continued to flex and the leg began to extend. The foot was dorsiflexed.

Although the gait of the model followed a bipedal pattern, it was less pronounced in its movement than that of *Homo sapiens* with slightly more shuffling rather than striding gait, with relatively straight legs throughout.

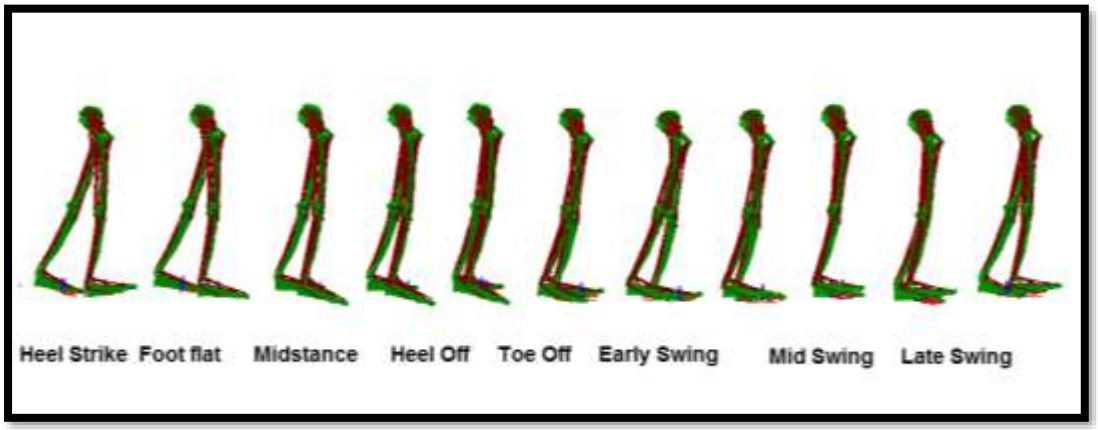

Figure 4-9: The pattern of locomotion produced in GaitSym for a stride of A.L. 288-1, based on the theoretical musculature determined by the Geometric Morphometric analysis

Regrettably, this study was unable to produce much quantative data from the model produced in GaitSym. However, further analysis of the joint angles observed in the model was undertaken using the angle measuring tool in Maya (2015), from the video produced in GaitSym (see Table 4.4). This showed a smaller range of motion at the hip in AL 288-1 than either chimpanzees or humans when compared to the data obtained by O'Neill *et al.* (2015) when they compared chimpanzees and humans walking bipedally. The minimum hip flexion observed (a measure of angle of extension) showed a value within the range of those obtained for humans, however, the maximum flexion at the hip was significantly less than either the chimpanzee or human range. At the knee, minimum flexion was within the range of O'Neill *et al*'s (2015) human sample, but showed a greatly reduced range of motion than either humans or chimpanzees, who both showed significantly greater maximum flexion at the knee. At the ankle, AL 2-881 showed greatest affinity to the chimpanzee sample, with all values falling within the observed range for this species. These findings indicate (possibly unsurprisingly given the method with which the model was constructed), a more human-like motion at the hip, intermediate at the knee and most non-human ape-like at the ankle.

Table 4-4 : Comparative joint angle minimum (Min), maximum (Max) and range of motion (ROM = Max – Min) values in degrees.

		Hip flexion	Knee flexion	Ankle flexion
Chimpanzees	Min	25 ± 9°	−92 ± 2°	−19 ± 8°
	Max	52 ± 6°	−14 ± 3°	19 ± 4°
	ROM	27 ± 4°	78 ± 1°	38 ± 5°
Humans	Min	−14 ± 3°	0 ± 1°	−18 ± 6°
	Max	35 ± 5°	−72 ± 1°	10 ± 5°
	ROM	48 ± 5°	73 ± 3°	28 ± 6°
AL 288-1	Min	-16.09°	0°	24.66°
	Max	5.95°	-24.18°	14.37°
	ROM	22.04°	24.18°	39.03°

Human data are matched to the chimpanzee data in dimensionless (i.e. relative-speed match) form (mean ± s.d.). Human and Chimpanzee data taken from O'Neill et al. (2015)

4.2 The Model

The model produced finds its place within an extensive debate about the locomotory pattern of *Australopithecus afarensis* based on comparative anatomical studies which ranges from claims of fully human-like striding bipedalism (Leakey and Hay, 1979; Lovejoy, 1979; 1980 etc.) to a bent-hip bent-knee gait (i.e.: Stern and Susman, 1981; 1983; 1991; 1993; Jungers and Stern, 1983) as seen in bipedally walking non-human apes. It is also part of a continuum in the research of locomotor modelling in both extant and fossil species (i.e. Kramer, 1999; Nagano et al. 2005; Wang et al.; Sellers et al. 2003; 2004; 2005; 2010; D'Aout et al., 2010 etc.) and hopefully seeks to combine the two.

4.21 Walking backwards

Unfortunately, there is no escaping the fact that the locomotion produced in this model was backwards. However, despite this, there are some positives. It was truly expected that combining muscle features and parameters in this way may in fact simply result in a model that fell over, or produced such force on joints or opposing musculature that there would be a catastrophic failure in the model. What was produced, however, was directional travel, and although backwards, the mode of locomotion was not outrageous.

It is believed that the model walked backwards owing to the nature of the driver options available within GaitSym. In bipedal walking, the initial step from a standing start is different from those that follow. As the drivers follow a cyclical pattern, the

initial step will always create a kind of 'shuffle' as the muscles on the non-dominant limb begin their cycle of activation part way through (so as heel strike is occurring in the dominant limb, the muscles in the non-dominant limb are activated as though they are just post toe-off).

Many studies overcome the problems of muscle activation in forward dynamics by using genetic algorithms to determine a muscle activation pattern (i.e: Sellers et al., 2003; 2004; 2005; 2010; 2013). By using genetic algorithms, you must select for certain traits that you want to be in your final model i.e. energy efficiency, walking forwards, not falling over. Then the model is run many hundreds of thousands of times, with random muscle activation patterns, selecting for these traits, until a pattern that best meets your requirements is obtained. This pattern, however, is unlikely to represent anything like a true biological pattern of muscle activation, and I would argue is therefore not necessarily biologically relevant. Such studies show what is possible within these constraints- i.e. *It is <u>possible</u> to produce an energetically efficient, forward travelling model of locomotion in species x that does not fall over* but this does not really mean that in a biological situation the species in question would use its muscles in that pattern or with the same degree of energetic efficiently. By using genetic algorithms there is a real danger of confirmation bias- we select for traits and then obtain them. Whilst the desired outcome is produced, the mechanisms by which it is produced are hidden. In studies of locomotion within the fossil record, we should be testing these mechanisms to ensure biological relevance, and as we do not know what the outcome of our queries should be, we should not be limiting the potential results in this way.

A further problem with genetic algorithms is that they are computationally expensive (Sellers et al. 2005). As a result, simple models with functionally grouped muscles are often used to limit the number of variables. The type of model used in this study, where muscle activation patterns are input, reduces the computational power required, as the need for genetic algorithms is removed. This in turn allows for a much more complex model of muscular anatomy to be produced and tested. This study showed that it is possible to use forward dynamic modelling and biologically representative muscle activation patterns in modelling locomotion in a fossil species, and builds on the work of Nagano et al. (2005) who showed that such modelling was possible using scaled human muscle variables. By using Geometric Morphometrics, this study was able to

theorize muscle parameters obtained from a variety of species and apply them in a forward dynamic model.

4.22 Walking forwards

When shown in reverse, so that the model walked forwards, the model showed a classic bipedal gait pattern with heel strike/initial contact showing flexion of the thigh at the hip, extension of the leg at the knee and a dorsiflexed foot. This was followed by a reduction in flexion of the thigh, moving towards extension and also flexion at the knee and plantar flexion of the foot in the foot flat/ loading response phase. A typical mid-stance period showed continued extension of the thigh, and extension of the knee, and the support of the body in one limb which was followed by expected heel off and toe off periods. The swing phase was less pronounced than in modern humans, and although the gait of the model followed a bipedal pattern, it was less pronounced in its movement than that of *Homo sapiens* with slightly more shuffling rather than striding gait. This is in accordance with what Hunt, (1994) proposes for the origin of bipedalism in arboreal and terrestrial food 'harvesting' behaviours and may reflect the use of bipedalism in an environment where large amounts of ranging were not required, as Kramer and Eck (2000) suggest. They posit that despite the relatively short legs found in *Australopithecus afarensis*, they were capable of effective bipedalism over shorter distances. Longer legs and travelling greater distances would not have been required.

An element of caution is however recommended when interpreting the locomotory pattern produced by this version. It is just a backwards walking model played in reverse, so the push off provided from toe off especially cannot be the same as in a forward walking model. Additionally, the model seems to produce less flexion and extension at the hip and knee than modern humans produce, so clearance of the substrate in the swing phase is also less. Certainly, it would have been greatly beneficial if the model had produced forward travel in order to test if the same pattern would be observed.

5. Conclusions

The focus of this study was a comprehensive 3D Geometric Morphometric analysis of the Os Coxa, the sacrum, the femur and the tibia in extant apes- *Pan paniscus, Pan troglodytes, Gorilla sp., Pongo pygmaeus* and *Homo sapiens.* Similarity in shape was assumed to indicate similarity in musculature between these species and *Australopithecus afarensis.* This was then tested by using this theoretical musculature to create a forward dynamic model to assess the locomotory style employed by A.L. 288-1, and compare it to existing theories of australopithecine locomotion, in particular the striding biped model and the bent knee bent hip model. When the model was created it showed a locomotory pattern similar to that of a striding biped, but with less 'swing' in the stride. The overarching purpose of this study was to see if this method for testing locomotion in fossil species worked, and therefore whether it could be used for other fossil specimens to determine their locomotory patterns.

5.1 Problems and limitations of the study

Whilst the principals in this study were fundamentally sound, there were certainly problems encountered within the process and limitations to what could be inferred by it.

During the data gathering process there were several issues including small sample sizes across all the groups and, in particular, the lack of *Pongo pygmaeus* specimens from both sexes. This meant that the study could not examine *Pongo pygmaeus* for sexual dimorphism in the lower limb, and the small sample size on this group overall meant that the results for *Pongo pygmaeus* have to be treated with caution. Additionally, both *Gorilla gorilla* and *Gorilla beringei* were used within the *Gorilla sp.* group, and some of the morphological variation observed within the *Gorilla sp.* group could possibly be attributed to this.

A further constraint was integral to 3D Geometric Morphometrics- the principle that landmarks must be found on all specimens under study. When species groups and especially fossil specimens are considered, this can mean that not all the structures are reliably observable in all groups and can therefore limit the landmarks and semilandmarks that can be used. This in turn limits the questions that can be answered. Unfortunately, this study could not use all desired landmarks for this reason, and was therefore unable to examine all exact muscle attachment sites.

The model itself was not a complete body which in turn could have had an impact on the locomotor style produced. As there was no torso, nor arms to swing the model may have lacked the forward momentum that these may have provided. Additionally, there was no fibula and the foot was a basic reconstruction rather than an exact replica of the foot of *Australopithecus afarensis.* However, missing or broken elements will always be a problem where fossil specimens are concerned. This means that using this method in the reconstruction of potential muscular behaviours in fossil species will only ever have merit where the specimens in question are relatively complete and minimal reconstruction is required or where there are multiple individuals that can be reliably attributed to the same species and composites made.

Additionally, the study used the assumption that the muscle activation pattern was that of a modern human. Unfortunately, it was beyond the scope of the study to test alternate muscle activation patterns (such as the muscle activation pattern observed in a bipedally walking chimpanzee) but this would be recommended future research.

The study could also have been improved further if improvements were made to the modelling process. It would have benefitted from more quantitative outputs such as energy used and additional options such as variation of the substrate, in order to test the locomotory styles under different conditions.

Furthermore, there were constraints implicit within GaitSym. The limitations created by the muscle driver type selection meant that there will always be an issue with the first step, unless genetic algorithms are used to create an optimised muscle activation pattern that can be fed into the model. This unfortunately would not allow for meaningful activation patterns in the muscles to be input but relies on computer generated optimal patterns that bear little relation to a true activation pattern.

As the techniques used in this study are relatively new, the equipment and software available are often complex to use and often are not stable, which can cause problems and form a barrier to easy repetition of this research. The techniques used can also be quite labour intensive and require the knowledge of several different computer programs and procedures.

Finally, the greatest limitation of the study is that forward travelling locomotion was not produced, and because of this, conclusions about the specific mode of locomotion in *A. afarensis* must be treated with caution.

5.2 Recommendations and Future research

New technologies are allowing new avenues of exploration into some of the oldest questions in palaeoanthropology. Digitisation of fossil specimens and museum reference collections are allowing these techniques to be used by researchers across the world, without damage or risk to the original specimens. As these collections grow and become more widely available, there will inevitably be great progress in the tools and methods available to researchers. As collections become digitised, policies as to the ownership and use of the data must be considered- regarding who owns the data and what constitutes fair use of the same (Gilissen, 2009). Accompanying this must be a push for more open source collections. Repeated digitisation of the same material negates the benefits of reduced risk to the collections and only the increased availability of such data for research purposes will counteract this. At this point in time, where data ownership of this type is unclear, the author is unable to confirm that all data used in this study would be available open source, as agreement must be obtained on an individual basis from each of the institutions kind enough to allow their specimens to be scanned.

Additionally, the tools for digital research in palaeoanthropology must be improved. Programs must be created with palaeoanthropology, and the specific questions it asks, in mind. The EVAN toolkit is such a program for Geometric Morphometrics, but I would advocate the creation of a forward-dynamic modelling system that could be used for non-locomotory studies, and, in locomotory studies, answer more of the questions important to palaeoanthropologists. This could only be done through greater interdisciplinary collaboration with the digital and programming community and has the potential to truly push the boundaries of the field.

The method put forward in this study could be used in its current form to study some of the exciting finds that have been made in recent years such as *Ardipithecus ramidus*, *Australopithecus sediba* and *Homo naledi*. All of these species pose questions regarding the primary manner of locomotion used, and perhaps this method would allow some light to be shed on these. Additionally, there would be great benefit to a greater exploration of potential differences in locomotion due to sex in the fossil record. We believe that some fossil species are highly sexually dimorphic, and perhaps

greater exploration of sexual dimorphism and locomotion would allow for a refinement of our understanding of sexually determined behaviours in the past.

Also, expansion on the current study is suggested. There would be a benefit to modifying the muscle activation pattern to one that is seen in apes when walking bipedally as this is significantly different to that of humans walking bipedally (D'Aout et al., 2004), and this may produce a different gait in the modelled species. Combination of the Geometric Morphometric techniques used here with finite element analysis (as used by Blemker and Delp, 2005) and assessments of energy efficiency (as per Nicolas et al., 2007 and 2009) would allow for the locomotion of *Australopithecus afarensis* in this model to be more quantitatively assessed. Additionally, as *Austrolpithecus afarensis* may be a highly sexually dimorphic species (Johanson et al. 1978; Johanson and White, 1979; Foley and Lee, 1989; McHenry, 1991), and the model could also be applied to a male (or composite male) of the species to assess if there are any differences in the locomotory style.

5.3 Conclusions and Reflections

The Geometric Morphometric analysis showed that there is a complex relationship between size and shape. The *Gorilla sp.* in particular showed a great deal of morphological difference due to its relatively massive size in comparison to the other groups, and this allometric effect was sometimes difficult to distinguish from effects that were purely to do with locomotion. Of course, the absolute size of the *Gorilla sp.* also has an impact on the nature of locomotion which it can undertake.

It was shown that the greater amount of arboreality seen in females in the *Gorilla sp.* in comparison to the males was reflected in the shape of the bones in the lower limb. Additionally, in the *Homo sapiens* group, allometric effects between the males and females were also observed, but these were further complicated by anatomical differences related to parturition.

When species were compared, there seemed to be a broad continuum reflected in the anatomy of each bone related to the amount of arboreality seen in the extant groups, with *Pongo pygmaeus* being shown to be the most arboreal, followed by *Pan paniscus.* *Pan troglodytes* was shown to be slightly more robust in all bones relative to *Pan paniscus* and this probably reflected this species greater size, but also slightly lesser

degree of arboreality. The *Gorilla sp.* were shown to be both the least arboreal and relatively largest.

The *Homo sapiens* group showed the most different shaped bones to all the species. This reflected the style of locomotion practised by this group, which, unlike in the non-human apes, shows very little arboreal component.

Australopithecus afarensis was shown to have a pelvis and femur most similar in shape to *Homo sapiens*. However, the tibia showed the greatest similarity in shape to *Pan* and some aspects of the morphology (particularly in the distal tibia) showed the greatest similarity to *Pongo pygmaeus*. This suggests a human-like hip in *A. afarensis* but an ankle perhaps still suited for locomotion in an arboreal context, with a greater degree of movement around this joint.

The model, although not without its problems, showed a locomotory style for *A. afarensis* consistent with a bipedal gait. The movements of flexion and extension at the hip and knee were however less pronounced than in *Homo sapiens* meaning that the locomotory style produced was less of a striding bipedal gait and more of a shuffling bipedal gait, with what can only be described as a 'stiff leg'. As in the Geometric Morphometric analysis, the hip was most human-like, the knee intermediate and the ankle ape-like, indicating that the anatomical adaptations to bipedalism were more pronounced at the hip than at the rest of the lower limb. Berge (1998) and Ward (2002) have pointed to biomechanical studies of australopithecine bipedalism suggesting marked differences in the way in which australopithecines walked in comparison with modern humans, and this study would seem to corroborate that. This study did not appear to show the 'waddling gait', with large rotational movements of the pelvis suggested by some (Zihlman and Hunter, 1972; Berge, 1991, 1994; Rak, 1991), but rather a stiff legged 'shuffle'. The apparent adaptation for arboreality and arboreal locomotion (as per Stern and Susman 1983, Susman et al. 1984, Hunt, 1994; Churchill et al., 2013; Da Silva e al. 2013, McHenry & Berger, 1998; Green & Alemsegoed, 2012) appear to be supported with this study, where both the Geometric Morphometric analysis and the model showed adaptations consistent with an ape-like ankle. This is in accordance with Hunt's (1994) proposal that bipedalism may have arisen as a response to small tree postural feeding, and harvesting

behaviours- with little requirement to travel bipedally for great distances, and the requirement to continue to use arboreal environments effectively.

This technique for assessment of locomotion in a fossil species has, I believe, some merit, although could be expanded to include additional elements to address potential differences in muscle activation patterns. The development of a purpose-built forward dynamic modelling program would also be of great benefit were such a study to be undertaken in the future. Although initially a labour intensive undertaking, once the comparative sample has been gathered and digitised, the Geometric Morphometric analyses on fossil specimens would be relatively quick and easy to do, and expansions to this study would be relatively easy and could be extremely informative for future locomotory studies.

6. References

Abitbol, M.M., 1988. Evolution of the ischial spine and of the pelvic floor in the Hominoidea. *American journal of physical anthropology*, *75*(1), pp.53-67.

Abitbol, M.M., 1995. Lateral view of Australopithecus afarensis: primitive aspects of bipedal positional behavior in the earliest hominids. Journal of human evolution, 28(3), pp.211-229.

Adams, D.C., Rohlf, F.J., and Slice, D.E. 2004. Geometric Morphometrics: Ten Years of Progress Following the 'Revolution'. Italian Journal of Zoology 71 (1): 5-16

Aiello, L. and Dean, C. 2002. An Introduction to Human Evolutionary Anatomy. Elsevier Academic Press: London.

Aiello, L.C., 1981. Locomotion in the Miocene Hominoidea. Aspects of human evolution, 21, pp.63-79.

Alexander RM (2003) Principles of Animal Locomotion. Princetown, NJ: Princetown University Press

Arsuaga, J.L., 1981. Iliac angular measurements in Australopithecus. Journal of Human Evolution, 10(4), pp.293IN1295-294302.,

Arsuaga, J.L., 1985. Antropología del hueso coxal: evolución, dimorfismo sexual y variabilidad (Doctoral dissertation).

Ashton, E.H. and Oxnard, C.E., 1964, January. Locomotor patterns in primates. In Proceedings of the Zoological Society of London (Vol. 142, No. 1, pp. 1-28). Blackwell Publishing Ltd.

Ashton, E.H., Flinn, R.M., Moore, W.J., Oxnard, C.E. and Spence, T.F., 1981. Further quantitative studies of form and function in the primate pelvis with special reference to Australopithecus. Journal of Zoology, 36(1), pp.1-98.

Bartholomew, G.A. and Birdsell, J.B., 1953. Ecology and the protohominids. American Anthropologist, 55(4), pp.481-498.

Benton R. 1965. *Morphological evidence for adaptations within the epaxial region of the primates*. In: Vagtborg H, editor. *The baboon in medical research*. Houston: University of Texas Press. Pp. 10–20.

Benton, R.S., 1976. Structural patterns in the Pongidae and Cercopithecidae. Yearb. phys. Anthrop, 18, pp.65-88.

Berge, C. 1991. Size- and locomotion-related aspects of hominid and anthropoid pelves: An osteometrical multivariate analysis. Human Evolution 6 (5-6):365-376

Berge, C. 1994. How did the australopithecines walk? A biomechanical study of the hip and thigh of Australopithecus afarensis. Journal of Human Evolution 26 (4): 259–273

Berge, C. and Kazmierczak, J.B., 1986. Effects of size and locomotor adaptations on the hominid pelvis: evaluation of australopithecine bipedality with a new multivariate method. Folia primatologica, 46(4), pp.185-204.

Berge, C. and Ponge, J.F., 1983. Les caractéristiques du bassin des Australopithèques (A. robustus, A. africanus et A. afarensis) sont-elles liées à une bipédie de type humain?. Bulletins et Mémoires de la Société d'Anthropologie de Paris, 10(3), pp.335-353.

Berge, C., 1984. Multivariate analysis of the pelvis for hominids and other extant primates: implications for the locomotion and systematics of the different species of australopithecines. Journal of Human Evolution, 13(7), pp.555-562.

Berge, C., 1990. Functional interpretation of the dimensions of the pelvis of Australpithecus afarensis (AL 288-1). Zeitschrift fur Morphologie und Anthropologie, 78(3), pp.321-330.

Berge, C., 1993. L'évolution de la hanche et du pelvis des hominidés: bipédie, parturition, croissance, allométrie. CNRS éditions.
Berge, C., 1998. Heterochronic processes in human evolution: an ontogenetic analysis of the hominid pelvis. American Journal of Physical Anthropology, 105(4), pp.441-459.
Bruce, G. and McIntyre, L. 2009. Mass graves at All Saints Church, Fishergate, York. York Historian 26: 79-84
Blemker, S.S. and Delp, S.L., 2005. Three-dimensional representation of complex muscle architectures and geometries. Annals of biomedical engineering, 33(5), pp.661-673.
Bookstein F. L. 1997. Landmark methods for forms without landmarks: Localizing group differences in outline shape. Medical Image Analysis 1: 225-243
Bookstein F. L., 1991, Morphometric Tools for Landmark Data: Geometry and Biology. Cambridge University Press: Cambridge.
Bookstein, F. L., P. Gunz, P. Mitteroecker, H. Prossinger, K. Schaefer, and H. Seidler. 2003. Cranial integration in Homo: singular warps analysis of the midsagittal plane in ontogeny and evolution. Journal of Human Evolution 44:167–187
Bookstein, F.L., Sampson, P.D., Connor, P.D., and Streissguth, A.P. 2002. Midline corpus callosum is a neuroanatomical focus of fetal alcohol damage. The Anatomical Record 269 (3): 162-174
Brunet, M., Guy, F., Pilbeam, D., Mackaye, H.T., Likius, A., Ahounta, D., Beauvilain, A., Blondel, C., Bocherens, H., Boisserie, J.R. and De Bonis, L., 2002. A new hominid from the Upper Miocene of Chad, Central Africa. Nature, 418(6894), pp.145-151.
Bruce, G. 2003. The Barbican Centre, York. Report on an Archaeological Evaluation. OSA Report No: OSA03EV08. *On Site Archaology Ltd.*
Bruce, G. & McIntyre, L. 2009. Mass graves at All Saints Church, Fishergate, York. *York Historian*. 26: 79-84.
Bryden, M.M. and Felts, W.J., 1974. Quantitative anatomical observations on the skeletal and muscular systems of four species of Antarctic seals. Journal of Anatomy, 118(Pt 3), p.589.
Carrier, D.R., 1984. The energetic paradox of human running and hominid evolution. Current Anthropology, 25(4), pp.483-495.
Cartmill, M. and Milton, K., 1977. The lorisiform wrist joint and the evolution of "brachiating" adaptations in the Hominoidea. American Journal of Physical Anthropology, 47(2), pp.249-272.;
Casey TM, 1992 Energetics of locomotion; in Alexander R McN (ed): *Mechanics of Animal Locomotion: Advances in Comparative and Environmental Physiology*. Berlin, Springer, vol 11, pp 251–276.
Christie, P.W., 1977, January. Form and function of the Afar ankle. In American Journal of Physical Anthropology 47 (1), pp. 123-123
Chumanov, E.S., Wall-Scheffler, C. and Heiderscheit, B.C., 2008. Gender differences in walking and running on level and inclined surfaces. *Clinical biomechanics*, *23*(10), pp.1260-1268.
Clutton-Brock, T.H., Harvey, P.H. and Rudder, B., 1977. Sexual dimorphism, socionomic sex ratio and body weight in primates. Nature.
Coolidge, H.J., 1933. Pan paniscus. Pigmy chimpanzee from south of the Congo river. American Journal of Physical Anthropology, 18(1), pp.1-59.

Corruccini, R.S. and Ciochon, R.L., 1976. Morphometric affinities of the human shoulder. American Journal of Physical Anthropology, 45(1), pp.19-37.
Crompton, R.H., Pataky, T.C., Savage, R., D'Aout, K., Bennet, M.R., Day, M.H., Bates, K., Morse, S and Sellers, W.I. 2012. Human-like external function of the foot, and fully upright gait, confirmed in the 3.66 million year old Laetoli hominin footprints by topographic statistics, experimental footprint-formation and computer simulation. Journal of the Royal Society Interface 9:707-719
Crompton, R.H., Sellers, W.I. and Thorpe, S.K., 2010. Arboreality, terrestriality and bipedalism. Philosophical Transactions of the Royal Society B: Biological Sciences, 365(1556), pp.3301-3314.,
Crompton, R.H., Thorpe, S., Weijie, W., Yu, L., Payne, R., Savage, R., Carey, T., Aerts, P., Van Elsacker, L., Hofstetter, A. and Günther, M., 2003. The biomechanical evolution of erect bipedality. COURIER-FORSCHUNGSINSTITUT SENCKENBERG, pp.135-146.
Crompton, R.H., Vereecke, E.E. and Thorpe, S.K.S., 2008. Locomotion and posture from the common hominoid ancestor to fully modern hominins, with special reference to the last common panin/hominin ancestor. Journal of Anatomy, 212(4), pp.501-543.
Cutting, J.E., Proffitt, D.R. and Kozlowski, L.T., 1978. A biomechanical invariant for gait perception. *Journal of Experimental Psychology: Human Perception and Performance*, *4*(3), p.357.
D'Août, K., Vereecke, E., Schoonaert, K., De Clercq, D., Van Elsacker, L. and Aerts, P., 2004. Locomotion in bonobos (Pan paniscus): differences and similarities between bipedal and quadrupedal terrestrial walking, and a comparison with other locomotor modes. Journal of Anatomy, 204(5), pp.353-361.
Deloison, Y., 1991. Les australopitheques marchaient-ils comme nous. Origine (s) de la Bipédie chez les Hominidés, pp.177-186.
DeSilva, J.M., 2009. Functional morphology of the ankle and the likelihood of climbing in early hominins. *Proceedings of the National Academy of Sciences*, *106*(16), pp.6567-6572.
DeSilva, J.M., 2011. A shift toward birthing relatively large infants early in human evolution. *Proceedings of the National Academy of Sciences*, *108*(3), pp.1022-1027.
Doran, D.M., 1992. The ontogeny of chimpanzee and pygmy chimpanzee locomotor behavior: a case study of paedomorphism and its behavioral correlates. Journal of Human Evolution, 23(2), pp.139-157.
Doran, D.M., 1993. Sex differences in adult chimpanzee positional behavior: the influence of body size on locomotion and posture. American Journal of Physical Anthropology, 91(1), pp.99-115.
Doran, D.M., 1996. Comparative positional behavior of the African apes. *Great ape societies*, p.213.
Dryden, I.L. and Mardia, K.V. 1998. Statistical Shape Analysis. John Wiley and Sons:New York
Feldesman, M.R., 1982. Morphometric analysis of the distal humerus of some Cenozoic catarrhines: the late divergence hypothesis revisited. American Journal of Physical Anthropology, 59(1), pp.73-95.
Fleagle, J.G., 1999. Primate Adaptations. In Fleagle, J.G., *Primate adaptation and evolution.* London: Academic Press (Part of Elsevier), pp.283-313
Fleagle, J.G., Stern, J.T., Jungers, W.L., Susman, R.L., Vangor, A.K. and Wells, J.P., 1981. Climbing: a biomechanical link with brachiation and with bipedalism. In Symp Zool Soc Lond (Vol. 48, pp. 359-375).

Flexscan 3D3, 2013. Copyright LMI Technologies. Canada.
Foley, R.A. and Elton, S., 1998. Time and energy: the ecological context for the evolution of bipedalism. In Primate Locomotion (pp. 419-433). Springer US.
Friederich, J.A. and Brand, R.A., 1990. Muscle fiber architecture in the human lower limb. Journal of biomechanics, 23(1), pp.91-95.
Gagneux, P. and Varki, A., 2000. Genetic differences between humans and great apes. Molecular phylogenetics and evolution, 18(1), pp.2-13.
GaitSym Sellers, 2014,
Gebo, D.L., 1992. Plantigrady and foot adaptation in African apes: implications for hominid origins. American Journal of Physical Anthropology, 89(1), pp.29-58.
Gebo, D.L., 1996. Climbing, brachiation, and terrestrial quadrupedalism: historical precursors of hominid bipedalism. American Journal of Physical Anthropology, 101(1), pp.55-92.
Gebo, D.L., 1996. Climbing, brachiation, and terrestrial quadrupedalism: historical precursors of hominid bipedalism. American Journal of Physical Anthropology, 101(1), pp.55-92.
Geomagic Wrap 12 OEM, 2010.Geomagic, Incorporated. USA.
Gilissen, E., 2009. Museum collections, scanning, and data access. J. Anthropol. Sci, 87, pp.223-226.
Gomberg, D.N., 1985. Functional differences of three ligaments of the transverse tarsal joint in hominoids. Journal of Human Evolution, 14(6), pp.553-562.
Gower, J. C. 1975. Generalized Procruses analysis. Psychometrika 40:33–51.
Grand, T.I., 1967. The functional anatomy of the ankle and foot of the slow loris (Nycticebus coucang). *American Journal of Physical Anthropology*, *26*(2), pp.207-218.
Gunz, P., Mitteroecker, P., and Bookstein, F.L. 2005. Semilandmarks in Three Dimensions. In Slice, D.E (ed). 2005. Modern Morphometrics in Physical Anthropology. Kluwer Academic / Plenum Publishers, New York.
Hager, L.D., 1996. Sex differences in the sciatic notch of great apes and modern humans. *American journal of physical anthropology*, *99*(2), pp.287-300.
Harcourt-Smith, W.E. and Aiello, L.C., 2004. Fossils, feet and the evolution of human bipedal locomotion. Journal of Anatomy, 204(5), pp.403-416.
Harcourt-Smith, W.E.H. 2007. *The Origins of Bipedal Locomotion.* In: Henke, W. and Tattersall, I. (eds.) 2007. *Handbook of Palaeoanthropology: Vol. 3.* Springer-Verlag.
Harmon, E.H. 2007. The shape of the hominoid proximal femur: a geometric morphometric analysis. Journal of Anatomy 210: 170-185
Harrison, T., 1991. The implications of Oreopithecus bambolii for the origins of bipedalism. Origine (s) de la bipédie chez les hominidés, pp.235-244.
Hunt, K.D., 1990, February. Implications of chimpanzee positional behavior for the reconstruction of early hominid locomotion and posture. In American Journal of Physical Anthropology Vol. 81 (2) pp. 242-242
Hunt KD(1992) Positional behavior ofPan troglodytesin theMahale Mountains and Gombe Stream National Parks, Tanza-nia.Am J Phys Anthropol87,83–107
Hunt, K.D., 1994. The evolution of human bipedality: ecology and functional morphology. Journal of Human Evolution, 26(3), pp.183-202.
Hunt, K.D., Cant, J.G., Gebo, D.L., Rose, M.D., Walker, S.E. and Youlatos, D., 1996. Standardized descriptions of primate locomotor and postural modes. Primates, 37(4), pp.363-387.

Hunt, K.D. 2016. Why are there apes? Evidence for the co-evolution of ape and monkey ecomorphology. *Journal of Anatomy* 228 (4) :630-685
Hutchinson, J.R., 2004. Biomechanical modeling and sensitivity analysis of bipedal running ability. I. Extant taxa. Journal of Morphology, 262(1), pp.421-440.
Isler, K., 2005. 3D-kinematics of vertical climbing in hominoids. American Journal of Physical Anthropology, 126(1), pp.66-81.
Jablonski, N.G. and Chaplin, G., 1993. Origin of habitual terrestrial bipedalism in the ancestor of the Hominidae. Journal of Human Evolution, 24(4), pp.259-280.
Johanson DC, Edey MA. 1981. Lucy-the Beginnings of Humankind. London : Penguin Books.
Johanson, D.C., Lovejoy, C.O., Kimbel, W.H., White, T.D., Ward, S.C., Bush, M.E., Latimer, B.M. and Coppens, Y., 1982. Morphology of the Pliocene partial hominid skeleton (AL 288-1) from the Hadar formation, Ethiopia. American Journal of Physical Anthropology, 57(4), pp.403-451.
Johanson, D.C. and Taieb, M. 1976. Plio-Pleistocene hominid discoveries in Hadar, Ethiopia. Nature 260: 293-297
Jolly, C.J., 1970. The seed-eaters: a new model of hominid differentiation based on a baboon analogy. Man, 5(1), pp.5-26.
Jungers, W.L. and Stern, J.T., 1983. Body proportions, skeletal allometry and locomotion in the Hadar hominids: a reply to Wolpoff. Journal of Human Evolution, 12(7), pp.673-684.
Jungers, W.L., 1982. Lucy's limbs: skeletal allometry and locomotion in Australopithecus afarensis. Nature, 297(5868), pp.676-678.
Jungers, W.L., 1984. Aspects of size and scaling in primate biology with special reference to the locomotor skeleton. American Journal of Physical Anthropology, 27(S5), pp.73-97.
Jungers, W.L., 1985. Body size and scaling of limb proportions in primates. In Size and scaling in primate biology (pp. 345-381). Springer US.
Jungers, W.L., 1991. Scaling of postcranial joint size in hominoid primates. Human Evolution, 6(5-6), pp.391-399.
Jungers, W.L., 1994. Ape and hominid limb length. Nature, 369, p.194.
Keith, A., 1903. The extent to which the posterior segments of the body have been transmuted and suppressed in the evolution of man and allied primates. Journal of anatomy and physiology, 37(Pt 1), p.18.
Keith, A., 1923. Hunterian Lectures on Man's Posture: Its Evolution and Disorders: Given at the Royal College of Surgeons of England. British medical journal, 1(3251), p.669.
Kendall, D.G. 1977. The Diffusion of Shape. Advances in Applied Probability 9 (3): 428-430
Kerrigan, D.C., Todd, M.K. and Croce, U.D., 1998. Gender Differences in Joint Biomechanics During Walking. Normative Study in Young Adults.
Kimbel, W.H., Johanson, D.C. and Rak, Y., 1994. The first skull and other new discoveries of Australopithecus afarensis at Hadar, Ethiopia. Nature, 368(6470), p.449.
Kimes, K.R., Siegel, M.I. and Sadler, D.L., 1981. Musculoskeletal scapular correlates of plantigrade and acrobatic positional activities in Papio cynocephalus anubis and Macaca fascicularis. American Journal of Physical Anthropology, 55(4), pp.463-472.

Klingenberg, C.P. and McIntyre, G.S., 1998. Geometric morphometrics of developmental instability: analyzing patterns of fluctuating asymmetry with Procrustes methods. Evolution, pp.1363-1375.
Klingenberg, C.P., Barluenga, M. and Meyer, A., 2002. Shape analysis of symmetric structures: quantifying variation among individuals and asymmetry. Evolution, 56(10), pp.1909-1920.
Klingenburg, C.P., 2015. Analyzing Fluctuating Asymmetry with Geometric Morphometrics: Concepts, Methods, and Applications. *Symmetry*7(2): 843-934
Kramer, P.A. and Eck, G.G., 2000. Locomotor energetics and leg length in hominid bipedality. *Journal of Human Evolution*, *38*(5), pp.651-666.
Kramer, P.A., 1999. Modelling the locomotor energetics of extinct hominids. Journal of Experimental Biology, 202(20), pp.2807-2818.
Larson, S.G., 1993. Functional morphology of the shoulder in primates. Postcranial adaptation in nonhuman primates, pp.45-69.
Latimer, B. and Lovejoy, C.O., 1989. The calcaneus of Australopithecus afarensis and its implications for the evolution of bipedality. American Journal of Physical Anthropology, 78(3), pp.369-386.
Latimer, B. and Lovejoy, C.O., 1990a. Hallucal tarsometatarsal joint in Australopithecus afarensis. American Journal of Physical Anthropology, 82(2), pp.125-133.
Latimer, B. and Lovejoy, C.O., 1990b. Metatarsophalangeal joints of Australopithecus afarensis. American Journal of Physical Anthropology, 83(1), pp.13-23.
Latimer, B., 1983, January. The Anterior Foot of *Australopithecus afarensis.* American Journal of Physical Anthropology 60 (2), pp. 217-217
Latimer, B., 1991. Locomotor adaptations in Australopithecus afarensis: the issue of arboreality. Origine (s) de la Bipédie chez les Hominidés, pp.169-176.
Latimer, B., Ohman, J.C. and Lovejoy, C.O., 1987. Talocrural joint in African hominoids: implications for Australopithecus afarensis. American Journal of Physical Anthropology, 74(2), pp.155-175.
Lele, S.R. and Richtsmeier, J.T., 2001. An invariant approach to statistical analysis of shapes. CRC Press.
Leong, A., 2006. Sexual dimorphism of the pelvic architecture: a struggling response to destructive and parsimonious forces by natural & mate selection. *McGill Journal of Medicine: MJM*, *9*(1), p.61.
Leutenegger, W., 1974. Functional aspects of pelvic morphology in simian primates. Journal of Human Evolution, 3(3), pp.207-222.
Lewis, O.J., 1981. Functional morphology of the joints of the evolving foot. In Symp Zool Soc London (Vol. 46, pp. 169-188).
Lewton, K.L., 2010. Locomotor function and the Evolution of the Primate Pelvis. Dissertation: Arizona State University.
Lovejoy, C.O. 1988. Evolution of human walking. Scientific American 259 (5): 118-25
Lovejoy, C.O., 1979. Reconstruction of the Pelvis of AL-288 (Hadar formation, Ethiopia. American Journal of Physical Anthropology 50 (3) pp. 460-460
Lovejoy, C.O., 1980. Hominid Origins-The Role of Bipedalism. American Journal of Physical Anthropology 52 (2) pp. 250-250
Lovejoy, C.O., 1981. The origin of man. Science, 211(4480), pp.341-350.
Lovejoy, C.O., 2005. The natural history of human gait and posture: Part 1. Spine and pelvis. Gait & posture, 21(1), pp.95-112.

Lovejoy, C.O., 2007. The natural history of human gait and posture: Part 3. The knee. Gait & posture, 25(3), pp.325-341.
Lovejoy, C.O., Suwa, G., Spurlock, L., Asfaw, B. and White, T.D., 2009. The pelvis and femur of Ardipithecus ramidus: the emergence of upright walking. Science, 326(5949), pp.71-71e6.
Lukas, K.E., Stoinski, T.S., Burks, K., Snyder, R., Bexell, S. and Maple, T.L., 2003. Nest building in captive Gorilla gorilla gorilla. *International journal of primatology*, *24*(1), pp.103-124.
Lycett, S.J. and von Cramon-Taubadel, N., 2013. Understanding the comparative catarrhine context of human pelvic form: a 3D geometric morphometric analysis. Journal of human evolution, 64(4), pp.300-310.
MacLatchy, L.M. and Bossert, W.H., 1996. An analysis of the articular surface distribution of the femoral head and acetabulum in anthropoids, with implications for hip function in Miocene hominoids. Journal of human evolution, 31(5), pp.425-453.
Mafart, B., Guipert, G., de Lumley, M and Subsol, G. 2004. Three-dimensional computer imaging of hominid fossils: a new step in human evolution studies. Canadian Association of Radiologists Journal 55 (4):264-270
Marchal, F., 1997. L'os coxal des hominide´s fossiles. Ph.D. Dissertation, Universite´ de la Me´diterrane´e Aix-Marseille II.
Marchal, F., 2000. A new morphometric analysis of the hominid pelvic bone. Journal of human evolution, 38(3), pp.347-365.
Marzke, M.W., 1983. Joint functions and grips of the Australopithecus afarensis hand, with special reference to the region of the capitate. Journal of Human Evolution, 12(2), pp.197-211.
Masi, S., Cipolletta, C. and Robbins, M.M., 2009. Western lowland gorillas (Gorilla gorilla gorilla) change their activity patterns in response to frugivory. *Am J Primatol*, *71*(2), pp.91-100.
Maya. Autodesk, 2015
McHenry, H.M. 1974. Biomechanical interpretation of the early hominid hip. Journal of Human Evolution 4: 343-355.
McHenry, H.M. 1978. Fore- and hind-limb proportions in Plio-Pleistocene hominids. American Journal of Physical Anthropology 49: 15-22.
McHenry, H.M. 2002. Introduction to the fossil record of human ancestry. In Hartwig, W.C., (ed.) 2002. The Primate Fossil Record. Cambridge, UK: Cambridge University Press
McHenry, H.M., 1975. Fossils and the mosaic nature of human evolution. *Science*, *190*(4213), pp.425-431.
McHenry, H.M., 1983. The capitate of Australopithecus afarensis and A. africanus. American Journal of Physical Anthropology, 62(2), pp.187-198.
Mehlman, P.T. and Doran, D.M., 2002. Influencing western gorilla nest construction at Mondika Research Center. *International Journal of Primatology*, *23*(6), pp.1257-1285.
Méndez, J. and Keys, A., 1960. Density and composition of mammalian muscle. Metabolism-Clinical and Experimental, 9(2), pp.184-188.
Minetti, A.E. and Alexander, R.M., 1997. A theory of metabolic costs for bipedal gaits. Journal of Theoretical Biology, 186(4), pp.467-476.
Morton, D.J., 1924. Evolution of the human foot II. American Journal of Physical Anthropology, 7(1), pp.1-52.

Myatt, J.P., Crompton, R.H., & Thorpe, S.K. 2011. Hindlimb muscle architecture in non-human great apes and a comparison of methods for analysing inter-species variation. *Journal of Anatomy.* 219, pp150–166
Nagano, A., Umberger, B.R., Marzke, M.W and Gerritsen, K.G.M. 2005. Neuromusculoskeletal Computer Modeling and Simulation of upright, straight-legged, bipedal locomotion of Australopithecus afarensis (AL 288-1). American Journal of Physical Anthropology 126:2-13
Napier, J.R. 1980. Hands. London: George Allen & Unwin
Napier, J.R. and Napier, P.H. 1985. The Natural History of the Primates. British Museum: London
Napier, J.R., 1967. Evolutionary aspects of primate locomotion. American Journal of Physical Anthropology, 27(3), pp.333-341.
Nicolas, G., Multon, F., and Berillon, G. 2007. From bone to bipedal locomotion using inverse kinematics. Journal of Biomechanics 40 (5):1048-1057
Nicolas, G., Multon, F., and Berillon, G. 2009. From bone to plausible bipedal locomotion. Part II: Complete motion synthesis for bipedal primates. Journal of Biomechanics 42 (8): 1127-1133colas et al. 2009
O'Higgins, P. 2000. The study of morphological variation in the hominid fossil record: biology, landmarks and geometry. Journal of Anatomy 197: 103-120
Ohman JC. 1986. The first rib of hominoids. American Journal of Physical Anthropology 70, pp 209–230.
O'Neill, M.C., Lee, L-F., Demes, B., Thompson, N.E., Larson, S.G., Stern, J.T. and Umberger, B.R. 2015. Three-dimensional kinematics of the pelvis and hind limbs in chimpanzee (*Pan troglodytes*) and human bipedal walking. *Journal of Human Evolution 86*:32-42
Orban, R., 1982. A biometrical comparative study of the os coxae of hominidae, pongidae and Australopithecus Sts 14. Man and His Origins, 21, pp.61-72.
Oxnard, C.E., 1967. The functional morphology of the primate shoulder as revealed by comparative anatomical, osteometric and discriminant function techniques. American Journal of Physical Anthropology, 26(2), pp.219-240.
Oxnard, C.E., 1968. A note on the fragmentary Sterkfontein scapula. American journal of physical anthropology, 28(2), pp.213-217.
Paciulli, L.M., 1995. Ontogeny of phalangeal curvature and positional behavior in chimpanzees. Am J Phys Anthropol, 20(Suppl), p.165.
Page, S.L. and Goodman, M., 2001. Catarrhine phylogeny: noncoding DNA evidence for a diphyletic origin of the mangabeys and for a human–chimpanzee clade. Molecular Phylogenetics and Evolution, 18(1), pp.14-25.
Palastanga, N., Soames, R., and Palastanga, D. 2008. Anatomy and Human Movement Pocketbook. Elsevier:China.
Payne R.C., Crompton RH, Isler K, Savage R, Vereecke EE, Gunther MM, Thorpe SKS, D'Aout K. 2006b. Morphological analysis of the hindlimb in apes and humans. II. Moment arms. J Anat 208:725–742.
Payne, R.C., Crompton, R.H., Isler, K., Savage, R., Vereecke, E.E., Günther, M.M., Thorpe, S.K.S. and D'Août, K., 2006. Morphological analysis of the hindlimb in apes and humans. I. Muscle architecture. *Journal of anatomy*, *208*(6), pp.709-724.
Phillips, R., O'Higgins, P., Bookstein, F., Green, B., George-Nashed, Y.S., Gunnarsson, H.P., Dalge, V., Gowigati, R. and Ali, O.B. 2010. Evan Toolbox. Copyright The EVAN Society.
Pierrynowski MR (1995) Analytical representation of muscle line of action and geometry. In: Allard P, Stokes IAF, Blanch JP, editors. Three-dimensional

analysis of human movement. Champaign, Illinois: Human Kinetic Publishers. 215–256
Plavcan, J.M. and Van Schaik, C.P., 1997. Intrasexual competition and body weight dimorphism in anthropoid primates. *American Journal of Physical Anthropology*, *103*(1), pp.37-68.
Prost, J.H. 1965. A Definitional System for the Classification of Primate Locomotion. American Anthropologist 67 (5): 1198-1214
Prost, J.H., 1980. Origin of bipedalism. *American Journal of Physical Anthropology*, *52*(2), pp.175-189.
Raichlen, D.A., Pontzer, H., Shapiro, L.J. and Sockol, M.D., 2009. Understanding hind limb weight support in chimpanzees with implications for the evolution of primate locomotion. American journal of physical anthropology, 138(4), pp.395-402.
Rak, Y., 1991. Lucy's pelvic anatomy: its role in bipedal gait. Journal of Human Evolution 20 (4): 283-290
Reed, K.E., 1997. Early hominid evolution and ecological change through the African Plio–Pleistocene. J. Hum. Evol. 32, 289–322.
Remis, M., 1995. Effects of body size and social context on the arboreal activities of lowland gorillas in the Central African Republic. *American Journal of Physical Anthropology*, *97*(4), pp.413-433.
Remis, M.J., 1998. The Gorilla Paradox. In Primate Locomotion (pp. 95-106). Springer US.
Remis, M.J., 1999. Tree structure and sex differences in arboreality among western lowland gorillas (Gorilla gorilla gorilla) at Bai Hokou, Central African Republic. *Primates*, *40*(2), pp.383-396.
Reynolds, E. and Hooton, E.A., 1936. Relation of the pelvis to erect posture. An exploratory study. American Journal of Physical Anthropology, 21(2), pp.253-278.
Reynolds, E., 1931. The evolution of the human pelvis in relation to the mechanics of the erect posture. Museum.
Richmond, B., 1999. Reconstructing locomotor behavior in early hominids: evidence from primate development. Journal of Human Evolution 36 (4) pp. 24-28
Richmond, B.G. and Strait, D.S., 2000. Evidence that humans evolved from a knuckle-walking ancestor. Nature, 404(6776), pp.382-385.
Richmond, B.G., 1997. Ontogeny of phalangeal curvature and locomotor behavior in lar gibbons. Am J Phys Anthropol Suppl, 24, p.197.
Richmond, B.G., Begun, D.R. and Strait, D.S. 2001. Origin of Human bipedalism: the knucklewalking hypothesis revisited. Yearbook of Physical Anthropology 44:71-105
Richtsmeier, J.T., Deleon, V.B. and Lele, S.R. 2002. The promise of geometric morphometrics. Yearbook of Physical Anthropology 45: 63-91
Robinson JT. 1972. Early hominid posture and locomotion. Chicago: University of Chicago Press.
Rodman, P.S. and McHenry, H.M., 1980. Bioenergetics and the origin of hominid bipedalism. American Journal of Physical Anthropology, 52(1), pp.103-106.
Rohlf, F. J., and D. E. Slice. 1990. Extensions of the Procrustes method for the optimal superimposition of landmarks. Systematic Zoology 39:40–59.
Rohlf, F. J., and M. Corti. 2000. The use of two-block partial least-squares to study covariation in shape. Systematic Biology 49:740–753
Rose, M.D. 1973. Quadrupedalism in Primates. Primates 14(4): 337-357

Rose, M.D., 1984. Food acquisition and the evolution of positional behaviour: the case of bipedalism. In Food acquisition and processing in primates (pp. 509-524). Springer US.
Rose, M.D., 1988. Another look at the anthropoid elbow. Journal of Human Evolution, 17(1-2), pp.193-224.
Rose, M.D., 1991. The process of bipedalization in hominids. Origine (s) de la bipédie chez les hominidés. CNRS, Paris, pp.37-48.
Rosenberg, K. and Trevathan, W., 2002. Birth, obstetrics and human evolution. *BJOG: An International Journal of Obstetrics & Gynaecology*, *109*(11), pp.1199-1206.
Ross, S.R. and Lukas, K.E., 2006. Use of space in a non-naturalistic environment by chimpanzees (Pan troglodytes) and lowland gorillas (Gorilla gorilla gorilla). *Applied Animal Behaviour Science*, *96*(1), pp.143-152.
Roth, V.L..1993 On Three-Dimensional Morphometrics, and on the Identification of Landmark Points, In: L.F. Marcus, E. Bello, and A. Garcia-Valdecasas (Eds.). 1993. Contributions to Morphometrics. Madrid, Museo Nacional de Ciencias Naturales, CSIC.
Ruff, C., 2003. Ontogenetic adaptation to bipedalism: age changes in femoral to humeral length and strength proportions in humans, with a comparison to baboons. Journal of Human Evolution, 45(4), pp.317-349.
Ruff, C.B., 2002. Long bone articular and diaphyseal structure in Old World monkeys and apes. I: locomotor effects. *American Journal of Physical Anthropology*, *119*(4), pp.305-342.
Russell, K.A., Palmieri, R.M., Zinder, S.M. and Ingersoll, C.D., 2006. Sex differences in valgus knee angle during a single-leg drop jump. *Journal of athletic training*, *41*(2), p.166.
Sarmiento, E.E. 1994. Terrestrial traits in the hands and feet of gorillas. Am Mus Nov 3091:1–56.
Sarmiento, E.E. 1998. Generalized quadrupeds, committed bipeds and the shift to open habitats: an evolutionary model of hominid divergence. Am Mus Nov 3250:1–78.
Sarmiento, E.E., 1985. Functional differences in the skeleton of wild and captive orang-utans and their adaptive significance (Doctoral dissertation, New York University).
Sarmiento, E.E., 1987. The phylogenetic position of Oreopithecus and its significance in the origin of the Hominoidea. American Museum novitates; no. 2881.
Schmid, P., 1983. Eine rekonstruktion des skelettes von AL 288-1 (Hadar) und deren konsequenzen. *Folia primatologica*, *40*(4), pp.283-306.
Schultz, A.H., 1930. The skeleton of the trunk and limbs of higher primates. Human Biology, 2(3), pp.303-438.
Schultz, A.H., 1936. Characters common to higher primates and characters specific for man. *The Quarterly Review of Biology*, *11*(3), pp.259-283.
Schultz, A.H., 1937. Proportions, variability and asymmetries of the long bones of the limbs and the clavicles in man and apes. Human Biology, 9(3), pp.281-328.
Schultz, A.H., 1961. Some factors influencing the social life of primates in general and of early man in particular. In Washburn, S.L. (ed) 1961. Social Life of Early Man. Chicago: Aldine
Schultz, A.H., 1969. The skeleton of the chimpanzee. In: Bourne, G.H. (ed.). 1969. The Chimpanzee. Basel: Karger, pp. 5G103

Scott, J.H., 1957. Muscle growth and function in relation to skeletal morphology. American journal of physical anthropology, 15(2), pp.197-234.
Sellers, W.I. 2013. *GaitSym 2013 Manual- Gait Simulation using Multibody Dynamics.* Available: http://www.animalsimulation.org
Sellers, W.I., Cain, G.M., Wang, W. and Crompton, R.H., 2005. Stride lengths, speed and energy costs in walking of Australopithecus afarensis: using evolutionary robotics to predict locomotion of early human ancestors. Journal of the Royal Society Interface, 2(5), pp.431-441.
Sellers, W.I., Dennis, L.A. and Crompton, R.H. 2003. Predicting the metabolic energy costs of bipedalism using evolutionary robotics. The Journal of Experimental Biology 206: 1127-1136
Sellers, W.I., Dennis, L.A., W-J, W. and Crompton, R.H., 2004. Evaluating alternative gait strategies using evolutionary robotics. Journal of Anatomy, 204(5), pp.343-351.
Sellers, W.I., Margetts, L., Bates, K.T. and Chamberlain, A.T., 2013. Exploring diagonal gait using a forward dynamic three-dimensional chimpanzee simulation. Folia Primatologica, 84(3-5), pp.180-200.
Sellers, W.I., Pataky, T.C., Caravaggi, P. and Crompton, R.H., 2010. Evolutionary robotic approaches in primate gait analysis. International Journal of Primatology, 31(2), pp.321-338.
Senut, B., 1978. Etude comparative des piliers de la palette humérale (Première partie). Cahiers d'Anthropologie Paris, (3), pp.1-8.
Senut, B., 1980. New data on the humerus and its joints in Plio-Pleistocene hominids. Collegium Antropologicum, 4(1), pp.87-93.
Senut, B., Pickford, M., Gommery, D., Mein, P., Cheboi, K and Coppens, Y. 2001. First hominid from the Miocene Lukeino Formation, Kenya). Comptes Rendus de l'Acadamie des Sciences. Paris, Sciences de la Terre et des planètes / Earth and Planetary Sciences 332: 137–144
Shapiro, S.S. and Wilk, M.B., 1965. An analysis of variance test for normality (complete samples). *Biometrika*, *52*(3-4), pp.591-611.
Shipman, P., 1986. Scavenging or hunting in early hominids: theoretical framework and tests. American Anthropologist, 88(1), pp.27-43.
Sigmon B. A. and Farslow D.L., 1986. *The primate hindlimb*. In: Swindler, D.R. and Erwin, J., 1986. *Comparative Primate Biology, Vol. I: Systematics, Evolution and Anatomy* pp. 671–718. New York: Alan R Liss Inc.
Sigmon, B.A., 1969. The scansorius muscle in pongids. *Primates*, *10*(3-4), pp.247-261.
Sigmon, B.A., 1974. A functional analysis of pongid hip and thigh musculature. Journal of Human Evolution, 3(2), pp.161IN3167-166IN14185.
Sigmon, B.A., 1975. Functions and evolution of hominid hip and thigh musculature. Primate functional morphology and evolution, pp.235-252.
Slice, D.E. 2005. Modern Morphometrics. In Slice, D.E (ed). 2005. Modern Morphometrics in Physical Anthropology. Kluwer Academic / Plenum Publishers, New York.
Slice, D.E. 2007. Geometric morphometrics. Annual Review of Anthropology 36:261-81
Sonntag, C.F., 1923. On the anatomy, physiology, and pathology of the chimpanzee. Proceedings of the Zoological Society of London 93 (2) pp. 323-429
Sonntag, C.F., 1924. 17. On the Anatomy, Physiology, and Pathology of the Orang-Outan. Journal of Zoology, 94(2), pp.349-450.

Stern, J.T. and Susman, R.L., 1981. Electromyography of the gluteal muscles in Hylobates, Pongo, and Pan: implications for the evolution of hominid bipedality. American Journal of Physical Anthropology, 55(2), pp.153-166.
Stern, J. T., and Larson, S.G. 1993. "Electromyographic study of the obturator muscles in non-human primates: implications for interpreting the obturator externus groove of the femur." Journal of Human Evolution 24(5): 403-427.
Stern, J.T. and Susman, R.L. 1983. The locomotor anatomy of Australopithecus afarensis. American Journal of Physical Anthropology 60 (30): 279-317
Stern, J.T. and Susman, R.L., 1991. Total morphological pattern" versus the "magic trait": conflicting approaches to the study of early hominid bipedalism. Origine (s) de la bipédie chez les Hominidés. Paris: Cahiers de Paleoanthropologie, CNRS. p, pp.99-112.
Stern, J.T., 1972. Anatomical and functional specializations of the human gluteus maximus. *American Journal of Physical Anthropology*, *36*(3), pp.315-339.
Steudel, K., 1981. Sexual dimorphism and allometry in primate ossa coxae. American journal of physical anthropology, 55(2), pp.209-215.
Straus, W.L., 1929. Studies on primate ilia. American Journal of Anatomy, 43(3), pp.403-460.
Sugardjito, J. and van Hooff, J.A.R.A.M., 1986. Age-sex class differences in the positional behaviour of the Sumatran orang-utan (Pongo pygmaeus abelii) in the Gunung Leuser National Park, Indonesia. Folia Primatologica, 47(1), pp.14-25.
Susman, R.L. and Demes, A.B., 1994. Relative foot length in Australopithecus afarensis and its implications for bipedality. Am J Phys Anthropol Suppl, 18, p.192.
Susman, R.L., Stern, J.T., and Jungers, W.L. 1984. Arboreality and bipedality in the Hadar hominids. Folia Primatologica 43 (2-3): 113-156
Swales, D.L.M. 2012. Life and Stress. A bio-cultural investigation into the later Anglo-Saxon population of the Black Gate cemetery, Newcastle-upon-Tyne. Unpublished PhD thesis. University of Sheffield.
Sylvester, A.D., 2013. A geometric morphometric analysis of the medial tibial condyle of African hominids. The Anatomical Record, 296(10), pp.1518-1525.
Sylvester, A.D., Merkl, B.C. and Mahfouz, M.R., 2008. Assessing AL 288-1 femur length using computer-aided three-dimensional reconstruction. Journal of human evolution, 55(4), pp.665-671.
Tao, W., Liu, T., Zheng, R. and Feng, H., 2012. Gait analysis using wearable sensors. Sensors, 12(2), pp.2255-2283.,
Tardieu C. 1979a. Analyse morpho-fonctionelle de l'articulation de genou chez les primates. Application aux hominides fossiles. These, Universite Pierre et Marie Curie, Paris IV.
Tardieu C. 1979b. Aspects biome´chaniques de l'articulation du genou chez les Primates. Bull Soc Anat Paris n° 4:66–86.
Tardieu C. 1983. L'articulation du genou, analyse morpho-fonctionelle chez les primates et les hominide´s fossiles. Paris: CNRS
Tardieu C. 1986a. The knee joint in three primates: application to Plio-pleistocene hominids and evolutionary implications. In: Taub D.M., and King F.A., (eds). 1986. Current perspectives in primate biology. New York: Van Nostrand. p 182–192
Tardieu C. 1986b. Evolution of the knee intraarticular menisci in primates and some fossil hominids. In: Else J.G.,and Lee P.C., (eds).1986. Primate evolution, vol. 1. Cambridge: Cambridge University Press. Pp. 183–190

Tardieu, C. and Preuschoft, H., 1996. Ontogeny of the knee joint in humans, great apes and fossil hominids: pelvi-femoral relationships during postnatal growth in humans. Folia Primatologica, 66(1-4), pp.68-81.
Taylor, A.B., 1995. Effects of ontogeny and sexual dimorphism on scapula morphology in the mountain gorilla (Gorilla gorilla beringel). *American journal of physical anthropology*, *98*(4), pp.431-445.
Taylor, A.B., 1997. Relative growth, ontogeny, and sexual dimorphism in Gorilla (Gorilla gorilla gorilla and G. g. beringei): Evolutionary and ecological considerations. *American Journal of Primatology*, *43*(1), pp.1-31.
Thorpe, S.K. and Crompton, R.H., 2005. Locomotor ecology of wild orangutans (Pongo pygmaeus abelii) in the Gunung Leuser Ecosystem, Sumatra, Indonesia: A multivariate analysis using log-linear modelling. American Journal of Physical Anthropology, 127(1), pp.58-78.
Thorpe, S.K. and Crompton, R.H., 2006. Orangutan positional behavior and the nature of arboreal locomotion in Hominoidea. American Journal of Physical Anthropology, 131(3), pp.384-401.
Thorpe, S.K., Holder, R.L. and Crompton, R.H., 2007. Origin of human bipedalism as an adaptation for locomotion on flexible branches. Science, 316(5829), pp.1328-1331.
Thorpe, S.K.S., Crompton, R.H. and Wang, W.J., 2004. Stresses exerted in the hindlimb muscles of common chimpanzees (Pan troglodytes) during bipedal locomotion. Folia Primatologica, 75(4), pp.253-265.
Trevathan, W., 2015. Primate pelvic anatomy and implications for birth. *Phil. Trans. R. Soc. B*, *370*(1663), p.20140065.
Turley, K., Guthrie, E.H. and Frost, S.R. 2011. The Anatomical Record 294: 217-230
Tuttle, R. and Basmajian, J.V., 1974. Electromyography of brachial muscles in Pan gorilla and hominoid evolution. American Journal of Physical Anthropology, 41(1), pp.71-90.
Tuttle, R., 1975. Parallelism, brachiation, and hominoid phylogeny. In Phylogeny of the Primates (pp. 447-480). Springer US.
Tuttle, R.H., 1981. Evolution of hominid bipedalism and prehensile capabilities. Philosophical Transactions of the Royal Society of London B: Biological Sciences, 292(1057), pp.89-94.
Umberger BR, Gerritsen KGM, Martin PE (2003) A model of human muscle energy expenditure. Computational Methods in Biomechanics and Biomedical Engineering 6: 99–111.
Uustal, H. and Baerga, E., 2004. Gait analysis. *Physical medicine and rehabilitation board review. 1st ed. New York: Demos Medical Publishing*.
Van Couvering, J.A. 2000. The Pliocene. In: Delson, E., Tattersall, I., Van Couvering, J.A., and Brooks, A.S. (eds) Encylopedia of human evolution and prehistory, 2nd edn. Garland,New York, pp 574–576
Vaughan, C.L. 2003. Theories of bipedal walking: an odyssey. Journal of Biomechanics 36:513-523
Videan, E.N. and McGrew, W.C., 2002. Bipedality in chimpanzee (Pan troglodytes) and bonobo (Pan paniscus): testing hypotheses on the evolution of bipedalism. American journal of physical anthropology, 118(2), pp.184-190.
Wang, W., Crompton, R.H., Carey, T.S., Günther, M.M., Li, Y., Savage, R. and Sellers, W.I., 2004. Comparison of inverse-dynamics musculo-skeletal models of AL 288-1 Australopithecus afarensis and KNM-WT 15000 Homo ergaster to

modern humans, with implications for the evolution of bipedalism. Journal of Human Evolution, 47(6), pp.453-478.
Wang, W.J. and Crompton, R.H., 2004. Analysis of the human and ape foot during bipedal standing with implications for the evolution of the foot. Journal of biomechanics, 37(12), pp.1831-1836.
Ward, C.V., 1993. Torso morphology and locomotion in Proconsul nyanzae. American Journal of Physical Anthropology, 92(3), pp.291-328.
Ward, C.V., 2002. Interpreting the posture and locomotion of Australopithecus afarensis: where do we stand?. American journal of physical anthropology, 119(S35), pp.185-215.
Ward, C.V., Leakey, M.G., Brown, B., Harris, J., Walker, A. 1999. South Turkwel: a new Pliocene hominid site in Kenya. J Hum Evol 36:69-95.
Warren, R.D & Crompton, R.H. 1998. Diet, Body Size and the Energy Costs of Locomotion in Saltatory Primates. *Folia Primatol* 69(suppl 1):86–100
Washburn, S.L., 1960. Tools and human evolution. Scientific American, 203, pp.62-75.
Washburn, S.L., 1967. Behaviour and the origin of man. Proceedings of the Royal Anthropological Institute of Great Britain and Ireland, (1967), pp.21-27.
Waterman, H.C., 1929. Studies on the evolution of the pelves of man and other primates. Bull. Am. Mus. Nat. Hist. 58, 585e642.
Watson, J.C., Payne, R.C., Chamberlain, A.T., Jones, R.K. and Sellers, W.I., 2008. The energetic costs of load-carrying and the evolution of bipedalism. *Journal of Human Evolution*, *54*(5), pp.675-683.
Weber, G.W. and Bookstein, F.L. 2011. Virtual Anthropology- A guide to a new interdisciplinary field. Springer-Verlag/Wein
Wells, J.C., 2015. Between Scylla and Charybdis: renegotiating resolution of the 'obstetric dilemma'in response to ecological change. Phil. Trans. R. Soc. B, 370(1663), p.20140067.
Wells, J.C., DeSilva, J.M. and Stock, J.T., 2012. The obstetric dilemma: an ancient game of Russian roulette, or a variable dilemma sensitive to ecology?. American journal of physical anthropology, 149(S55), pp.40-71.
Wheeler, P.E., 1984. The evolution of bipedality and loss of functional body hair in hominids. Journal of Human Evolution, 13(1), pp.91-98.
Wheeler, P.E., 1988. Stand tall and stay cool.New Sci 118(1613): 62–65
Wheeler, P.E., 1991. The influence of bipedalism on the energy and water budgets of early hominids. Journal of Human Evolution, 21(2), pp.117-136.
Wheeler, P.E., 1993. The influence of stature and body form on hominid energy and water budgets; a comparison of Australopithecus and early Homo physiques. Journal of human evolution, 24(1), pp.13-28.
Wheeler, P.E., 1994. The foraging times of bipedal and quadrupedal hominids in open equatorial environments (a reply to Chaplin, Jablonski & Cable, 1994). Journal of human evolution, 27(6), pp.511-517.
Whitcome, K.K., Shapiro, L.J. and Lieberman, D.E., 2007. Fetal load and the evolution of lumbar lordosis in bipedal hominins. Nature, 450(7172), pp.1075-1078.
White, T.D., 1994. Ape and hominid limb length. Nature, 369, p.194.
White, T.D., Hart, W.K., Walter, R.C., WoldeGabriel, G., de Heinzelin, J., Clark, J.D., Asfaw, B. and Vrba, E., 1993. New discoveries of Australopithecus at Maka in Ethiopia. Nature, 366(6452), pp.261-265.

Wittman, A.B. and Wall, L.L., 2007. The evolutionary origins of obstructed labor: bipedalism, encephalization, and the human obstetric dilemma. Obstetrical & gynecological survey, 62(11), pp.739-748.
Wolpoff, M.H., 1983. Lucy's lower limbs: long enough for Lucy to be fully bipedal?. Nature, 304(5921), pp.59-61.
Wolpoff, M.H., 1983a. Lucy's little legs. Journal of Human Evolution, 12(5), pp.443-453.
Wrangham, R.W., 1980. An ecological model of female-bonded primate groups. Behaviour, 75(3), pp.262-300.
Yirga, S., 1987. Interrelation between ischium, thigh extending muscles and locomotion in some primates. Primates, 28(1), pp.79-86.
Zelditch, M.L., Swiderski, D.L., and Sheets, H.D. 2012. Geometric Morphometrics for Biologists: A Primer. Second Edition. Elsevier: London
Zheng N, Fleisig GS, Escamilla RF, Barrentine SW (1998) An analytical model of the knee for estimation of internal forces during exercise. Journal of Biomechanics 31: 963–967.2
Zihlman, A.L. and Cramer, D.L., 1978. Skeletal differences between pygmy (Pan paniscus) and common chimpanzees (Pan troglodytes). Folia Primatologica, 29(2), pp.86-94.
Zihlman, A.L. and Hunter, W.S., 1972. A biomechanical interpretation of the pelvis of Australopithecus. Folia Primatologica, 18(1-2), pp.1-19.
Zihlman, A.L., Mcfarland, R.K. and Underwood, C.E., 2011. Functional anatomy and adaptation of male gorillas (Gorilla gorilla gorilla) with comparison to male orangutans (Pongo pygmaeus). The Anatomical Record, 294(11), pp.1842-1855.
Zuckerman, S., Ashton, E.H., Flinn, R.M., Oxnard, C.E. and Spence, T.F., 1973. Some locomotor features of the pelvic girdle in primates. In Symp. Zool. Soc. Lond (Vol. 33, No. 71, p. 165).

7. Appendix

Generalised Procrustes Analysis

In every case, the Procrustes Distances showed that the specimens within the species groups were more alike to each other, than the species groups were to each other.

The *Pongo pygmaeus* group displayed the smallest Procrustes Distances for each bone. This is probably due to a combination of this group having had the both smallest sample, and that sample consisting of only male specimens. Figure 7-1 illustrates the total variance for each species subset.

Table 7-1: Procrustes Distances for each bone and species

	Group	Procrustes Distance		Group	Procrustes Distance
OS COXA	All	1.90828	SACRUM	All	2.25542
	Pan paniscus	0.06354		*Pan paniscus*	0.19697
	Pan troglodytes	0.09040		*Pan troglodytes*	0.34413
	Gorilla sp.	0.09024		*Gorilla sp.*	0.29439
	Homo sapiens	0.10582		*Homo sapiens*	0.17680
	Pongo pygmaeus	0.03178		*Pongo pygmaeus*	0.14199
FEMUR	Group	Procrustes Distance	TIBIA	Group	Procrustes Distance
	All	0.17216		All	0.17720
	Pan paniscus	0.00905		*Pan paniscus*	0.01449
	Pan troglodytes	0.01663		*Pan troglodytes*	0.01663
	Gorilla sp.	0.02509		*Gorilla sp.*	0.01859
	Homo sapiens	0.01182		*Homo sapiens*	0.01117
	Pongo pygmaeus	0.00870		*Pongo pygmaeus*	0.00555

Principal Components Analyses and ANOVA

Principal Components Analyses were conducted in order to determine how the shapes of each bone varied across each species. Principal components were selected on the basis that they explained the greatest percentage of the variation, whilst simultaneously providing the greatest separation between groups. In all cases, this was Principal Component 1 and Principal Component 2.

Sex was considered to be a potential source of variation within the species subsets, and so in order to explore this, Principal Components Analyses were conducted on each species subset. The Principal Components Analyses were also conducted on the overall shape of each bone using all landmarks and semilandmarks across all species groups. Furthermore, in order to greater explore the shape of the bones in more specific areas, the 'true landmarks' were used in combination with each semilandmark set. This was done in order to focus the possible muscular anatomy for the fossil species.

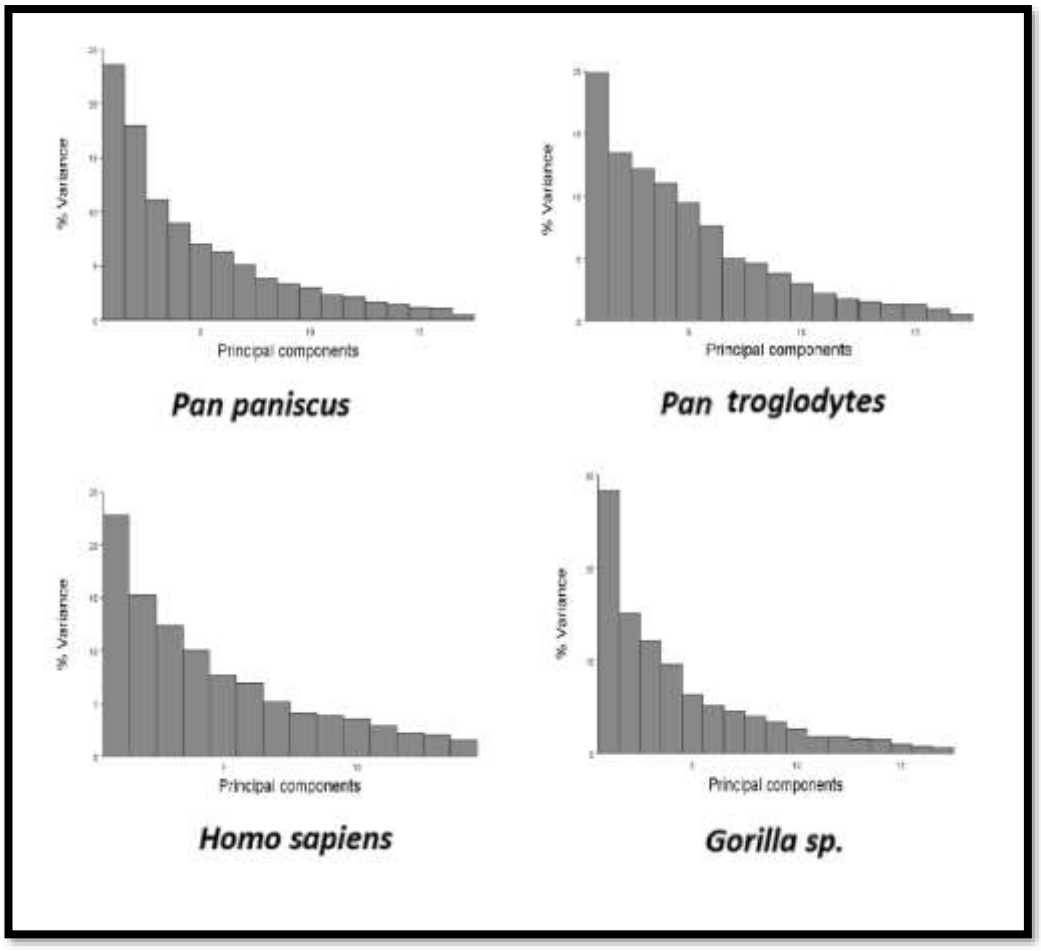

Figure 7-1 Percentage of the variance in the Os Coxa by each Principal Component in the analysis of all Landmarks and Semilandmarks within each species subsample

Table 7-2 Shapiro-Wilk tests for normality for each sex within the species subsets, including all Landmarks and Semilandmarks of the Os Coxa

		Sex	Stat.	df	Sig.			Sex	Stat.	df	Sig.
Pan paniscus	PC 1	female	0.862	9	0.100	*Pan troglodytes*	PC 1	female	0.941	9	0.596
		male	0.944	8	0.652			male	0.899	10	0.213
	PC 2	female	0.902	9	0.265		PC 2	female	0.900	9	0.253
		male	0.930	8	0.513			male	0.850	10	0.057
Gorilla sp.	PC 1	female	0.921	10	0.364	*Homo sapiens*	PC 1	female	0.909	8	0.347
		male	0.972	8	0.915			male	0.929	7	0.539
	PC 2	female	0.951	10	0.675		PC 2	female	0.853	8	0.102
		male	0.969	8	0.892			male	0.970	7	0.896

Table 7-3 Levene's Tests for Homogeneity of Variance of the Os Coxa for Each Species Subset

Species	Principal Component	Levene's Statistic	df1	df2	Sig.
Pan paniscus	PC1	.891	1	15	.360
	PC2	.189	1	15	.670
Pan troglodytes	PC1	1.845	1	17	.192
	PC2	.010	1	17	.921
Gorilla sp.	PC1	4.196	1	16	.057
	PC2	.002	1	16	.967
Homo sapiens	PC1	.769	1	13	.396
	PC2	2.441	1	13	.142

Table 7-4: ANOVA of all Landmarks & Semilandmarks of the Os Coxa in Each Species Subset

	Pan paniscus						*Pan troglodytes*					
	PC1			PC2			PC1			PC2		
	Between groups	Within groups	Total	Between groups	Within groups	Total	Between groups	Within groups	Total	Between groups	Within groups	Total
Sum of squares	.001	.012	.013	.000	.007	.007	.001	.016	.017	.000	.012	.012
df	1	15	16	1	15	16	1	17	18	1	17	18
Mean square	.001	.001		.001	.001		.001	.001		.000	.001	
F	1.437			.519			1.377			.224		
Sig.	.249			.482			.257			.642		
	Gorilla sp.						*Homo sapiens*					
	PC1			PC2			PC1			PC2		
	Between groups	Within groups	Total	Between groups	Within groups	Total	Between groups	Within groups	Total	Between groups	Within groups	Total
Sum of squares	.006	.020	.025	.001	.013	.014	.008	.016	.024	.004	.012	.016
df	1	16	17	1	16	17	1	13	14	1	13	14
Mean square	.006	.001		.000	.001		.008	.001		.004	.001	
F	4.622			.449			7.084			4.895		
Sig.	.047			.512			.020			.045		

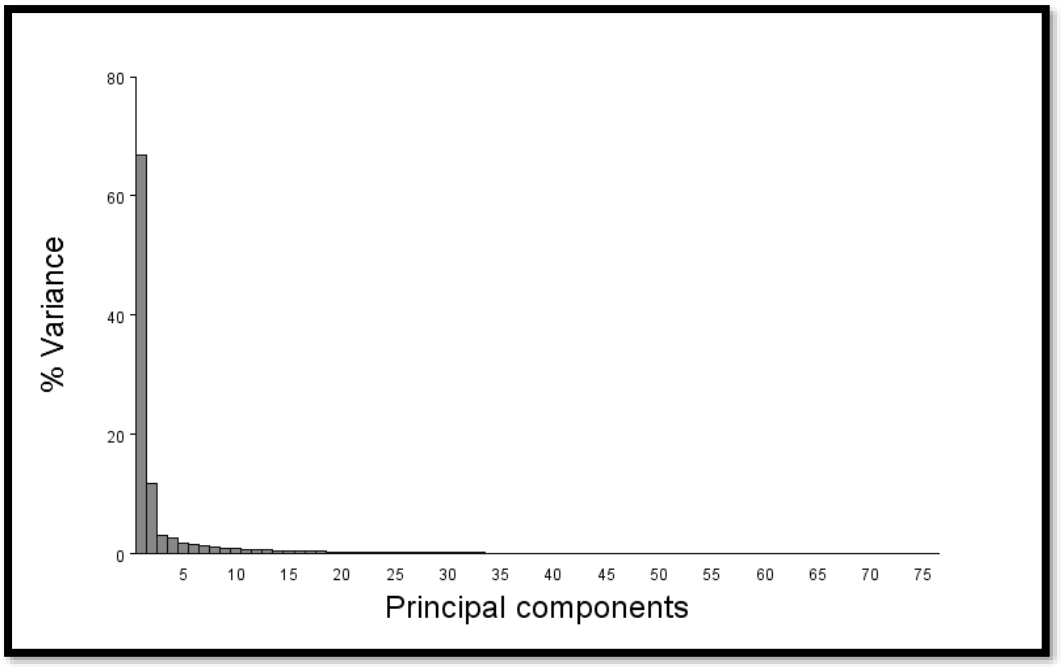

Figure 7-2: Percentage of the Total Variance Explained by Each Principal Component in the Principal Components Analysis of the Os Coxa Using All Landmarks and Semilandmarks

Table 7-5: Shapiro-Wilk test for normality for each species, including all Landmarks and Semilandmarks of the Os Coxa

	Species	Statistic	df	Sig.
Principal Component 1	*Pan paniscus*	.946	16	.338
	Pan troglodytes	.938	19	.240
	Gorilla sp.	.965	18	.704
	Homo sapiens	.965	15	.774
	Pongo pygmaeus	.917	7	.447
Principal Component 2	*Pan paniscus*	.929	16	.073
	Pan troglodytes	.906	19	.062
	Gorilla sp.	.961	18	.630
	Homo sapiens	.940	15	.379
	Pongo pygmaeus	.941	7	.644

Table 7-6: Analysis of Variance for Principal Components 1 & 2 For All Landmarks and Semilandmarks Across All Species in the Os Coxa

		Sum of Squares	df	Mean Square	F	Sig.
PC1	Between Groups	1.167	4	.292	882.577	.000
	Within Groups	.024	73	.000		
	Total	1.191	77			
PC2	Between Groups	.180	4	.045	113.886	.000
	Within Groups	.029	73	.000		
	Total	.209	77			

Table 7-7

Tukey Post Hoc Homogeneous Subsets for Principal Components 1 & 2 of the Os Coxa for all Species

Principal Component 1

Species	N	Subset for alpha=0.05 1	2	3	4
Pan paniscus	17	-.0931871530374			
Pan troglodytes	19	-.0799237492844			
Pongo pygmaeus	7		-.0357427303152		
Gorilla sp.	18			-.0128988516084	
Homo sapiens	15				.2406904542709
Sig.		.329	1.000	1.000	1.000

Principal Component 2

Species	N	Subset for alpha=0.05 1	2	3
Pan paniscus	17	-.041378389931210		
Homo sapiens	15	-.021152377617327	-.021152377617327	
Pan troglodytes	19		-.015031802966157	
Pongo pygmaeus	7		-.014890084025519	
Gorilla sp.	18			.086671808485278
Sig.		.073	.924	1.000

Means for groups in homogeneous subsets are displayed.
Uses Harmonic Mean Sample Size = 13.372.
The group sizes are unequal. The harmonic mean of the group sizes is used. Type I error levels are not guaranteed.

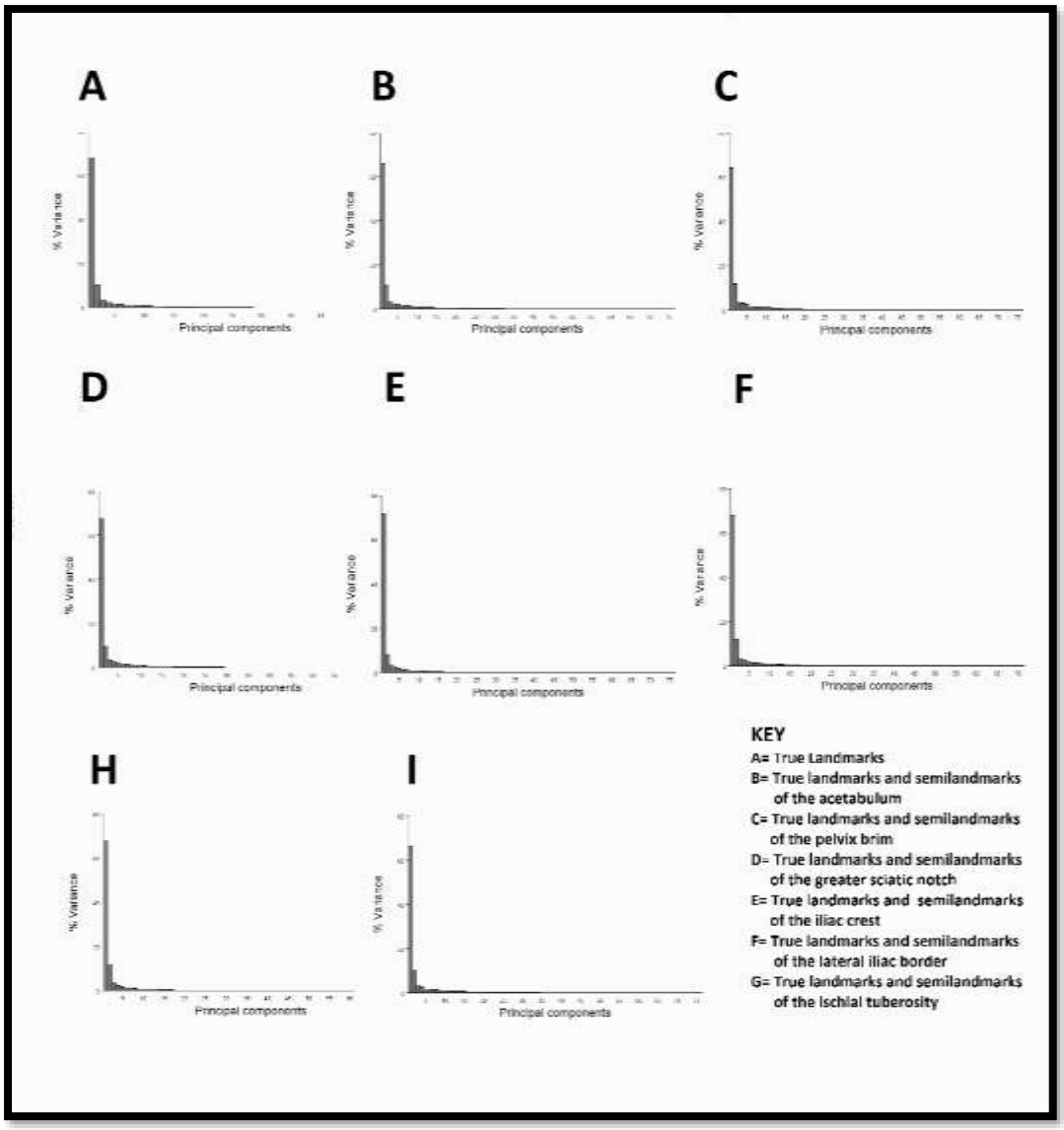

Figure 7-3: The Percentage of the Variance Explained by Each Principal Component for Each Semilandmark set of the Os Coxa

Table 7-8: Shapiro-Wilk Tests for Normality of Each Semilandmark Set in the Os Coxa for Each Species

		True Landmarks			*Acetabulum*			*Pelvic Brim*			*Greater Sciatic Notch*			*Iliac Crest*			*Lateral Iliac Border*			*Ischial Tuberosity*		
	Species	**Stat**	**df**	**Sig.**	**Stat**	**df**	**Sig.**	**Stat**	**df**	**Sig.**	**Stat**	**df**	**Sig.**	**Stat**	**df**	**Sig.**	**Stat**	**df**	**Sig.**	**Stat**	**df**	**Sig.**
P	*Pan paniscus*	.941	17	.335	.944	19	.310	.955	17	.471	.913	19	.083	.930	17	.172	.981	19	.953	.926	17	.149
C	*Pan troglodytes*	.898	19	.044	.883	19	.024	.902	19	.052	.887	19	.028	.943	19	.293	.923	19	.131	.927	19	.156
1	*Gorilla sp.*	.949	18	.411	.964	18	.674	.942	18	.316	.955	18	.516	.970	18	.789	.956	18	.519	.937	18	.262
	Homo sapiens	.953	15	.580	.967	15	.804	.902	15	.102	.947	15	.484	.939	15	.371	.960	15	.701	.959	15	.669
	Pongo pygmaeus	.951	7	.743	.910	7	.399	.976	7	.939	.842	7	.103	.890	7	.276	.932	7	.567	.959	7	.814
P	*Pan paniscus*	.881	17	.033	.923	17	.130	.923	17	.129	.916	17	.096	.917	17	.098	.902	17	.053	.875	17	.018
C	*Pan troglodytes*	.937	19	.230	.931	19	.180	.954	19	.453	.931	19	.179	.929	19	.163	.903	19	.056	.960	19	.573
2	*Gorilla sp.*	.957	18	.544	.944	18	.336	.954	18	.500	.950	18	.421	.942	18	.312	.963	18	.665	.923	18	.145
	Homo sapiens	.926	15	.239	.861	15	.025	.901	15	.098	.897	15	.086	.937	15	.343	.958	15	.659	.898	15	.089
	Pongo pygmaeus	.848	7	.118	.848	7	.117	.826	7	.073	.881	7	.233	.912	7	.410	.919	7	.463	.938	7	.623

Underlined data indicates data that were not normal

Table 7-9: Levene's Test for Homogeneity of Variance for Each Semilandmark Set Principal Components 1 & 2

	True Landmarks				*Acetabulum*				*Pelvic Brim*				*Greater Sciatic Notch*				*Iliac Crest*				*Lateral Iliac Border*				*Ischial Tuberosity*			
	Levene Statistic	**df1**	**df2**	**Sig.**	**Levene Statistic**	**df1**	**df2**	**Sig.**	**Levene Statistic**	**df1**	**df2**	**Sig.**	**Levene Statistic**	**df1**	**df2**	**Sig.**	**Levene Statistic**	**df1**	**df2**	**Sig.**	**Levene Statistic**	**df1**	**df2**	**Sig.**	**Levene Statistic**	**df1**	**df2**	**Sig.**
PC 1	.256	4	71	.905	.721	4	73	.580	.479	4	73	.751	.649	4	73	.629	.278	4	73	.891	.363	4	73	.834	.387	4	73	.817
PC 2	2.498	4	71	.050	1.628	4	73	.176	2.146	4	73	.084	2.441	4	73	.054	2.173	4	73	.080	2.891	4	73	.058	2.521	4	73	.048

Table 7-10: ANOVAs for Principal Components 1 & 2 for Each Semilandmark Set of the Os Coxa

			Sum of Squares	*df*	*Mean Square*	*F*	*Sig.*
True landmarks	PC1	Between Groups	1.695	4	.424	662.818	.000
		Within Groups	.045	71	.001		
		Total	1.740	75			
	PC2	Between Groups	.228	4	.057	109.473	.000
		Within Groups	.037	71	.001		
		Total	.265	75			
Acetabulum	PC1	Between Groups	1.820	4	.455	792.081	.000
		Within Groups	.042	73	.001		
		Total	1.862	77			
	PC2	Between Groups	.276	4	.069	116.950	.000
		Within Groups	.043	73	.001		
		Total	.319	77			
Pelvic Brim	PC1	Between Groups	1.577	4	.394	710.009	.000
		Within Groups	.041	73	.001		
		Total	1.617	77			
	PC2	Between Groups	.269	4	.067	146.897	.000
		Within Groups	.033	73	.000		
		Total	.303	77			
Greater Sciatic Notch	PC1	Between Groups	1.754	4	.439	717.419	.000
		Within Groups	.045	73	.001		
		Total	1.799	77			
	PC2	Between Groups	.227	4	.057	109.042	.000
		Within Groups	.038	73	.001		
		Total	.265	77			
Iliac Crest	PC1	Between Groups	1.209	4	.302	539.710	.000
		Within Groups	.041	73	.001		
		Total	1.250	77			
	PC2	Between Groups	.116	4	.029	91.500	.000
		Within Groups	.023	73	.000		
		Total	.139	77			
Lateral Iliac Border	PC1	Between Groups	1.688	4	.422	683.174	.000
		Within Groups	.045	73	.001		
		Total	1.733	77			
	PC2	Between Groups	.274	4	.068	141.135	.000
		Within Groups	.035	73	.000		
		Total	.309	77			
Ischial Tuberosity	PC1	Between Groups	1.373	4	.343	730.333	.000
		Within Groups	.034	73	.000		
		Total	1.407	77			
	PC2	Between Groups	.193	4	.048	105.071	.000
		Within Groups	.033	73	.000		
		Total	.226	77			

Table 7-11: Tukey Post Hoc Homogeneous Subsets for Principal Components 1 & 2 of the Os Coxa for the True Landmarks in all Species

Principal Component 1

Species	N	Subset for alpha = 0.05		
		1	2	3
Pan paniscus	17	-.114749552374190		
Pan troglodytes	19	-.100109606452085		
Pongo pygmaeus	7		-.039559608913859	
Gorilla sp.	18		-.012183992900675	
Homo sapiens	15			.290614162146109
Sig.		.571	.051	1.000

Principal Component 2

Species	N	Subset for alpha = 0.05			
		1	2	3	4
Gorilla sp.	18	-.0961285667348			
Pongo pygmaeus	7		-.0022151136950		
Pan troglodytes	19		.0126588749330	.0126588749330	
Homo sapiens	15			.0276767512331	
Pan paniscus	17				.05281146416393
Sig.		1.000	.453	.443	1.000

Means for groups in homogeneous subsets are displayed.
a. Uses Harmonic Mean Sample Size = 13.279.
b. The group sizes are unequal. The harmonic mean of the group sizes is used. Type I error levels are not guaranteed.

Table 7-12: Tukey Post Hoc Homogeneous Subsets for Principal Components 1 & 2 of the Os Coxa for the True Landmarks And Semilandmarks of the Acetabulum in all Species

Principal Component 1					
		Subset for alpha = 0.05			
Species	N	1	2	3	4
Homo sapiens	15	-.29785605063518			
Gorilla sp.	18		.00853258196170		
Pongo pygmaeus	7			.03639009089643	
Pan troglodytes	19				.107178909886327
Pan paniscus	17				.116675843171153
Sig.		1.000	1.000	1.000	.850
Principal Component 2					
		Subset for alpha = 0.05			
Species	N	1	2	3	4
Gorilla sp.	18	-.10525354770604			
Pongo pygmaeus	7		.00306953656371		
Pan troglodytes	19		.01672969564432	.01672969564432	
Homo sapiens	15			.03222849050368	.032228490503686
Pan paniscus	17				.054486788846286
Sig.		1.000	.611	.489	.148

Means for groups in homogeneous subsets are displayed.
a. Uses Harmonic Mean Sample Size = 13.279.
b. The group sizes are unequal. The harmonic mean of the group sizes is used. Type I error levels are not guaranteed.

Table 7-13: Tukey Post Hoc Homogenous Subsets for Principal Components 1 & 2 of the Os Coxa for the True Landmarks And Semilandmarks of the Pelvic Brim in all Species

Principal Component 1				
		Subset for alpha = 0.05		
Species	N	1	2	3
Homo sapiens	15	-.279971594505358		
Gorilla sp.	18		.017022295251868	
Pongo pygmaeus	7		.037579060964744	
Pan troglodytes	19			.094006176936804
Pan paniscus	17			.107812493903247
Sig.		1.000	.185	.572
Principal Component 2				
		Subset for alpha = 0.05		
Species	N	1	2	3

Pan paniscus	17	-.0538953801001			
Homo sapiens	15		-.0279328059809		
Pan troglodytes	19		-.0170290653650	-.0170290653650	
Pongo pygmaeus	7			-.0035803055206	
Gorilla sp.	18				.1035351585916
Sig.		1.000	.689	.496	1.000

Means for groups in homogeneous subsets are displayed.
a. Uses Harmonic Mean Sample Size = 13.279.
b. The group sizes are unequal. The harmonic mean of the group sizes is used. Type I error levels are not guaranteed.

Table 7-14: Tukey Post Hoc Homogenous Subsets for Principal Components 1 & 2 of the Os Coxa for the True Landmarks And Semilandmarks of the Greater Sciatic Notch in all Species

Principal Component 1					
		Subset for alpha = 0.05			
Species	**N**	**1**	**2**	**3**	**4**
Pan paniscus	17	-.12084092102125			
Pan troglodytes	18	-.10097392218202			
Pongo pygmaeus	7		-.04093746482102		
Gorilla sp.	19			-.0079206022506	
Homo sapiens	15				.29109283883843
Sig.		.328	1.000	1.000	1.000
Principal Component 2					
		Subset for alpha = 0.05			
Species	**N**	**1**	**2**	**3**	**4**
Gorilla sp.	19	-.08906654634355			
Pongo pygmaeus	7		-.00377293322499		
Pan troglodytes	18		.01004250739735	.0100425073973	
Homo sapiens	15			.0310033033534	.03100330335342
Pan paniscus	17				.05226870436315
Sig.		1.000	.611	.203	.191

Means for groups in homogeneous subsets are displayed.
a. Uses Harmonic Mean Sample Size = 13.279.
b. The group sizes are unequal. The harmonic mean of the group sizes is used. Type I error levels are not guaranteed.

Table 7-15: Tukey Post Hoc Homogenous Subsets for Principal Components 1 & 2 of the Os Coxa for the True Landmarks And Semilandmarks of the Iliac Crest in all Species

Principal Component 1

Species	N	Subset for alpha = 0.05			
		1	2	3	4
Pan paniscus	17	-.106535712041221			
Pan troglodytes	19	-.081895436148405			
Pongo pygmaeus	7		-.040214775725108		
Gorilla sp.	18			.007402738153993	
Homo sapiens	15				.238540442648902
Sig.		.073	1.000	1.000	1.000

Principal Component 2

Species	N	Subset for alpha = 0.05			
		1	2	3	4
Gorilla sp.	18	-.067488538975797			
Pan troglodytes	19		.000692068956628		
Pongo pygmaeus	7		.012389466123399	.012389466123399	
Homo sapiens	15			.024446202694684	.024446202694684
Pan paniscus	17				.033413582300873
Sig.		1.000	.444	.413	.693

Means for groups in homogeneous subsets are displayed.
a. Uses Harmonic Mean Sample Size = 13.279.
b. The group sizes are unequal. The harmonic mean of the group sizes is used. Type I error levels are not guaranteed.

Table 7-16: Tukey Post Hoc Homogenous Subsets for Principal Components 1 & 2 of the Os Coxa for the True Landmarks And Semilandmarks of the Ischial Tuberosit in all Species

Principal Component 1				
		Subset for alpha = 0.05		
Species	**N**	**1**	**2**	**3**
Homo sapiens	15	-.262939518647563		
Gorilla sp.	19		.025166707877191	
Pongo pygmaeus	7		.039443424055381	
Pan troglodytes	18			.088524240811897
Pan paniscus	17			.094001305173993
Sig.		1.000	.520	.974

Principal Component 2				
		Subset for alpha = 0.05		
Species	**N**	**1**	**2**	**3**
Gorilla sp.	19	-.082777983785031		
Pongo pygmaeus	7		.001514518065100	
Pan troglodytes	18		.015874052695905	
Homo sapiens	15		.019082928119822	
Pan paniscus	17			.048336719103684
Sig.		1.000	.316	1.000

Means for groups in homogeneous subsets are displayed.

a. Uses Harmonic Mean Sample Size = 13.279.

b. The group sizes are unequal. The harmonic mean of the group sizes is used. Type I error levels are not guaranteed.

Table 7-17: Tukey Post Hoc Homogenous Subsets for Principal Components 1 & 2 of the Os Coxa for the True Landmarks And Semilandmarks of the Lateral Iliac Border in all Species

Principal Component 1				
		Subset for alpha = 0.05		
Species	N	1	2	3
Pan paniscus	17	-.112093922596398		
Pan troglodytes	18	-.095706976274245		
Pongo pygmaeus	7		-.039946209382140	
Gorilla sp.	19		-.022733287220364	
Homo sapiens	15			.290096359689706
Sig.		.513	.463	1.000
Principal Component 2				
		Subset for alpha = 0.05		
Species	**N**	**1**	**2**	**3**
Pan paniscus	17	-.054179881360231		
Homo sapiens	15		-.026581422869099	
Pan troglodytes	18		-.021616517152968	
Pongo pygmaeus	7		.000166712496700	
Gorilla sp.	19			.099452496956688
Sig.		1.000	.052	1.000

Means for groups in homogeneous subsets are displayed.

a. Uses Harmonic Mean Sample Size = 13.279.

b. The group sizes are unequal. The harmonic mean of the group sizes is used. Type I error levels are not guaranteed.

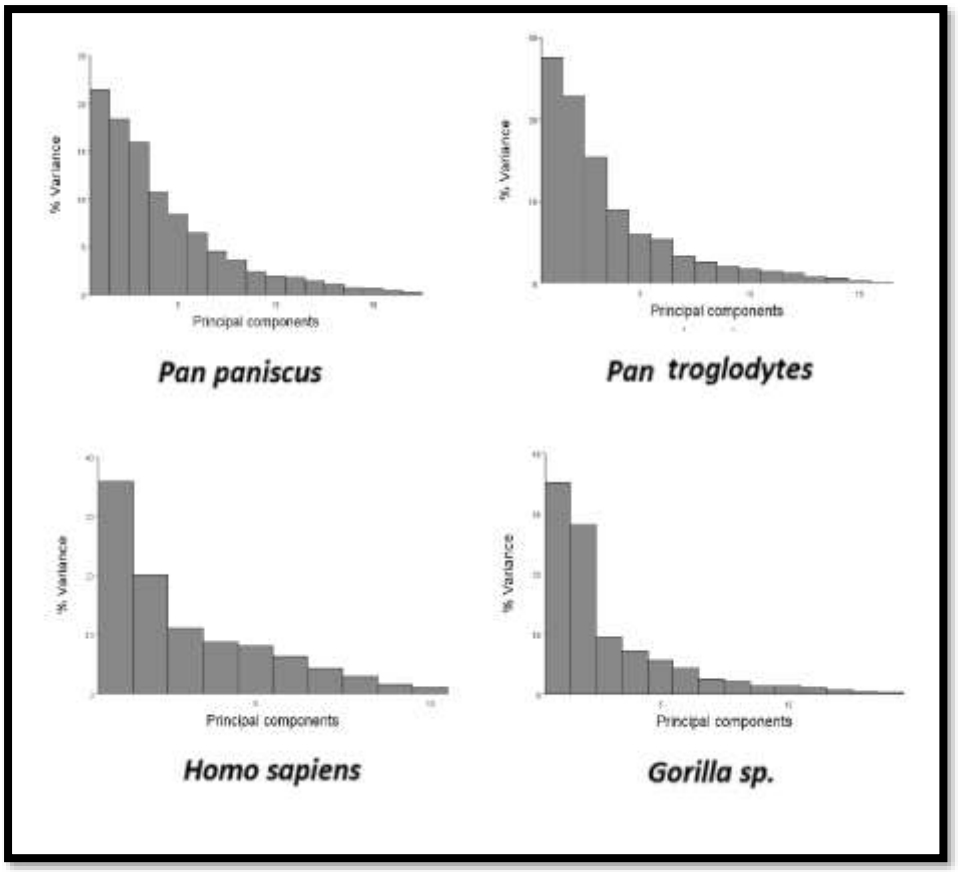

Figure 7-4 Percentage of the variance in the Shape of the Sacrum Explained by each Principal Component in the analysis of all Landmarks and Semilandmarks within each species subsample

Table 7-18: Shapiro-Wilk tests for normality for each sex within the species subsets, including all Landmarks and Semilandmarks of the Sacrum

		sex	Statistic	df	Sig.			sex	Statistic	df	Sig.
Pan paniscus	PC 1	female	.928	9	.466	*Pan troglodytes*	PC 1	female	.892	9	.210
		male	.954	8	.756			male	.902	9	.262
	PC 2	female	.931	9	.491		PC 2	female	.986	9	.987
		male	.925	8	.474			male	.931	9	.495
Gorilla sp.	PC 1	female	.881	9	.160	*Homo sapiens*	PC 1	female	.981	7	.964
		male	.839	7	.110			male	.884	5	.328
	PC 2	female	.923	9	.414		PC 2	female	.923	7	.495
		male	.929	7	.545			male	.943	5	.685

Table 7-19: Levene's Tests for Homogeneity of Variance of the Sacrum for Each Species Subset

Species	Principal Component	Levene's Statistic	df1	df2	Sig.
Pan paniscus	PC1	.210	1	15	.653
	PC2	1.562	1	15	.231
Pan troglodytes	PC1	.297	1	16	.594
	PC2	2.852	1	16	.111
Gorilla sp.	PC1	.607	1	14	.449
	PC2	6.858	1	14	.020
Homo sapiens	PC1	4.270	1	10	.066
	PC2	.009	1	10	.928

Table 7-20: Analysis of Variance for all Landmarks & Semilandmarks of the Sacrum in Each Species Subset

	Pan paniscus						*Pan troglodytes*					
	PC1			PC2			PC1			PC2		
	Between groups	Within groups	Total	Between groups	Within groups	Total	Between groups	Within groups	Total	Between groups	Within groups	Total
Sum of squares	.007	.018	.026	.003	.022	.025	.001	.046	.047	.001	.077	.078
df	1	15	16	1	15	16	1	16	17	1	16	17
Mean square	.007	.001		.003	.001		.001	.003		.001	.005	
F	6.077			2.204			.450			.115		
Sig.	.026			.158			.512			.739		
	Gorilla sp.						*Homo sapiens*					
	PC1			PC2			PC1			PC2		
	Between groups	Within groups	Total	Between groups	Within groups	Total	Between groups	Within groups	Total	Between groups	Within groups	Total
Sum of squares	.037	.058	.095	.000	.046	.046	.005	.030	.034	.001	.015	.017
df	1	14	15	1	14	15	1	10	11	1	10	11
Mean square	.037	.004		.000	.003		.005	.003		.001	.002	
F	9.083			.005			1.536			.857		
Sig.	.009			.945			.243			.376		

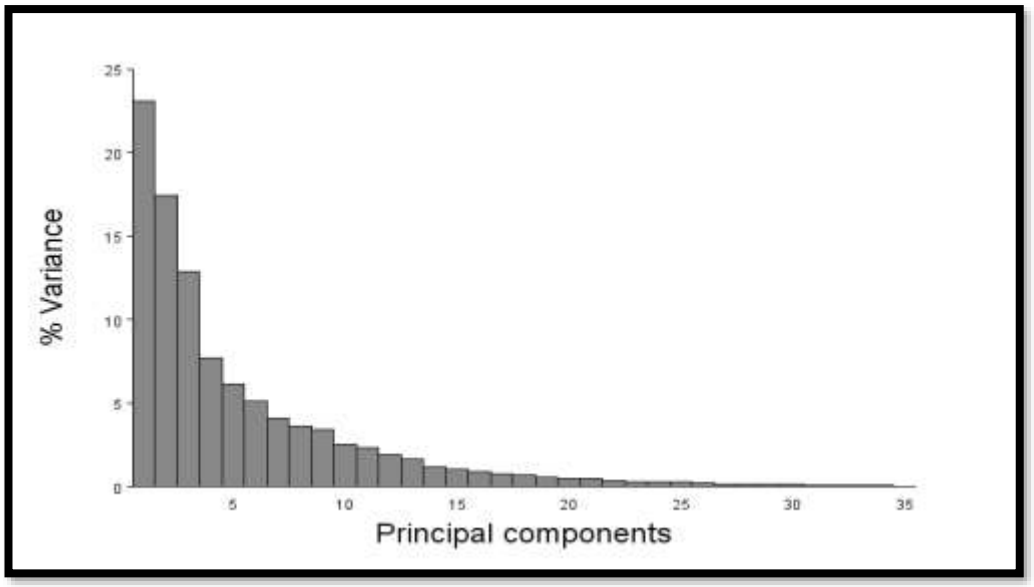

Figure 7-5: Percentage of the Total Variance Explained by Each Principal Component in the Principal Components Analysis of the Sacrum Using All Landmarks and Semilandmarks

Table 7-21 Shapiro-Wilk test for normality for each species, including all Landmarks and Semilandmarks of the Sacrum

	Species	Statistic	df	Sig.
Principal Component 1	*Pan paniscus*	.958	17	.593
	Pan troglodytes	.975	18	.885
	Gorilla sp.	.904	16	.094
	Homo sapiens	.929	12	.370
	Pongo pygmaeus	.944	7	.673
Principal Component 2	*Pan paniscus*	.978	17	.933
	Pan troglodytes	.980	18	.948
	Gorilla sp.	.973	16	.888
	Homo sapiens	.940	12	.498
	Pongo pygmaeus	.904	7	.354

Table 7-22: Analysis of Variance for Principal Components 1 & 2 for All Landmarks and Semilandmarks Across All Species in the Sacrum

		Sum of Squares	df	Mean Square	F	Sig.
PC1	Between Groups	.548	4	.137	34.668	.000
	Within Groups	.257	65	.004		
	Total	.805	69			
PC2	Between Groups	.034	4	.009	2.998	.025
	Within Groups	.187	65	.003		
	Total	.221	69			

Table 7-23: Games-Howell Post Hoc for Principal Component 1 of the Sacrum comparing all Species

Species (I)	Species (J)	Mean Difference (I-J)	Std. Error	Sig.
Pan paniscus	*Pan troglodytes*	-.11156329502*	.01574677735	.000
	Gorilla sp.	-.04143264547	.02212678006	.361
	Homo sapiens	-.26148046080*	.01882698287	.000
	Pongo pygmaeus	-.13525589584*	.03750544298	.049
Pan troglodytes	*Pan paniscus*	.11156329502*	.01574677735	.000
	Gorilla sp.	.07013064955*	.02341894514	.044
	Homo sapiens	-.14991716575*	.02032997491	.000
	Pongo pygmaeus	-.02369260082	.03828199118	.968
Gorilla sp.	*Pan paniscus*	.04143264547	.02212678006	.361
	Pan troglodytes	-.07013064955*	.02341894514	.044
	Homo sapiens	-.22004781532*	.02559182054	.000
	Pongo pygmaeus	-.09382325037	.04131760216	.232
Homo sapiens	*Pan paniscus*	.26148046080*	.01882698287	.000
	Pan troglodytes	.14991716577*	.02032997491	.000
	Gorilla sp.	.22004781532*	.02559182054	.000
	Pongo pygmaeus	.12622456495	.03964851997	.069
Pongo pygmaeus	*Pan paniscus*	.13525589584*	.03750544298	.049
	Pan troglodytes	.02369260082	.03828199118	.968
	Gorilla sp.	.09382325037	.04131760216	.232
	Homo sapiens	-.12622456495	.03964851997	.069

Table 7-24: Games-Howell Post Hoc for Principal Component 2 of the Sacrum comparing all Species

Species (I)	Species (J)	Mean Difference (I-J)	Std. Error	Sig.
Pan paniscus	*Pan troglodytes*	.04977196010	.01865069323	.085
	Gorilla sp.	.01444840629	.01694439009	.911
	Homo sapiens	.05455023424*	.01485283128	.010
	Pongo pygmaeus	.04228464580	.02412370723	.455
Pan troglodytes	*Pan paniscus*	-.04977196010	.01865069323	.085
	Gorilla sp.	-.03532355381	.02115593829	.466
	Homo sapiens	.00477827414	.01952096224	.999
	Pongo pygmaeus	-.00748731430	.02724728647	.999
Gorilla sp.	*Pan paniscus*	-.01444840629	.01694439009	.911
	Pan troglodytes	.03532355381	.02115593829	.466
	Homo sapiens	.04010182795	.01789782009	.197
	Pongo pygmaeus	.02783623950	.02610897580	.820
Homo sapiens	*Pan paniscus*	-.05455023424*	.01485283128	.010
	Pan troglodytes	-.00477827414	.01952096224	.999
	Gorilla sp.	-.04010182795	.01789782009	.197
	Pongo pygmaeus	-.01226558844	.02480267847	.986
Pongo pygmaeus	*Pan paniscus*	-.04228464580	.02412370723	.455
	Pan troglodytes	.00748731430	.02724728647	.999
	Gorilla sp.	-.02783623950	.02610897580	.820
	Homo sapiens	.01226558844	.02480267847	.986

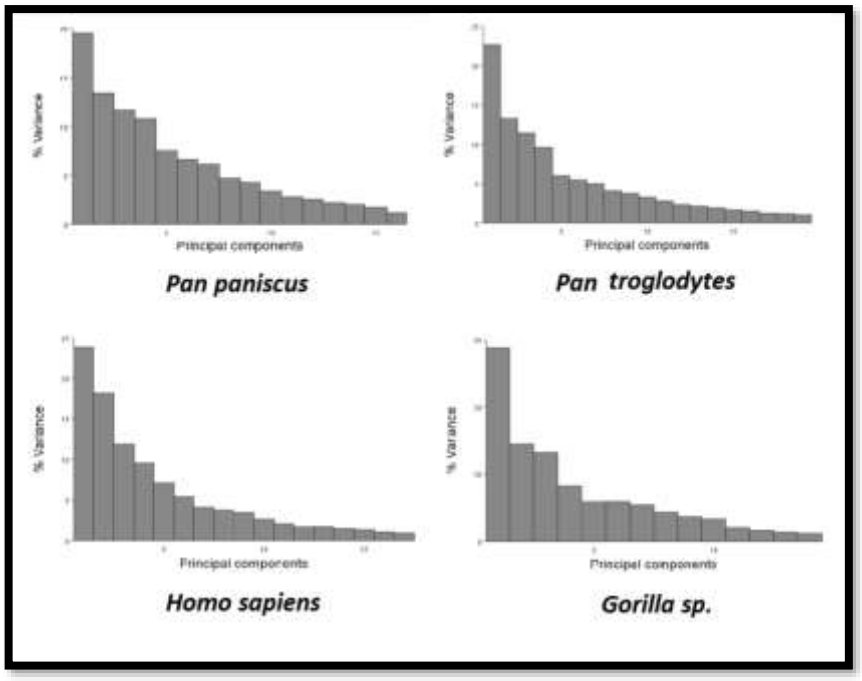

Figure 7-6: Percentage of the Variance in the Femur by each Principal Component in the Analysis of all Landmarks and Semilandmarks within Each Species Subsample

Table 7-25 Shapiro-Wilk tests for normality for each sex within the species subsets, including all Landmarks and Semilandmarks of the Femur

		sex	Statistic	df	Sig.			sex	Statistic	df	Sig.
Pan paniscus	PC 1	female	0.985	9	0.984	*Pan troglodytes*	PC 1	female	0.912	10	0.294
		male	0.951	8	0.722			male	0.926	10	0.413
	PC 2	female	0.922	9	0.41		PC 2	female	0.962	10	0.806
		male	0.901	8	0.295			male	0.915	10	0.315
Gorilla sp.	PC 1	female	0.956	10	0.739	*Homo sapiens*	PC 1	female	0.869	8	0.148
		male	0.883	8	0.203			male	0.891	7	0.281
	PC 2	female	0.967	10	0.862		PC 2	female	0.901	8	0.297
		male	0.943	8	0.645			male	0.963	7	0.846

Table 7-26: Levene's Tests for Homogeneity of Variance of Femur for Each Species Subset

Species	Principal Component	Levene's Statistic	df1	df2	Sig.
Pan paniscus	PC 1	.237	1	15	.633
	PC 2	1.968	1	15	.181
Pan troglodytes	PC 1	.164	1	18	.690
	PC 2	.929	1	18	.348
Gorilla sp.	PC 1	1.229	1	16	.284
	PC 2	.065	1	16	.801
Homo sapiens	PC 1	.025	1	13	.877
	PC 2	.009	1	13	.924

Table 7-27: ANOVA of all Landmarks & Semilandmarks of the Femur in Each Species Subset

	Pan paniscus						*Pan troglodytes*					
	PC1			PC2			PC1			PC2		
	Between groups	Within groups	Total	Between groups	Within groups	Total	Between groups	Within groups	Total	Between groups	Within groups	Total
Sum of squares	.000	.001	.001	.000	.001	.001	.000	.002	.002	.000	.002	.002
df	1	15	16	1	15	16	1	18	19	1	18	19
Mean square	.000	.000		.000	.000		.000	.000		.000	.000	
F	2.121			1.170			.408			.032		
Sig.	.166			.297			.531			.860		
	Gorilla sp.						*Homo sapiens*					
	PC1			PC2			PC1			PC2		
	Between groups	Within groups	Total	Between groups	Within groups	Total	Between groups	Within groups	Total	Between groups	Within groups	Total
Sum of squares	.001	.002	.003	.001	.002	.003	.001	.001	.002	.000	.001	.001
df	1	16	17	1	16	17	1	13	14	1	13	14
Mean square	.001	.000		.001	.000		.001	.000		.000	.000	
F	6.018			7.308			7.365			6.023		
Sig.	.026			.016			.018			.029		

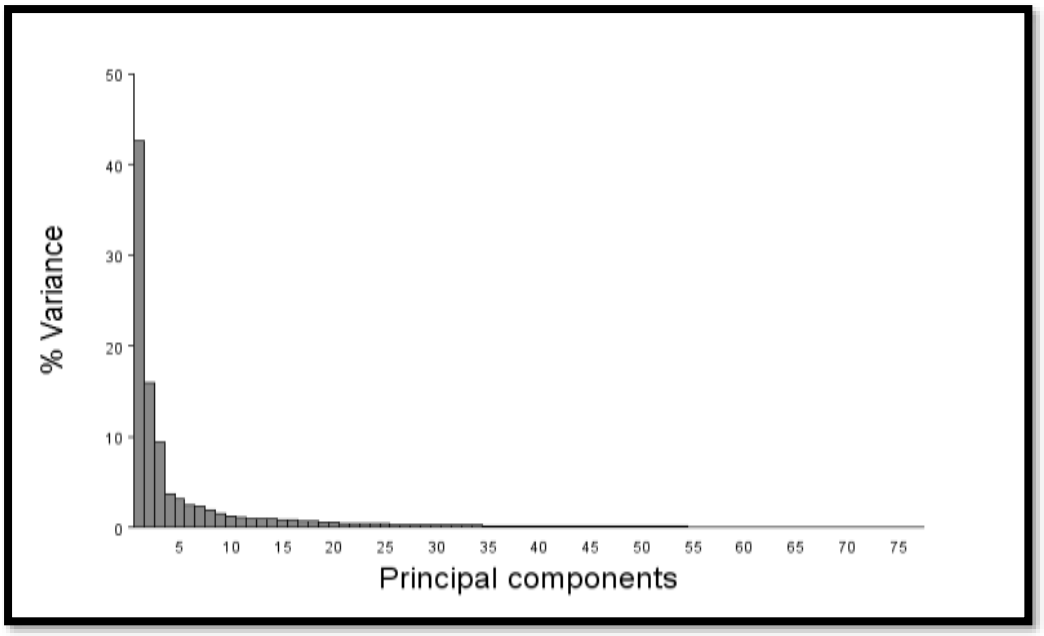

Figure 7-7: Percentage of the Variance Explained by each Principal Component in the Analysis of All Landmarks and Semilandmarks of the Femur

Table 7-28: Shapiro-Wilk test for normality for each species, including all Landmarks and Semilandmarks of the Femur

		Statistic	df	Sig.
Principal Component 1	*Pan paniscus*	.978	17	.936
	Pan troglodytes	.953	20	.410
	Gorilla sp.	.953	18	.473
	Homo sapiens	.947	15	.481
	Pongo pygmaeus	.906	7	.370
Principal Component 2	*Pan paniscus*	.965	17	.728
	Pan troglodytes	.954	20	.432
	Gorilla sp.	.974	18	.863
	Homo sapiens	.941	15	.401
	Pongo pygmaeus	.734	7	.009*

Table 7-29: Between Groups ANOVA for Principal Components 1 and 2 for all Landmarks and Semilandmarks of the Femur

		Sum of Squares	df	Mean Square	F	Sig.
PC 1	Between Groups	.065	5	.013	118.389	.000
	Within Groups	.008	72	.000		
	Total	.073	77			
PC 2	Between Groups	.020	5	.004	38.671	.000
	Within Groups	.007	72	.000		
	Total	.027	77			

Table 7-30

Tukey Post Hoc Homogeneous Subsets for Principal Components 1 & 2 of the Femur for all Landmarks and Semilandmarks across all Species groups

Principal Component 1					
		Subset for alpha=0.05			
Species	N	1	2	3	4
Gorilla sp.	18	-.0449920611			
Pongo pygmaeus	7		-.0152710686		
Pan troglodytes	20			.0032424723	
Pan paniscus	17			.0138929365	
Homo sapiens	15				.0394283067
Sig.		1.000	1.000	.078	1.000

Principal Component 2				
		Subset for alpha=0.05		
Species	N	1	2	3
Pongo pygmaeus	7	-.0449797714		
Homo sapiens	15		-.0083282745	
Gorilla sp.	18			.0036537117
Pan troglodytes	20			.0088082384
Pan paniscus	17			.0126729329
Sig.		1.000	1.000	.160

Means for groups in homogeneous subsets are displayed.
Uses Harmonic Mean Sample Size = 13.372.
The group sizes are unequal. The harmonic mean of the group sizes is used. Type I error levels are not guaranteed.

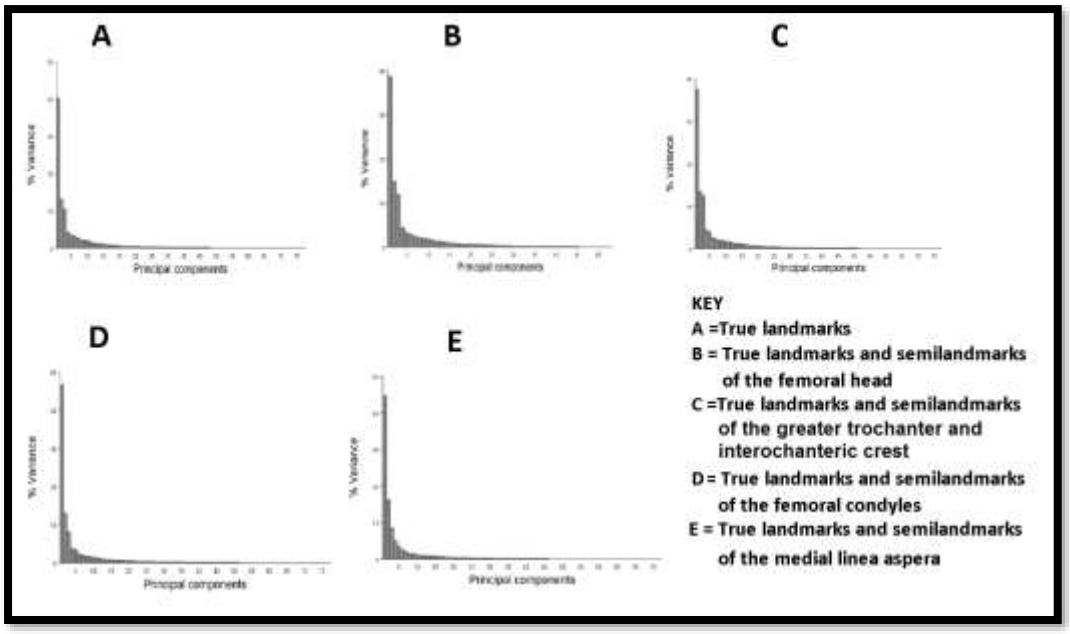

Figure 7-8: The Percentage of the Variance Explained by Each Principal Component for Each Semilandmark set of the Femur

Table 7-31: Shapiro-Wilk Tests for Normality for the True Landmarks and each Semilandmark Set for the Femur

		True Landmarks			*Femoral head*			*Greater trochanter and intertrochanteric crest*			*Femoral Condyles*			*Medial linea aspera*		
	Species	**Stat,**	**df**	**Sig.**	**Statistic**	**df**	**Sig.**	**Statistic**	**df**	**Sig.**	**Statistic**	**df**	**Sig.**	**Statistic**	**df**	**Sig.**
PC 1	***Pan paniscus***	.946	17	.393	.946	17	.399	.963	17	.698	.948	17	.432	.925	17	.181
	Pan troglodytes	.947	20	.330	.951	20	.381	.914	20	.075	.960	20	.550	.967	20	.681
	Gorilla sp.	.971	18	.818	.943	18	.332	.968	18	.764	.891	18	.040*	.939	18	.279
	Homo sapiens	.948	15	.493	.945	15	.444	.965	15	.776	.961	15	.717	.962	15	.731
	Pongo pygmaeus	.917	7	.444	.932	7	.572	.908	7	.384	.907	7	.372	.942	7	.654
PC 2	***Pan paniscus***	.979	17	.947	.931	17	.224	.985	17	.988	.958	17	.591	.948	17	.433
	Pan troglodytes	.971	20	.780	.976	20	.873	.973	20	.808	.957	20	.493	.953	20	.411
	Gorilla sp.	.967	18	.746	.948	18	.392	.930	18	.198	.984	18	.979	.991	18	.999
	Homo sapiens	.931	15	.286	.923	15	.212	.928	15	.250	.942	15	.403	.954	15	.583
	Pongo pygmaeus	.936	7	.599	.955	7	.777	.925	7	.507	.801	7	.042*	.778	7	.024*

* Not normally distributed

Table 7-32: Levene's Test for Homogeneity of Variance for the True Landmarks and each Semilandmark Set for the Femur

	True landmarks				*Femoral head*				*Greater trochanter and intertrochanteric crest*				*Femoral condyles*				*Medial linea aspera*			
	Levene Statistic	df1	df2	Sig.	Levene Statistic	df1	df2	Sig.	Levene Statistic	df1	df2	Sig.	Levene Statistic	df1	df2	Sig.	Levene Statistic	df1	df2	Sig.
PC1	1.399	4	72	.243	1.812	4	72	.136	.994	4	72	.416	1.773	4	72	.144	2.320	4	72	.065
PC2	2.595	4	72	.043	1.396	4	72	.244	.995	4	72	.416	1.976	4	72	.107	1.105	4	72	.361

Table 7-33: ANOVAs of each Semilandmark Set of the Femur

			Sum of Squares	*df*	*Mean Square*	*F*	*Sig.*
True landmarks	PC1	Between Groups	.048	4	.012	103.252	.000
		Within Groups	.008	72	.000		
		Total	.056	76			
	PC2	Between Groups	.015	4	.004	37.875	.000
		Within Groups	.007	72	.000		
		Total	.022	76			
Femoral head	PC1	Between Groups	.050	4	.013	93.750	.000
		Within Groups	.010	72	.000		
		Total	.060	76			
	PC2	Between Groups	.013	4	.003	26.333	.000
		Within Groups	.009	72	.000		
		Total	.022	76			
Greater trochanter and intertrochanteric crest	PC1	Between Groups	.068	4	.017	142.436	.000
		Within Groups	.009	72	.000		
		Total	.077	76			
	PC2	Between Groups	.017	4	.004	38.049	.000
		Within Groups	.008	72	.000		
		Total	.025	76			
Femoral Condyles	PC1	Between Groups	.074	4	.018	118.684	.000
		Within Groups	.011	72	.000		
		Total	.085	76			
	PC2	Between Groups	.018	4	.004	59.702	.000
		Within Groups	.005	72	.000		
		Total	.023	76			
Medial Linea aspera	PC1	Between Groups	.096	4	.024	141.447	.000
		Within Groups	.012	72	.000		
		Total	.108	76			
	PC2	Between Groups	.028	4	.007	44.823	.000
		Within Groups	.011	72	.000		
		Total	.040	76			

Table 7-34: Tukey Post Hoc Homogenous Subsets for Principal Components 1 & 2 of the Femur for the True Landmarks in all Species

Principal Component 1				
		Subset for alpha=0.05		
Species	N	1	2	3
Gorilla sp.	18	-.033961774897404		
Pongo pygmaeus	7	-.023999156904044		
Pan troglodytes	20		.002373510021630	
Pan paniscus	17		.007311094172769	
Homo sapiens	15			.038328418935589
Sig.		.129	.759	1.000

Principal Component 2			
Species	N	1	2
Pan paniscus	17	-.019138706631401	
Pan troglodytes	20	-.009197888795069	
Gorilla sp.	18		.007576444028150
Homo sapiens	15		.015285499166295
Pongo pygmaeus	7		.017562509292111
Sig.		.078	.076

Uses Harmonic Mean Sample Size = 13.372.

The group sizes are unequal. The harmonic mean of the group sizes is used. Type I error levels are not guaranteed.

Table 7-35: Tukey Post-Hoc Tests showing the Homogeneous Subsets when only the True landmarks and Semilandmarks of the Femoral Head for each Principal Component

Principal Component 1

Species	N	Subset for alpha = 0.05			
		1	2	3	4
Homo sapiens	15	-.036492214647085			
Pan paniscus	17		-.011504276876409		
Pan troglodytes	20		-.002589450098101		
Pongo pygmaeus	7			.023669613473532	
Gorilla sp.	18				.036441424605699
Sig.		1.000	.280	1.000	1.000

Principal Component 2

Species	N	Subset for alpha = 0.05		
		1	2	3
Pan paniscus	17	-.010447195239703		
Gorilla sp.	18	-.008683981308863		
Pan troglodytes	20	-.000946693952811	-.000946693952811	
Homo sapiens	15		.006136310862734	
Pongo pygmaeus	7			.036009246601007
Sig.		.183	.467	1.000

Means for groups in homogeneous subsets are displayed.
a. Uses Harmonic Mean Sample Size = 13.372.
b. The group sizes are unequal. The harmonic mean of the group sizes is used. Type I error levels are not guaranteed.

Table 7-36: Tukey Post-Hoc Tests showing the Homogeneous Subsets when only the True landmarks and Semilandmarks of the greater trochanter and intertrochanteric crest for each Principal Component

Principal Component 1					
		Subset for alpha = 0.05			
Species	**N**	**1**	**2**	**3**	**4**
Gorilla sp.	18	-.041669618979883			
Pongo pygmaeus	7		-.025924413170371		
Pan troglodytes	20			.002398885164202	
Pan paniscus	17			.011471953546812	
Homo sapiens	15				.044475572412568
Sig.		1.000	1.000	.212	1.000

Principal Component 2					
		Subset for alpha = 0.05			
Species	**N**	**1**	**2**	**3**	**4**
Pan paniscus	17	-.018429800949768			
Pan troglodytes	20	-.008403373283869	-.008403373283869		
Gorilla sp.	18		.001610344999192		
Homo sapiens	15			.015046552467142	
Pongo pygmaeus	7				.029603114300817
Sig.		.109	.110	1.000	1.000

Means for groups in homogeneous subsets are displayed.
a. Uses Harmonic Mean Sample Size = 13.372.
b. The group sizes are unequal. The harmonic mean of the group sizes is used. Type I error levels are not guaranteed.

Table 7-37: Tukey Post-Hoc Tests showing the Homogeneous Subsets when only the True landmarks and Semilandmarks of the Femoral Condyles for each Principal Component

Principal Component 1

Species	N	Subset for alpha = 0.05			
		1	2	3	4
Gorilla sp.	18	-.044375803673521			
Pongo pygmaeus	7		-.026399755401137		
Pan troglodytes	20			.004514706069343	
Pan paniscus	17			.010192470488206	
Homo sapiens	15				.045632605533317
Sig.		1.000	1.000	.764	1.000

Principal Component 2

Species	N	Subset for alpha = 0.05		
		1	2	3
Pongo pygmaeus	7	-.021810867806111		
Homo sapiens	15	-.018418997320797		
Gorilla sp.	18		-.005658315160012	
Pan troglodytes	20			.011374543212365
Pan paniscus	17			.019252902924395
Sig.		.848	1.000	.140

Means for groups in homogeneous subsets are displayed.
a. Uses Harmonic Mean Sample Size = 13.372.
b. The group sizes are unequal. The harmonic mean of the group sizes is used. Type I error levels are not guaranteed.

Table 7-38: Tukey Post-Hoc Tests showing the Homogeneous Subsets when only the True landmarks and Semilandmarks of the Medial Linea Aspera for each Principal Component

Principal Component 1

Species	N	Subset for alpha = 0.05				
		1	2	3	4	5
Gorilla sp.	18	-.05784679312948				
Pongo pygmaeus	7		-.01283723816724			
Pan troglodytes	20			.00573732488602		
Pan paniscus	17				.02009056720192	
Homo sapiens	15					.04250579860949
Sig.		1.000	1.000	1.000	1.000	1.000

Principal Component 2

Species	N	Subset for alpha = 0.05		
		1	2	3
Pongo pygmaeus	7	-.057330590919675		
Homo sapiens	15		-.005342151081544	
Gorilla sp.	18		.005340962921746	.005340962921746
Pan troglodytes	20			.010510978868874
Pan paniscus	17			.011018976175100
Sig.		1.000	.191	.768

Means for groups in homogeneous subsets are displayed.
a. Uses Harmonic Mean Sample Size = 13.372.
b. The group sizes are unequal. The harmonic mean of the group sizes is used. Type I error levels are not guaranteed.

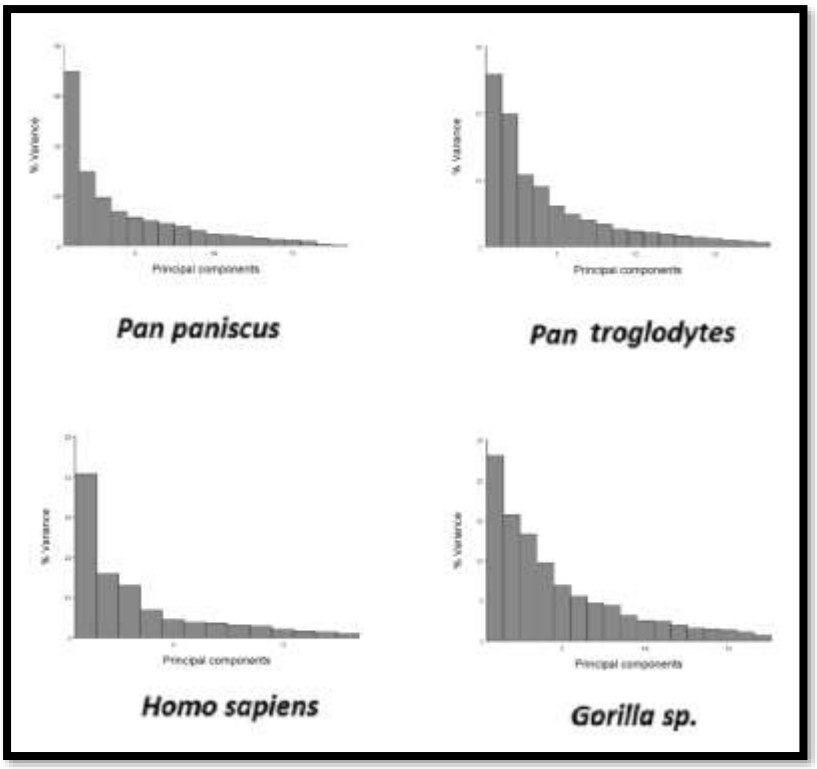

Figure 7-9: Percentage of the variance in the Tibia by each Component in the analysis of all Landmarks and Semilandmarks within each species subsample

Table 7-39: Shapiro-Wilk tests for normality for each sex within the species subsets, including all Landmarks and Semilandmarks of the Tibia

		sex	Statistic	df	Sig.			sex	Statistic	df	Sig.
Pan paniscus	PC 1	female	.920	9	.392	*Pan troglodytes*	PC 1	female	.949	9	.676
		male	.936	8	.568			male	.928	10	.426
	PC 2	female	.929	9	.469		PC 2	female	.962	9	.823
		male	.932	8	.536			male	.864	10	.085
Gorilla sp.	PC 1	female	.900	10	.221	*Homo sapiens*	PC 1	female	.927	7	.526
		male	.955	8	.763			male	.860	7	.152
	PC 2	female	.973	10	.917		PC 2	female	.939	7	.632
		male	.848	8	.090			male	.926	7	.517

Table 7-40: Levene's Tests for Homogeneity of Variance of the Tibia for Each Species Subset

Species	Principal Component	Levene's Statistic	df1	df2	Sig.
Pan paniscus	PC1	.004	1	15	.951
	PC2	.464	1	15	.506
Pan troglodytes	PC1	.065	1	17	.801
	PC2	1.382	1	17	.256
Gorilla sp.	PC1	.514	1	16	.484
	PC2	.866	1	16	.366
Homo sapiens	PC1	.071	1	12	.795
	PC2	2.270	1	12	.158

Table 7-41: ANOVA of all Landmarks & Semilandmarks of the Tibia in Each Species Subset

	Pan paniscus						*Pan troglodytes*					
	PC1			PC2			PC1			PC2		
	Between groups	Within groups	Total	Between groups	Within groups	Total	Between groups	Within groups	Total	Between groups	Within groups	Total
Sum of squares	.001	.003	.003	.000	.002	.002	.000	.004	.004	.000	.003	.003
df	1	15	16	1	15	16	1	17	18	1	17	18
Mean square	.001	.000		.000	.000		.000	.000		.000	.000	
F	3.034			.626			.000			1.824		
Sig.	.102			.441			.993			.195		
	Gorilla sp.						*Homo sapiens*					
	PC1			PC2			PC1			PC2		
	Between groups	Within groups	Total	Between groups	Within groups	Total	Between groups	Within groups	Total	Between groups	Within groups	Total
Sum of squares	.001	.004	.004	.001	.002	.003	.002	.003	.005	.000	.002	.002
df	1	16	17	1	16	17	1	12	13	1	12	13
Mean square	.001	.000		.001	.000		.002	.000		.000	.000	
F	2.260			11.403			9.132			.572		
Sig.	.152			.004			.011			.464		

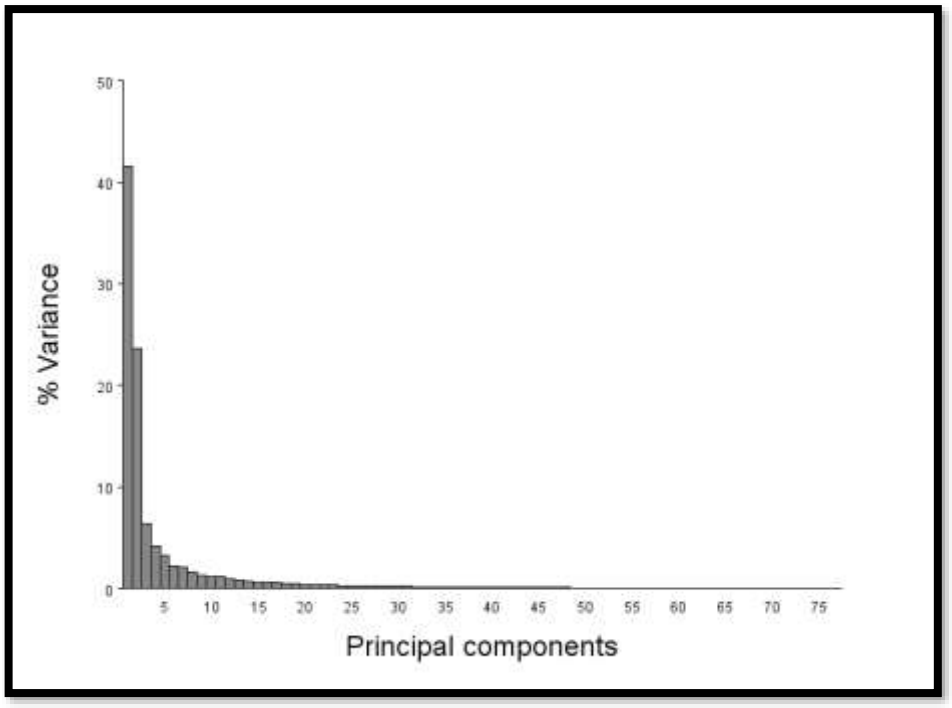

Figure 7-10: Percentage of the Variance Explained by each Principal Component in the Analysis of All Landmarks and Semilandmarks of the Tibia

Table 7-42 Shapiro-Wilk test for normality for each species, including all Landmarks and Semilandmarks of the Tibia

		Statistic	df	Sig.
Principal Component 1	*Pan paniscus*	.944	17	.375
	Pan troglodytes	.961	19	.598
	Gorilla sp.	.953	18	.467
	Homo sapiens	.950	14	.557
	Pongo pygmaeus	.955	7	.773
Principal Component 2	*Pan paniscus*	.965	17	.724
	Pan troglodytes	.970	19	.777
	Gorilla sp.	.951	18	.435
	Homo sapiens	.899	14	.109
	Pongo pygmaeus	.878	7	.219

Table 7-43: ANOVA of Principal Components 1 & 2 of All Landmarks and Semilandmarks of the Tibia Across Species Groups

		Sum of Squares	df	Mean Square	F	Sig.
PC1	Between Groups	.067	4	.017	200.898	.000
	Within Groups	.006	70	.000		
	Total	.073	74			
PC2	Between Groups	.026	4	.007	39.498	.000
	Within Groups	.012	70	.000		
	Total	.038	74			

Table 7-44: Tukey Post Hoc Homogeneous Subsets for Principal Components 1 & 2 of the Tibia for all Species Using all Landmarks and Semilandmarks

Principal Component 1				
		Subset for alpha=0.05		
Species	N	1	2	3
Homo sapiens	14	-.057343778028426		
Pongo pygmaeus	7		.002090854065954	
Pan paniscus	17		.004102078958904	
Pan troglodytes	19		.007298976296479	
Gorilla sp.	18			.032994624571917
Sig.		1.000	.591	1.000
Principal Component 2				
		Subset for alpha=0.05		
Species	N	1	2	3
Pan paniscus	17	-.022975244947172		
Pan troglodytes	19	-.011636488184431		
Pongo pygmaeus	7		.007766045737427	
Homo sapiens	14		.014392941342830	.014392941342830
Gorilla sp.	18			.025122403837824
Sig.		.171	.680	.216

Means for groups in homogeneous subsets are displayed.
Uses Harmonic Mean Sample Size = 13.372.
The group sizes are unequal. The harmonic mean of the group sizes is used. Type I error levels are not guaranteed.

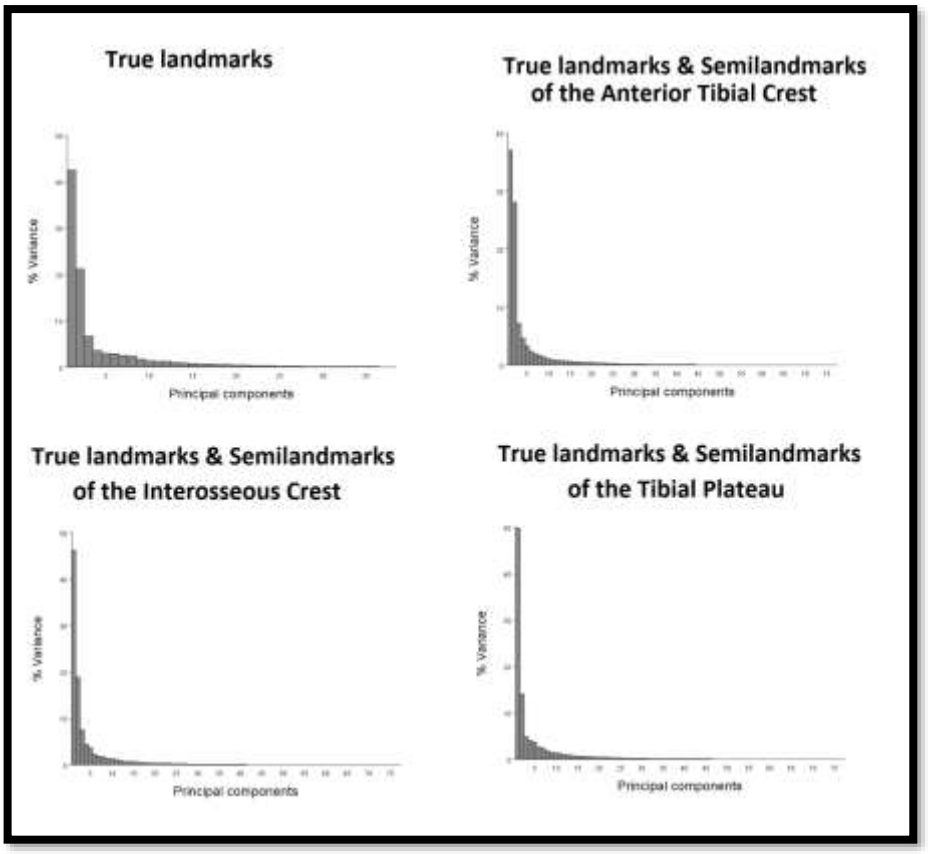

Figure 7-11: The Percentage of the Variance Explained by Each Principal Component for Each Semilandmark set of the Tibia

Table 7-45: Shapiro-Wilk Tests for Normality for True landmarks and each Semilandmark Set of the Tibia

		True Landmarks			*Anterior Tibial Crest*			*Interosseous Crest*			*Tibial Plateau*		
	Species	Stat	df	Sig.	Stat	df	Sig.	Stat	df	Sig.	Stat	df	Sig.
PC1	*Pan paniscus*	.984	17	.986	.939	17	.304	.905	17	.084	.955	17	.549
	Pan troglodytes	.952	19	.430	.971	19	.790	.886	19	.027*	.985	19	.983
	Gorilla sp.	.915	18	.104	.965	18	.693	.963	18	.656	.958	18	.571
	Homo sapiens	.960	14	.726	.955	14	.636	.967	14	.841	.950	14	.556
	Pongo pygmaeus	.856	7	.139	.826	7	.074	.908	7	.382	.912	7	.407
PC2	*Pan paniscus*	.976	17	.916	.966	17	.740	.963	17	.681	.981	17	.966
	Pan troglodytes	.955	19	.479	.971	19	.796	.968	19	.727	.968	19	.729
	Gorilla sp.	.862	18	.013*	.930	18	.197	.955	18	.515	.923	18	.146
	Homo sapiens	.928	14	.284	.901	14	.116	.909	14	.153	.922	14	.231
	Pongo pygmaeus	.896	7	.308	.905	7	.365	.950	7	.728	.874	7	.199

* Not normally distributed

Table 7-46: Levene's Test for Homogeneity of Variance for True Landmarks and each Semilandmark Set of the Tibia

	True Landmarks				*Anterior Tibial Crest*				*Interosseous Crest*				*Tibial Plateau*			
	Levene Statistic	df1	df2	Sig.	Levene Statistic	df1	df2	Sig.	Levene Statistic	df1	df2	Sig.	Levene Statistic	df1	df2	Sig.
PC1	1.516	4	70	.207	.453	4	70	.770	.715	4	70	.585	1.809	4	70	.137
PC2	1.116	4	70	.356	.557	4	70	.694	1.514	4	70	.208	2.308	4	70	.066

Table 7-47: ANOVAs of the True Landmarks and each Semilandmark set for the Tibia

			Sum of Squares	*df*	*Mean Square*	*F*	*Sig.*
True landmarks	**PC1**	**Between Groups**	**.039**	**4**	**.010**	**110.006**	**.000**
		Within Groups	**.006**	**70**	**.000**		
		Total	**.045**	**74**			
	PC2	**Between Groups**	**.014**	**4**	**.003**	**32.547**	**.000**
		Within Groups	**.007**	**70**	**.000**		
		Total	**.021**	**74**			
Anterior Tibial Crest	**PC1**	**Between Groups**	**.056**	**4**	**.014**	**190.625**	**.000**
		Within Groups	**.005**	**70**	**.000**		
		Total	**.061**	**74**			
	PC2	**Between Groups**	**.029**	**4**	**.007**	**39.837**	**.000**
		Within Groups	**.013**	**70**	**.000**		
		Total	**.042**	**74**			
Interosseous Crest	**PC1**	**Between Groups**	**.070**	**4**	**.018**	**188.976**	**.000**
		Within Groups	**.007**	**70**	**.000**		
		Total	**.077**	**74**			
	PC2	**Between Groups**	**.019**	**4**	**.005**	**30.564**	**.000**
		Within Groups	**.011**	**70**	**.000**		
		Total	**.029**	**74**			
Tibial Plateau	**PC1**	**Between Groups**	**.068**	**4**	**.017**	**91.105**	**.000**
		Within Groups	**.013**	**70**	**.000**		
		Total	**.081**	**74**			
	PC2	**Between Groups**	**.015**	**4**	**.004**	**36.631**	**.000**
		Within Groups	**.007**	**70**	**.000**		
		Total	**.022**	**74**			

Table 7-48: Tukey Post-Hoc Homogeneous Subsets for Principal Components 1 & 2 of the Tibia for all Species Using True Landmarks

Principal Component 1					
		Subset for alpha = 0.05			
Species	N	1	2	3	4
Gorilla sp.	18	-.030455024857868			
Pongo pygmaeus	7		-.010675565921681		
Pan troglodytes	19		-.000665882428039	-.000665882428039	
Pan paniscus	17			.003054955903724	
Homo sapiens	14				.038832630193684
Sig.		1.000	.059	.848	1.000

Principal Component 2			
		Subset for alpha = 0.05	
Species	N	1	2
Pan paniscus	17	-.014445028632504	
Pongo pygmaeus	7	-.014279940524303	
Pan troglodytes	19	-.005185829029959	
Gorilla sp.	18		.014742494344628
Homo sapiens	14		.017339354207856
Sig.		.150	.966

Means for groups in homogeneous subsets are displayed.
a. Uses Harmonic Mean Sample Size = 13.113.
b. The group sizes are unequal. The harmonic mean of the group sizes is used. Type I error levels are not guaranteed.

Table 7-49: Tukey Post Hoc Homogeneous Subsets for Principal Components 1 & 2 of the Tibia for all Species Using True Landmarks and Semilandmarks of the Anterior Tibial Crest

Principal Component 1					
		Subset for alpha = 0.05			
Species	N	1	2	3	4
Homo sapiens	14	-.049317086291790			
Pan paniscus	17		-.004341371828289		
Pan troglodytes	19			.005962920501802	
Pongo pygmaeus	7			.012283693552195	
Gorilla sp.	18				.033323634376233
Sig.		1.000	1.000	.334	1.000

Principal Component 2				
		Subset for alpha = 0.05		
Species	N	1	2	3
Homo sapiens	14	-.023314559104839		
Gorilla sp.	18	-.022380130394648		
Pongo pygmaeus	7		.000873101428793	
Pan troglodytes	19		.010389333379993	.010389333379993
Pan paniscus	17			.024905940307621
Sig.		1.000	.380	.057

Means for groups in homogeneous subsets are displayed.
a. Uses Harmonic Mean Sample Size = 13.113.
b. The group sizes are unequal. The harmonic mean of the group sizes is used. Type I error levels are not guaranteed.

Table 7-50: Tukey Post-Hoc Homogeneous Subsets for Principal Components 1 & 2 of the Tibia for all Species Using True Landmarks and Semilandmarks of the Interosseous Crest

Principal Component 1				
		Subset for alpha = 0.05		
Species	N	1	2	3
Homo sapiens	14	-.061926208049392		
Pongo pygmaeus	7		-.009460290610847	
Pan troglodytes	19			.012812473054619
Pan paniscus	17			.015302958934837
Gorilla sp.	18			.022359236489153
Sig.		1.000	1.000	.095

Principal Component 2					
		Subset for alpha = 0.05			
Species	N	1	2	3	4
Gorilla sp.	18	-.026106222693863			
Pongo pygmaeus	7		-.007647685566312		
Homo sapiens	14		.000056939233073	.000056939233073	
Pan troglodytes	19			.009007465564740	.009007465564740
Pan paniscus	17				.016289351490487
Sig.		1.000	.504	.351	.560

Table 7-51: Tukey Post Hoc Homogeneous Subsets for Principal Components 1 & 2 of the Tibia for all Species Using True Landmarks and Semilandmarks of the Tibial Plateau

Principal Component 1					
		Subset for alpha = 0.05			
Species	N	1	2	3	4
Homo sapiens	14	-.045271963755737			
Pan paniscus	17		-.007636373117053		
Pan troglodytes	19		-.002282962903093	-.002282962903093	
Pongo pygmaeus	7			.009201248180659	
Gorilla sp.	18				.045900094813244
Sig.		1.000	.854	.211	1.000

Principal Component 2				
		Subset for alpha = 0.05		
Species	N	1	2	3
Pan paniscus	17	-.014891334383234		
Pongo pygmaeus	7	-.010813945808998		
Pan troglodytes	19	-.007271692242201		
Gorilla sp.	18		.011443397951403	
Homo sapiens	14			.022693125618612
Sig.		.316	1.000	1.000